

**THE STUDY OF  
FAINT GALACTIC OPEN CLUSTERS**

*A Thesis  
Submitted For The Degree of  
Doctor of Philosophy In The Faculty of Science*

BANGALORE UNIVERSITY

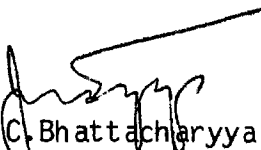
*By*  
G. S. D. BABU


INDIAN INSTITUTE OF ASTROPHYSICS  
BANGALORE  
INDIA


APRIL 1985

## DECLARATION

I hereby declare that the matter embodied in this thesis is the result of the investigations carried out by me in the Indian Institute of Astrophysics, Bangalore and the Department of Physics, Central College, Bangalore, under the supervision of Late Prof. M.K.V.Bappu (until his sudden demise in August 1982), Prof. J.C.Bhattacharyya (since September 1982) and Dr. M.N. Anandaram. This work has not been submitted for the award of any degree, diploma, associateship, fellowship, etc. of any University or Institute.

  
J.C. Bhattacharyya  
Supervisor

  
M.N. Anandaram  
Supervisor

  
(G.S.D. Babu)  
Candidate

Bangalore  
Dated: 9 April 1985

### **DEDICATION**

I dedicate this thesis to the memory of Late Prof. M.K.V.Bappu.

## ACKNOWLEDGEMENTS

I will remain deeply indebted forever to Late Prof. M.K.V.Bappu, who initiated me into the study of clusters and gave me the opportunity to work under his invaluable guidance until his untimely death. No words can express my gratitude for the ever helpful inspiration and continued encouragement provided to me by him during his lifetime. May his soul rest in peace.

The present work was carried out by me as a member of the Indian Institute of Astrophysics, Bangalore. I wish to thank the Director and the authorities of the Institute for providing me with all the facilities to carry out this work, including the funds for visiting Australia.

It is a pleasure to acknowledge the painstaking efforts taken by my supervisors Prof. J.C.Bhattacharyya and Dr. M.N.Ananda Ram in seeing to the successful completion of this thesis. I am highly obliged to Prof. Bhattacharyya for accepting the task of supervising the thesis at a critical juncture when Prof. Bappu suddenly passed away. Thanks are also due to the members of the Doctoral Committee headed successively by Prof. K.N.Kuchela, Prof.P.Pasramasivaiah, Late Prof. N.Madaiah and Prof. N.G.Puttaswamy along with Prof. S.Chandrasekhar and Prof. B.C.Chandrasekhar for looking after the progress of my thesis work.

I wish to express my heartfelt thanks to Prof. D.S.Mathewson, Director of the Mount Stromlo and Siding Spring Observatories (MSSSO) in Australia for the kind hospitality extended towards me during my stay at these observatories.

I specially thank Dr. N.Visvanathan of MSSSO for taking a lot of interest in my programme and for making my trip to Australia a reality. I am grateful to him and Dr. V.L.Ford for generously granting me the observing time on the telescopes at the Mount Stromlo and Siding Spring Observatories. I shall remain highly indebted to Dr. Visvanathan for taking care of all my problems, thus making a very pleasant stay for me in Australia.

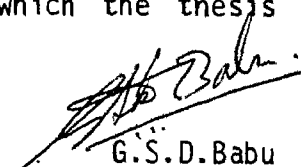
I am also thankful to Drs. J.B.Newell, E.M.Green, B.Pettersson, D.Carter, P.Harding, H.Morrison and many others at Mount Stromlo Observatory (MSO) for their help and cooperation at various stages of my work there. Drs. Green and Petterson were very kind in showing me the telescopes at the Siding Spring Observatory (SSO) along with the accessories with which I had to work.

I give my special thanks to Dr. John Dawe of SSO, who readily helped me whenever I was in need and always cheered me up with a smile during my long spells of night observations. My thanks are due to Drs. S. Tritton and D. Malin for making me feel at home during my stay at SSO. I thank one and all at MSO and SSO.

I am grateful to Dr. U. C. Joshi of Physical Research Laboratories, Ahmedabad and Dr. R. Sagar of Kumaon University, Nainital for their continued help and encouragement right from the beginning of my work on clusters. I would like to thank Prof. R. F. Garrison of David Dunlap Observatory, Ontario, Canada and Prof. G. Lynga of Lund Observatory, Lund, Sweden for their valuable comments and helpful discussions.

My sincere thanks to all my colleagues in the Institute, who gave me their time and support throughout my work. I am especially thankful to Drs. D. C. V. Mallik, N. Kameswara Rao and R. Rajamohan for patiently going through the entire manuscript and for giving me very valuable suggestions. I gratefully acknowledge the enormous help given to me by Mr. K. Kuppaswamy, Mr. M. J. Rosario and Mr. K. Jayakumar during the time of my observations with the telescopes at Kavalur Observatory. I am thankful to Ms. A. Vagiswari and the staff of the Library for their immense help in connection with various references. I thank Ms. Sandra Rajiva for her help in editing the thesis. I also thank my colleagues in the Drawing Section, especially Mr. Hari Inbaraj, for preparing all the drawings. The typing was done by Miss. K. Padmavathi and Mr. K. Thiyagarajan for whom I extend my gratitude. I am similarly grateful to Mr. Md. Khan for his help at the copying machine and to Mr. R. Krishnamoorthy for the binding work.

Finally, I am grateful to my wife Mary as well as to my sons, Christopher Summeet and Paul Amit, for their encouragement and cooperation throughout the period during which the thesis work was carried out.

  
G. S. D. Babu

## CONTENTS

|                   |  | <u>Page</u> |
|-------------------|--|-------------|
| ABSTRACT          | ...  | i - iii     |
| <b>CHAPTER 1.</b> | <b>INTRODUCTION</b>  | <b>1</b>    |
| 1.1.              | Open Clusters  | 2           |
| 1.2.              | Classification of Open Clusters  | 4           |
| 1.2.1.            | According to Appearance  | 4           |
| 1.2.2.            | Based on HR-diagram  | 5           |
| 1.3.              | Young Open Clusters as Spiral Arm Tracers  | 6           |
| 1.4.              | Plan of the Thesis   | 12          |
| <br>              |  |             |
| <b>CHAPTER 2.</b> | <b>SELECTION OF YOUNG CLUSTERS AND THEIR PROVISIONAL MEMBERSHIP</b>                    | <b>14</b>   |
| 2.1.              | Modified Objective-Grating Camera  | 20          |
| 2.2.              | Spectral Types from the Modified Objective-Grating Spectroscopy                        | 21          |
| 2.3.              | Magnitudes from the Images of the Sky Survey Charts                                    | 29          |
| 2.4.              | HR-diagrams and the Provisional Membership of the Open Clusters                        | 36          |
| 2.4.1.            | OC1 537 (Dolidze 25)   | 38          |
| 2.4.2.            | OC1 598 (NGC 2414)   | 40          |
| 2.4.3.            | OC1 618 (NGC 2384)   | 45          |
| 2.4.4.            | OC1 626 (NGC 2421)   | 50          |
| 2.5.              | Conclusions  | 50          |
| <br>              |  |             |
| <b>CHAPTER 3.</b> | <b>PROCEDURES FOR THE OBSERVATIONS AND FOR THE DETERMINATION OF CLUSTER PARAMETERS</b> | <b>55</b>   |
| 3.1.              | Photoelectric Photometry   | 56          |
| 3.1.1.            | The Photoelectric Photometer   | 56          |

|                |           |  |     |           |
|----------------|-----------|--|-----|-----------|
|                | 3.1.2.    | The Observational and<br>Reduction Procedures                      | ... | 58        |
|                | 3.1.3.    | Computation of Standard<br>Magnitudes                              | ... | 60        |
|                | 3.2.      | Photographic Photometry  | ... | 61        |
|                | 3.2.1.    | Direct Photography   | ... | 62        |
|                | 3.2.2.    | Analysis of the Photographs  | ... | 64        |
|                | 3.3.      | Procedure for the Determi-<br>nation of Cluster Membership         | ... | 67        |
|                | 3.3.1.    | Photometric Criteria   | ... | 67        |
|                | 3.3.2.    | Kinematic Criteria   | ... | 70        |
|                | 3.3.3.    | Statistical Criteria   | ... | 70        |
|                | 3.3.4.    | Spectroscopic Criteria   | ... | 71        |
|                | 3.4.      | Procedure for the Determi-<br>nation of Reddening                  | ... | 72        |
|                | 3.5.      | Intrinsic Magnitudes and<br>Colours                                | ... | 77        |
|                | 3.6.      | Procedure for the Determi-<br>nation of Distance to the<br>Cluster | ... | 78        |
|                | 3.7.      | Procedure for the Determi-<br>nation of Age                        | ... | 79        |
| <b>CHAPTER</b> | <b>4.</b> | <b>OBSERVATIONS AND RESULTS</b>                                    | ... | <b>83</b> |
|                | 4.1.      | OC1 427 (Czernik 20)   | ... | 86        |
|                | 4.1.1.    | Selection and Observations   | ... | 86        |
|                | 4.1.2.    | Membership   | ... | 93        |
|                | 4.1.3.    | Reddening  | ... | 95        |
|                | 4.1.4.    | Distance   | ... | 95        |
|                | 4.1.5.    | Age of the Cluster   | ... | 96        |
|                | 4.2.      | OC1 493 (Czernik 25)   | ... | 98        |
|                | 4.2.1.    | Selection and Observations   | ... | 98        |
|                | 4.2.2.    | Membership   | ... | 104       |
|                | 4.2.3.    | Reddening  | ... | 104       |
|                | 4.2.4.    | Distance   | ... | 106       |
|                | 4.2.5.    | Age of the Cluster   | ... | 106       |

|        |                            |     |     |
|--------|----------------------------|-----|-----|
| 4.3.   | OC1 501 (NGC 2236)         | ... | 108 |
| 4.3.1. | Selection and Observations | ... | 108 |
| 4.3.2. | Membership                 | ... | 114 |
| 4.3.3. | Reddening                  | ... | 115 |
| 4.3.4. | Distance                   | ... | 117 |
| 4.3.5. | Age of the Cluster         | ... | 119 |
| 4.4.   | OC1 506 (Cr 97)            | ... | 119 |
| 4.4.1. | Selection and Observations | ... | 119 |
| 4.4.2. | Membership                 | ... | 125 |
| 4.4.3. | Reddening                  | ... | 127 |
| 4.4.4. | Distance                   | ... | 127 |
| 4.4.5. | Age of the Cluster         | ... | 128 |
| 4.5.   | OC1 556 (Haffner 3)        | ... | 128 |
| 4.5.1. | Selection and Observations | ... | 131 |
| 4.5.2. | Membership                 | ... | 136 |
| 4.5.3. | Reddening                  | ... | 139 |
| 4.5.4. | Distance                   | ... | 140 |
| 4.5.5. | Ages of the Two Clusters   | ... | 140 |
| 4.6.   | OC1 585 (NGC 2374)         | ... | 142 |
| 4.6.1. | Selection and Observations | ... | 143 |
| 4.6.2. | Membership                 | ... | 148 |
| 4.6.3. | Reddening                  | ... | 150 |
| 4.6.4. | Distance                   | ... | 151 |
| 4.6.5. | Age of the Cluster         | ... | 153 |
| 4.7.   | OC1 674 (Haffner 14)       | ... | 153 |
| 4.7.1. | Selection and Observations | ... | 154 |
| 4.7.2. | Membership                 | ... | 158 |
| 4.7.3. | Reddening                  | ... | 161 |
| 4.7.4. | Distance                   | ... | 161 |
| 4.7.5. | Age of the Cluster         | ... | 163 |
| 4.8.   | OC1 692 (Haffner 20)       | ... | 163 |
| 4.8.1. | Selection and Observations | ... | 163 |
| 4.8.2. | Membership                 | ... | 167 |
| 4.8.3. | Reddening                  | ... | 167 |
| 4.8.4. | Distance                   | ... | 170 |
| 4.8.5. | Age of the Cluster         | ... | 170 |



|                |           |  |     |            |
|----------------|-----------|--|-----|------------|
|                | 4.9.      | OC1 694 (Haffner 17)   | ... | 172        |
|                | 4.9.1.    | Selection and Observations   | ... | 172        |
|                | 4.9.2.    | Membership   | ... | 174        |
|                | 4.9.3.    | Reddening  | ... | 177        |
|                | 4.9.4.    | Distance   | ... | 179        |
|                | 4.9.5.    | Age of the Cluster   | ... | 179        |
|                | 4.10.     | OC1 715 (NGC 2588)   | ... | 181        |
|                | 4.10.1    | Selection and Observations   | ... | 181        |
|                | 4.10.2.   | Membership   | ... | 184        |
|                | 4.10.3.   | Reddening  | ... | 187        |
|                | 4.10.4.   | Distance   | ... | 187        |
|                | 4.10.5.   | Age of the Cluster   | ... | 189        |
|                | 4.11.     | OC1 762 (Ruprecht 69)  | ... | 189        |
|                | 4.11.1.   | Selection and Observations   | ... | 191        |
|                | 4.11.2.   | Membership   | ... | 194        |
|                | 4.11.3.   | Reddening  | ... | 194        |
|                | 4.11.4.   | Distance   | ... | 197        |
|                | 4.11.5.   | Age of the Cluster   | ... | 199        |
|                | 4.12.     | OC1 798 (NGC 3105)   | ... | 199        |
|                | 4.12.1.   | Selection and Observations   | ... | 200        |
|                | 4.12.2.   | Membership   | ... | 205        |
|                | 4.12.3.   | Reddening  | ... | 211        |
|                | 4.12.4.   | Distance   | ... | 212        |
|                | 4.12.5.   | Age of the Cluster   | ... | 214        |
| <b>CHAPTER</b> | <b>5.</b> | <b>EVOLUTIONARY ASPECTS OF THE<br/>SELECTED CLUSTERS AND THEIR<br/>RELATIONSHIP TO THE STRUCTURE<br/>OF THE GALAXY</b> | ... | <b>215</b> |
|                | 5.1.      | Evolutionary Aspects   | ... | 215        |
|                | 5.2.      | Presence of Gas-Dust in<br>Clusters  | ... | 220        |
|                | 5.3.      | Relationship of the Open<br>Clusters to the Structure<br>of the Galaxy   | ... | 224        |
| <b>CHAPTER</b> | <b>6.</b> | <b>SUMMARY AND FUTURE PROSPECTS</b>  | ... | <b>229</b> |
|                |           | <b>REFERENCES</b>  | ... | <b>234</b> |

## ABSTRACT

The topic of this thesis was originally suggested by Late Prof. M.K.V.Bappu and was undertaken with two major aims. The first was to obtain the luminosities of stars contained in the very distant and hitherto not well-studied clusters. The second aim was to use the younger of these clusters as spiral arm tracers to substantiate the existing optical picture of our Galaxy's spiral structure. In this thesis, the portion covered was restricted to the anticenter direction of the Galaxy ( $160^\circ < \text{gal. long.} < 280^\circ$ ) so that an attempt may be made to optically study the remotest galactic parts. This is made slightly easier because in this direction, the complications due to the effects of interstellar extinction are less than those in the direction of the galactic center.

As the first step, one hundred and four not well-studied clusters were chosen from the catalogue of open clusters in the given range of galactic longitudes. Then thirty two of them were observed with the modified objective grating method (Hoag & Schroeder, 1970), so as to get an approximate estimate of spectral types of the individual stars in each cluster region. These spectral types were combined with their respective visual magnitudes determined from the image sizes on the already existing sky survey charts, to construct the approximate HR-diagram of each cluster. Out of them, six were found to have stars of spectral type B3 or earlier on the respective main-sequence bands and were categorised as young. Six more bluer clusters

were selected based on the visual inspection of the blue and red prints of the sky survey charts.

All these twelve clusters were photometrically observed using the facilities at Kavalur Observatory in India and at Siding Spring Observatory in Australia. In general, the stars which appeared to be members, out of the observed ones, in each of the programme clusters, have been found to be in the range of 10 to 30, with one exception, for which 55 members have been counted.

Each one of these clusters is found to be showing some amount of luminosity spread, which is mainly caused by stars of differing ages, supporting the earlier suggestion that star formation in clusters is not coeval. Their ages are in the range of  $6.0 \times 10^6$  to  $5.9 \times 10^8$  years.

Their distances are found to be ranging from 0.6 kpc to 7.1 kpc and their colour excesses,  $E(B-V)$ , are in the range of 0.00 mag to 1.20 mag. It is clearly seen from the present work that as the cluster distance increases, the value of  $E(B-V)$  increases. That is, the amount of interstellar matter increases in the line of sight column with the increasing distance from the Sun in the plane of the Galaxy.

Out of the twelve clusters studied here, four are located along the Cygnus-Orion arm and one is a definite member of the Sagittarius-Carina arm. The existence of the outer Perseus spiral feature is substantiated by four clusters at distances of about 4 to 5.5 kpc in the direction of the galactic longitude

170° to 220°, some evidence for which was found earlier by Moffat & Vogt (1973). There is a clear indication that this outer feature is probably extending into the Puppis group of clusters which seems to be the junction for the merging of the local arm with the outer Perseus arm. This is supported by one of the presently studied clusters which is located at a distance of about 6.5 kpc in the galactic longitude of about 245°.

There is an indication of a feature which is originating from the Orion-Cygnus arm at a distance of about 4.5 kpc and extending upto a distance of about 8 kpc towards the galactic longitude of 280°. This inference is based on the location of one of the programme clusters at a distance of about 7 kpc in the direction of galactic longitude 270° along with two other already known clusters in the same area. Even though there is some suggestion of this branching off feature from the radio studies, this is perhaps its first indication from the optical observations.

\*\*\*\*\*

## CHAPTER 1

### INTRODUCTION

Besides galaxies, the smaller stellar aggregates are generally divided into three categories: globular clusters, open clusters and stellar associations.

Globular clusters are very compact objects containing hundreds of thousands of stars and belong to an older category called Population II. Open clusters contain a few tens to a few hundred stars and are relatively loosely packed. The term 'stellar association' was introduced by Ambartsumian (1949) to designate loose groups of stars, either of the massive O-B types or of the very young T Tauri stars. They are more loosely packed than the open clusters and are dynamically unstable.

All the stellar aggregates are usually designated according to their number listing in various catalogues. A few of the common ones are given below:

- M : Messier Catalogue (Watson, 1949)
- NGC : New General Catalogue of Nebulae and Clusters (Dreyer, 1888)
- IC : Index Catalogue (Dreyer, 1895, 1908)
- Tr : Trumpler Catalogue (Trumpler, 1922)
- Me1 : Melotte Catalogue (Melotte, 1915)
- OC1/GC1: Catalogue of Star clusters and Associations (Alter et al., 1970).

The last one is a modern card catalogue with an extensive bibliography and contains 1039 open clusters, 11 stellar

groups, 70 O-associations, 125 globular clusters and 28 extragalactic objects.

Recently, the International Astronomical Union introduced a more general numbering system for clusters according to their right ascension and declination. For example, Praesepe cluster is designated as C0837+201, which indicates that it is a cluster situated at a right ascension of  $08^{\text{h}} 37^{\text{m}}$  and a declination of  $+20^{\circ}.1$ .

Out of the three stellar groups mentioned above, it is well known that open clusters are vital for determining galactic structure, for checking theories of stellar evolution and for calibrating absolute luminosities. The more clusters investigated, the better these factors become known. With this in view, a photometric programme to study the open clusters, not investigated so far, has been taken up here. The card catalogue compiled by Alter et al. (1970) has been found to be the best one for picking out such clusters. The role of young open clusters as the spiral arm tracers of our Galaxy has been chosen as the main aim of this work.

### 1.1. Open Clusters

The stars in any given open cluster are localized in space and probably were formed out of the same interstellar material. These stars are assumed to have a nearly identical chemical composition and a common evolutionary history. As the stars evolve, their positions in the Hertzsprung-Russell (HR) diagram keep changing and the appearance of the cluster

HR-diagram at any epoch contains important clues concerning the evolution of the member stars.

The main sequence (MS) in the HR-diagram represents stars of homogenous chemical composition. Hydrogen in the core of these stars is being converted into helium by thermonuclear reactions. When about 10% of hydrogen in the core is exhausted, a star evolves off the MS, rapidly to start with, and finally reaches the region of red giants. Since the total nuclear fuel available is proportional to the mass  $M$  of the star, and the rate at which the fuel is consumed is proportional to the star's luminosity  $L$ , the evolution times are expected to scale roughly as  $M/L$ . Thus, stars with large masses and correspondingly larger luminosities, like O type stars, would leave the main sequence sooner than, say, the M dwarfs, which have small masses and smaller luminosities. Hence, in practice the age of the cluster can be judged by the spectral type of the hottest star still left on the main sequence. These considerations lead to the conclusion that clusters with O and early B stars are rather young ( $\lesssim 10^7$  years) and may be expected to be found physically near the places of their origin, which are generally in the region of spiral arms. This is due to the fact that the random velocities in the galaxy tend to smear out these clusters over the plane within about  $10^8$  years (Schmidt-Kaler, 1965).

Further, the stars within a cluster are all at nearly the same distance from us. Hence, the differences in their apparent magnitudes ( $m_v$ ) are essentially equal to the differences in their

absolute magnitudes ( $M_V$ ). Thus, if the absolute magnitudes of some stars in the cluster are known independently, then the  $M_V$  of the rest of the stars can be determined; from this in turn, a more reliable distance modulus for the cluster as a whole can be established.

## 1.2. Classification of Open Clusters

A proper classification of an open cluster should describe its intrinsic conditions, like its dynamical and spectral properties, outlines, dimensions and star distributions. Various attempts have been made at classifying these clusters by Shapley (1930), Trumpler (1930), Collinder (1931), Alter (1942), Markarian (1950) and others. Out of all these classifications, that by Trumpler (1930) has been most widely used. His classification was based on two different characteristics of the clusters: the physical appearances and the spectra of the member stars.

### 1.2.1. According to appearance

Since the dimensions of a cluster are governed by its gravitational potential and are related to its constitution, a classification on the basis of appearance has significance. Trumpler (1930) used Roman numerals I to IV to indicate decreasing central concentration for the cluster as given below:

- I. Detached clusters with strong central concentration.
- II. Detached clusters with little central concentration.
- III. Detached clusters with no noticeable concentration, in which the stars are more or less thinly, but nearly uniformly scattered.



IV. Clusters not well detached but passing gradually into the environs, appearing like a star field condensation.

Likewise, numerals 1 to 3 have been used for showing the increasing range between magnitudes of the member stars of the cluster according to the following scheme:

1. Most cluster stars are nearly of the same apparent brightness (e.g. NGC 7789).
2. Medium range exists in the brightness of the stars (e.g. NGC 2254).
3. Cluster is composed of bright and faint stars; generally a few very bright and some moderately bright stars stand out from a host of faint ones (e.g. Pleiades).

Lastly, letters are used to indicate the number of stars.

- p : Poor clusters with less than 50 stars.
- m : Moderately rich clusters with 50 to 100 stars.
- r : Rich clusters with more than 100 stars.

Thus, for example, the cluster Tr 1 has been classified as of type 1 3 p, which means that it is a detached cluster with strong central concentration. It is composed of bright and faint stars; it is a poor cluster with less than 50 stars.

#### 1.2.2. Based on HR-diagram

Another important classification of open clusters is the one which depends upon the spectra of the individual stars. Trumpler (1925, 1930) schematically classified the HR-diagrams of the clusters into types characterized by a combination of the numbers 1, 2, 3 and of the letters o, b, a, f. The numbers designate the relative proportion of late - type giants

as given below:

1. The giant branch is entirely missing and all cluster stars belong to the main branch from O to M.
2. A relatively small number of stars are in the giant branch.
3. The majority of the more luminous stars are yellow or red giants.

The letter following the number indicates the spectral class of the earliest stars on the MS: o, b, a, f stand for O, B, A, F stars respectively. Thus, for 1, only 'o' and 'b' are possible, occasionally extending to 'a'. For 2 and 3 only 'a' and later are expected.

This classification scheme was later slightly modified (Trumpler & Weaver, 1953) through the inclusion of an additional number indicating the spectral subtype of the earliest main sequence star. For instance, type 1 - b3 would indicate a cluster with no red giant stars and having main sequence stars of spectral type B3 and later.

### **1.3. Young Open clusters as Spiral Arm Tracers**

It was Baade & Mayall (1951), who for the first time found that the spiral arms in the Andromeda galaxy, M 31, were most clearly traced by the emission nebulae and by the young OB stars. Clusters and associations of these young stars were specially helpful in outlining the spiral structure. Soon after this, Morgan, Sharpless & Osterbrock (1952) examined the distribution of OB associations and their nebulosities

in our Galaxy by obtaining their distances. The following three parallel sections of spiral arms were clearly delineated in this work.

1. The Orion arm: it is the arm in which the Sun is located.
2. The Perseus arm: it is a portion of an outer arm and is about 2500 parsecs away from the Orion arm.
3. The Sagittarius arm: it is a portion of an inner arm and is at a distance of about 1500 to 2000 parsecs from the Orion arm.

It is interesting to note at this juncture that the first comprehensive study of the open clusters and their distribution in space done much earlier by Trumpler (1930) shows the Perseus arm and also gives an indication of the Sagittarius and Carina features. However, he had not segregated the young clusters from his sample and thus was not able to definitively establish the spiral features of our Galaxy.

Fig.1.1 shows the Morgan - Sharpless - Osterbrock diagram updated by Schmidt - Kaler in 1965. This diagram shows the positions of the clusters and associations with O to B2 stars and of the associated emission nebulae in the galactic plane. The above mentioned three sections of the spiral arms found here are shown rather neatly as:

- the Perseus arm ( $80^\circ < \text{gal. long.} < 180^\circ$ )
- the Orion - Cygnus arm ( $60^\circ < \text{gal. long.} < 210^\circ$ ) and
- the Sagittarius - Carina arm ( $285^\circ < \text{gal. long.} < 45^\circ$ ).

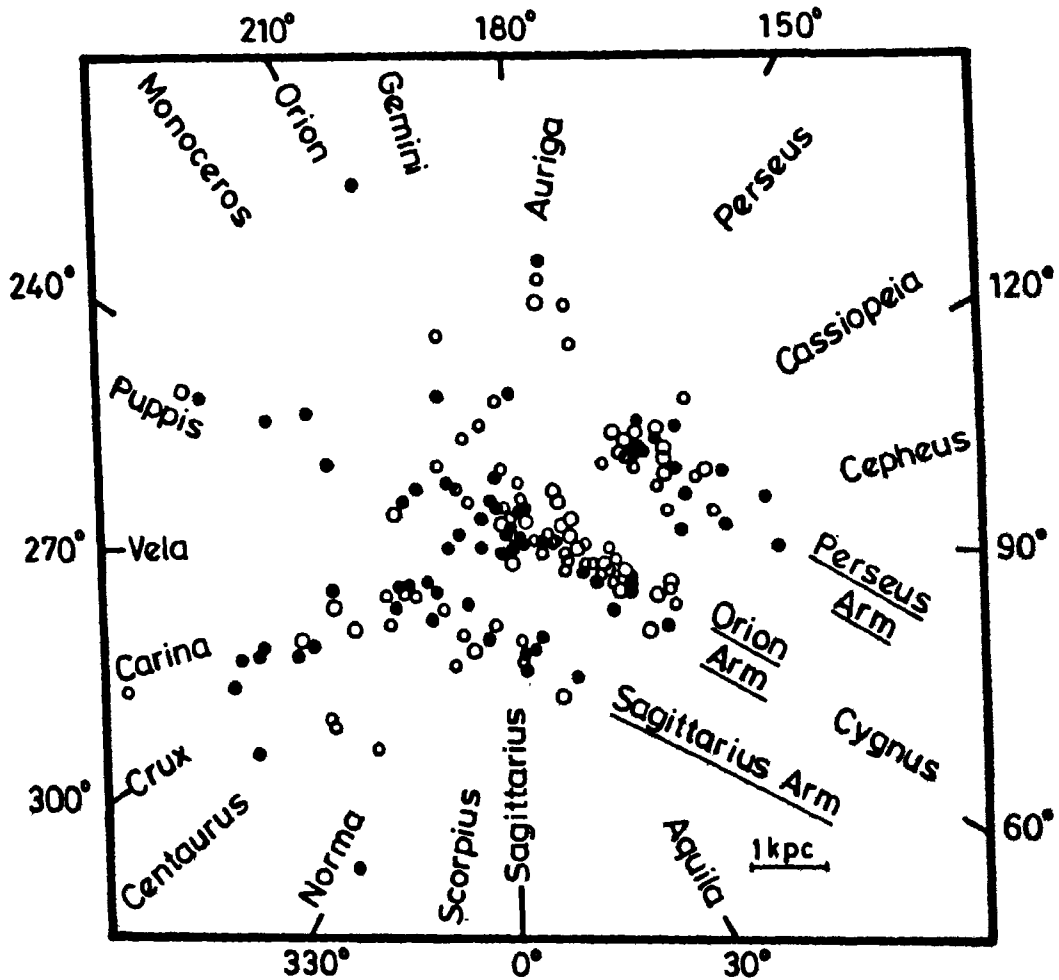


**Fig. 1.1.** Optical spiral structure of the Galaxy. The Sun is at the centre of the diagram. The galactic centre is in the direction toward 0° gal. longitude at a distance of 10 kpc from the Sun. The principal observed sections of the Sagittarius, Orion and Perseus arms are shown. The directions from the Sun towards some of the key constellations along the band of the Milky Way are marked along the periphery of the diagram. (Morgan-Osterbrock-Sharp less diagram updated by Schmidt - Kaler in 1965).

On the basis of this diagram, Becker could assert that the pitch angle of the three spiral arms averages close to  $25^\circ$  (cf. Bok, 1971). It is now obvious that since the locations of the young open clusters are not much different from the places of their origin, a knowledge of their distances and directions may be expected to trace the star forming regions, which are generally the spiral features. And Becker (1963) showed that the young open clusters with stars of spectral type B2 or earlier are good spiral tracers.

These optical observations are superimposed on the radio map of the Galaxy (cf. Bok, 1971) and it is quite clear from this composite picture (cf. Fig.1.2), that the radio structures of our Galaxy show very good agreement with those found optically, albeit in a limited region. One can also find many spurs and bifurcations originating from the major spiral features, like for example, the Vela connecting arm. Several external spiral galaxies also show such 'extra' features.

Further, there are some indications of two inner features known as the Norma - Scutum arm and the Norma Internal arm. And recently, a possible outermost portion of the Galaxy has been indicated by a few young open clusters along with some HII regions (Jackson, FitzFerald & Moffat, 1979) as shown in Fig.1.3. This lies beyond the Perseus arm in the anticentre direction and is named as the Outer Perseus arm. Thus, the young open clusters have been vitally responsible for the present day knowledge of the structure of our Galaxy.

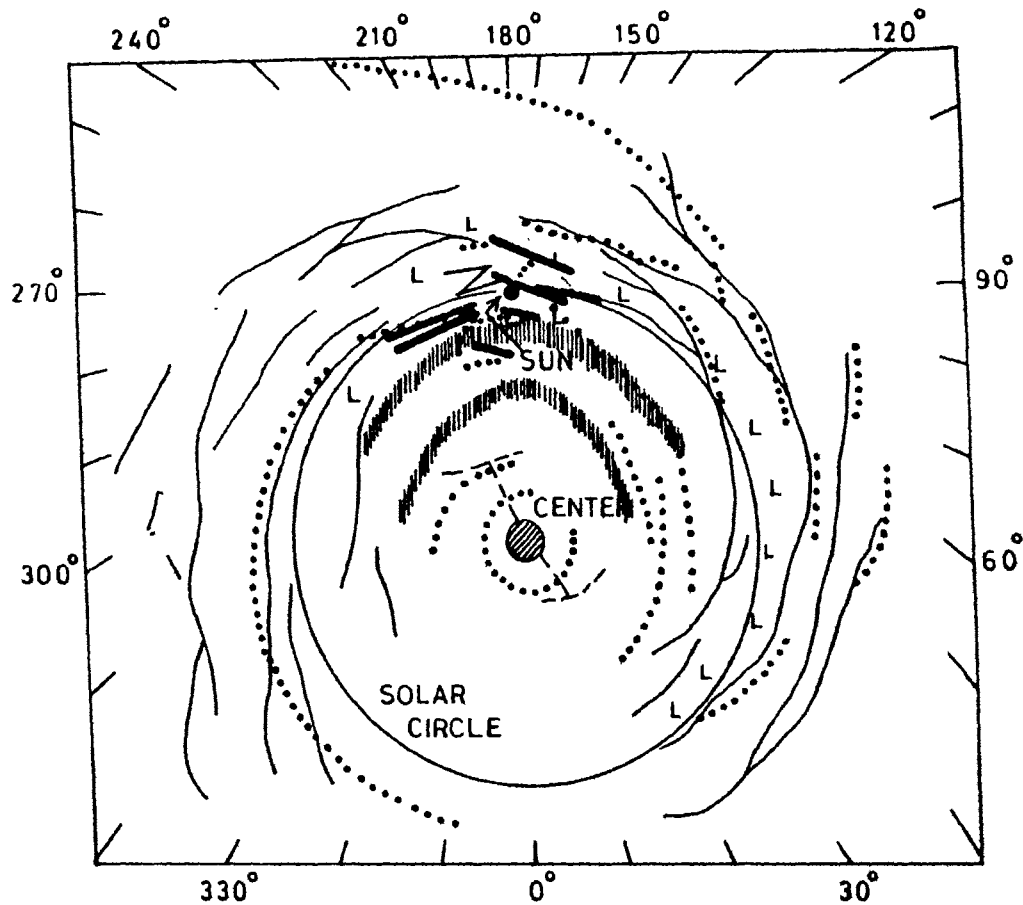


**Fig. 1.2** Superimposed maps of the neutral hydrogen distribution in the Galaxy as interpreted by Kerr (1969) and by Weaver (1970). These are shown respectively, by thin lines and dotted lines. The hatched areas indicate where the location is uncertain. The points marked 'L' denote regions deficient in neutral hydrogen. The optical features are shown by thick lines. The radius of the solar circle is 10 kpc. Galactic longitude is shown around the edge of the map.

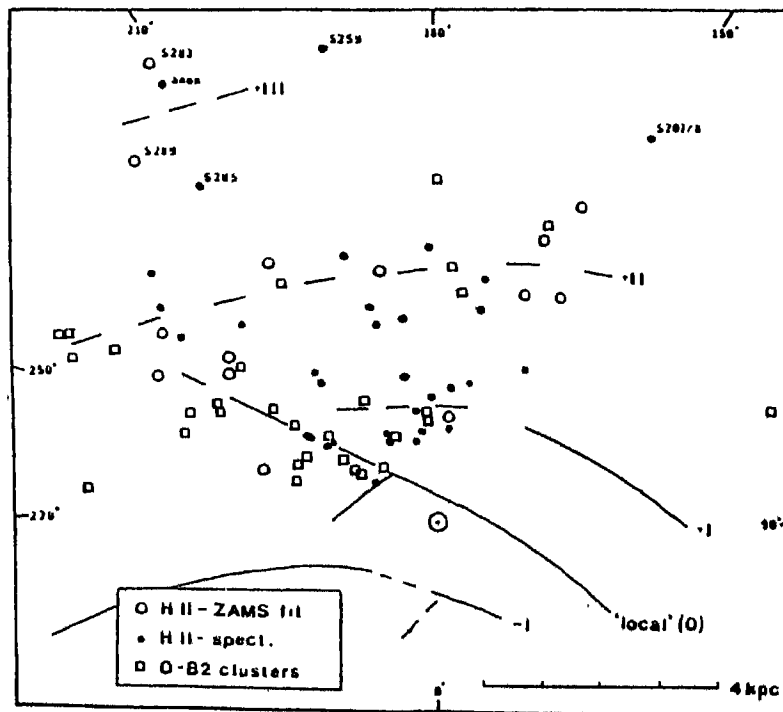


Fig. 1.3. Positions of H II regions and O-B2 clusters plotted on the galactic plane in the longitude range  $150^\circ$  to  $260^\circ$ . Well determined spiral features are shown as solid lines while tentative features are shown as dashed lines (Diagram taken from Jackson, FitzGerald & Moffat, 1979).

#### 1.4. Plan of the Thesis

In the light of the above discussions, the present study of faint young open clusters, which was originally suggested by Late Prof. M.K.V.Bappu was undertaken with two major aims. The first was to obtain the luminosities of stars contained in the very distant hitherto not well-studied clusters. If these clusters were found young enough, then they could as well be used as spiral arm tracers. This led to the second aim of substantiating the existing optical picture of the spiral structure of our Galaxy. In this regard, since there was enough scope for this study in the anticentre direction with a possibility of reaching much greater distances, the galactic longitude region between  $160^\circ$  and  $280^\circ$  was chosen. Thus, the most complicated effects of the interstellar extinction, which exist towards the galactic centre direction, were avoided. The optical observational techniques of spectral type-luminosity classification and the broad band UBV photometry have been selected for carrying out this investigation.

This thesis is comprised of six chapters including this first chapter which is an introductory one. In this chapter, a brief description of the terminology relevant to the topic of star clusters is given along with a brief account of the present state of knowledge concerning the star clusters.

The second chapter deals with the selection of young clusters and their provisional membership. A new technique of combining the spectral types of individual stars obtained



from the modified objective-grating spectroscopy and the V magnitudes estimated from the image diameters on the sky survey charts has been used for this purpose.

The instrumentation and the procedures used for observations and their reduction are described in the third chapter. Methods for the determination of the cluster parameters such as membership, reddening, distance and age are also mentioned.

In chapter four, the observations and results of UBV photometry of the star clusters OC1 427, 493, 501, 506, 556, 585, 674, 692, 694, 715, 762 and 798 have been discussed. Various parameters of these clusters have been determined from the above mentioned observations.

These cluster parameters are discussed in the fifth chapter in connection with their non-coeval nature, the presence of non-uniform reddening and their relationship to the structure of the Galaxy. The location of some of these young clusters in the anticentre direction of the Galaxy strongly supports the existence of an outer spiral feature at distances of about 4 to 5 kpc. A feature, which is branching off from the local arm and extending towards the Carina arm is indicated for the first time through optical observations.

Finally, the sixth chapter summarises the work done in this study. A few suggestions for the future programmes are also included.

\*\*\*\*\*

## CHAPTER 2\*

### SELECTION OF YOUNG CLUSTERS AND THEIR PROVISIONAL MEMBERSHIP

There are about 400 open clusters in the galactic longitude region of  $160^\circ$  to  $280^\circ$  according to the catalogue by Alter *et al.*, (1970). Out of them a total of 72 clusters have no information whatsoever regarding their magnitudes or their earliest spectral types. 92 clusters are listed as having stars of magnitude 12 or fainter with no information on spectral types. 24 others are given as having the earliest spectral type of B3 or earlier, with nothing known about the magnitudes. All these 188 clusters were then carefully examined on the corresponding sky survey charts, where a total of 104 appeared to be likely physical groupings. These are listed in Table 2.1. In order to find out the most probable spiral arm tracers from among these physical groupings, which may later on be subjected to a more detailed photometric work, the following technique has been chosen. This technique involves the construction of crude HR-diagrams, for which the spectral types obtained from the modified objective grating spectroscopy and the visual magnitudes determined from the image diameters of stars on the sky survey charts were used. These diagrams have been used for estimating the provisional membership of stars in the clusters as well as

The results included in this chapter have partly been published, *vide*: G.S.D.Babu, 1983, "Membership of stars in faint galactic open clusters", *J. Astrophys. Astr.* **4**, 235.

**Table 2.1** The coordinates and the Trumpler classification of the not-well-studied clusters, which appeared to be likely physical groupings on the sky survey charts in the galactic longitude region of 160° to 280°. The earliest spectral types and the brightest magnitudes in these clusters are also given wherever available. (Source: Alter et al., 1970).

| Sl. No. | OC1 | IAU No.   | l      | b      | Earliest sp. type | Brightest mag. | Trumpler class |
|---------|-----|-----------|--------|--------|-------------------|----------------|----------------|
| (1)     | (2) | (3)       | (4)    | (5)    | (6)               | (7)            | (8)            |
| * 1     | 406 | C0431+451 | 158.60 | -1.58  | B3                |                | III 1m         |
| 2       | 414 | C0458+443 | 162.33 | 1.61   |                   | 15.0           | II 2p          |
| * 3     | 426 | C0424+308 | 168.29 | -12.30 |                   |                | IV 2p          |
| * 4     | 427 | C0516+394 | 168.30 | 1.32   |                   |                | II 2r          |
| * 5     | 435 | C0511+326 | 173.17 | - 3.48 |                   |                | III 2p         |
| 6       | 443 | C0454+287 | 174.09 | - 8.85 |                   |                | III 2m         |
| * 7     | 453 | C0501+237 | 179.15 | -10.52 |                   |                | IV 1p          |
| 8       | 461 | C0445+131 | 185.79 | -19.81 |                   |                | IV 2p          |
| * 9     | 478 | C0630+205 | 192.61 | 5.44   |                   | 15.0           | II 2p          |
| 10      | 483 | C0524+070 | 196.58 | -15.10 |                   |                | IV 2p          |
| * 11    | 487 | C0600+104 | 198.06 | - 5.81 |                   | 15.0           | II 3r          |
| * 12    | 489 | C0545+073 | 198.98 | -10.40 |                   |                | III 2p         |
| * 13    | 490 | C0555+078 | 199.80 | - 8.05 |                   | 15.0           | III 3p         |
| * 14    | 492 | C0635+109 | 201.78 | 2.13   |                   | 14.0           | II 2p          |
| * 15    | 493 | C0610+070 | 202.31 | - 5.26 |                   |                | II 2p          |
| * 16    | 501 | C0627+068 | 204.37 | - 1.69 |                   | 12.5           | III 2p         |
| * 17    | 506 | C0628+059 | 205.37 | - 1.76 | B0                |                | IV 3p          |
| * 18    | 512 | C0628+049 | 206.19 | - 2.28 |                   |                | II 3p          |
| * 19    | 519 | C0619+023 | 207.42 | - 5.52 |                   |                | IV 2p          |
| 20      | 526 | C0700+064 | 208.55 | 5.52   |                   |                | II 2p          |
| 21      | 531 | C0635+012 | 210.38 | - 2.36 |                   |                | I 2p           |
| 22      | 533 | C0641+016 | 210.68 | - 0.88 |                   |                | III 1p         |
| * 23    | 534 | C0655+032 | 210.80 | 2.89   |                   | 15.0           | II 1p          |

---

| 1    | 2   | 3         | 4      | 5      | 6 | 7    | 8      |
|------|-----|-----------|--------|--------|---|------|--------|
| 24   | 535 | C0643+018 | 210.80 | 0.30   |   |      | III 2p |
| * 25 | 544 | C0628-041 | 214.35 | - 6.51 |   |      | III 1p |
| 26   | 551 | C0717-010 | 217.23 | 5.95   |   | 15.0 | II 2p  |
| 27   | 552 | C0719-008 | 217.29 | 6.31   |   |      | III 2p |
| 28   | 555 | C0719-032 | 219.36 | 5.17   |   | 13.0 | I 1p   |
| * 29 | 556 | C0701-060 | 219.83 | 0.02   |   | 14.0 | II 2p  |
| 30   | 566 | C0704-107 | 224.35 | - 1.45 |   |      | III 2p |
| 31   | 569 | C0653-132 | 225.30 | - 5.02 |   |      | III 2p |
| 32   | 570 | C0655-131 | 225.43 | - 4.62 |   | 14.0 | III 2m |
| 33   | 573 | C0659-135 | 226.20 | - 3.92 |   | 12.0 | IV 2p  |
| * 34 | 581 | C0736-105 | 227.85 | 5.38   |   |      | II 1p  |
| * 35 | 585 | C0721-131 | 228.43 | 1.04   |   |      | II 3p  |
| 36   | 588 | C0727-138 | 229.67 | 1.85   |   |      | II 3p  |
| 37   | 600 | C0722-169 | 231.78 | - 0.62 |   | 14.0 | I 2p   |
| 38   | 603 | C0658-204 | 232.22 | - 7.32 |   | 14.0 | III 2m |
| 39   | 605 | C0701-207 | 232.90 | - 6.84 |   | 16.0 | I 3m   |
| * 40 | 615 | C0747-171 | 234.96 | 4.53   |   | 14.0 | III 2p |
| * 41 | 620 | C0738-189 | 235.48 | 1.78   |   |      | II 1p  |
| 42   | 628 | C0743-202 | 237.20 | 2.15   |   | 12.0 | III 2p |
| * 43 | 630 | C0758-189 | 237.85 | 5.82   |   |      | II 1p  |
| 44   | 632 | C0728-232 | 238.01 | - 2.43 |   | 13.0 | III 2p |
| 45   | 636 | C0746-211 | 238.34 | 2.32   |   | 12.0 | III 2p |
| 46   | 645 | C0750-223 | 239.71 | 2.37   |   | 14.0 | III 2p |
| * 47 | 654 | C0735-264 | 241.65 | - 2.58 |   | 12.0 | II 2m  |
| 48   | 656 | C0746-257 | 242.28 | - 0.07 |   | 14.0 | III 1p |
| * 49 | 661 | C0721-294 | 242.68 | - 6.79 |   | 14.0 | II 3m  |
| 50   | 662 | C0750-261 | 243.04 | 0.52   |   | 14.0 | I 3p   |

---

---

| 1    | 2   | 3         | 4         | 5      | 6      | 7    | 8      |
|------|-----|-----------|-----------|--------|--------|------|--------|
| * 51 | 669 | C0755-257 | 243.30    | 1.65   |        | 14.0 | II 2p  |
| * 52 | 670 | C0745-271 | 243.33    | - 0.93 | OB     |      | I 2p   |
|      | 53  | 672       | C0713-312 | 243.58 | - 9.17 | 13.0 | III 2p |
|      | 54  | 673       | C0751-268 | 243.80 | 0.37   | 14.0 | III 2p |
|      | 55  | 674       | C0742-282 | 243.99 | - 2.06 | 14.0 | III 2m |
|      | 56  | 677       | C0759-270 | 244.81 | 1.66   | 15.0 | II 1p  |
| * 57 | 681 | C0757-284 | 245.77    | 0.52   |        | 12.0 | III 1p |
|      | 58  | 683       | C0748-297 | 245.86 | - 1.74 |      | II 3p  |
| * 59 | 684 | C0756-287 | 246.02    | 0.28   |        | 12.0 | III 2p |
|      | 60  | 686       | C0812-268 | 246.30 | 4.31   | 12.0 | III 2p |
|      | 61  | 691       | C0810-277 | 246.78 | 3.41   | 15.0 | III 2m |
|      | 62  | 692       | C0754-302 | 247.01 | - 0.94 | 14.0 | II 3p  |
|      | 63  | 693       | C0758-301 | 247.32 | - 0.15 | 14.0 | IV 2p  |
|      | 64  | 694       | C0750-317 | 247.72 | - 2.53 | 15.0 | III 3p |
| * 65 | 704 | C0822-289 | 249.24    | 4.82   |        |      | III 1p |
|      | 66  | 705       | C0803-318 | 249.32 | - 0.17 | 13.0 | III 2p |
|      | 67  | 706       | C0821-293 | 249.45 | 4.49   |      | II 1p  |
|      | 68  | 707       | C0813-306 | 249.58 | 2.29   | 14.0 | IV 2p  |
|      | 69  | 709       | C0819-301 | 249.90 | 3.70   |      | II 2m  |
| * 70 | 710 | C0809-318 | 250.03    | 0.95   |        | 15.0 | III 2p |

---

| 1  | 2   | 3         | 4      | 5     | 6  | 7    | 8      |
|----|-----|-----------|--------|-------|----|------|--------|
| 71 | 712 | C0812-318 | 250.43 | 1.55  |    | 12.0 | I 2p   |
| 72 | 715 | C0821-328 | 252.28 | 2.45  |    |      | II 1p  |
| 73 | 717 | C0817-343 | 253.02 | 0.92  |    | 12.0 | III 1p |
| 74 | 718 | C0823-340 | 253.47 | 2.07  |    | 14.0 | IV 2p  |
| 75 | 724 | C0819-360 | 254.67 | 0.27  | B5 |      | IV 1p  |
| 76 | 725 | C0820-360 | 254.82 | 0.52  |    |      | III 2p |
| 77 | 728 | C0836-345 | 255.60 | 3.97  |    | 13.0 | I 3p   |
| 78 | 729 | C0842-357 | 257.27 | 4.22  |    | 14.0 | III 1p |
| 79 | 731 | C0829-385 | 257.83 | 0.43  |    | 13.0 | III 3m |
| 80 | 732 | C0838-378 | 258.47 | 2.29  |    | 15.0 | III 2p |
| 81 | 738 | C0800-442 | 259.57 | -7.30 |    | 13.0 | I 3p   |
| 82 | 741 | C0802-461 | 261.35 | -8.00 |    |      | IV 2p  |
| 83 | 744 | C0817-452 | 262.12 | -5.20 |    | 15.0 | I 1p   |
| 84 | 749 | C0919-368 | 263.00 | 9.00  |    | 13.0 | II 1p  |
| 85 | 756 | C0917-403 | 265.29 | 6.34  |    |      | II 2m  |
| 86 | 758 | C0831-481 | 265.80 | -5.01 |    | 13.0 | II 3p  |
| 87 | 759 | C0840-469 | 265.85 | -3.03 |    | 13.0 | I 3m   |
| 88 | 762 | C0843-474 | 266.45 | -2.99 |    | 14.0 | III 2p |
| 89 | 765 | C0918-449 | 268.64 | 3.20  |    | 12.0 | III 2p |
| 90 | 769 | C0859-507 | 270.76 | -3.03 |    | 14.0 | III 2p |

| 1   | 2   | 3         | 4      | 5     | 6  | 7    | 8      |
|-----|-----|-----------|--------|-------|----|------|--------|
| 91  | 770 | C0940-438 | 270.80 | 6.73  |    | 13.0 | III 1p |
| 92  | 774 | C0920-509 | 273.16 | -0.77 |    | 12.0 | II 2p  |
| 93  | 777 | C0953-467 | 274.53 | 5.92  |    | 14.0 | I 3p   |
| 94  | 780 | C0927-525 | 275.03 | -1.17 |    | 14.0 | IV 2p  |
| 95  | 782 | C0927-534 | 275.69 | -1.85 |    | 15.0 | I 2p   |
| 96  | 784 | C0925-549 | 276.47 | -3.12 |    | 14.0 | II 3p  |
| 97  | 786 | C0920-560 | 276.79 | -4.43 |    | 12.0 | II 3p  |
| 98  | 788 | C0943-537 | 277.70 | -0.47 |    | 12.0 | II 3p  |
| 99  | 790 | C0949-529 | 277.79 | 0.64  | B1 |      | I 3p   |
| 100 | 791 | C0947-543 | 278.48 | -0.59 |    | 12.0 | I 3p   |
| 101 | 794 | C0956-544 | 279.51 | 0.12  |    |      |        |
| 102 | 795 | C0919-601 | 279.55 | -7.50 |    | 15.0 | II 3p  |
| 103 | 798 | C0959-545 | 279.92 | 0.29  |    |      | I 3p   |
| 104 | 799 | C0959-548 | 280.18 | 0.15  |    | 15.0 | I 3p   |

Note: The clusters, which were observed with the modified objective grating camera are shown with an asterisk (\*).

the cluster reality to the first approximation. An attempt has then been made to pick out the young clusters containing stars of spectral type B5 or earlier. However, due to some unavoidable circumstances, the modified objective grating spectroscopy could not be done for several of the above mentioned clusters, for which only visual estimates were made.

### 2.1. Modified Objective - Grating Camera

Objective prism surveys (e.g. Stephenson & Sanduleak, 1971) have generally been effective in the identification of OB stars brighter than  $\sim 12$  mag. The limitation is partly due to the telescope aperture sizes and partly due to the conventional techniques used for spectral classification. However, one can now reach much fainter stars, up to  $\sim 15$  mag, with the help of a simple method introduced by Hoag & Schroeder (1970). In this method, a transmission grating is placed in the converging light beam of a telescope immediately in front of the focal plane to obtain low dispersion spectra. From such spectra, one can, with relative ease, identify emission lines in objects such as Wolf-Rayet stars and can separate the early type stars with prominent UV continua from stars of later spectral type.

Although the transmission grating photographs do not cover as extensive an area of the sky as covered by Schmidt objective prism plates, they have the advantage of a larger light collecting power and larger plate scale of the moderate telescope. McCarthy & Miller (1973), Miller & Graham (1974) and Muzzio & McCarthy (1973) had employed this modified objective



grating technique in the searches for faint OB stars in various sections of the Milky Way. Bok (1980) also recommended this Hoag-Schroeder technique for application to the faint open clusters so as to press these searches to even larger distances to aid the study of the structure of our Galaxy.

In the present study, a transmission grating with 300 lines  $\text{mm}^{-1}$ , blazed at  $6200\text{\AA}$  in the first order was used. The grating was placed at a distance of 25 mm in front of the photographic plate. Both the plate holder and the grating were fixed in a wooden box of 17cm x 17cm x 15cm size, which was mounted at the Cassegrain focus of the Kavalur 102-cm telescope. The details of the instrument are shown in Fig.2.1. In order to save the already faint starlight from further absorption, no extra optical elements like the field corrector for example, were introduced in the path of the light. The exposed area was 16 arcmin x 16 arcmin. This, being centrally situated in the available 40 arcmin diameter field, was expected to have negligible image distortions. This arrangement gave a dispersion of  $970\text{\AA} \text{mm}^{-1}$  in the first order.

Kodak 103a-0 emulsion plates were used along with this set up because of their sensitivity in the blue-violet region. Further, being a coarse grain emulsion, it is much faster than many others.

## **2.2. Spectral Types from the Modified Objective-Grating Spectroscopy**

One advantage of using a grating with smaller number of grooves is that the zero order images seen in the same plate,

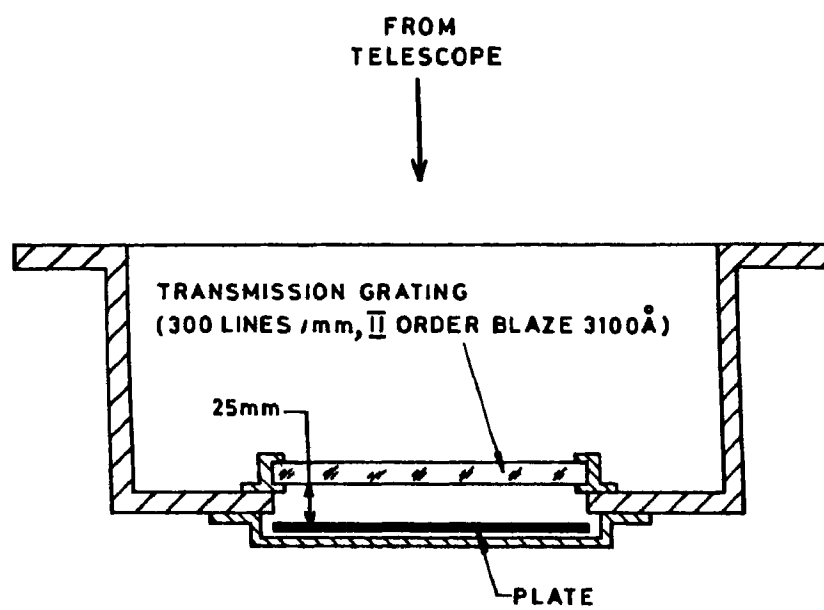


Fig. 2.1. Schematic diagram of the instrument used for obtaining the objective grating spectra with a dispersion of  $970 \text{ \AA mm}^{-1}$  in the first order.

provide an excellent means of identifying the stars. They are especially useful in the relatively crowded fields of clusters. Once the stars are identified, the images of their other two orders may be utilized for determining the individual spectral types.

Fig.2.2 shows a selection of MK standard stars ranging in spectral type from O to M, which have been photographed with the above instrument. The widening of the images was avoided and the telescope was guided during the exposure in order to further save the light of the faint stars. The final picture on the plate shows three images corresponding to each star. They are:

- i) the zero-order images, which appear as small dots, being essentially the undispersed stellar images;
- ii) the first-order images, which show a dispersion of  $970\text{\AA mm}^{-1}$ .
- iii) the second-order images, where the dispersion is  $485\text{\AA mm}^{-1}$ .

While these low dispersions, the 103a-0 emulsion and the unwidened images, combine to make the photography faster, they limit the appearances of the images to only some gross features. Such features include the strong UV continuum in O and early B type stars, the Balmer jump in A stars, the G band in the G stars, the H and K lines of Ca II in the late G and K type stars and a few molecular bands, such as TiO bands in the M stars. However, the shape of the intensity distribution in the first and the second-order images is a good indicator for estimating the approximate spectral types of the individual stars. Especially, the second-order images, owing to the  $3100\text{\AA}$

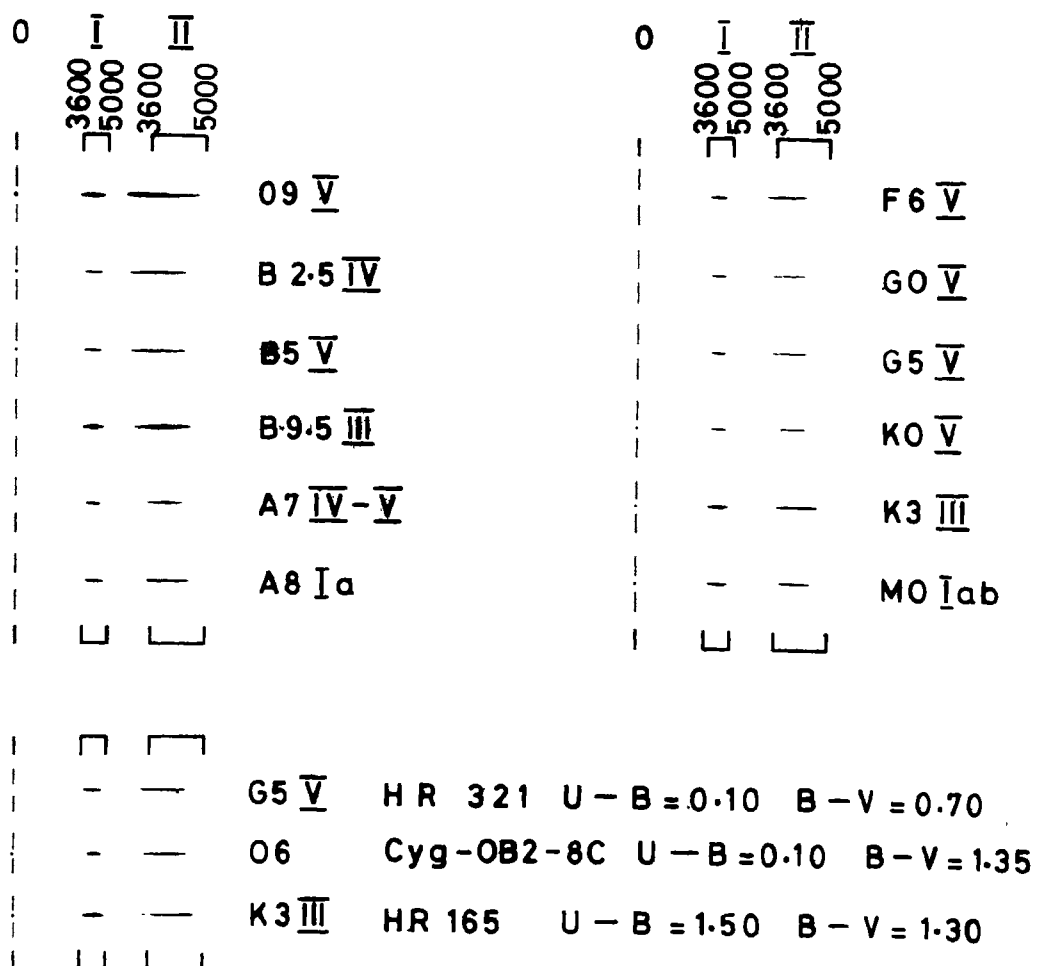


Fig. 2.2. A sample of MK standards used for calibrating the objective-grating spectra based mainly on the shape of the energy distribution in the first and second orders. The three spectra at the bottom are shown as an example of the effects of interstellar extinction on an early-type star compared with the unreddened late-type stars.

blaze in this order, are more suited for picking out the OB stars which possess strong UV and blue continuum.

The images of any star are visually compared with those of the standard stars in Fig.2.2 and the spectral type that matches best, is attributed to the programme star. In some cases, interpolation between the spectral types of the standard stars is also done. In order to estimate the errors, the images of a few stars with known spectral types have been selected. They have been compared with those in Fig.2.2 to get the unbiased estimates of the respective spectral types. This shows a maximum uncertainty of about four spectral subclasses.

Even though this technique is based on the intensity distribution in the continuum, the effect of interstellar extinction has not proved a limitation. In order to show this, Hoag & Schroeder (1970) and Miller & Graham (1974) observed some early type stars with large extinctions along with some unreddened late type stars. They pointed out that even though a greater fraction of the light is concentrated at red wavelengths in these low dispersion images, the early-type stars showed long and faded out UV trail with no obvious breaks, which was not so in the case of the late-type stars. This is illustrated in Fig.2.2, where a heavily obscured early-type star of the Cyg-OB2 association is included. Its apparent (U-B) colour matches with that of a G5 V star and the apparent (B-V) colour matches with that of a K3 III star. Thus, there is a likelihood of misclassifying this star in the absence of any other informa-

tion. But, the smooth second-order image of the Cyg star clearly indicates that the blue region is affected by interstellar extinction and what one sees is only the less affected red region. Therefore, the conclusion was that it must be an early type star, though it was not possible to fix the actual spectral type within the normal limits of accuracy.

This technique was tried on twentyeight well-studied open clusters, randomly selected from the literature. Ten of them, taken from the works of Hoag et al. (1961), Becker (1963), Vogt & Moffat (1972, 1973) and Moffat & vogt (1975) are presented here. Some basic data on these clusters are given in Table 2.2.

The spectral type estimates of the stars in these clusters are plotted against the corresponding V mag given by the earlier authors, in Fig. 2.3. Each diagram in this figure is thus an HR-diagram of the given cluster. It may be noticed here that the member stars, denoted by filled circles, clearly form the main-sequence and the non-members, denoted by crosses, are generally away from the main sequence. These diagrams agree well with the corresponding colour-magnitude diagrams given by the authors mentioned, demonstrating the feasibility of obtaining the spectral types from the modified objective-grating spectra and the soundness of the technique. Thus assured, this technique has been applied to the programme clusters, in order to pick out those which contain stars of spectral type B5 or earlier.

Table 2.2. Some basic data on ten well-established clusters which are included in the present work.

| OC1 | Cluster Name | IAU number | l deg | b deg | Trumpler type | No. of members | Distance kpc | Earliest spectral type |               | Magnitude range |
|-----|--------------|------------|-------|-------|---------------|----------------|--------------|------------------------|---------------|-----------------|
|     |              |            |       |       |               |                |              | Litt.(ref)             | Present study |                 |
| 148 | NGC 6871     | C2004+356  | 72.6  | +2.1  | IV3p          | 22             | 1.6          | O9(1)                  | B0            | 6.8-11.9        |
| 411 | NGC 1664     | C0447+436  | 161.7 | -0.4  | III1p         | 8              | 1.3          | A0(1)                  | B8            | 7.5-12.5        |
| 537 | Dolidze 25   | C0542+003  | 211.9 | -1.3  | IV2p          | 10             | 5.3          | O (2)                  | B2            | 8.9-13.6        |
| 598 | NGC 2414     | C0731-153  | 231.4 | +2.0  | I3m           | 7              | 4.2          | BI(3)                  | B2            | 8.2-13.4        |
| 618 | NGC 2384     | C0722-209  | 235.4 | -2.4  | IV3p          | 9              | 3.3          | B0(3)                  | B3            | 9.1-13.3        |
| 621 | NGC 2367     | C0718-218  | 235.6 | -3.9  | IV3p          | 9              | 2.9          | B1(3)                  | B3            | 9.4-13.3        |
| 626 | NGC 2421     | C0734-205  | 236.2 | +0.1  | I2m           | 18             | 1.9          | B0.5(2)                | B2            | 10.5-13.8       |
| 635 | Trumpler 7   | C0725-239  | 238.3 | -3.4  | II3p          | 12             | 1.6          | B1(3)                  | B2            | 9.1-13.0        |
| 713 | Ruprecht 55  | C0810-324  | 250.7 | +0.8  | IV2p          | 8              | 4.4          | B2(2)                  | B2            | 8.5-12.7        |
| 754 | Pismis 6     | C0837-460  | 264.8 | -2.9  | II2p          | 8              | 1.7          | B2(4)                  | B1            | 8.9-13.2        |

References: 1. Becker (1963); 2. Moffat & Vogt (1975); 3. Vogt & Moffat (1972); 4. Vogt & Moffat (1973).

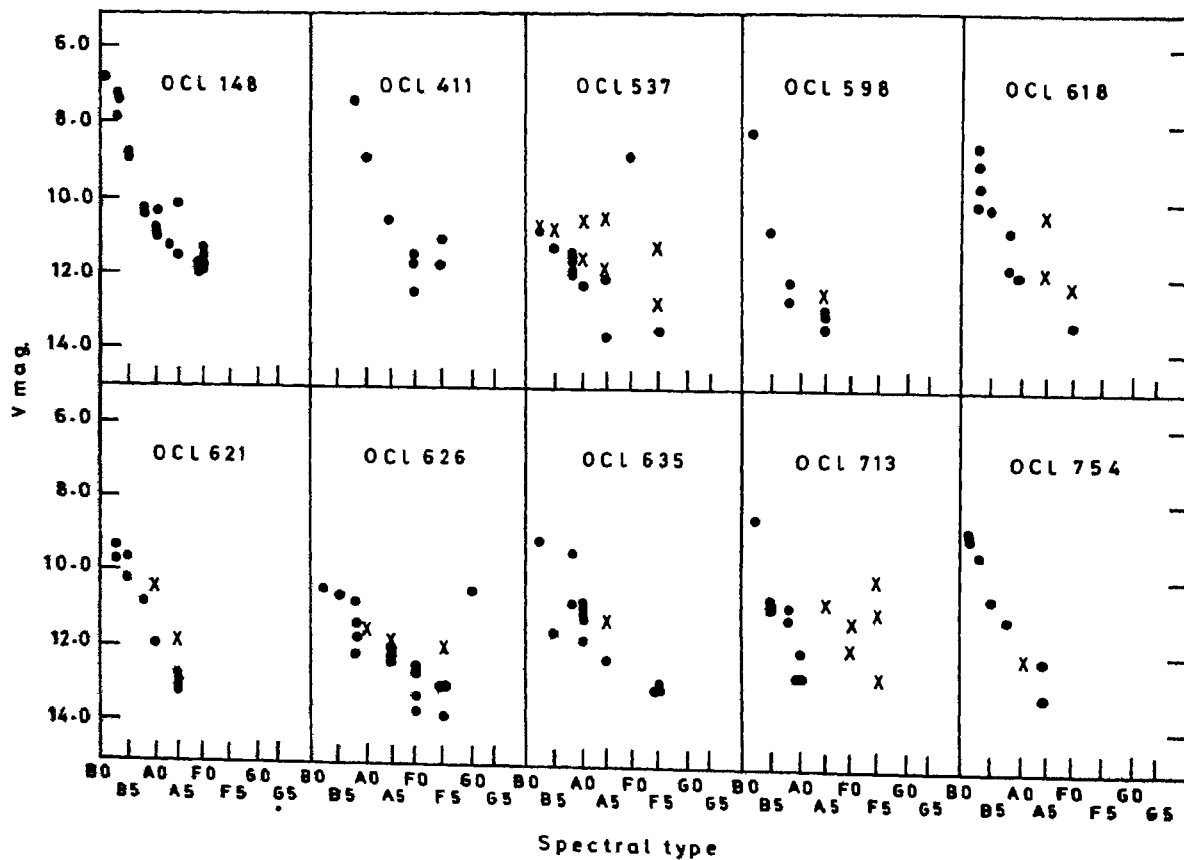


Fig. 2.3. Spectral types estimated on the basis of the objective-grating spectra for the individual stars of a few known clusters are plotted against their known V magnitudes. Crosses denote probable non-members based on previous work.



Out of the list of the 104 'unknown' clusters (cf. Table 2.1), mentioned earlier, 32 could actually be observed during the available observing time. 6 of them show stars of B5 or earlier, with two appearing to be slightly brighter than the other four clusters. Their brightness indicates the nearness of these clusters to the Sun as compared to the rest. Due to the time bound nature of the programme and due to the insufficient observing time, the remaining 72 clusters were visually inspected on the blue and red prints of the sky survey charts. The procedure here, was to look for stars which are brighter on the blue prints. This method, though crude, was found useful in the preliminary stages. Sky survey charts of Palomar Observatory, of UK-Schmidt Telescope and of European southern Observatory were used for this purpose, from which a further set of 6 open clusters were picked up.

Thus, a total of 12 open clusters were finally selected, all of which were considered to be belonging to the young category. Table 2.3 gives their available data as compiled in the catalogue by Alter et al. (1970). All these clusters are located in the galactic plane (b ranging from  $-3^\circ$  to  $+3^\circ$ ). This fact, further supports their young nature.

### **2.3. Magnitudes from the images of the sky survey charts**

Following the procedure given by Bappu (1978) the contact copies of both blue and red sky survey charts containing the field of each selected cluster were subjected to a photographic

Table 2.3. Compilation of the available data for the selected clusters

| Cluster<br>OCID Name             | 1              | 2                | 3              | 4                                | 5      | 6                    | 7              | 8                                     | 9       | 10   | 11     | 12  | 13  |
|----------------------------------|----------------|------------------|----------------|----------------------------------|--------|----------------------|----------------|---------------------------------------|---------|------|--------|---|---|
|                                  | AD<br>(Arcmin) | Dist<br>(Parsec) | LD<br>(Parsec) | No. Mag<br>of (bright-<br>stars) | E(B-V) | Earliest<br>Sp. type | Mag<br>(Total) | Trumpler<br>class<br>(Ruppre-<br>cht) | Remarks | Ref. |        |   |   |
| 427 Czernik 20                   | 18             |                  |                | 325                              |        |                      |                |                                       | II 2r   |      |        |   | Czernik 1966                                    |
| 493 Czernik 25                   | 7              |                  |                | 44                               |        |                      |                |                                       | II 2p   |      |        |   | Czernik 1966                                    |
| 501 NGC 2236<br>Tr, Sh,<br>Cr 94 | 11             |                  |                | 171                              |        |                      | 12.5           |                                       |         |      |        |   | Roberts 1899                                    |
|                                  | 5              | 8320             | 12.1           | 50                               |        |                      |                |                                       |         |      |        | One of the most<br>remote open<br>cluster | Reinmuth 1926<br>Shapley 1930a<br>Shapley 1930b |
|                                  | 6              | 2290             | 4.0            |                                  |        |                      |                |                                       |         |      |        |   | Trumpler 1930                                   |
|                                  | 7              | 4750             | 9.7            | 15                               |        |                      |                | 11.9                                  |         |      |        |   | Collinder 1931a                                 |
|                                  | 3.5            | 4750             | 4.9            | 18                               |        |                      |                | 11.4                                  |         |      |        |   | Collinder 1931b                                 |
|                                  | 12             | 1600             | 5.6            |                                  |        |                      |                |                                       |         |      |        | Relation to<br>Milky Way                  | Bok 1949  |
|                                  |                | 3430             | 9.0            | 109                              |        |                      |                | 0.51                                  | A0      |      |        |   | Barhatova 1950                                  |
|                                  |                | 3400             |                |                                  |        |                      |                | 0.51                                  | A0      |      | III 2p |   | Rahim 1970<br>Becker et al. 1971                |



|     | 1              | 2       | 3    | 4   | 5     | 6  | 7  | 8    | 9 | 10   | 11     | 12 | 13              |
|-----|----------------|---------|------|-----|-------|----|----|------|---|------|--------|----|-----------------|
| 762 | Ruprecht<br>69 | 1.4x2.2 |      |     |       | 20 | 14 |      |   |      | III 2p |    | Ruprecht 1960   |
| 798 | NGC<br>3105    | 2.5     | 4680 | 3.4 |       |    |    |      |   |      | I 3p   |    | Trumpler 1930   |
|     | Tr, Sh         | 1.5     | 3980 | 1.7 | 15    |    |    |      |   |      |        |    | Shapley 1930    |
|     | Cr 214         | 2.5     | 7150 | 5.2 | 10    |    |    |      |   | 11.1 |        |    | Collinder 1931a |
|     |                | 8       | 2370 | 5.5 |       |    |    |      |   |      |        |    | Barhatova 1950  |
|     |                | 2       |      |     | 20;   |    |    |      |   |      |        |    | Hogg 1965       |
|     |                |         |      |     | mem-  |    |    |      |   |      |        |    |                 |
|     |                |         |      |     | bers: |    |    |      |   |      |        |    |                 |
|     |                |         |      |     | 17    |    |    |      |   |      |        |    |                 |
|     |                |         | 8000 |     |       |    |    | 1.09 |   |      |        |    | Moffat 1974     |
|     |                |         | 5500 |     |       |    |    | 1.08 |   |      |        |    | FitzGerald 1977 |

technique called single stage 'sabattiering'. This technique gives the isophots of all the images present in the photograph. From these isophots, the diameters  $\phi_{blue}$  (on the blue-prints) and  $\phi_{red}$  (on the red prints) of the relevant stellar images were obtained in mm using an X-Y coordinate measuring engine. Image diameters of several stars of known B and V magnitudes were also measured on the same copies for constructing the calibration curves relating the image diameters to the stellar magnitudes. In this connection, following van den Bergh (1957), the known B magnitudes were directly plotted against the corresponding blue print image diameters; from this, the blue (or B) magnitudes were obtained for the stars whose blue print image diameters could be measured. The expression that was used in the linear portion was:

$$B = Y\phi_{blue} + Z_{blue} \quad .2.1$$

where the coefficients Y and Z are constants for the given chart. In the same way, the red magnitudes (denoted as  $m_r$ ) were obtained for the stars whose red print image diameters could be measured. The expression for the linear portion in this case was

$$m_r = S\phi_{red} + Z_{red} \quad 2.2$$

However,  $m_r$  includes a colour term, for which the relation is given by van den Bergh (1957) as:

$$m_r = V - \frac{2}{3} (B-V). \quad 2.3$$

Thus, with B and  $m_r$  known, one can obtain V as

$$V = 0.6 m_r + 0.4 B \quad 2.4$$

Figures 2.4 and 2.5 show some examples of the calibration curves

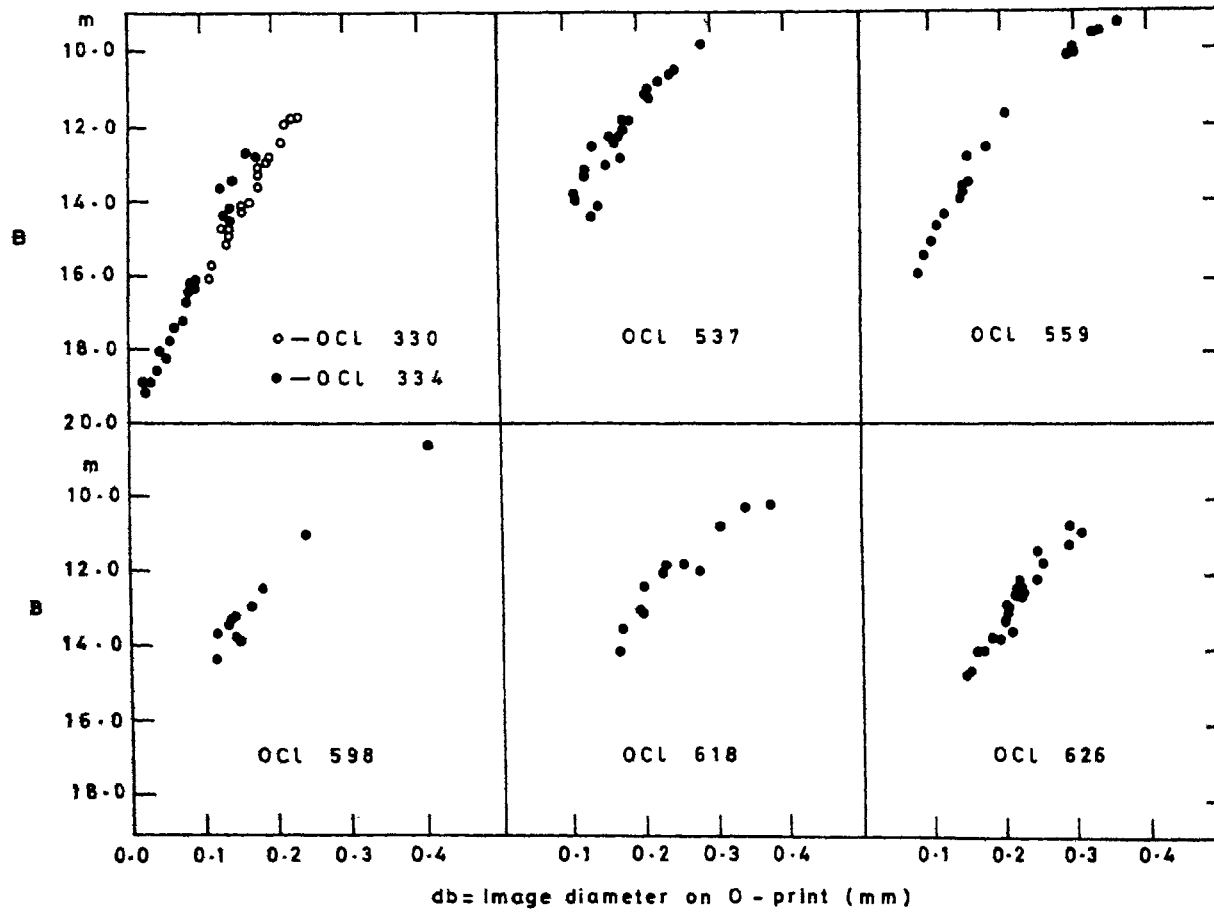


Fig. 2.4. Relationship between the POSS chart O-print image diameters of the individual stars belonging to various clusters and their corresponding B magnitudes.

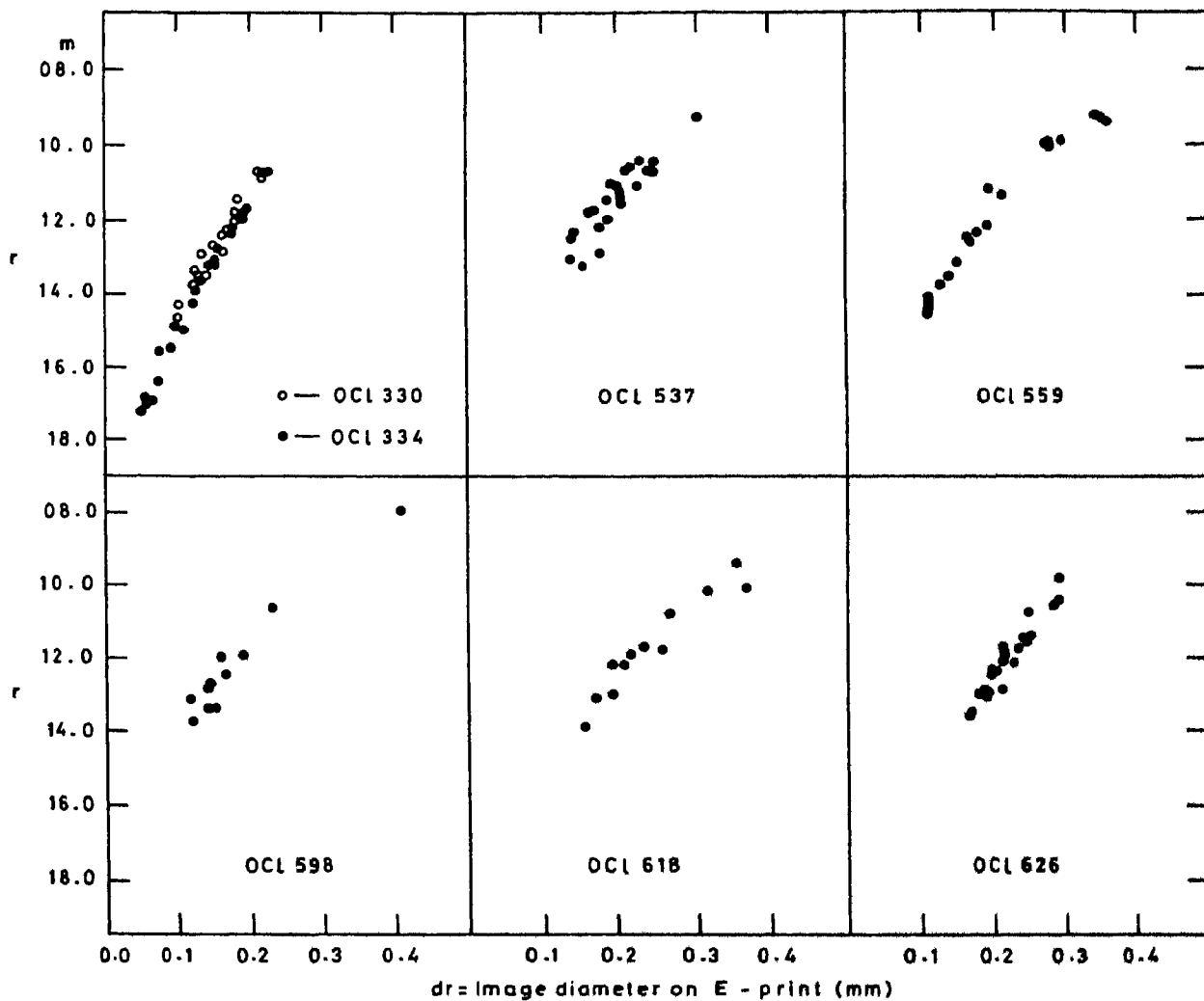


Fig. 2.5. Relationship between the POSS chart E-print image diameters of the individual stars belonging to various clusters and their corresponding red magnitudes expressed as  $r = V - \frac{2}{3} (B-V)$ , where  $r$  is same as  $m_r$ .

between the image diameters and the respective magnitudes for some of the known clusters representing different Palomar Observatory Sky Survey (POSS) Charts.

It may be noted that in both these figures, the curves for stars fainter than  $B$  or  $m_r = 11.0$  (whenever available) are linear.

For the diagrams shown in Fig.2.4, the value of  $Y$  ranges from  $-27.5$  to  $-33.5$  and  $Z_{\text{blue}}$  ranges from  $17$  to  $21$ . For the diagrams shown in Fig.2.5, the value of  $S$  ranges from  $-31.5$  to  $-35.5$  and  $Z_{\text{red}}$  ranges from  $19$  to  $21$ .

Using these values of  $B$  and  $m_r$  in equation 2.4 one obtains the value of  $V$  for each star. Following this procedure, the  $B$  and  $V$  magnitudes of the stars in the fields of the selected clusters were obtained.

#### **2.4. HR Diagrams and the Provisional Membership of Stars in the Open Clusters**

It is found that the average uncertainties involved in the technique of obtaining  $B$  and  $V$  magnitudes from the sky survey charts are of the order of  $0.3$  to  $0.4$  mag. Therefore, it is hazardous to consider the  $(B-V)$  colours from these measurements which could have otherwise been used in constructing the respective HR diagrams. In view of this, the spectral types determined from the objective grating measurements (described in Section 2.2) and the  $V$  mag derived from the sky survey charts (cf. Section 2.3) were made use of in obtaining the respective approximate HR-diagrams of six of the selected clusters. For the other



six, this technique was not applied.

Now the primary requirement is to make sure, that the star of the earliest spectral type seen in the field of any given cluster is not a field star, but a probable member of the cluster. The fulfilment of the following two conditions should suffice in establishing such a membership.

i) The star should be reasonably close to the densest region of the physical group as seen on the sky survey photograph.

ii) The star should fall into the evolutionary main sequence band of the spectral type - magnitude diagram, which is formed by most of the stars in the field.

Thus, if the star was to the left of the main sequence, it might not be a member of the cluster even though its spectral type was the earliest of all the stars in the field. On the other hand, the stars falling to the right of the main sequence might be giant members or not members at all. However, the latter were not crucial in the picking up of the young clusters, and were, therefore ignored.

In constructing these approximate HR diagrams, the effects of reddening on V were neglected. If the reddening is uniform across the given cluster, it will introduce only a lateral shift in V, while a non-uniform reddening may create a larger scatter in the main sequence. However, since this HR diagram is not intended for any further detailed study, the unknown absorption in V mag is unimportant at this juncture.

Thus all the stars, which fall on to the main sequence band were given a provisional membership of the corresponding cluster and whichever cluster was found to consist of stars of B5 or earlier spectral types on the main sequence was considered to be a young cluster.

This technique has been tested on a few well-established clusters, four of which are presented here as a sample. The respective star charts are shown in Figures 2.6, 2.8, 2.10, 2.12, which are the enlarged copies of the corresponding POSS maps. The numbering of the stars as given by the earlier authors has been retained; these are named as 'known' stars. The numbering is continued for a few 'additional' stars which on the basis of the present study, are also believed to be probable members of the respective clusters, with a few exceptions.

In the diagrams shown for each of these clusters, part (a) of the figure includes all the stars for which the spectral types as well as the V (POSS) magnitudes are obtained by using the techniques mentioned above. Part (b) shows the diagram after removing all the possible non-members from the diagram in part (a). Part (c) reproduces the colour magnitude diagram given by the earlier authors. The following subsections briefly describe each of these four clusters.

#### 2.4.1. OC1 537 (Dolidze 25)

This cluster has been observed earlier by Moffat and Vogt (1975). The field is shown in Fig.2.6 where eleven 'addi-

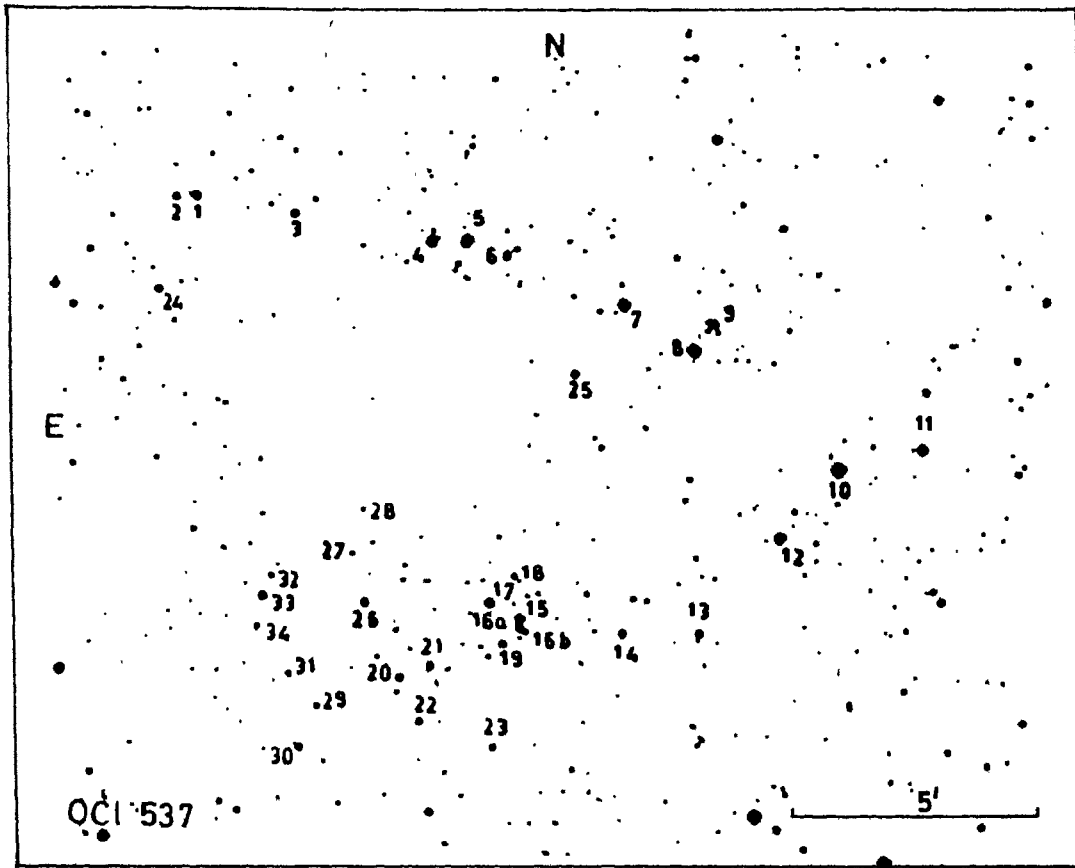


Fig. 2.6. Field of OC1 537 (Dolidze 25).

tional' stars (24 to 34) have been introduced. The spectral types and V magnitudes have been determined for a total of twenty-nine stars, twenty of them being the 'known' stars. Table 2.4 compiles the results.

In Fig.2.7a, we have considered seven 'known' stars (2, 5,6,7, 8, 20 and 21) as non-members, in agreement with the earlier work. However, Moffat & Vogt consider three more stars (3, 4 and 14) as non-members. Out of the 'additional' stars 25 and 26 could well be non-members. An inspection of the star field along with the HR-diagram shows that the bulk of the cluster is concentrated in the lower half of the photograph, which makes the membership of 1 and 24 doubtful. Thus, in Fig.2.7b, a sequence of seventeen stars is found - seven of them being 'additional' which, in all likelihood, are representative of the cluster. Fig.2.7c is plotted using (B-V) and V values of Moffat & Vogt, which have not been corrected for interstellar extinction. A comparison of this with the clear sequence in Fig.2.7b indicates that our method is quite effective in differentiating a reddened early-type member star from an unreddened late-type field star.

#### 2.4.2. OC 1 598 (NGC 2414)

Vogt & Moffat (1972) have observed eleven stars of this cluster and considered ten of these eleven as members. The field is shown in Fig.2.8, where four 'additional' stars (12 to 15) are also numbered. The spectral types and V magnitudes were obtained for all the numbered stars excepting star 15. Table 2.5 lists the results.

Table 2.4. OC1 537 (Dolidze 25)

| Star No. | Spectral type | V    | Membership | Star No. | Spectral type | V    | Membership |
|----------|---------------|------|------------|----------|---------------|------|------------|
| 1        | B5            | 11.1 | m ?        | 18       | F5            | 13.5 | m          |
| 2        | A5            | 11.8 | ...        | 19       | A5            | 12.8 | m          |
| 3        | A0            | 11.5 | ...        | 20       | F5            | 11.5 | ...        |
| 4        | B2            | 10.6 | ...        | 21       | F5            | 13.2 | ...        |
| 5        | B5            | 10.4 | ...        | 22       | A5            | 12.7 | m          |
| 6        | A5            | 11.7 | ...        | 24       | B8            | 11.7 | m ?        |
| 7        | A0            | 10.6 | ...        | 25       | K0            | 11.7 | ...        |
| 8        | A5            | 10.3 | ...        | 26       | G5            | 11.4 | ...        |
| 9        | A0            | 11.9 | m          | 27       | F5            | 14.4 | m          |
| 10       | F0            | 8.9  | m          | 28       | F5            | 14.5 | m          |
| 12       | B2            | 11.0 | m          | 31       | F0            | 13.5 | m          |
| 13       | B8            | 12.3 | m          | 32       | F0            | 13.4 | m          |
| 14       | B8            | 11.9 | ...        | 33       | B8            | 11.6 | m          |
| 15       | B8            | 11.5 | m          | 34       | F5            | 14.0 | m          |
| 17       | B8            | 11.7 | m          |          |               |      |            |

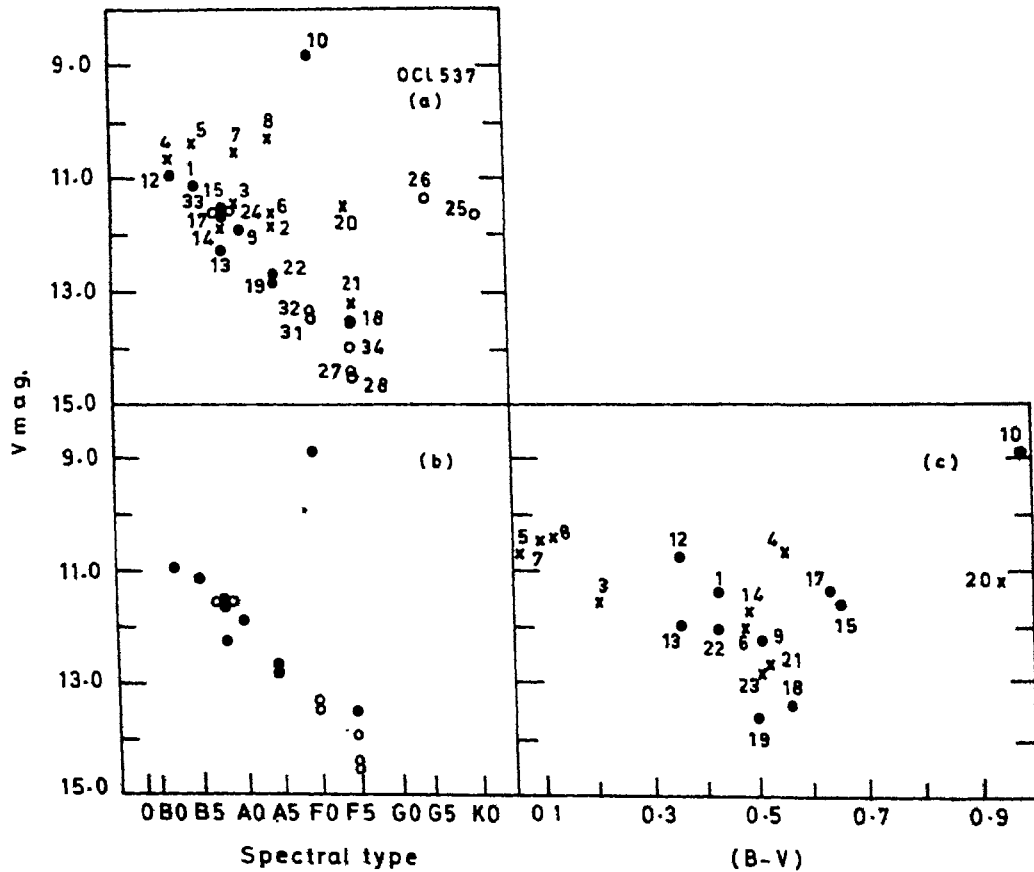


**Fig. 2.7a.** Spectral types of all the individual stars of OC1 537 which could be estimated on the basis of the objective-grating spectra, plotted against the corresponding V magnitudes from POSS charts. The filled circles and the crosses denote members and non-members of the cluster, respectively (Moffat & Vogt, 1975). The open circles represent the stars added in the present work.

**b.** Spectral type versus magnitude (HR) diagram of OC1 537 after removing all the possible non-members of the cluster.

**c.** The colour-magnitude diagram of OC1 537 as given by Moffat & Vogt (1975).

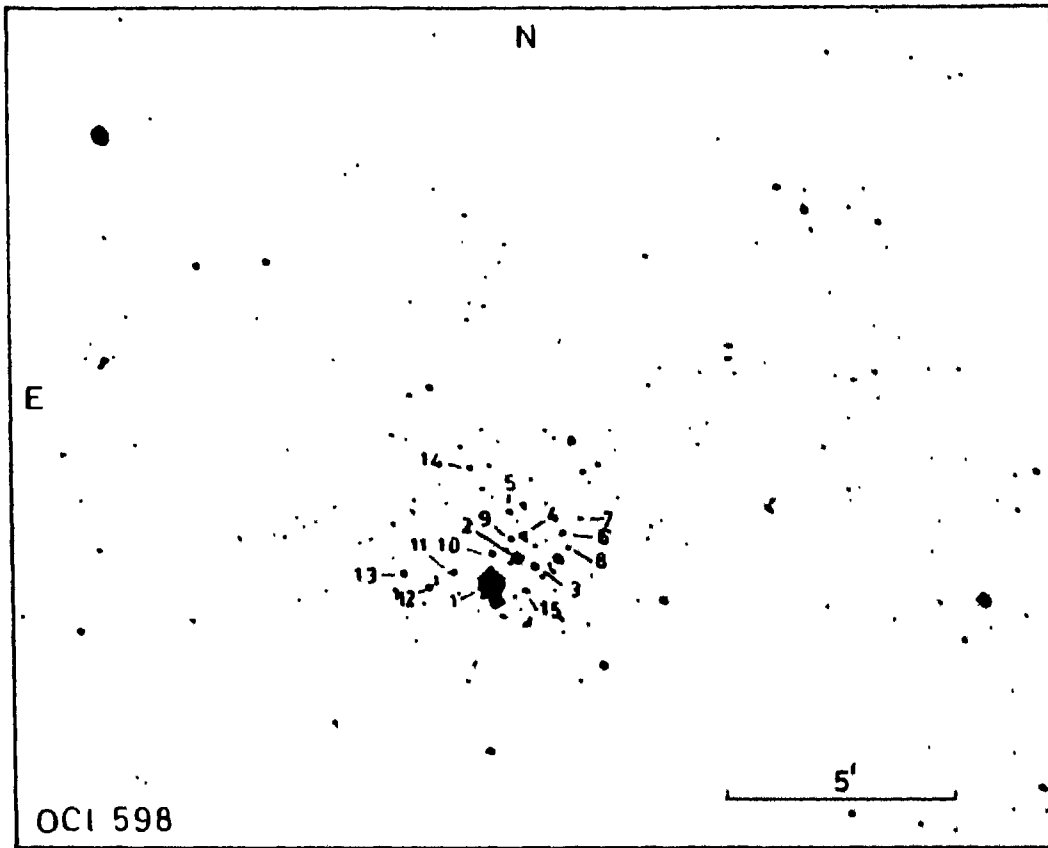


Fig. 2.8. Field of OCI 598 (NGC 2414).

Table 2.5. OC1 598 (NGC 2414)

| Star No. | Spectral type | V    | Membership | Star No | Spectral type | V    | Membership |
|----------|---------------|------|------------|---------|---------------|------|------------|
| 1        | B2            | 8.2  | m          | 8       | ...           | 14.0 | ...        |
| 2        | B5            | 10.7 | m          | 9       | ...           | 13.3 | ...        |
| 3        | B8            | 11.9 | m          | 10      | ...           | 13.0 | . .        |
| 4        | B8            | 12.6 | m          | 11      | A5            | 13.3 | m          |
| 5        | F0            | 13.0 | ...        | 12      | K0            | 12.4 | ...        |
| 6        | A5            | 13.3 | m          | 13      | B5            | 12.2 | m          |
| 7        | F0            | 14.2 | m          | 14      | B8            | 13.5 | . .        |

---

---



Though star 12 appears to be within the physical group of the cluster as seen in the photograph, it could well be a foreground, late-type star (Fig.2.9a). Star 5 has already been termed a non-member by Vogt & Moffat. Fig.2.9b shows a sequence with the most likely members, the earliest spectral type being B2. This sequence matches closely with the one given by Vogt & Moffat (Fig.2.9c).

#### 2.4.3. OC1 618 (NGC 2384)

Fifteen stars of this cluster have been observed by Vogt & Moffat (1972), four of which turned out to be non-members. Five 'additional' stars have been numbered (16 to 20) in the present work as shown in Fig.2.10. For stars 6 and 7 the spectral types could not be estimated due to the overlapping of the other stars' spectra, while stars 1, 2 and 10 turned out to be too bright to obtain meaningful V magnitudes from the images on the corresponding POSS photographs. The results are compiled in Table 2.6.

Among the remaining fifteen stars 3, 14 and 15 are 'known' non-members and star 17 appears to lie away from the general sequence. This last one could be a background A-type star (Fig. 2.11a). Fig.2.11b shows a sequence of seven 'known' and four 'additional' members. The earliest spectral type appears to be B3. There is good agreement between this and the colour magnitude diagram given by Vogt & Moffat (Fig.2.11c).

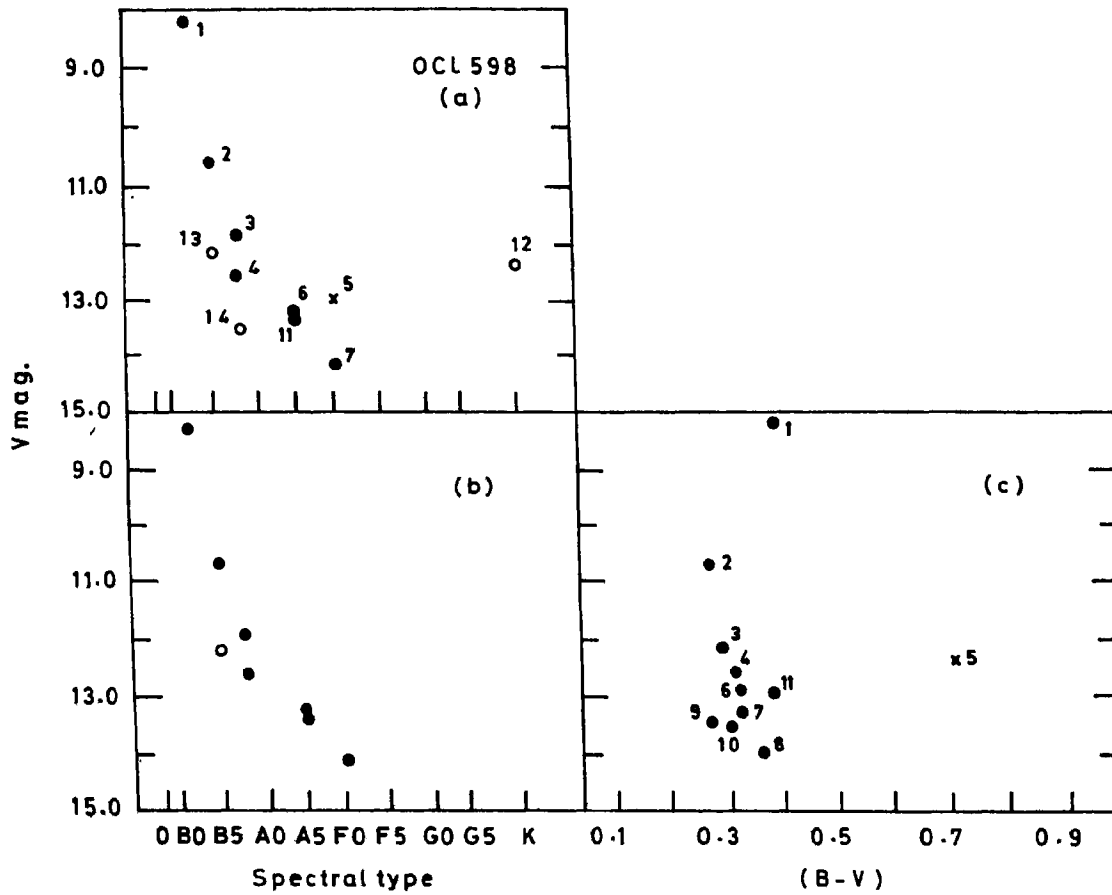


**Fig. 2.9a.** Spectral type plotted against V magnitude for stars of OCL 598. The filled circles and the cross denote the members and the non-member respectively. The open circles represent the stars added in the present work.  
**b.** Spectral type versus magnitude diagram after deleting all the possible non-members.  
**c.** Colour-magnitude diagram as given by Vogt & Moffat (1972).

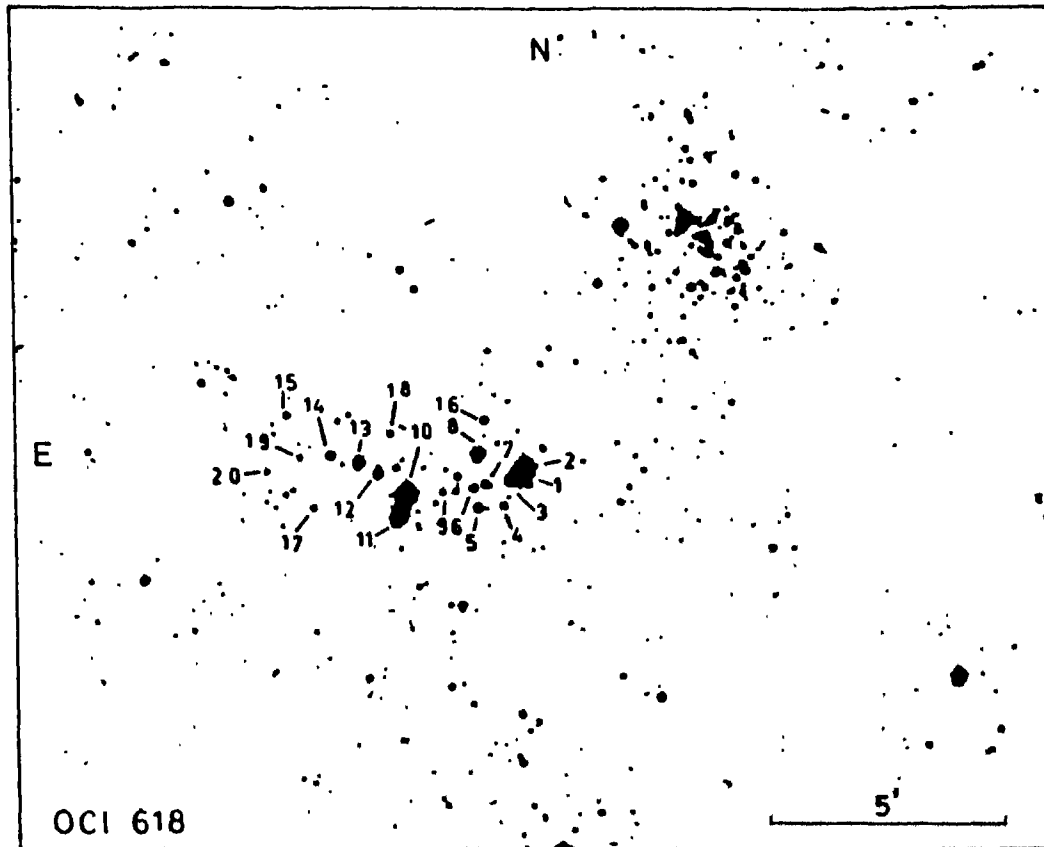


Fig. 2.10. Field of OC1 618 (NGC 2384).

Table 2.6. OC1 618 (NGC 2384)

| Star No. | Spectral type | V     | Membership | Star No. | Spectral type | V    | Membership |
|----------|---------------|-------|------------|----------|---------------|------|------------|
| 1        | B3            | ...   | ...        | 11       | B3            | 9.6? | m          |
| 2        | B3            |       | ...        | 12       | B8            | 11.4 | m          |
| 3        | A5            | 11.0? | ...        | 13       | B8            | 10.7 | m          |
| 4        | F0            | 13.5  | m          | 14       | A5            | 10.5 | ...        |
| 5        | A0            | 12.0  | m          | 15       | F0            | 12.7 | ...        |
| 6        | ...           | 12.7  | ...        | 16       | A5            | 12.4 | m          |
| 7        | ...           | 12.4  | ...        | 17       | A0            | 13.2 | ...        |
| 8        | B5            | 10.1  | m          | 18       | F0            | 13.4 | m          |
| 9        | F5            | 13.9  | m          | 19       | F5            | 13.9 | m          |
| 10       | B0            | ...   | ...        | 20       | F5            | 13.3 | m          |

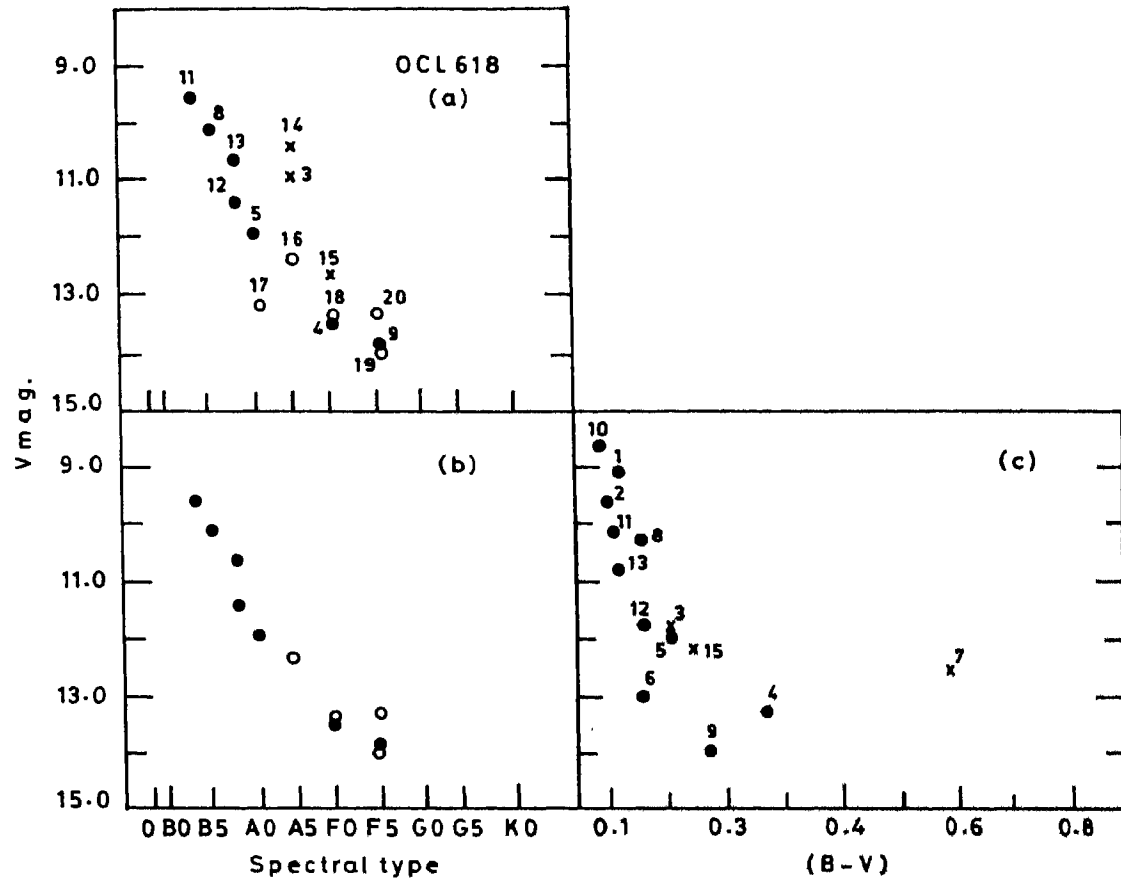


Fig. 2.11a. Spectral type plotted against V magnitude for stars of OCL 618. The filled circles, crosses and open circles denote the members, non-members and 'additional' stars respectively.  
b. Spectral type versus magnitude diagram after deleting all the possible non-members.  
c. Colour-magnitude diagram as given by Vogt & Moffat (1972).

#### 2.4.4. OC1 626 (NGC 2421)

Moffat & Vogt (1975) have observed twenty-eight stars in this cluster, out of which six have been termed as non-members. Fifteen 'additional' stars have been number here as shown in Fig.2.12. The spectral types could not be estimated for stars 18, 19, 21, 23, 26, 28, 32, 39 and 40 whereas the V magnitudes are lacking for only four stars (24, 25, 39 and 40), mainly due to crowding effects. Table 2.7 shows the results.

Thus, out of the forty-three stars, only thirty-two could be included in Fig.2.13a where stars 6, 7, 12 and 15 are 'known' non-members and stars 29, 35, 36 and 37 are 'additional' non-members. Stars 38, 41 and 42 are very close to the known red giant star 5 and, therefore, are adopted as members of the giant branch. Thus, Fig.2.13b shows sixteen 'known' members and eight 'additional' members of this cluster, with the earliest spectral type as B2. The sequence in this part seems to be matching fairly well with the colour magnitude diagram given by Moffat & Vogt which is shown in Fig.2.13c.

#### **2.5. Conclusions**

On the basis of these experimentations, it may be concluded that the new technique of combining spectral types (from the objective-grating spectroscopy) and the V magnitudes (from the sky survey chart image diameters) works well to establish the cluster reality. Telescope time is needed only for the objective-grating spectroscopy, while the other parameter can be obtained from the already available survey charts. It is also possible to

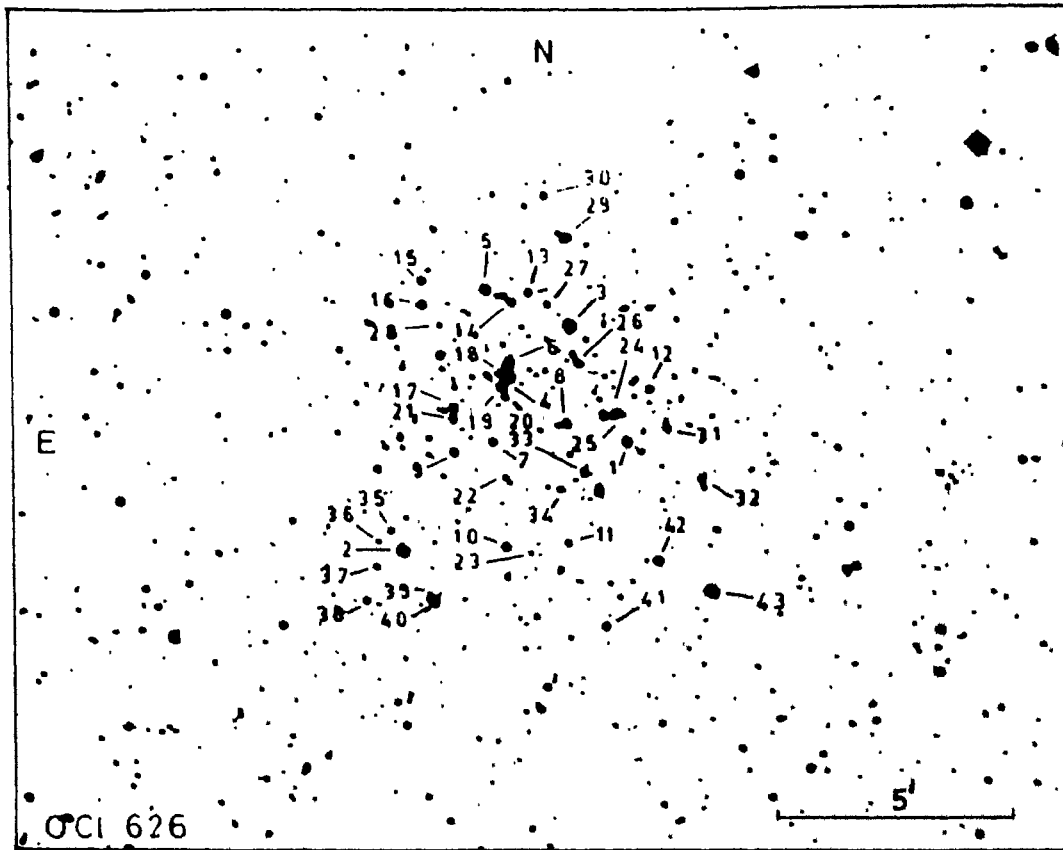
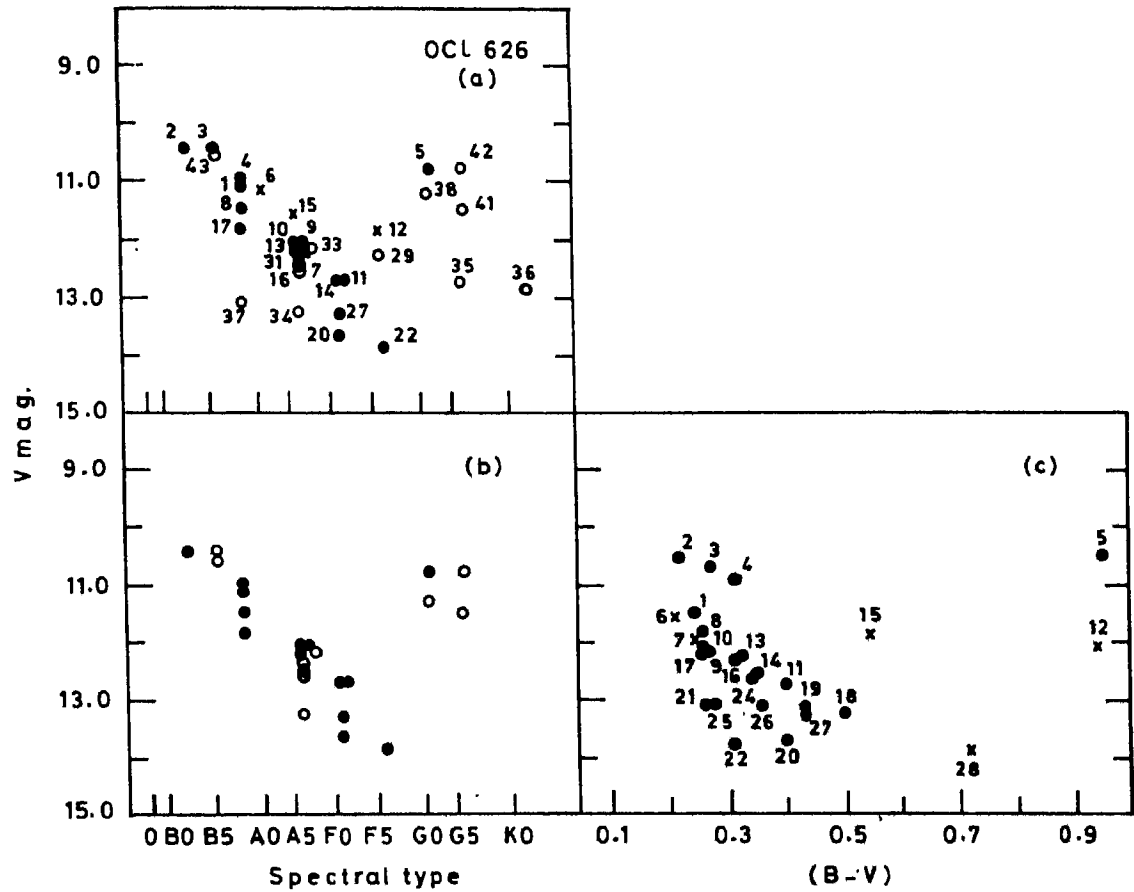


Fig. 2.12. Field of OC1 626 (NGC 2421).

Table 2.7 OC1 626 (NGC 2421)

| Star No. | Spectral type | V    | Membership | Star No. | Spectral type | V     | Membership |
|----------|---------------|------|------------|----------|---------------|-------|------------|
| 1        | B8            | 11.2 | m          | 22       | F5            | 13.9  | m          |
| 2        | B2            | 10.5 | m          | 23       | ..            | 13.1  | ...        |
| 3        | B5            | 10.4 | m          | 24       | F0            | ...   | ...        |
| 4        | B8            | 11.0 | m          | 25       | F5            | ...   | ...        |
| 5        | G0            | 10.8 | gm         | 26       | ...           | 12.8  | ...        |
| 6        | A0            | 11.2 | ...        | 27       | F0            | 13.3  | m          |
| 7        | A5            | 12.1 | ...        | 28       | ...           | 13.9  | ...        |
| 8        | B8            | 11.5 | m          | 29       | F0            | 12.3  | ...        |
| 9        | A5            | 12.1 | m          | 30       | A5            | 12.5  | m          |
| 10       | A5            | 12.0 | m          | 31       | A5            | 12.4  | m          |
| 11       | F0            | 12.7 | m          | 32       | ...           | 12.9  | ...        |
| 12       | F5            | 11.9 | ...        | 33       | A5            | 12.2? | m          |
| 13       | A5            | 12.2 | m          | 34       | A5            | 13.3  | m          |
| 14       | F0            | 12.7 | m          | 35       | G5            | 12.7  | ...        |
| 15       | A5            | 11.7 | ...        | 36       | K0            | 13.8  | ...        |
| 16       | A5            | 12.5 | m          | 37       | B8            | 13.1  | ...        |
| 17       | B8            | 11.8 | m          | 38       | G0            | 11.2  | gm         |
| 18       | ..            | 12.9 | ...        | 41       | G5            | 11.5  | gm         |
| 19       | ..            | 12.2 | ...        | 42       | G5            | 10.7  | gm         |
| 20       | F0            | 13.6 | m          | 43       | B5            | 10.6  | m          |
| 21       | ..            | 12.8 | ...        |          |               |       |            |





**Fig. 2.13a.** Spectral type plotted against V magnitude for stars of OCL 626. The filled circles, crosses and open circles represent the members, non-members and 'additional' stars respectively.

b. Spectral type versus magnitude diagram after deleting all the possible non-members.

c. Colour-magnitude diagram as given by Moffat & Vogt (1975).

observe much fainter stars with this method and thereby pick out the young clusters at greater distances. The method of visually inspecting the sky survey charts for the bluer clusters is crude; but it is found to be useful in the initial stages.

\*\*\*\*\*

## CHAPTER 3

### PROCEDURES FOR OBSERVATIONS AND FOR THE DETERMINATION OF CLUSTER PARAMETERS

The clusters selected in the previous chapter, have been subjected to more detailed photometric observations. Brief descriptions of these photometric procedures employed for obtaining the standard magnitudes and colours of stars in the UBV system of Johnson & Morgan (1953) are discussed in the first two sections of this chapter. Then the procedures for the determination of cluster members and for finding the interstellar reddening in the case of any given cluster are presented in the next two sections. Finally, the procedures for the determination of their distances and ages are given in the last portions of this chapter.

The photoelectric and photographic observations discussed in this study were obtained by using the facilities at the following observatories.

1. Kavalur Observatory, Indian Institute of Astrophysics, India.  
(Longitude =  $78^{\circ} 49'.6$  E, Latitude =  $+12^{\circ} 34'.6$ ; Altitude = 725 m).
2. Siding Spring Observatory, Australian National University, Australia.  
(Longitude =  $149^{\circ} 04'.0$  E, Latitude =  $-31^{\circ} 16'.6$ ; Altitude = 1150 m).

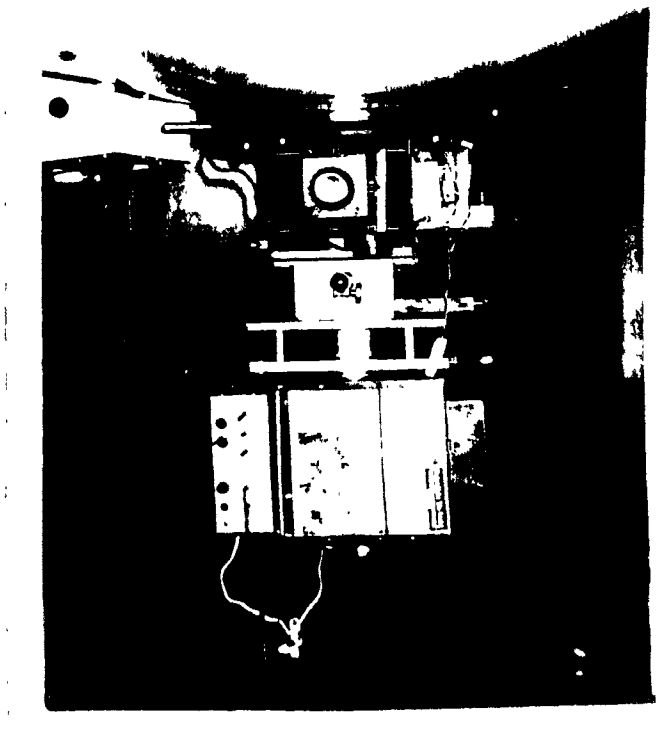
### 3.1. Photoelectric Photometry

The photoelectric observations of the selected young clusters were made with the 102-cm telescope (F/13) at Kavalur Observatory and the 61-cm telescope (F/18) at Siding Spring Observatory. The photometer, the procedure for observations and the reduction techniques are briefly described below.

#### 3.1.1. The Photoelectric Photometer

A schematic diagram of the photometer is given in Fig.3.1. It consists of the following components.

- i) A field viewer consisting of a plane mirror  $M_1$  and a wide-angle field eyepiece E. The mirror can be shifted away from the path of light to allow the light to go through to the next stage. The eyepiece can be given X-Y motions and this provision may be used for off-set guiding on nearby field stars.
- ii) A diaphragm disc (or slide) D having circular apertures to admit small portions of sky, generally several seconds of arc, located at the Cassegrain focus of the telescope.
- iii) A microscope M for viewing the diaphragm aperture.
- iv) A filter disc (or slide) F having U, B and V filters of the Johnson and Morgan Photometric system (Johnson & Morgan, 1953).
- v) A Fabry lens L fixed in front of the photomultiplier tube for imaging the objective of the telescope on to the photocathode.



Photograph of the photoelectric photometer attached to the 102-cm telescope of the Kavalur Observatory.

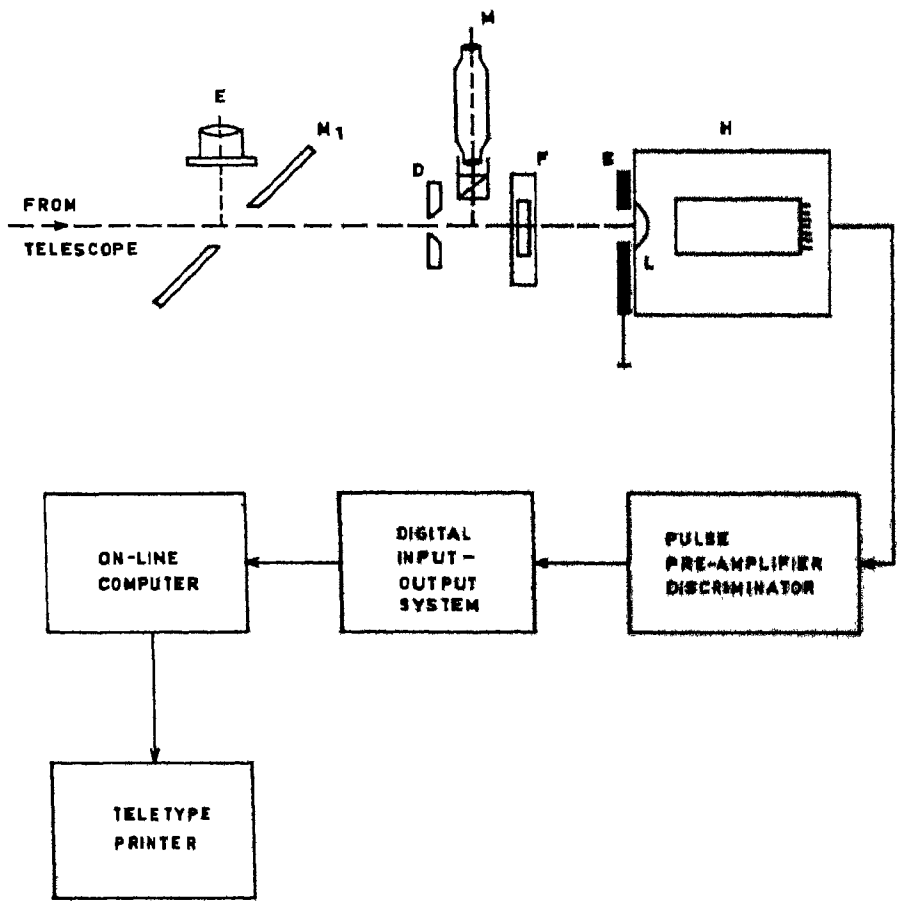


Fig. 3.1. Schematic diagram of the photoelectric photometer; (see text for the explanation of the symbols).

- vi) An EMI 9558 B or 9658 R photomultiplier tube having an effective photocathode of about 50 mm in diameter. The normal dark current of this tube is reduced by cooling.
- vii) A photomultiplier housing H, which is designed for cooling the photomultiplier tube by charging it with dry ice. Proper magnetic and electrostatic shielding are also provided for the photomultiplier tube.

All the photoelectric observations were obtained employing standard pulse counting techniques. A block diagram of the electronic system used is included in Fig.3.1. The on-line computer reads the pulse at regular intervals as selected by the built-in real time clock and then prints out the number of counts on the teletype printer according to the observer's commands.

### 3.1.2. The Observational and Reduction Procedures

After identifying the cluster field, a programme star was placed at the centre of one of the diaphragm apertures. Usually, the aperture of 1 mm was used. Sometimes, to eliminate the presence of other stars in the vicinity of the programme star, a smaller aperture of 0.6 mm had to be chosen. At least three observations through each filter U, B and V were taken in the order:

Star + Sky, Sky only.

The integration time in the case of faint stars was generally kept at 20 seconds, while for the brighter ones, 5 or 10 seconds were sufficient. By subtracting the (sky) measurement from the (star + sky) measurement in each case for each filter, the counts for the star were obtained and the mean of three observations was taken. These were then converted to counts per sec. At least two stars in the vicinity of the cluster were observed on each night in order to evaluate atmospheric extinction. The number of observations on each night for the purpose of extinction determination averaged around 3 for every two hours.

A number of standard stars, covering a wide range of spectral classes, selected from the photometric sequences given by Landolt (1973), were also observed on each night and were used for the determination of instrumental constants.

The mean count rate ( $n$ ) of a star for a given filter was transformed to magnitude scale with the expressions

$$\begin{aligned}v &= - 2.5 \log n_v \\b &= - 2.5 \log n_b \\u &= - 2.5 \log n_u.\end{aligned}\tag{3.1}$$

Whence the observed colour indices are given by

$$(b-v) = - 2.5 \log \left( \frac{n_b}{n_v} \right)\tag{3.2}$$

$$\text{and } (u-b) = - 2.5 \log \left( \frac{n_u}{n_b} \right).\tag{3.3}$$

The airmass ( $X$ ) was calculated using the expression (Hardie, 1962)

$$\begin{aligned}
 X = & \sec Z - 0.0018167 (\sec Z - 1) \\
 & - 0.002875 (\sec Z - 1)^2 \\
 & - 0.0008083 (\sec Z - 1)^3
 \end{aligned}
 \tag{3.4}$$

$$\text{where } \sec Z = (\sin \phi \sin \delta + \cos \phi \cos \delta \cos h)^{-1}.
 \tag{3.5}$$

In this expression,  $\phi$ ,  $\delta$  and  $h$  were respectively the observer's latitude, the declination of the star and its instantaneous hour angle. Then, the  $v$ ,  $(b-v)$  and  $(u-b)$  values of the stars observed for extinction purposes were plotted against the corresponding instantaneous airmass values. From these plots, the atmospheric extinction coefficients  $K_v$ ,  $K_{(b-v)}$  and  $K_{(u-b)}$  were determined using the method of least squares. The observed quantities  $v$ ,  $(b-v)$  and  $(u-b)$  of all the other stars were then corrected for atmospheric extinction so as to obtain their instrumental magnitudes and colours by the use of the following relations, the resulting values being denoted by the zero subscripts.

$$v_0 = v - K_v X
 \tag{3.6}$$

$$(b-v)_0 = (b-v) - K_{(b-v)} X
 \tag{3.7}$$

$$(u-b)_0 = (u-b) - K_{(u-b)} X.
 \tag{3.8}$$

### 3.1.3. Computation of Standard Magnitudes

The systemic transformations of these instrumental magnitudes and colours to the standard ones were done by using the equations

$$V = v_0 + \epsilon (B-V) + \zeta_v
 \tag{3.9}$$



$$(B-V) = \mu (b-v)_0 + \zeta_{bv} \quad 3.10$$

$$\text{and } (U-B) = \psi (u-b)_0 + \zeta_{ub} \quad 3.11$$

Here  $\epsilon, \mu, \psi$  are the transformation coefficients and  $\zeta_v, \zeta_{bv}, \zeta_{ub}$  are the zero-point constants determined from the observations of the standard stars. Rufener (1968) has shown that  $\zeta$  values depend upon the nightly atmospheric extinction and on the photometric system. However, since the standard stars were observed on all the nights, the effects of these variations could be taken care of. Thus the instrumental magnitudes and colours of all the programme stars were transformed into the standard ones. The mean internal errors (derived from the different measurements of the same star) of the observation in  $V, (B-V)$  &  $(U-B)$  were respectively found to be between 0.02 to 0.03, 0.02 to 0.045 and 0.05 to 0.10 mag. within a magnitude range of  $V = 12.0$  to  $15.5$  mag. The larger errors were applicable to the fainter stars. These standard magnitudes and colours form the basic data for further discussions. The plot between  $(U-B)$  and  $(B-V)$  is called the colour - colour diagram and is abbreviated as CCD. The plot between  $(U-B)$  and  $V$  is called the short wavelength colour - magnitude diagram, while the one between  $(B-V)$  and  $V$  is called the long wavelength colour - magnitude diagram. Both these names are abbreviated as CMDs.

### 3.2. Photographic Photometry

When the stars are faint and the field is too crowded for photoelectric photometry, direct photography with suitable filter and plate combinations becomes very useful. Since the

stars in the open clusters chosen for this study, are generally fainter than 12 mag and most of them appear to be having fields with stars situated quite closely to each other, they were photographed using the following instrument for direct photography. These photographs were then analysed to obtain the photographic magnitudes of the individual stars.

### 3.2.1. Direct Photography

A schematic diagram of the instrument is shown in Fig.3.2. This was used with the 102-cm telescope at Kavalur Observatory and the 1-m telescope at Siding Spring Observatory to obtain the U, B and V photographs of the selected clusters. For this purpose, the following plate and filter combinations were generally used.

IIa-0 + Schott UG 2 for U

IIa-0 + Schott GG 13 for B

IIa-D + Schott GG 14 for V

In some cases, 103a-0 emulsion was used instead of IIa-0. The exposure times for obtaining the B and V pictures were usually between 45 and 60 minutes while the range for the U pictures was 90 to 100 minutes. During these exposures, guiding of the telescope was done by using the guiding probe (cf. Fig.3.2).

The field covered at the Cassegrain focal plane of the Kavalur telescope was 40 arcmin diameter with a plate scale of  $15.9 \text{ arcsec mm}^{-1}$ . The field of the Siding Spring Telescope was 60 arcmin diameter and its plate scale was  $25 \text{ arc sec mm}^{-1}$ .

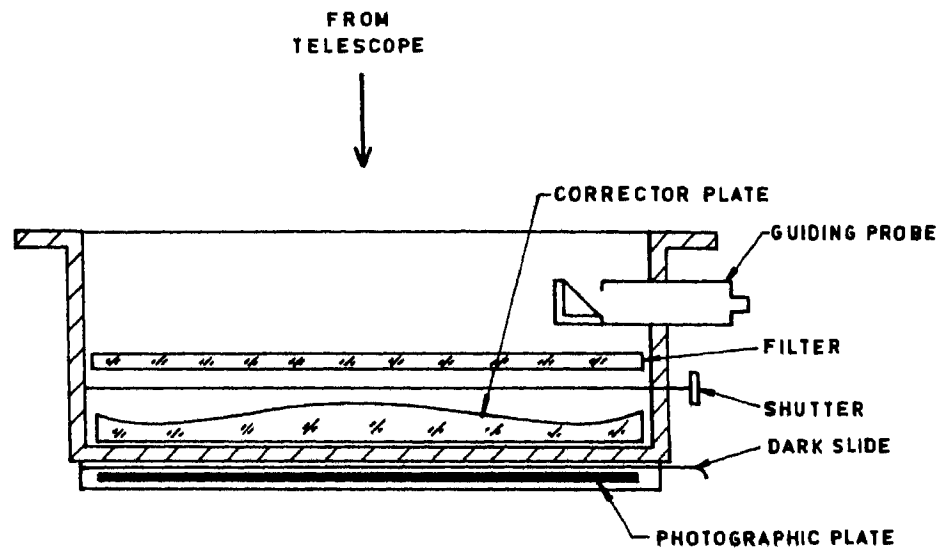
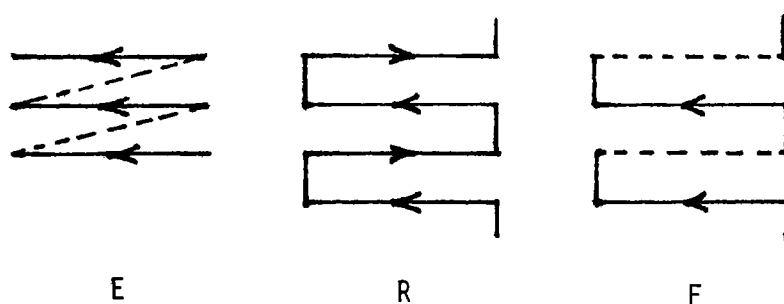


Fig. 3.2. A schematic diagram of the instrument used for direct photography.

### 3.2.2. Analysis of the Photographs

The images of the stars in the field of the cluster on each plate were measured using the PDS microdensitometer at Mount Stromlo Observatory of the Australian National University in Australia. A schematic diagram of this instrument is shown in Fig.3.3 and the procedure followed for obtaining the photographic magnitudes is given below.

The plate to be scanned was fixed on to the glass platten of the PDS microdensitometer and each star in the field of the cluster was centred on the view screen by moving the glass platten. Its position was then recorded on a floppy disc as X and Y coordinates of the platten. The carriage with the platten would then move to these positions in a sequential order in the automatic scanning mode. In this auto mode, the pattern traced out by the reading spot on the plate is one of the three forms, EDGE (E), RASTER (R) or FLIPPED RASTER (F) as shown below:



A programme called FORNAX written in FORTRAN and designed to run under the DEC RT-11 operating system, was used for scanning. It permits the user to define the size, resolution and format of a rectangular scan pattern and to perform this

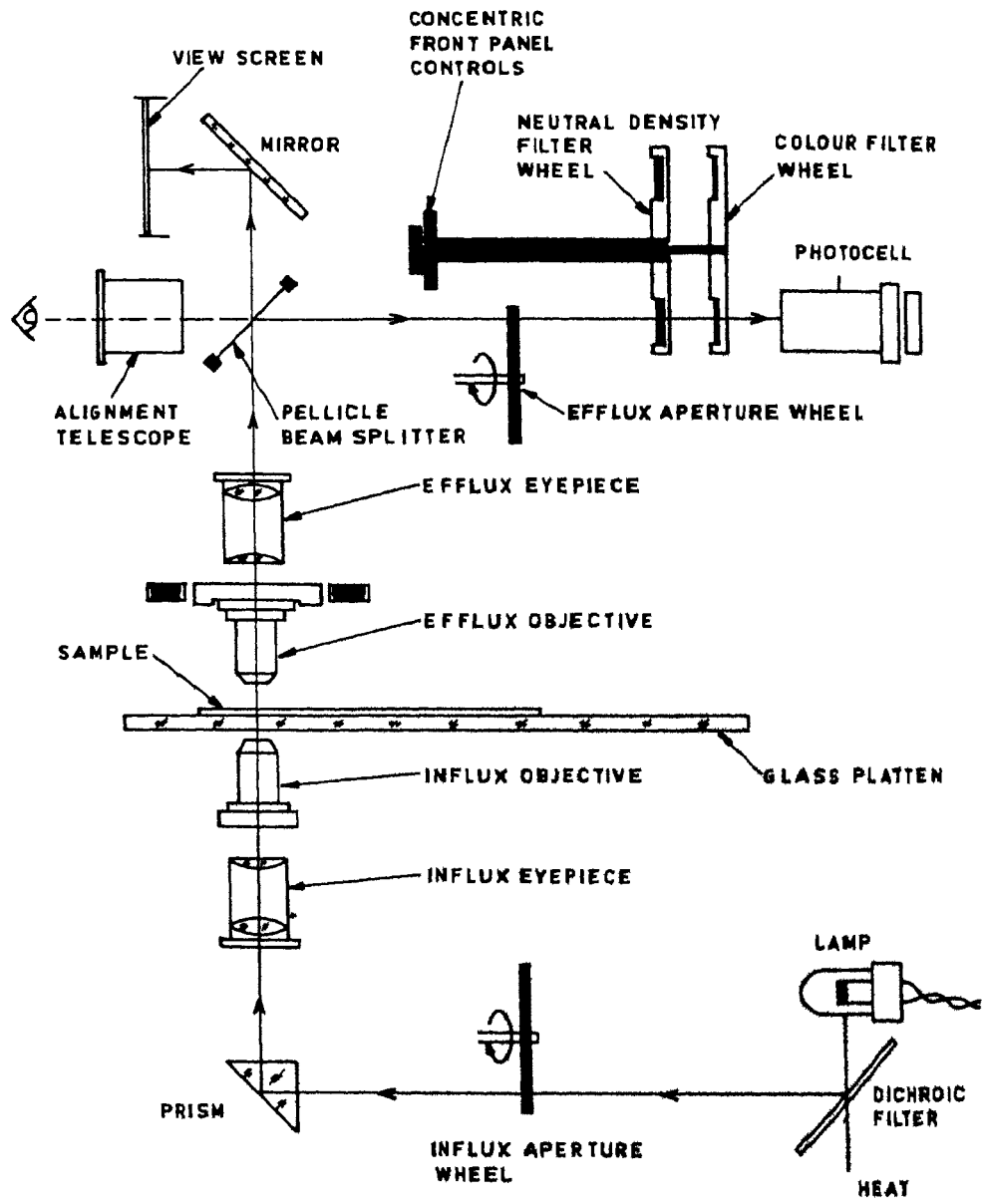


Fig.3.3. A schematic diagram of the PDS microdensitometer.

scan either at nominated position of the stage or at a series of locations which are stored on floppy disc as pairs of coordinates. In this study, the flipped raster (i.e., F) was selected with a scanning speed of  $30 \mu\text{m sec}^{-1}$ . A total of 61 steps in both X and Y axes were covered, the step size being  $20 \mu\text{m}$  in both X and Y. The efflux and influx apertures were kept at  $30 \mu\text{m}$  for all the scans. And all the measurements were done in density mode.

The measured data were recorded on the magtape and the scanning was monitored on the teletype printer. During this monitoring, the counts in each step of the middle line (i.e., line 31 in this case) were printed.

The data collected on magtape was processed on the VAX 11/780 computer with the help of a software package called APEX. In this programme, which was developed by Newell and Harding at Mount Stromlo Observatory, the density of the stellar images were transformed to an arbitrary magnitude scale for each of U, B and V plates.

These arbitrary U, B, V magnitudes (denoted as  $m'_{pg}$ ) for the programme stars in each cluster were standardized in the following manner: the photoelectrically observed stars were individually picked from each plate and their photoelectric magnitudes  $V_{pe}$ ,  $B_{pe}$ ,  $U_{pe}$  (denoted as  $m_{pe}$ ) were separately plotted against the corresponding arbitrary photographic magnitudes  $m'_{pg}$ . In these plots, the stars in the range of 12 to 17 mag in  $V_{pe}$  and  $B_{pe}$  were found to show good linear relationships. The same stars in the case of  $U_{pe}$  however, showed a slightly larger scatter.

All the measured values of  $m'_{pg}$  on a given plate were then converted into the  $m_{pe}$  scale with the help of the plots mentioned above. For only one cluster (OC1 585), the X-Y coordinate measuring engine was used (Babu, 1985) in the same manner as was done for the sky survey charts, where the image diameters were transformed to photographic magnitudes (cf. Section 2.3). The uncertainties in these standardized values were found to be  $\lesssim \pm 0.15$  mag in B and V, about  $\pm 0.2$  mag in U.

In this way, the photographic magnitudes and colours of as many stars as possible in the fields of all the 12 clusters were determined. These are listed in the respective tables of the individual clusters, which are dealt with in the next chapter.

### **3.3. Procedure for the Determination of Cluster Membership**

The first requirement for the determination of cluster parameters and for the investigation of different problems concerning clusters, is the separation of cluster stars from field stars (van Altena, 1972; Slovak, 1977). This determination of cluster membership can be accomplished through any one, or more, of the following criteria.

#### 3.3.1. Photometric Criteria

In this method, the determination of cluster membership is based on the assumption that the stars in a given cluster have the same chemical composition and are formed at the same

time. Therefore, the cluster stars should show a well defined sequence in their colour - colour diagram (CCD) and the colour - magnitude diagrams (CMDs) as expected from the theory of stellar evolution. Thus, an inspection of the CCD and of the two CMDs would normally reveal a sequence of several stars which is parallel, or nearly so, to some part of the zero-age-main sequence (ZAMS), in at least one of the three diagrams, if the cluster is real. If this was not the case the cluster was considered to be a random group of field stars.

If the result was positive, there were two cases to be considered.

Case (a): The sequence was present in all the three diagrams. This implies non-variable reddening across the cluster. The procedure described in Section 3.4 is then used to determine the mean reddening to deredden the CMDs.

Case (b): The sequence was apparent only in the short wavelength CMD. This implies variable reddening across a young cluster in which the MS is nearly parallel to the reddening line in the short wavelength CMD (but not so in the long wavelength CMD). In older, sparse clusters with variable reddening, the problem of membership is more difficult. For such clusters, one needs spectral types also. For young clusters with variable reddening each star was corrected individually to obtain the dereddened CMDs, as has been described in Section 3.4.

The final determination of membership was made under ~~the~~ assumption that a member, must fulfil the following criteria:



1. The reddening of the star must be compatible with the majority of stars, which in turn, could be cluster members. However, in the case of the reddening being variable it becomes more difficult.
2. The location of the star in both CMDs must correspond to the same possible evolutionary stage in the cluster.

Then if,

- (a) the star is located below the ZAMS in one or both CMDs, it may be inferred to be a background star;
- (b) the star is located on the ZAMS in one CMD and above it in the other, a foreground star is implied;
- (c) the star is located above the ZAMS in both CMDs, the following subcases arise:
  - i. If the star is too faint to be a post-main-sequence member, according to known evolutionary tracks (e.g. Wilde, 1968), then it is a foreground star.
  - ii. If the brightness of the star is compatible with that of the brightest known cluster members, then it is possibly a giant member.
  - iii. If the star is one of the faintest observed and the cluster is very young, then it is possibly a pre-main-sequence contracting member.

### 3.3.2. Kinematic Criteria

In this method it is assumed that the kinematic properties of the cluster members are similar but are different from those of the field stars. Relative proper motions and radial velocity measurements are used for this purpose. The latter limits the method to stars brighter than about 12.0 mag (Moffat, 1972) while the former permits one to go up to approximately the sixteenth magnitude (van Altena, 1972) with a telescope of moderate size. A method for the determination of cluster membership from proper motion study has been given by Vasilevskis et al. (1958), and the same has also been adopted for computers by Sanders (1971a). However, none of the clusters selected in this work have known proper motion studies, and therefore, this method could not be applied here for the determination of the cluster members.

### 3.3.3. Statistical Criteria

In this method the density of field stars, estimated from outside the cluster region, is used to estimate the number of field stars present in the cluster region. In this case, it is assumed that the density of the field stars is uniform across the whole field. Such a method was first used by Ozsvath (1960) for the old rich cluster NGC 7789. Vogt (1971) used it in a more refined way, for the young rich clusters  $\eta$  and  $\chi$  Persei in which the variation of reddening across the measured fields was taken into account. Moffat (1972) has applied this method for a number of other clusters. The method in brief, is as follows:

Photographic UBV magnitudes are obtained for all stars in a region which well encloses the cluster. Another field, the total area of which is at least as large as that of the cluster region itself and is located far enough from the cluster centre, is also selected. However, this field should not be so far that the space density and mean reddening differ appreciably from that in the direction of the cluster. When this condition is satisfied, a statistical subtraction of the number of comparison field stars from the number of stars in the cluster region will reveal a net positive difference. However, this method only enables an estimation of the total membership of a cluster, but does not help in the determination of individual membership (Sagar & Joshi, 1978a). As such, since the requirement was for the individual membership of the programme clusters, only an approximate estimate of the field stars inside the cluster boundaries was made by visual inspection of the sky survey charts. This appears to be almost negligible due to the very small angular diameters of these clusters.

#### 3.3.4. Spectroscopic Criteria

In this method the membership is based on the fit between spectral - luminosity type (MKK classification) and position in the colour-magnitude diagram, taking into account the effects of stellar evolution. The limitation of this method is, that one cannot apply it for stars fainter than  $V \sim 12$  mag (Moffat, 1972) with telescopes of moderate size. However, the method described in Chapter 2, is capable of reaching up to about 15 mag with some tolerable uncertainties.

One may also note that while using the photometric criteria, there is no a priori way of identifying unusual stars. Therefore, astrophysically important peculiar objects, the runaway stars for instance, may not be recognized as such, while the kinematic methods help to identify them.

In light of the above discussions and in the absence of the proper motion studies, the photometric method has been given the preference, along with the provisional membership obtained from the modified objective grating - sky survey chart work being the starting point, if available. Thus, the individual membership in each cluster was determined and the results have been tabulated in the next chapter, along with the respective clusters. In general, out of the observed stars, those which appeared to be members in each of the programme clusters, have been found to be in the range of 10 to 30, with just one exception, for which 55 members have been counted.

#### **3.4. Procedure for the Determination of Reddening**

A fair knowledge of the interstellar reddening is necessary to determine intrinsic properties of the cluster stars. In UBV photometry, this reddening can be determined with the help of (U-B), (B-V) colour-colour diagram (Becker & Stock, 1954). Stars reddened by interstellar absorption are found displaced with respect to the unreddened stars of the same intrinsic colour parallel to the reddening line, the slope of which is given by the ratio of the colour excesses,

$$\frac{E(U-B)}{E(B-V)} = 0.72 \text{ (cf. Johnson \& Morgan, 1953).}$$

Thus, a comparison of the (U-B) versus (B-V) diagram of the main sequence (MS) stars for a given (reddened) cluster with the unreddened main sequence would reveal the amount of reddening. One would expect to find the reddened MS stars of the cluster displaced parallel to the reddening line by an amount equal to the colour excesses  $E(B-V)$  and  $E(U-B)$ , as is shown schematically in Fig.3.4. Thus, the interstellar reddening in the direction of the cluster can be determined.

The photometric sequences of open clusters in the colour-colour diagrams exhibit dispersions from one case to another. The causes of dispersion in a cluster sequence are differential extinction, stellar evolution, stellar duplicity, stellar rotation, differences in chemical composition, dispersion in ages of cluster stars, dispersion in the distances, presence of non-member stars and the inaccuracies in the data (Burki, 1975). The effect of differential reddening (or extinction) on the young cluster sequences is more because of the presence of the interstellar matter either inside, or in the vicinity of the cluster, or the circumstellar shells around the cluster stars (Burki, 1975; Wallenquist, 1975). If one considers only the MS member stars of the cluster, then the various effects mentioned above (apart from the differential extinction) produce dispersion of the order of 0.09 mag in the (U-B) versus (B-V) diagram (Burki, 1975).

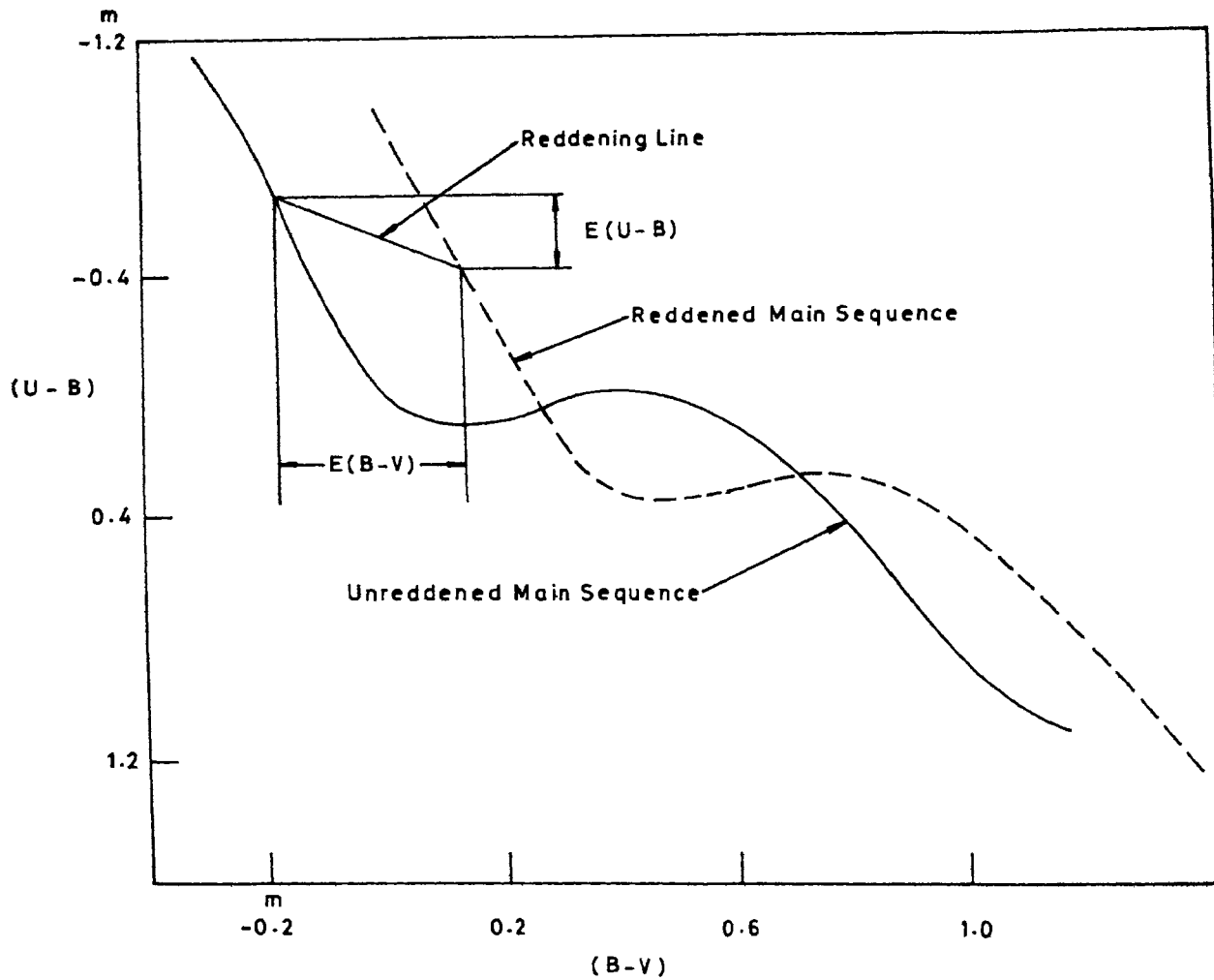


**Fig. 3.4.** Schematic description of the method of measuring  $E(B-V)$  and  $E(U-B)$  in the  $(B-V)$ ,  $(U-B)$  diagram. Unreddened MS is taken from Schmidt-Kaler (1965).

Consequently, the MS cluster members with dispersions  $\delta(B-V)$  larger than 0.09 mag which corresponds to  $\Delta E(B-V) \approx 0.11$  mag, (cf. Fig.3.5) clearly indicate the presence of non-uniform extinction across the cluster. For this reason, following Burki (1975), the minimum and maximum colour excesses were determined by fitting the measured MS stars to the intrinsic MS, as shown schematically in Fig.3.5. The difference  $\Delta E(B-V)$  between the maximum and minimum colour excesses is a measure of the differential extinction.

The reddening can also be determined using the Q-method of Johnson & Morgan (1953). The parameter Q of the UBV system is defined as

$$Q = (U-B) - \frac{E(U-B)}{E(B-V)} (B-V) \quad 3.12$$

$$\text{with } (B-V)_0 = 0.332 Q. \quad 3.13$$

However, this is valid only for O, B stars lying on the MS (Johnson & Morgan, 1953). The colour excess for such stars is then determined using the expression (Go lay, 1974),

$$E(B-V) = (B-V) \frac{(U-B) - \chi (B-V) - 0.05(B-V)^2}{3.012 - 0.05 (B-V)} \quad 3.14$$

$$\text{wherein } \chi = 0.62 - 0.3(B-V)_0 \text{ for } (B-V)_0 < - 0.09 \text{ mag} \quad 3.15$$

$$\text{and } \chi = 0.66 + 0.08(B-V)_0 \text{ for } (B-V)_0 > - 0.09 \text{ mag} \quad 3.16$$

as given by Kamp (1974).

The colour excess  $E(U-B)$  is then calculated using the expression

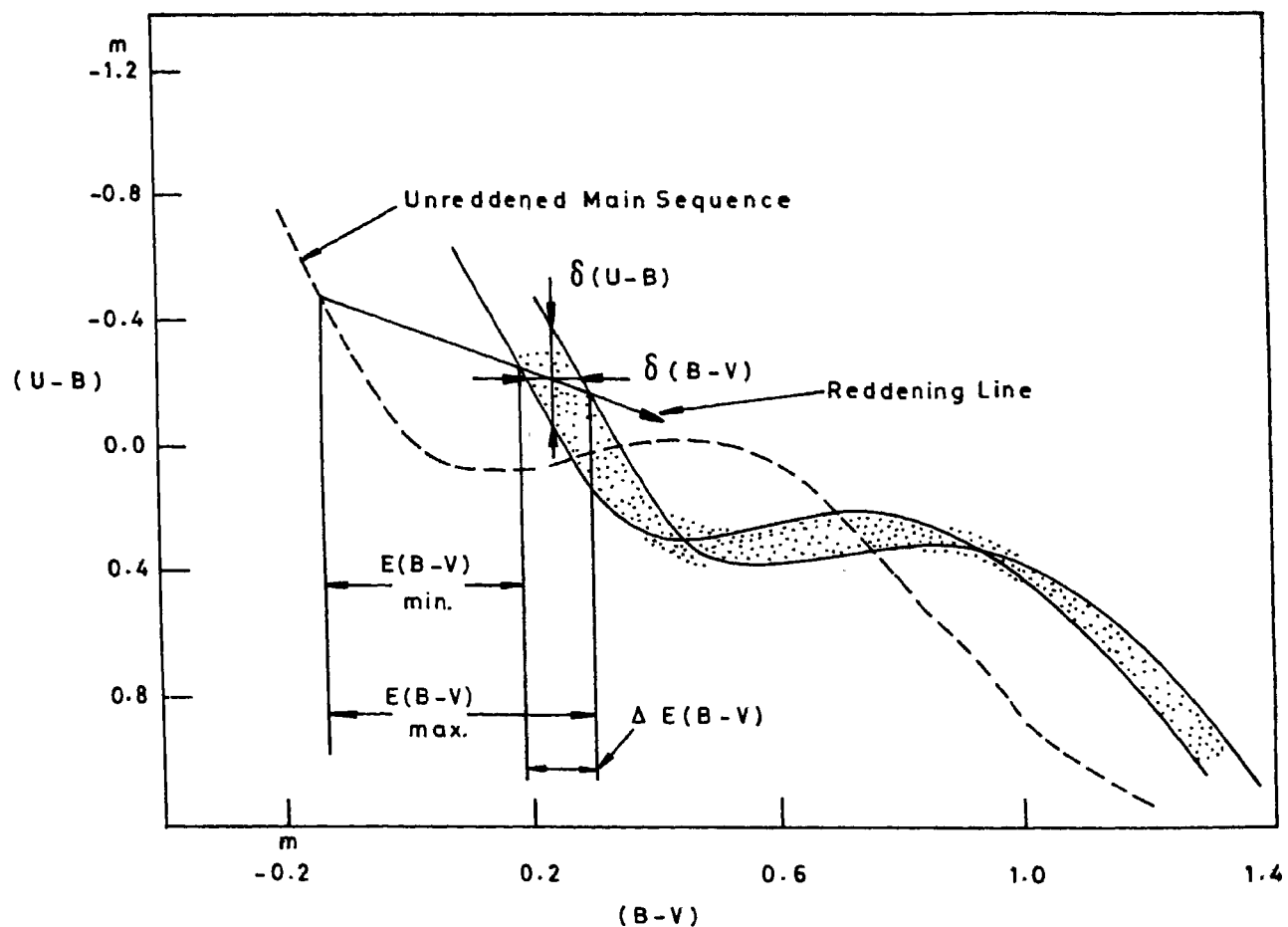


**Fig. 3.5.** Schematic description of the method of measuring  $\Delta E(B-V)$  in the  $(B-V)$ ,  $(U-B)$  diagram. The shaded area is the region occupied by the MS cluster members.  $E(B-V)_{\min}$  and  $E(B-V)_{\max}$  are the minimum and maximum  $(B-V)$  colour excesses of the stars.  $\delta(U-B)$  and  $\delta(B-V)$  are respectively the dispersion of the cluster MS in  $(U-B)$  and in  $(B-V)$ , at a given spectral type. Unreddened MS is taken from Schmidt-Kaler (1965).



$$E(U-B) = [X + 0.05 E(B-V)] E(B-V). \quad 3.17$$

### 3.5. Intrinsic Magnitudes and Colours

The intrinsic V magnitudes and the colours of the cluster stars were determined by correcting them for the reddening across the cluster. When the reddening was found variable, the corrections were applied individually to the cluster star. Otherwise, a mean value of the reddening was used. The total absorption  $A_V$  was calculated, from the relation

$$A_V = R.E(B-V)$$

using the value of the above mentioned  $E(B-V)$ . Following the discussions by Moffat & Schmidt-Kaler (1976), the ratio of total-to-selective absorption R is taken as 3.25, which is considered valid for all regions of the Galaxy with a mean error  $\pm 0.05$ , except perhaps for very local higher values in the young T Tauri stars. The intrinsic V magnitudes and the colours (denoted by subscript 'o') have then been calculated using the expressions

$$V_o = V - A_V \quad 3.18$$

$$(B-V)_o = (B-V) - E(B-V) \quad 3.19$$

$$\text{and } (U-B)_o = (U-B) - E(U-B). \quad 3.20$$

These intrinsic values were then used to construct the two main diagrams for the study of these clusters. They are the plots between  $(U-B)_o$  and  $V_o$  and the one between  $(B-V)_o$  and  $V_o$ . It is found that the  $E(B-V)$  of the programme clusters range from a quantity as small as 0.00 mag to about 1.20 mag.

And the range of  $A_V$  is found to be from 0.00 mag to 3.55 mag.

### 3.6. Procedure for the Determination of Distance to the Cluster

It is logical to assume that all the stars of a cluster are situated approximately at the same distance from the Sun. The distance modulus to the cluster is determined using  $V_0$ ,  $(B-V)_0$  and  $V_0$ ,  $(U-B)_0$  CMDs of the cluster. Theoretically, for young clusters, the distance determined from  $V_0$ ,  $(U-B)_0$  CMD is more reliable than that determined from the  $V_0$ ,  $(B-V)_0$  CMD since the upper part of the ZAMS is much less steep in the former diagram (Becker & Fenkart, 1970, 1971). In this work, the distance modulus of each cluster has been determined by fitting the standard ZAMS given by Schmidt-Kaler (1965) on to their respective  $V_0$ ,  $(B-V)_0$  and  $V_0$ ,  $(U-B)_0$  diagrams and the corresponding average value of the distance modulus ( $V_0-M$ ) has been adopted for the given cluster.

Once the distance modulus is known, the distance  $D$  to the cluster (in parsecs) can be calculated from the relation

$$\log D = 0.2 (V_0 - M) + 1 \quad 3.21$$

The uncertainty of the photometric distance determination is caused, first of all, by the inaccuracy in estimating the amount of absorption and secondly by the inaccuracy of the photometric zero point. These effects, if present, would change the distance modulus systematically by several tenths of a magnitude.

The absolute mean error  $E(D)$  in distance determination can be estimated from

$$E(D) = \pm 0.4605 [D \cdot E(V_0 - M)]. \quad 3.22$$

According to Becker (1963, 1972), the minimum uncertainty of the distance modulus determination is of the order of 10 per cent. Applying this method, the distances of the programme clusters have been found to be in the range of 0.6 kpc to 7.1 kpc with the mean error ranging from about  $\pm 0.10$  kpc to  $\pm 0.7$  kpc.

### 3.7. Procedure for the Determination of Age

The most widely used methods of age determination for open clusters are single parameter methods such as turn-off point (Sandage, 1957b, 1963; Gray, 1963), the brightest star on the MS (Lindoff, 1968), the bluest star and the second bluest star on the MS (Taff & Littleton, 1973; Harris, 1976) etc. The main feature of all these methods is their simplicity. Thus in order to estimate the age of a cluster, it would be sufficient to know the position of a few cluster members (the brightest, the bluest) in the HR - diagram. However, these single parameter methods are rather approximate, and often ages determined for the same cluster by different authors differ by factors of 2 to 5 (Palous et al., 1977).

The comparison of a cluster HR - diagram with sets of isochrones gives a considerably more accurate estimate of the cluster age (Palous et al., 1977). In this way, a majority of the evolved cluster members are taken into account.

The accuracy of age determination on the basis of isochrones depends on the following factors, (cf. Palous et al., 1977).

1. The accuracy of the observational data relating to the cluster HR-diagram.
2. The effects influencing star positions on the HR-diagram such as unresolved double stars, rotation of early type stars, circumstellar envelopes of young stars etc. Systematic errors may be introduced by the chemical composition variations from cluster to cluster, as well as by the uncertainties in the determination of distances and interstellar absorptions. Piskunov (1977) indicates that the variation of the chemical composition from cluster to cluster is a major source of error in age estimation. However, since the effect of this factor decreases as the stellar mass increases, it is relatively small on age estimation of the young cluster.
3. The evolutionary stage of the star (e.g. the giant phase, main sequence phase, gravitational contraction phase, etc.). According to Piskunov (1977) the error in age determination based on stars of equal masses, but evolving to or off the ZAMS, is about 2 orders of magnitude. For instance, the evolution in the gravitational contraction phase is relatively faster than the hydrogen burning or the giant phase of evolution.

4. The uncertainty due to the transformations

$$(B-V)_0 \rightarrow \log T_e \text{ and } M_V \rightarrow \log \frac{L}{L_\odot} .$$

However, it has been noted by Palous et al., (1977) that age uncertainties caused by the above effects are of the same order of magnitude as those introduced by random errors in  $V_0$  and  $(B-V)_0$  of each star in the HR - diagram. The same authors have also shown that while the absolute error in age estimation increases with cluster age, the relative error depends only slightly on the cluster age, decreasing somewhat for old clusters. The mean relative error has been found to be about 40%; the best determinations give about 20%, the worst about 70%.

In the present work, the isochrones given by Barbaro et al., (1969) have been used for stars evolving off the ZAMS in estimating the stellar ages. On the other hand, for stars in the stage of gravitational contraction, those computed by Iben (1965) have been used. These curves in the plane of  $(M_V, (B-V)_0)$  have been taken from the work of Joshi (1980).

The ages have also been derived by the method given by Sandage (1975b) for clusters which distinctly show the turn-off points. The age  $t$ , of the cluster is determined using the expression

$$t = 1.10 \times 10^{10} \frac{M}{L} \tag{3.23}$$

where  $M$  and  $L$  are mass and luminosity respectively, both in solar units. These two quantities correspond to the absolute

magnitude at the turn-off point and are taken from Schmidt-Kaler (1965).

The ages of the clusters covered in this study are in the range of  $6.0 \times 10^6$  to  $5.9 \times 10^8$  yrs.

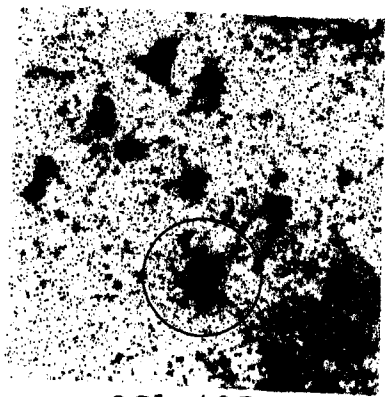
\*\*\*\*\*

## CHAPTER 4

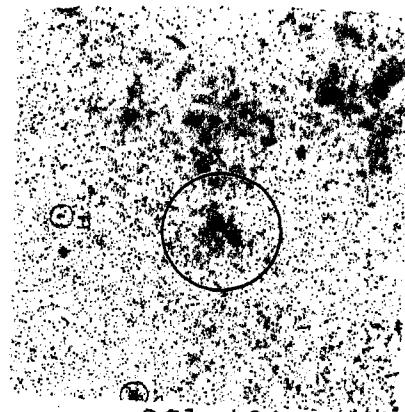
### OBSERVATIONS AND RESULTS

Out of the twelve clusters selected for the photometric observations, there are seven for which very little information exists. The remaining five clusters have some estimates of distances, though there seems to be a sizeable amount of discrepancy among the values given by various authors for any one cluster. The amount of interstellar reddening has been calculated only for two of these clusters, namely, OC1 501 and OC1 798. For OC1 501, RGU photometry is available, while UBV photometry is available for OC1 798. The latter has been specifically chosen as a test cluster to check the procedures followed in the present work. It is found that the results obtained for this cluster by FitzGerald, Jackson & Moffat (1977) match very closely with those obtained in the present work. The available information for the twelve clusters is compiled in Table 2.3, most of which comes from the OC1 catalogue.

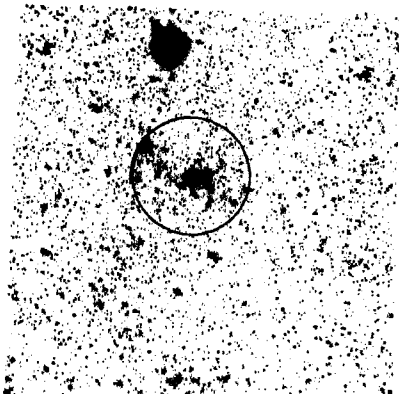
A brief description of the observations and the results obtained for each of these clusters are given in this chapter. The fields of these clusters, as seen directly on the respective sky survey charts, are presented in Fig.4.1. Excepting for OC1.798, the enlarged finding charts are made from the copies of the blue plates of the corresponding sky



OC1 427



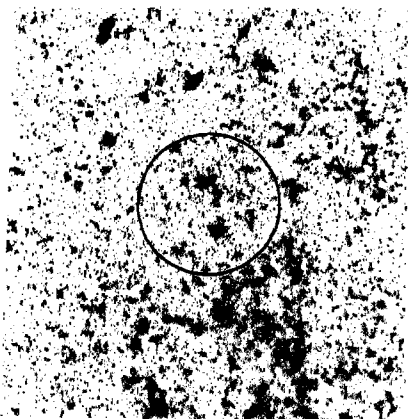
OC1 493



OC1 501



OC1 506



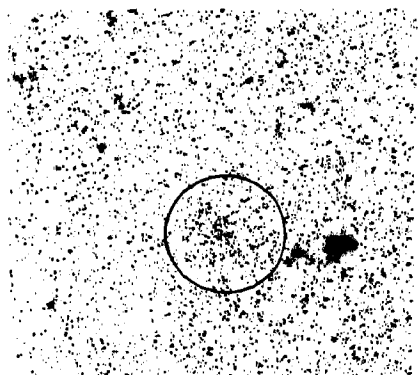
OC1 556



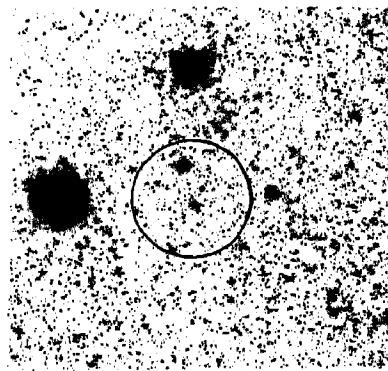
OC1 585

Fig. 4.1 The fields of the selected clusters as seen directly on the respective sky survey charts. The circles are drawn only for indicating the locations of the clusters.

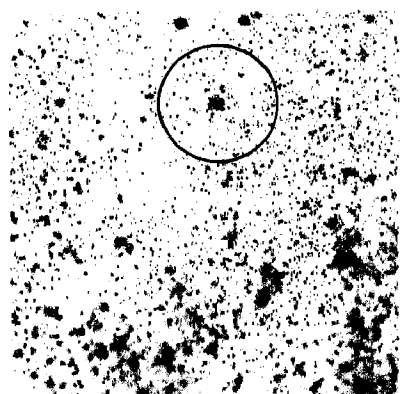




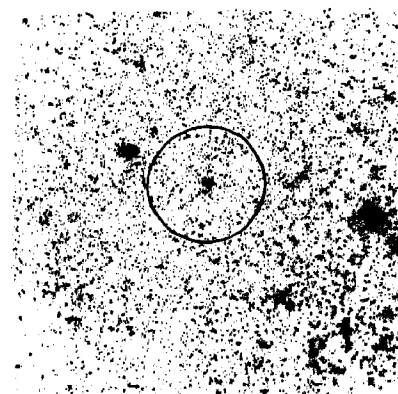
OCl 674



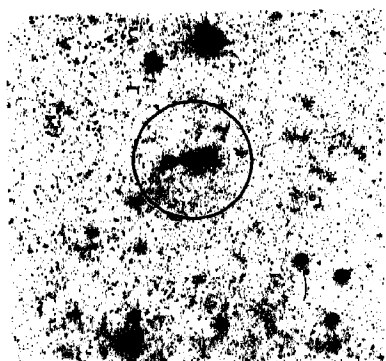
OCl 692



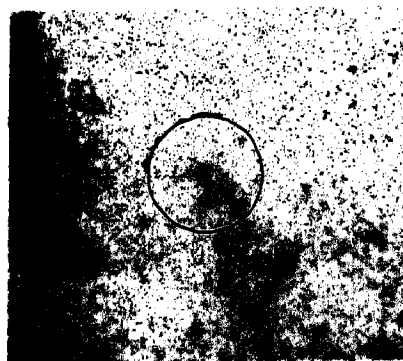
OCl 694



OCl 715



OCl 762



OCl 798

Fig. 4.1 (Continued)

survey charts. In all cases, the numbering of the individual stars, done in this work, has been used. For ten of them, this is the first numbering attempt. The following notations have been used in all the diagrams of this chapter.

|  |    |   |
|--|----|---|
| Filled circles or filled triangles     | }] | Members observed through photoelectric photometry |
| Unfilled circles or unfilled triangles | }] | Members observed through photographic photometry  |
| Half-filled circles                    | :  | Doubtful members                                  |
| Crosses                                | :  | Non-members                                       |

#### 4.1. OC1 427 (Czernik 20)

Czernik (1966) was the first one to consider this group of stars as a cluster with three hundred and twenty five possible members and estimated its angular diameter as 18 arcmin. Accordingly, Ruprecht (1966) classified it as II 2 r in the Trumpler system. The richness is obvious on the finding chart, which is displayed in Fig.4.2. This is the only 'rich' cluster in the present programme.

##### 4.1.1. Selection and Observations

This cluster was selected on the basis of the objective grating spectroscopy (cf. Chapter 2). The exposure time was 75 minutes on a 103a-0 emulsion and from this plate, spectral types could be assigned for a total of sixteen stars. This small number was due to the fact that the first and second order spectra of most of the stars were lost in the richness of the cluster.

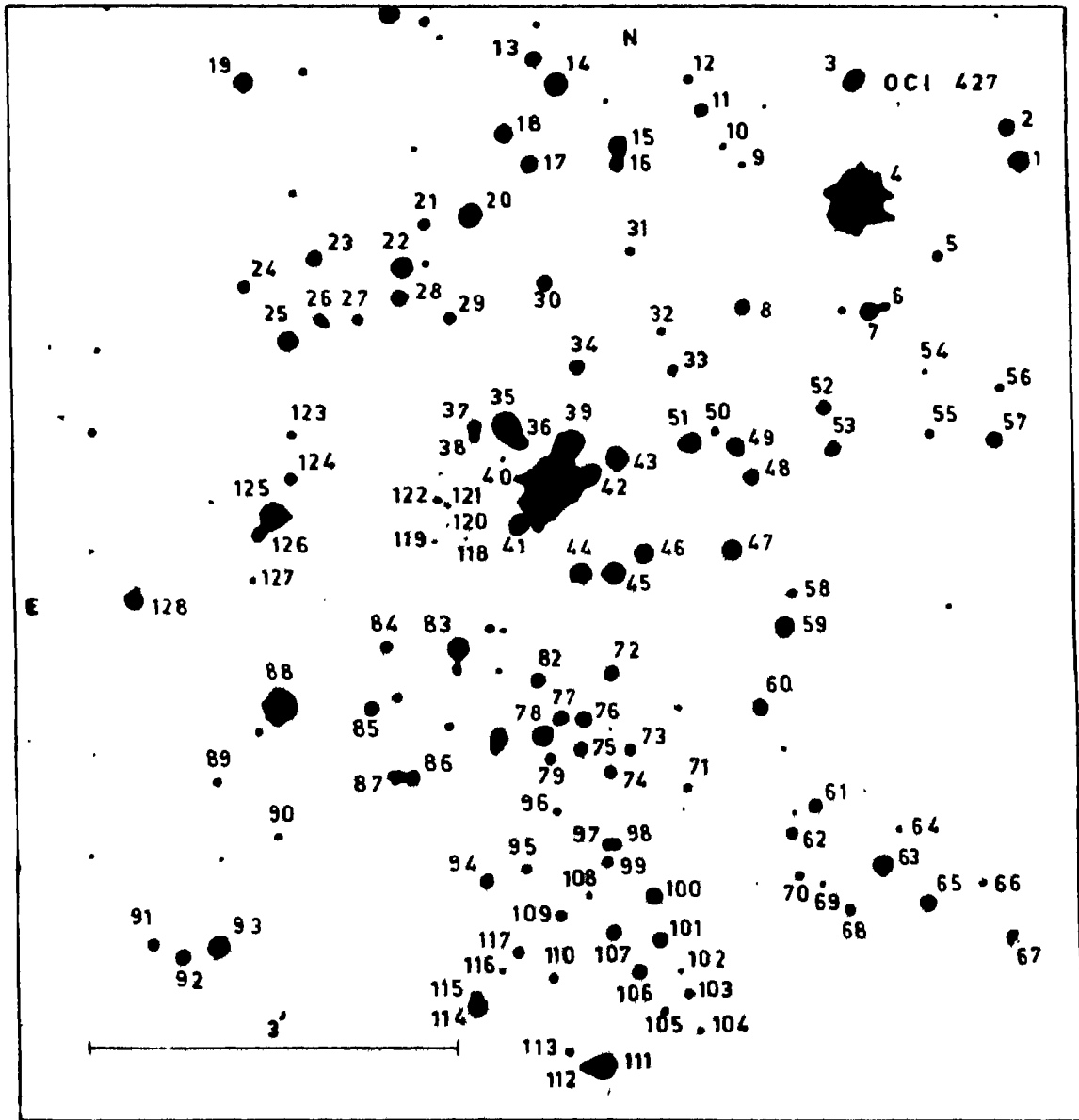


Fig. 4.2. Finding chart for the field of OC1 427.

The estimated spectral types are listed in Table 4.1 along with the V(POSS) magnitudes. Stars 4 and 40 show spectral types of B0 and B2 respectively with star 88 showing type B5. In the V(POSS) magnitude - spectral type plot shown in Fig.4.3, star 88 appears slightly to the right of the MS and therefore considered only as a doubtful member. Star 4 is perhaps too bright for this cluster. Further, its location is marginally away from the 'rich' area, thus making it a probable non-member. Stars 20 and 35 are considered as non-members, while stars 45 and 46 could be belonging to the giant category.

The photoelectric observations of this cluster were done using the 61-cm telescope at Siding Spring Observatory (cf. Section 3.1). Standardized magnitudes and colours for a total of twelve stars were obtained and the values are included in Table 4.1. The coefficients of the atmospheric extinction, the transformation coefficients and the zero-point constants (cf. Equations 3.6 to 3.11) are given below.

$$\begin{array}{llll} K_V = 0.165 & \epsilon = 5.435 & \zeta_V = 0.303 & \zeta \\ K_{(b-v)} = 0.155 & \mu = 0.034 & \zeta_{bv} = 0.785 & \text{values} \\ & & & \text{unchanged?} \\ K_{(u-b)} = 0.200 & \psi = 2.225 & \zeta_{ub} = -2.693 & \end{array}$$

The U, B, V photographs of this cluster were taken with the help of 102-cm telescope at Kavalur Observatory (cf. Section 3.2.1). The plate and filter combination along with the exposure times are as follows.

**Table 4.1.** The observational data for individual stars in the open cluster OC1 427.

| Star<br>No.               | Spectral<br>type | V<br>(Sky<br>survey) | V      | (B-V) | (U-B)  | $V_0$  | $(B-V)_0$ | $(U-B)_0$ | E(B-V) | Member-<br>ship |
|---------------------------|------------------|----------------------|--------|-------|--------|--------|-----------|-----------|--------|-----------------|
| 1                         | 2                | 3                    | 4      | 5     | 6      | 7      | 8         | 9         | 10     | 11              |
| Photoelectric photometry: |                  |                      |        |       |        |        |           |           |        |                 |
| 4                         | B0               | 8.8                  | 9.122  | 0.013 | -0.204 | -      | -         | -         | -      | -               |
| 8                         | -                | -                    | 14.454 | 0.270 | -0.178 | 13.154 | -0.13     | -0.46     | 0.4    | m               |
| 20                        | A0               | 12.2                 | 12.630 | 0.675 | 0.822  | -      | -         | -         | -      | -               |
| 30                        | B8               | 14.2                 | 14.669 | 0.381 | -0.033 | 13.073 | -0.11     | -0.39     | 0.491  | m               |
| 46                        | K5               | -                    | 12.234 | 1.449 | 1.120  | 10.755 | 0.994     | 0.795     | 0.455  | m               |
| 59                        | B5               | 12.2                 | 12.592 | 0.194 | -0.621 | 11.084 | -0.27     | -0.95     | 0.464  | m               |
| 83                        | -                | -                    | 11.725 | 1.434 | 1.134  | 10.246 | 0.979     | 0.809     | 0.455  | m               |
| 85                        | -                | -                    | 14.448 | 0.423 | 0.198  | 12.943 | -0.04     | -0.14     | 0.463  | m               |
| 88                        | B5               | 10.9                 | 10.526 | 0.198 | -0.348 | 9.33   | -0.17     | -0.61     | 0.368  | m?              |
| 93                        | -                | -                    | 12.192 | 0.197 | -0.587 | 10.707 | -0.26     | -0.92     | 0.457  | m               |
| Photographic photometry:  |                  |                      |        |       |        |        |           |           |        |                 |
| 2                         | -                | -                    | 13.44  | -0.11 | 0.15   | -      | -         | -         | -      | -               |
| 3                         | -                | -                    | 13.67  | 0.68  | 0.15   | -      | -         | -         | -      | -               |
| 11                        | -                | -                    | 15.44  | 0.33  | -0.15  | 13.90  | -0.14     | -0.49     | 0.47   | m               |
| 12                        | -                | -                    | 16.79  | 0.68  | -0.10  | -      | -         | -         | -      | -               |
| 13                        | -                | -                    | 14.98  | 0.39  | 0.24   | 13.65  | -0.02     | -0.06     | 0.41   | m               |
| 14                        | B5               | 13.0                 | 12.84  | 0.21  | -0.56  | 11.35  | -0.25     | -0.88     | 0.46   | m               |
| 15                        | -                | -                    | 13.80  | 0.28  | 0.17   | -      | -         | -         | -      | -               |
| 16                        | -                | -                    | 14.95  | 1.06  | 0.35   | -      | -         | -         | -      | -               |
| 17                        | -                | -                    | 14.30  | 0.50  | 0.33   | 12.82  | 0.04      | 0.00      | 0.46   | m               |
| 18                        | -                | -                    | 14.05  | 0.34  | -0.07  | 12.60  | -0.11     | -0.39     | 0.45   | m               |
| 19                        | -                | -                    | 12.71  | 0.25  | -0.47  | 11.18  | -0.22     | -0.80     | 0.47   | m?              |
| 22                        | -                | -                    | 13.17  | 0.25  | -0.55  | 11.50  | -0.26     | -0.92     | 0.51   | m               |
| 23                        | -                | -                    | 13.88  | 0.28  | -0.13  | 12.57  | -0.12     | -0.42     | 0.40   | m               |

| 1  | 2  | 3    | 4     | 5    | 6     | 7     | 8     | 9     | 10   | 11 |
|----|----|------|-------|------|-------|-------|-------|-------|------|----|
| 24 | -  | -    | 14.07 | 0.84 | 0.12  | -     | -     | -     | -    | -  |
| 25 | B5 | 12.6 | 12.80 | 0.23 | -0.57 | 11.23 | -0.26 | -0.92 | 0.49 | m  |
| 28 | -  | -    | 14.50 | 0.33 | -0.10 | 13.04 | -0.12 | -0.42 | 0.41 | m  |
| 29 | -  | -    | 15.94 | 1.00 | 0.95  | -     | -     | -     | -    | -  |
| 35 | A5 | 12.5 | 12.07 | 0.78 | -0.14 | -     | -     | -     | -    | -  |
| 37 | -  | -    | 16.14 | 0.61 | 0.65  | 14.66 | 0.15  | 0.33  | 0.46 | m  |
| 39 | -  | -    | 12.72 | 0.24 | -0.55 | 11.15 | -0.25 | -0.90 | 0.49 | m  |
| 40 | B2 | 11.7 | 11.47 | 0.15 | -0.45 | 10.34 | -0.20 | -0.69 | 0.35 | m  |
| 41 | -  | -    | 14.94 | 0.68 | 0.24  | 13.46 | 0.22  | -0.09 | 0.46 | m  |
| 42 | -  | -    | 16.02 | 0.82 | 0.57  | 14.54 | 0.37  | 0.24  | 0.46 | m  |
| 43 | B8 | 13.6 | 13.47 | 0.25 | -0.31 | 12.11 | -0.17 | -0.61 | 0.42 | m  |
| 44 | B5 | 12.9 | 13.25 | 0.25 | -0.42 | 11.77 | -0.21 | -0.74 | 0.46 | m  |
| 45 | K0 | 12.4 | 11.97 | 1.28 | 0.97  | 10.49 | 0.82  | 0.64  | 0.46 | m  |
| 47 | B5 | 12.5 | 12.90 | 0.20 | -0.58 | 11.44 | -0.25 | 0.90  | 0.45 | m  |
| 48 | -  | -    | 14.29 | 0.25 | 0.38  | -     | -     | -     | -    | -  |
| 49 | -  | -    | 14.36 | 0.20 | -0.06 | 13.49 | -0.07 | -0.25 | 0.27 | m  |
| 51 | -  | -    | 12.26 | 1.21 | 0.99  | 10.78 | 0.76  | 0.66  | 0.46 | m  |
| 52 | -  | -    | 14.54 | 0.29 | -0.35 | 12.95 | -0.20 | -0.69 | 0.49 | m  |
| 53 | -  | -    | 14.19 | 1.12 | -0.22 | -     | -     | -     | -    | -  |
| 55 | -  | -    | 14.41 | 1.89 | 0.61  | -     | -     | -     | -    | -  |
| 56 | -  | -    | 16.62 | 0.82 | -0.59 | -     | -     | -     | -    | -  |
| 57 | -  | -    | 13.70 | 0.28 | -0.16 | 12.37 | -0.13 | -0.46 | 0.41 | m  |
| 60 | -  | -    | 13.47 | 0.24 | -0.41 | 12.01 | -0.21 | -0.73 | 0.45 | m  |
| 61 | -  | -    | 12.98 | 1.51 | 1.29  | 11.51 | 1.06  | 0.97  | 0.46 | m  |
| 62 | -  | -    | 15.39 | 0.52 | -0.58 | -     | -     | -     | -    | -  |
| 63 | -  | -    | 12.51 | 0.26 | -0.63 | 10.73 | -0.29 | -1.01 | 0.55 | m  |
| 65 | -  | -    | 13.57 | 0.33 | -0.17 | 12.05 | -0.14 | -0.51 | 0.47 | m  |
| 66 | -  | -    | 17.02 | 0.23 | -0.53 | -     | -     | -     | -    | -  |
| 67 | -  | -    | 12.38 | 1.21 | 0.94  | 10.90 | 0.76  | 0.62  | 0.46 | m  |
| 68 | -  | -    | 15.83 | 1.08 | -1.20 | -     | -     | -     | -    | -  |
| 70 | -  | -    | 16.40 | 0.80 | 0.24  | 14.92 | 0.35  | -0.08 | 0.46 |    |

---

| (1) | (2) | (3)  | (4)   | (5)  | (6)   | (7)   | (8)   | (9)   | (10) | (11) |
|-----|-----|------|-------|------|-------|-------|-------|-------|------|------|
| 71  | -   | -    | 16.51 | 0.81 | 1.01  | -     | -     | -     | -    |      |
| 72  | -   | -    | 15.58 | 0.81 | 0.18  | -     | -     | -     | -    |      |
| 73  | -   | -    | 15.92 | 0.55 | 0.11  | 13.81 | -0.10 | -0.36 | 0.65 | m    |
| 75  | -   | -    | 15.76 | 0.59 | 0.22  | 14.28 | 0.13  | -0.10 | 0.46 | m    |
| 76  | -   | -    | 14.51 | 0.38 | -0.14 | 12.81 | -0.14 | -0.52 | 0.52 | m    |
| 77  | -   | -    | 15.40 | 0.49 | -0.01 | 13.39 | -0.13 | -0.46 | 0.62 | m    |
| 78  | -   | -    | 13.44 | 0.25 | -0.37 | 12.02 | -0.19 | -0.68 | 0.44 | m    |
| 80  | -   | -    | 15.75 | 0.68 | 0.54  | 14.27 | 0.22  | 0.21  | 0.46 | m    |
| 81  | -   | -    | 13.99 | 0.27 | -0.16 | 12.74 | -0.12 | -0.44 | 0.39 | m    |
| 82  | -   | -    | 15.29 | 0.51 | 0.35  | 13.81 | 0.05  | 0.03  | 0.46 | m    |
| 84  | -   | -    | 15.77 | 0.64 | 0.37  | 14.29 | 0.18  | 0.05  | 0.46 | m    |
| 86  | B8  | 14.2 | 14.40 | 0.27 | 0.01  | 13.29 | -0.07 | -0.24 | 0.34 | m    |
| 87  | B8  | 14.0 | 14.32 | 0.38 | 0.11  | 12.90 | -0.06 | -0.21 | 0.44 | m    |
| 89  | -   | -    | 15.92 | 1.49 | -0.03 | -     | -     | -     | -    | -    |
| 90  | -   | -    | 15.24 | 1.48 | 0.24  | -     | -     | -     | -    | -    |
| 91  | -   | -    | 14.43 | 0.31 | -0.36 | 12.75 | -0.21 | -0.74 | 0.52 | m    |
| 92  | -   | -    | 13.65 | 0.29 | -0.17 | 12.28 | -0.13 | -0.48 | 0.42 | m    |
| 100 | -   | -    | 13.68 | 0.44 | -0.06 | 11.85 | -0.13 | -0.48 | 0.57 | m    |
| 101 | -   | -    | 14.31 | 0.41 | 0.61  | -     | -     | -     | -    |      |
| 106 | -   | -    | 14.16 | 0.48 | 0.25  | 11.91 | -0.09 | -0.30 | 0.69 | m    |
| 107 | -   | -    | 14.45 | 0.36 | 0.01  | 12.99 | -0.21 | -0.75 | 0.45 | m    |
| 111 | -   | -    | 12.11 | 0.24 | -0.50 | 10.60 | -0.23 | -0.84 | 0.47 | m    |
| 112 | -   | -    | 15.82 | 0.71 | 1.25  | -     | -     | -     | -    | -    |
| 114 | -   | -    | 12.90 | 0.26 | -0.47 | 11.31 | -0.23 | -0.82 | 0.49 | m    |

---

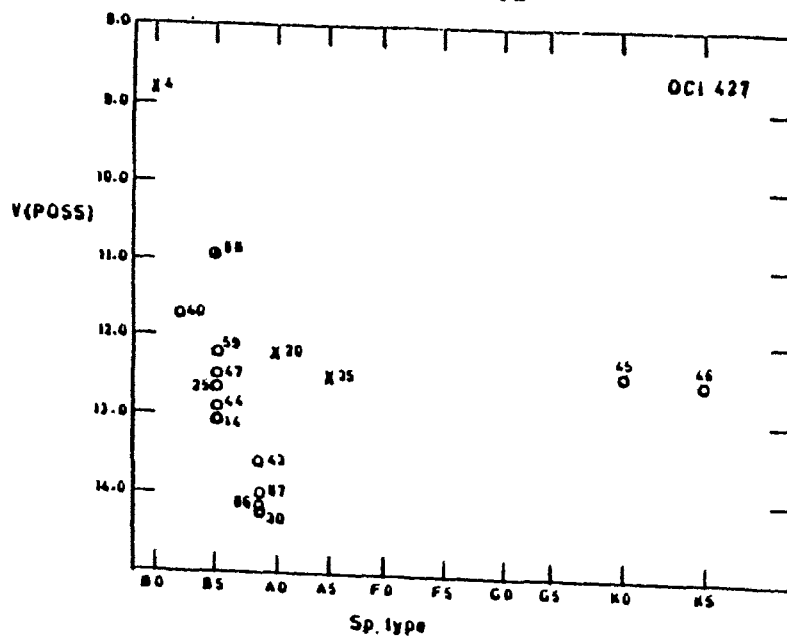


Fig. 4.3. Spectral types obtained from the modified objective-grating spectra plotted against the V magnitudes estimated from the POSS charts, for the stars in the field of OC1 427.

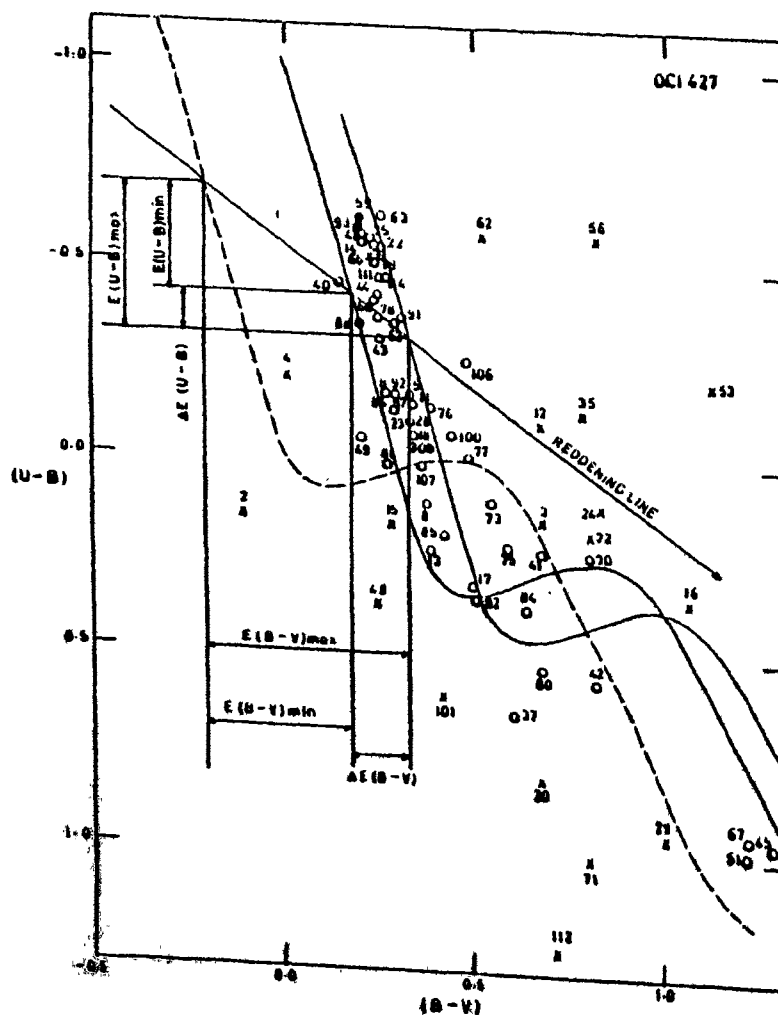


Fig. 4.4. The colour-colour diagram (CCD) of OC1 427. The dashed line is the unreddened main sequence (MS) taken from Schmidt-Kaler (1965).



| <u>Plate</u> | <u>Filter</u> | <u>Exposure time</u> |
|--------------|---------------|----------------------|
| 103a-0       | UG2           | 60 min for U         |
| 103a-0       | GG13          | 60 min for B         |
| IIa-D        | GG11          | 60 min for V         |

From these plates, the photographic magnitudes were obtained for a total of seventyseven stars (including the twelve photoelectrically observed stars) on an arbitrary scale, which were then standardized using the above mentioned photoelectric observations (cf. Section 3.2.2). These magnitudes and colours are also listed in Table 4.1.

#### 4.1.2. Membership

In the absence of any other information about this cluster, only photometric criteria were used to determine the membership of the individual stars. The CCD and the two CMD's of this cluster were examined for this purpose as described in Section 3.3. Figs. 4.4, 4.5 & 4.6 respectively show the CCD, the (B-V) vs. V diagram and the (U-B) vs. V diagram. In spite of the slightly larger scatter a majority of the stars appear to be forming a sequence in all the three diagrams. By marking the boundaries for the stars in the most likely sequence on the CCD and by picking out the same stars on the two CMD's, a total of fiftyfive stars have been adopted as the most probable members of the cluster out of the observed seventyseven stars. Six of the members are seen to be located in the region of red giants. Only star 88 appears to be a little too bright to be a member, if the giants are considered as

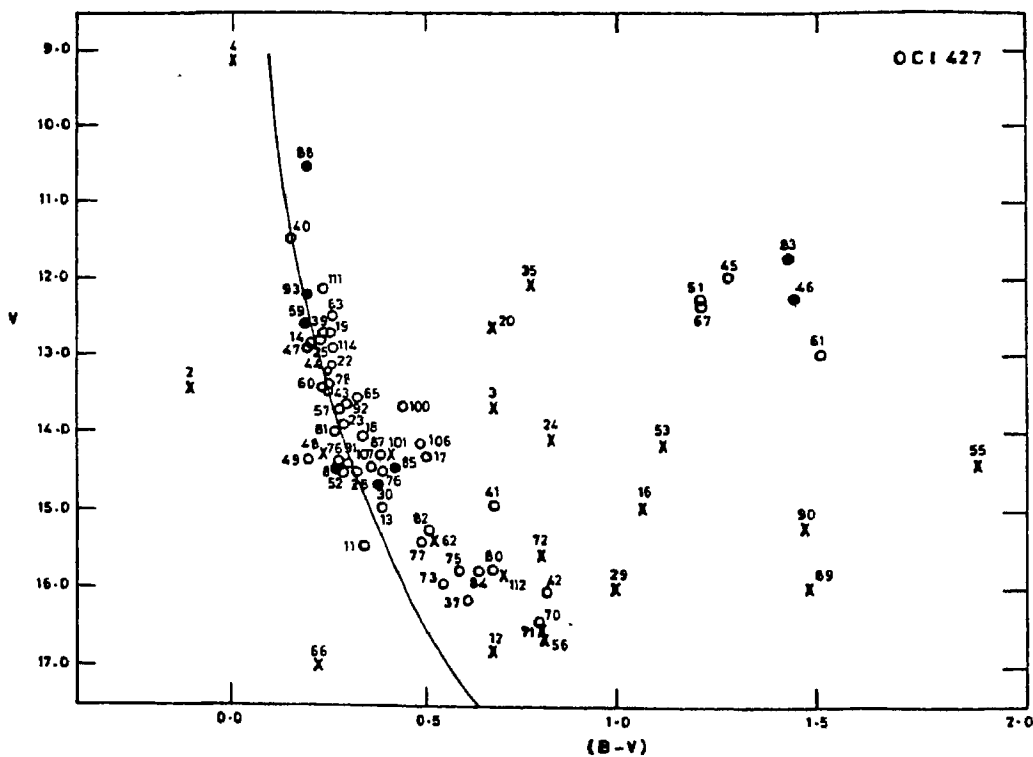


Fig. 4.5. The  $(B-V)$ ,  $V$  diagram (CMD) of OC1 427. The solid curve represents the zero age main sequence (ZAMS) fitted onto the cluster CMD.

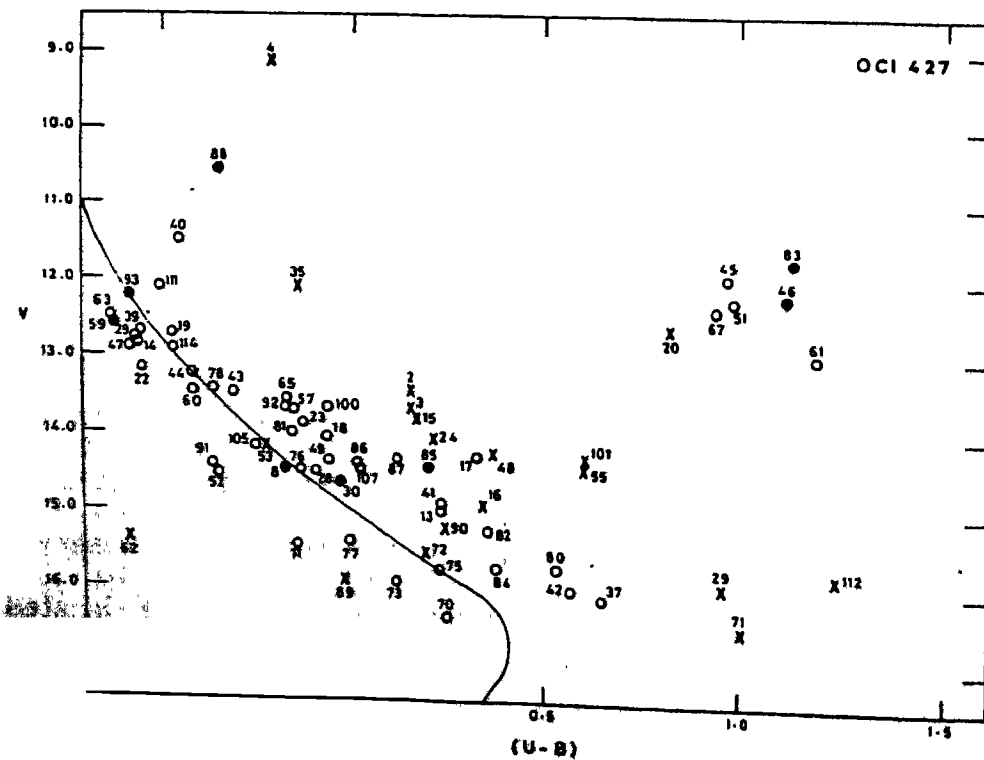


Diagram (CMD) of OC1 427. The solid curve represents the ZAMS fitted onto the cluster CMD.

members. Therefore, it (star 88) is taken as a doubtful member. All the members are denoted by 'm' in Table 4.1, with the doubtful members as m?.

#### 4.1.3. Reddening

The CCD in Fig. 4.4 shows a sequence formed by most of the stars. The boundaries of this sequence show a difference between  $E(B-V)_{\max}$  and  $E(B-V)_{\min}$  as

$$\Delta E(B-V) = 0.15 \text{ mag.}$$

Similarly  $\Delta E(U-B) = 0.11 \text{ mag.}$

These, being slightly larger than the values due to the natural dispersion (cf. Section 3.4), suggest a variable extinction across the field of the cluster. Hence the stars were corrected individually for the interstellar reddening, which was found to vary between  $E(B-V)_{\max} = 0.53 \text{ mag}$  and  $E(B-V)_{\min} = 0.38 \text{ mag}$ . Similarly  $E(U-B)_{\max} = 0.38 \text{ mag}$  and  $E(U-B)_{\min} = 0.27 \text{ mag}$ . The individual  $E(B-V)$  values have been included in Table 4.1.

Using these individual  $E(B-V)$  values, the corresponding values of  $A_V$  were obtained and were found to be between 1.72 mag and 1.24 mag. These, in turn, were used to correct the observed  $V$  values. All these corrected magnitudes and colours are included in Table 4.2 as  $V_0$ ,  $(B-V)_0$  and  $(U-B)_0$ .

#### 4.1.4. Distance

The value of the distance modulus of this cluster has been determined by fitting the ZAMS given by Schmidt-Kaler (1965) onto the  $V_0$ ,  $(B-V)_0$  and  $V_0$ ,  $(U-B)_0$  diagrams as shown in Fig. 4.7. The estimates of the true distance modulus as obtained from

these two CMD's are respectively 13.25 mag and 13.05 mag, yielding an average value of 13.15 mag. Then the distance to the cluster based on Equation 3.21 is

$$D = 4.16 \pm 0.14 \text{ kpc.}$$

#### 4.1.5. Age of Cluster

The HR-diagram of the cluster is plotted in Fig.4.8 for the above mentioned true distance modulus of 13.15 mag. On this diagram, the isochrones given by Barbaro et al. (1969) have been drawn in order to determine the age from the MS and post-MS stars. Star nos.88 and 40, indicate the slightly evolved phase and show a range in age as  $2.2 \times 10^7$  to  $3.7 \times 10^7$  years. The red giant stars give a slightly older age range of  $5.0 \times 10^7$  to  $7.1 \times 10^7$  years.

There are a few stars, which are apparently located in the pre-MS contracting phase. According to the isochrones given by Iben (1965) for this phase, it is found that they are between  $1.0 \times 10^6$  and  $1.75 \times 10^6$  years. Since most of the stars in the upper part of the MS, are in the age range of  $1.0 \times 10^7$  to  $2.2 \times 10^7$ , the cluster appears to be young enough to contain the pre-MS contracting stars. This aspect throws some doubts on the membership of the stars in the red giant area. However, dispersion in ages of cluster stars is possible, since star formation in clusters is not necessarily takes place over an interval of approximately (cf. Herbig, 1962; Iben & Talbot, 1966; Williams

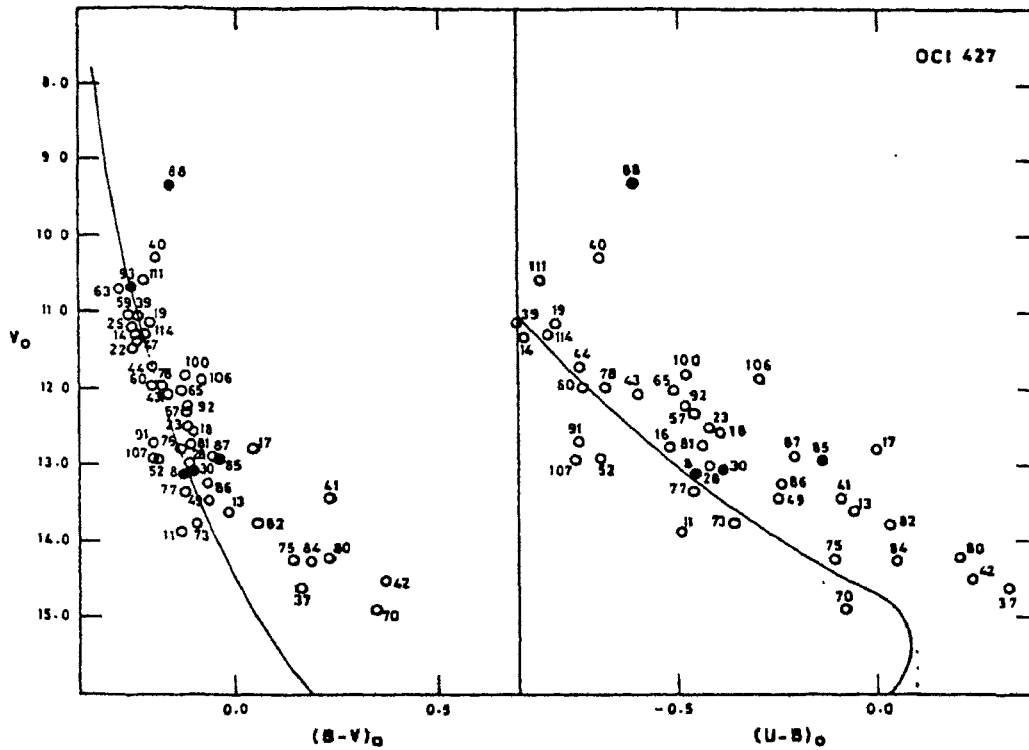


Fig. 4.7. The intrinsic  $(B-V)_0$ ,  $V_0$  and  $(U-B)_0$ ,  $V_0$  diagrams (CMDs) of OC1 427. The solid curves represents the ZAMS, taken from Schmidt-Kaler (1965), fitted onto the cluster CMDs.

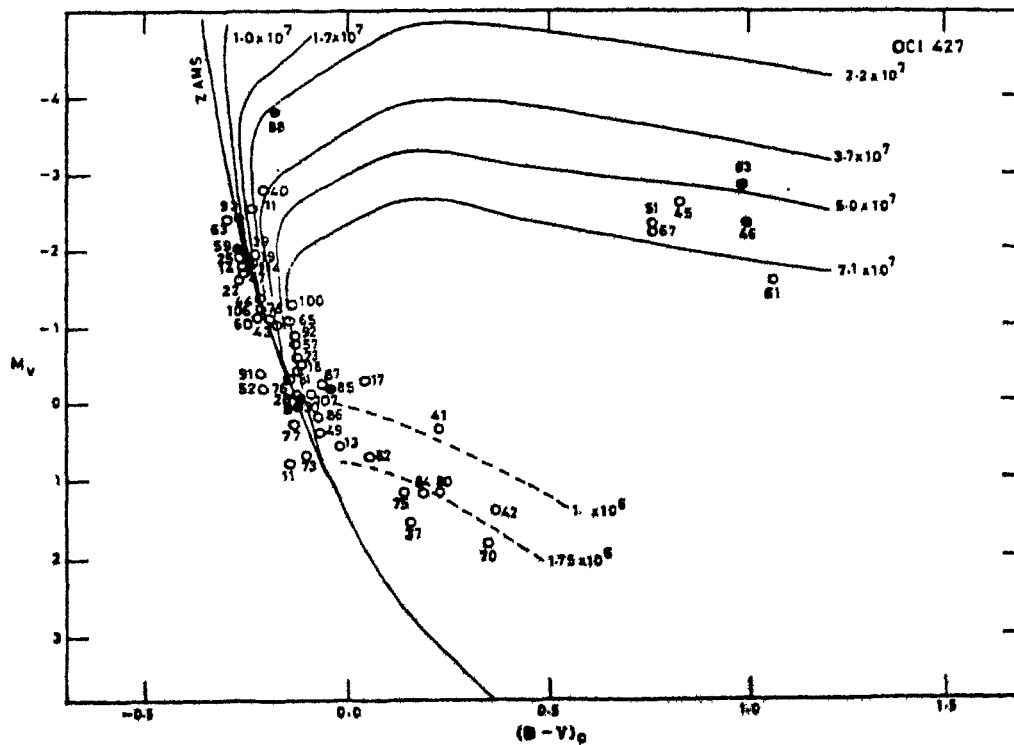


Fig. 4.8. HR-diagram of OC1 427. The post-MS isochrones are from Barbaro et al. (1969) and the dashed lines represent the pre-MS isochrones taken from Iben (1965). The ages are indicated in years alongside the isochrones.

& Cremin, 1969; McNamara, 1976; Piskunov, 1977; Götz, 1977; Sagar & Joshi, 1978a, 1978b, 1979).

The age of this cluster has also been determined on the basis of the earliest  $(B-V)_0$  on the MS. This value is - 0.26 mag and yields an age of  $1 \times 10^7$  years. Thus the total dispersion in age seems to be from  $1.0 \times 10^7$  to  $7.1 \times 10^7$  years, if the pre-MS stars are not considered. However, the cluster is young enough to be taken as a spiral arm tracer.

#### 4.2. OC1 493 (Czernik 25)

This cluster was also first identified by Czernik (1966), who estimated its angular diameter to be 7 arcmin with fortyfour stars in it. Ruprecht (1966) classified it as II 2 p in the Trumpler system. Fig.4.9 gives the finding chart for this cluster.

##### 4.2.1. Selection and observations

A photograph of this cluster using the objective grating spectroscopic technique (cf. Section 2.2) taken with an exposure time of 80 minutes, yielded spectral types for a total of fifteen stars in the field of the cluster. From a plot between these spectral types and the  $V(\text{POSS})$  magnitudes shown in Fig.4.10 (cf. Table 4.2), star 4 is seen to be on the main sequence, with a spectral type of B3. Stars 27 and 28 appear to have just evolved from the main sequence and stars 31 and 36 are likely members of its giant branch. Stars 16, 20, 21 and 23 are considered to be non-members since their location on this diagram is very different from the

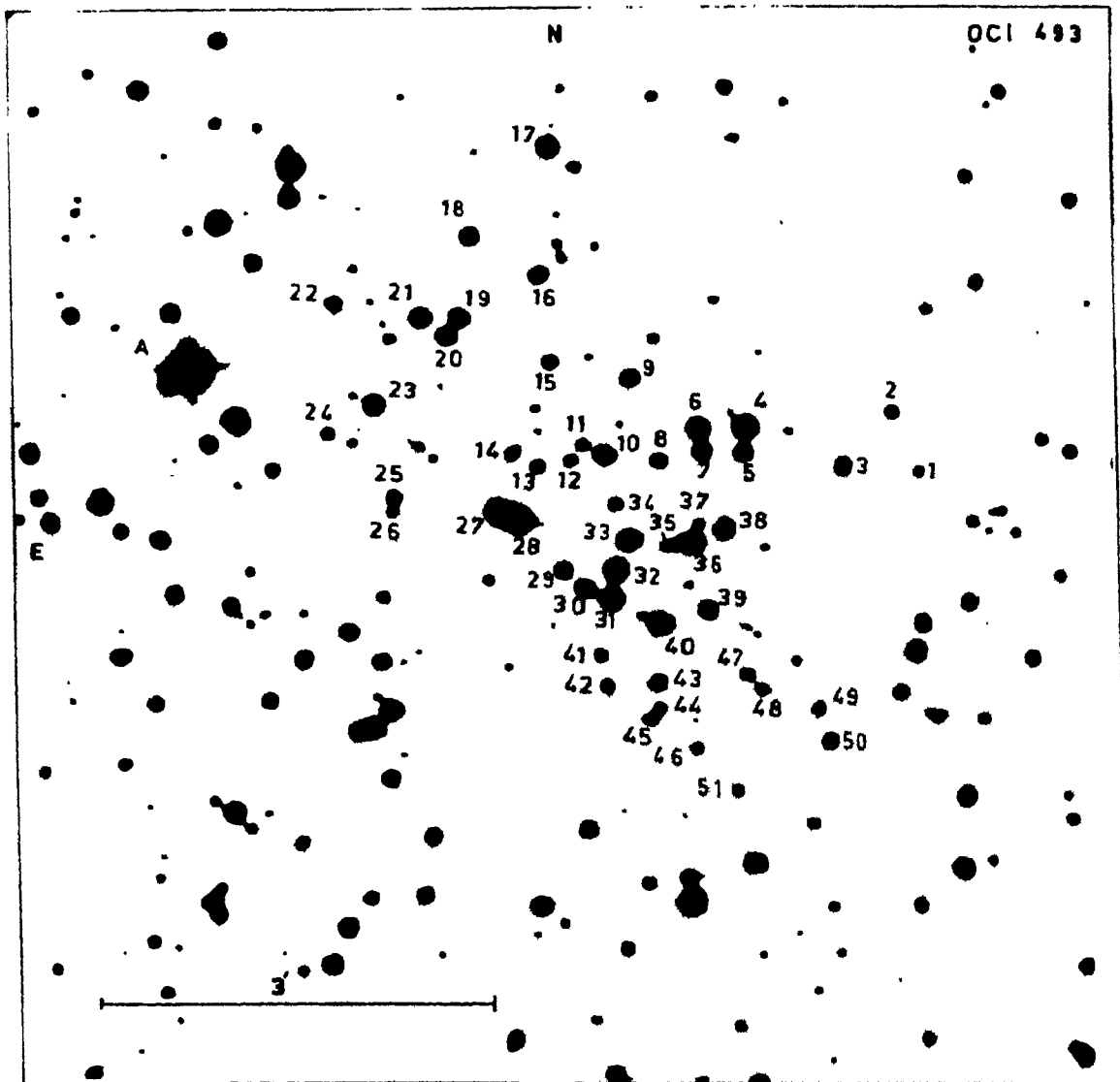


Fig. 4.9. Finding chart for the field of OC1 493.

**Table 4.2.** The observational data for individual stars in the open cluster OC1 493.

| Star No.                  | Spectral Type | V (Sky survey) | V      | (B-V) | (U-B)  | $V_0$  | $(B-V)_0$ | $(U-B)_0$ | Membership |
|---------------------------|---------------|----------------|--------|-------|--------|--------|-----------|-----------|------------|
| 1                         | 2             | 3              | 4      | 5     | 6      | 7      | 8         | 9         | 10         |
| Photoelectric photometry: |               |                |        |       |        |        |           |           |            |
| 4                         | B3            | 13.6           | 13.935 | 0.358 | -0.469 | 12.034 | -0.227    | -0.899    | m          |
| 7                         | -             | -              | 14.987 | 0.414 | -0.248 | 13.086 | -0.171    | -0.678    | m          |
| 8                         | B8            | 15.0           | 15.024 | 0.496 | -0.015 | 13.123 | -0.089    | -0.445    | m          |
| 23                        | G5            | 14.5           | 14.390 | 0.849 | 0.792  | -      | -         | -         | -          |
| 27                        | A0            | 12.3           | 12.627 | 0.516 | 0.395  | 10.726 | -0.069    | -0.035    | m          |
| 28                        | B8            | 12.3           | 12.462 | 0.487 | 0.179  | 10.561 | -0.098    | -0.251    | m          |
| 30                        | A0            | 15.0           | 15.402 | 0.548 | 0.194  | 13.501 | -0.037    | -0.236    | m          |
| 31                        | K5            | 12.5           | 13.087 | 0.524 | 1.316  | 11.186 | 0.939     | 0.886     | m          |
| 32                        | -             | -              | 13.780 | 0.540 | 0.451  | 11.879 | -0.045    | 0.021     | m          |
| 33                        | B5            | 14.0           | 14.300 | 0.357 | -0.363 | 12.399 | -0.228    | -0.793    | m          |
| 38                        | B8            | 14.6           | 14.469 | 0.467 | 0.209  | 12.568 | -0.118    | -0.221    | m          |
| 39                        | -             | -              | 15.009 | 0.621 | 0.409  | 13.198 | 0.036     | -0.021    | m          |
| 40                        | -             | -              | 13.627 | 0.499 | 0.285  | 11.726 | -0.086    | -0.145    | m          |
| Photographic photometry:  |               |                |        |       |        |        |           |           |            |
| 3                         | K0            | 15.0           | 15.14  | 0.93  | 1.13   | -      | -         | -         | -          |
| 5                         | -             | -              | 15.51  | 0.18  | 0.20   | -      | -         | -         | -          |
| 6                         | -             | -              | 14.09  | 0.53  | 0.41   | 12.19  | -0.06     | -0.03     | m          |
| 9                         | -             | -              | 14.39  | 0.56  | 0.35   | 12.49  | -0.03     | -0.09     | m          |
| 10                        | -             | -              | 15.56  | 0.61  | 0.58   | 13.65  | 0.02      | 0.15      | m          |
| 15                        | -             | -              | 15.70  | 0.93  | 1.65   | -      | -         | -         | -          |
| 16                        | B5            | 15.0           | 14.93  | 0.76  | 0.99   | -      | -         | -         | -          |
|                           |               |                | 14.02  | 0.41  | 0.32   | -      | -         | -         | -          |
|                           |               |                | 15.59  | 0.12  | 0.22   | -      | -         | -         | -          |
|                           |               |                | 13.98  | 1.51  | 1.76   | -      | -         | -         | -          |
|                           |               |                | 14.85  | 0.87  | 1.22   | -      | -         | -         | -          |
|                           |               |                | 14.58  | 0.89  | 0.69   | -      | -         | -         | -          |



---

| (1) | (2) | (3)  | (5)   | (6)  | (7)  | (8)   | (9)  | (10) | (11) |
|-----|-----|------|-------|------|------|-------|------|------|------|
| 29  |     |      | 15.68 | 0.70 | 0.48 | 13.78 | 0.12 | 0.05 | m    |
| 36  | K5  | 12.7 | 13.02 | 1.46 | 1.19 | 11.12 | 0.87 | 0.76 | m    |
| 43  |     |      | 14.93 | 0.91 | 1.28 | -     | -    | -    | -    |
| 50  |     |      | 15.63 | 0.91 | 1.20 | -     | -    | -    | -    |
| 51  |     |      | 13.06 | 0.42 | 0.11 | -     | -    | -    | -    |
| 52  |     |      | 14.21 | 0.60 | 0.46 | -     | -    | -    | -    |

---

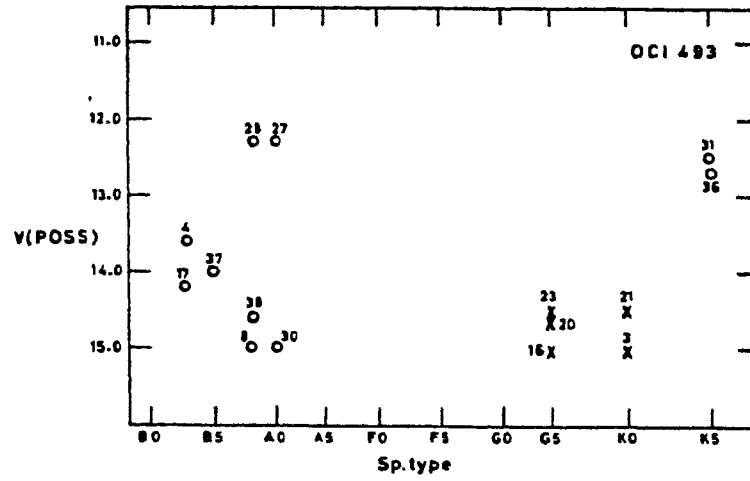


Fig. 4.10. Spectral types obtained from the modified objective-grating spectra plotted against the V magnitudes estimated from the POSS charts, for the stars in the field of OC1 493.

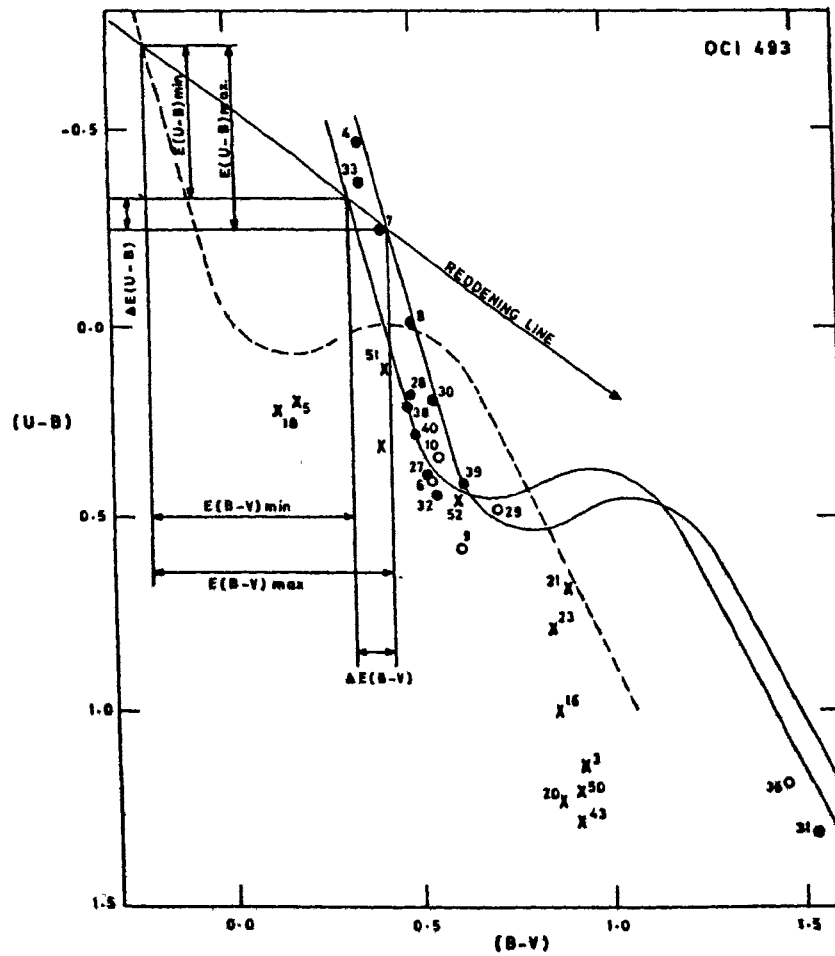


Fig. 4.11. The colour-colour diagram (CCD) of OC1 493. The dashed line is the unreddened main sequence (MS) taken from Schmidt-Kaler (1965).

general trend for the rest of the stars. Since star 4 is of spectral type B3 and is on the main sequence, this cluster is considered as a young one.

The photoelectric observations of this cluster were done using the 61-cm telescope of the Siding Spring Observatory (cf. Section 3.1). Standardized magnitudes and colours for a total of thirteen stars were obtained and the values are included in Table 4.2. The atmospheric extinction coefficients, the transformation coefficients and the zero-point constants (cf. Equations 3.6 to 3.11) are tabulated below.

$$\begin{array}{llll}
 K_V = 0.170 & \epsilon = 5.595 & \zeta_V = 0.298 & ? \text{ interchanged?} \\
 K_{b-v} = 0.125 & \mu = 0.005 & \zeta_{bv} = 0.849 & ? \\
 K_{u-b} = 0.223 & \psi = 2.385 & \zeta_{ub} = -2.857 & 
 \end{array}$$

The direct photography of this cluster was done using the 1-m telescope at Siding Spring Observatory (cf. Section 3.2.1). The plate and filter combination along with the exposure times are as under.

| <u>Plate</u> | <u>Filter</u> | <u>Exposure time</u> |
|--------------|---------------|----------------------|
| II a-0       | UG 2          | 60 minutes for U     |
| 103 a-0      | GG 13         | 30 minutes for B     |
| II a-D       | GG 14         | 30 minutes for V     |

From these plates, the photographic magnitudes were obtained for a total of thirtyone (including the thirteen photoelectrically observed ones) on an arbitrary scale, which were then standardized using the above mentioned photoelectric observations.

(cf. Section 3.2.2). These magnitudes and colours are also listed in Table 4.2.

#### 4.2.2. Membership

The photometric criteria (cf. Section 3.3.1) alone were used to determine the membership of the individual stars, due to lack of any other information regarding this cluster. The CCD of this cluster, shown in Fig.4.11, indicates a clear sequence for some stars. By making the boundaries for the stars forming the most likely sequence in this diagram and by picking out the same stars on the two CMD's (cf. Figs. 4.12 and 4.13), a total of seventeen stars have been adopted as the most probable members of the cluster out of the observed thirtyone stars. Two of the members (stars 31 and 36) probably belong to the giant branch. Stars 27 and 28 are the brightest and probably a little evolved members of this cluster. All these members are denoted by 'm' in Table 4.2.

#### 4.2.3. Reddening

The CCD in Fig.4.11 shows a sequence formed by a majority of the stars and the boundaries of this sequence show that

$$\Delta E (B-V) = 0.11 \text{ mag}$$

$$\text{and } \Delta E (U-B) = 0.08 \text{ mag.}$$

Since these values are same as the ones due to the natural dispersion (cf. Section 3.4), it is presumed that the inter-stellar extinction is non-variable across the field of the cluster. Hence the following mean colour excesses have been adopted.

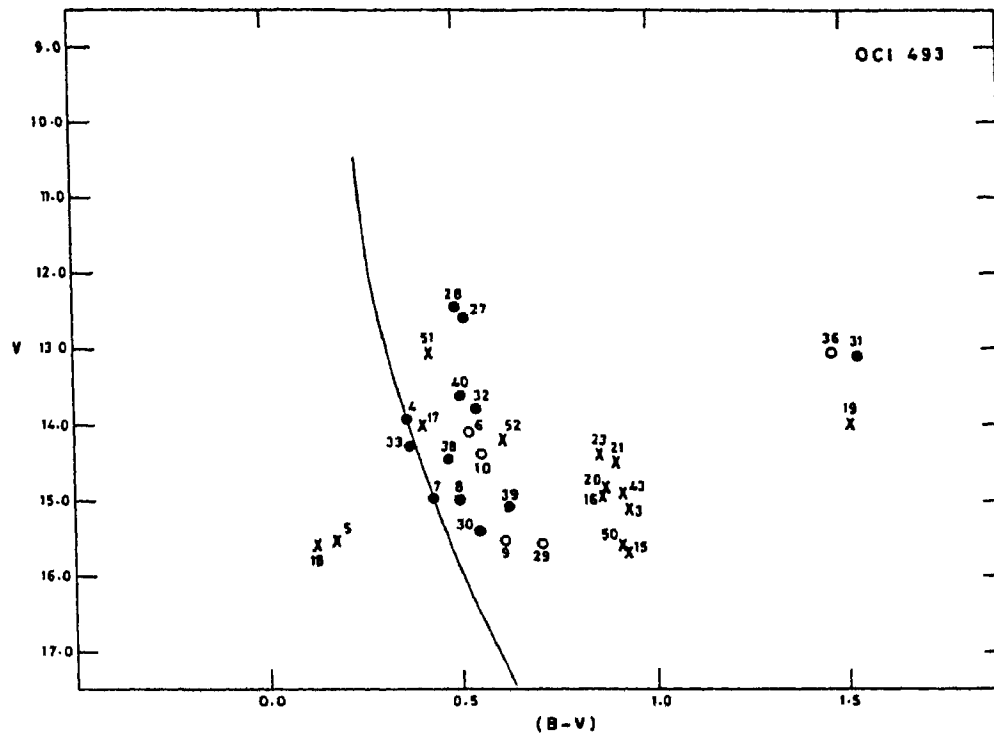


Fig. 4.12. The  $(B-V)$ ,  $V$  diagram (CMD) of OC1 493. The solid curve represents the zero age main sequence (ZAMS) fitted onto the cluster CMD.

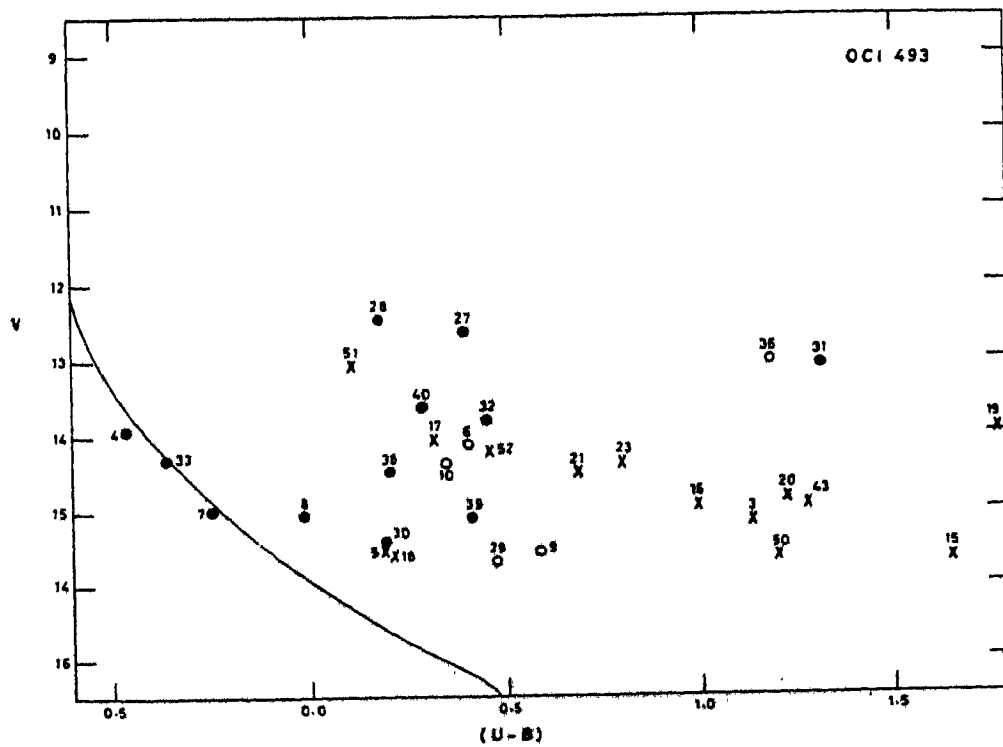


Fig. 4.13. The  $(U-B)$ ,  $V$  diagram (CMD) of OC1 493. The solid curve represents the ZAMS fitted onto the cluster CMD.

$$\begin{aligned} E(B-V) &= [1/2 [ E(B-V)_{\max} + E(B-V)_{\min} ] \\ &= 1/2 [ 0.64 + 0.53 ] = 0.585 \text{ mag} \end{aligned}$$

and similarly

$$E(U-B) = 1/2 [ 0.47 + 0.39 ] = 0.43 \text{ mag.}$$

Then  $A_V = 1.901 \pm 0.029 \text{ mag.}$

Using these values in Equations 3.18 to 3.20, the intrinsic magnitudes and colours were calculated. These are included in Table 4.2 and denoted as  $V_0$ ,  $(B-V)_0$  and  $(U-B)_0$ .

#### 4.2.4. Distance

The ZAMS given by Schmidt-Kaler (1965) has been fitted onto the cluster main sequences shown in Fig.4.14 in order to determine the true distance modulus of the cluster. They are found to be 13.65 mag and 13.84 mag in the long and short wavelength CMD's respectively, giving an average value of 13.75 mag. Then the distance to the cluster based on Equation 3.21 is

$$D = 5.63 \pm 0.26 \text{ kpc.}$$

#### 4.2.5. Age of the Cluster

Fig.4.15 shows the HR-diagram of the cluster, plotted for the true distance modulus of 13.75 mag. The post-MS isochrones indicate an age range of  $3.7 \times 10^7$  to  $5.0 \times 10^7$  years, while the MS appears to be following the curve of  $1.2 \times 10^7$  years. It is quite likely that the fainter stars, which are

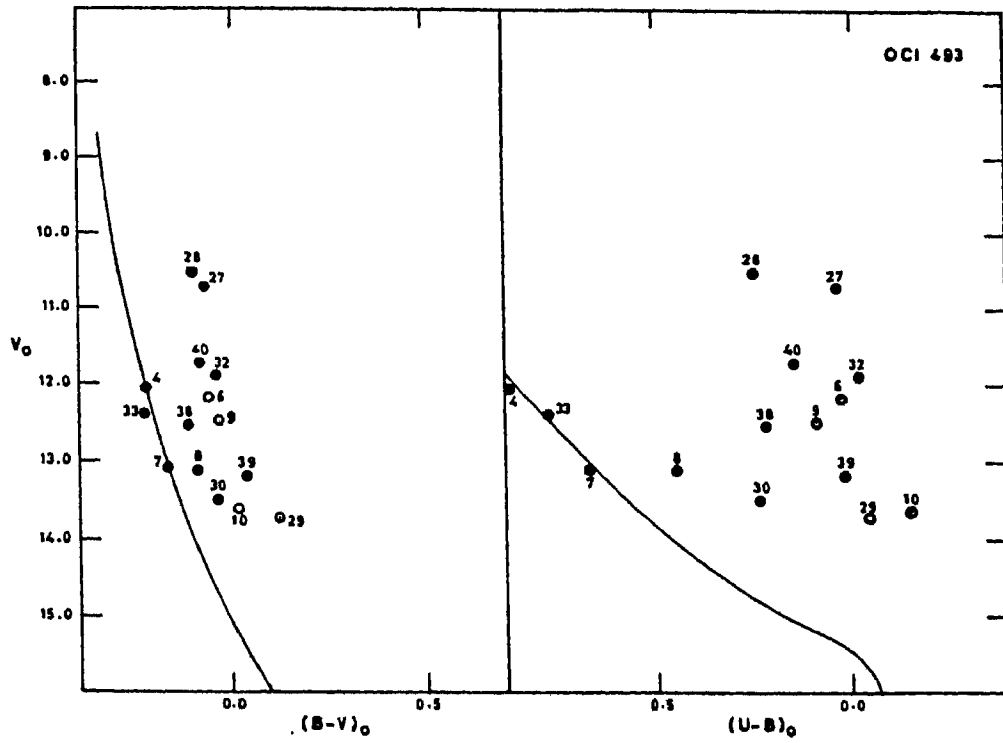


Fig. 4.14. The intrinsic  $(B-V)_0$ ,  $V_0$  and  $(U-B)_0$ ,  $V_0$  diagrams (CMDs) of OC1 493. The solid curves represent the ZAMS, taken from Schmidt-Kaler (1965), fitted onto the cluster CMDs.

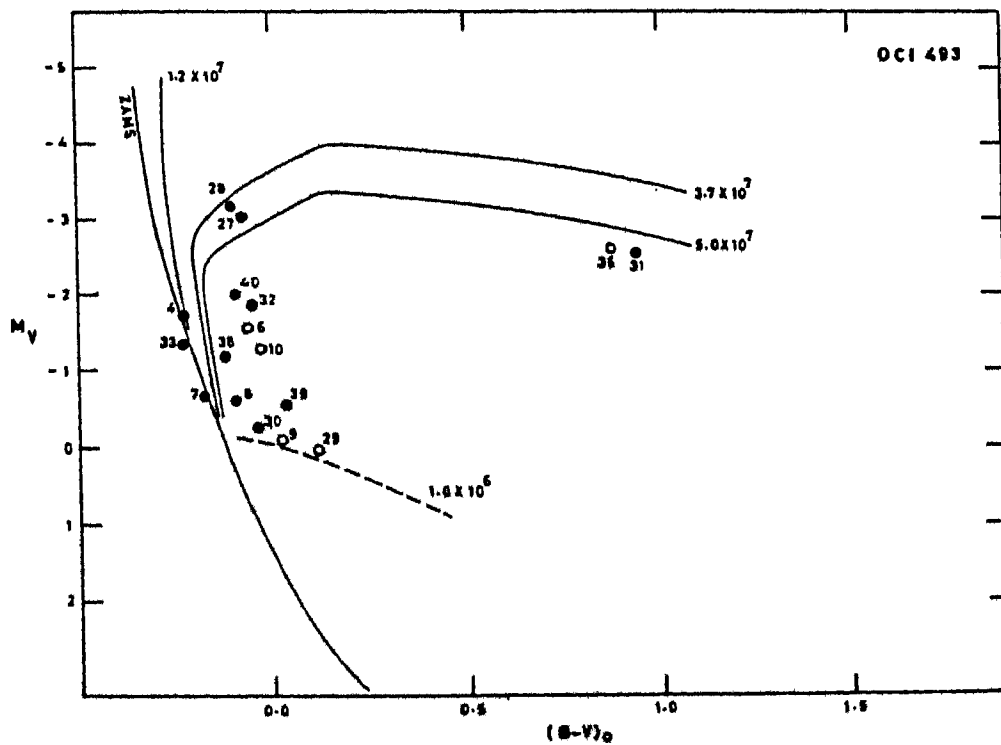


Fig. 4.15. HR-diagram of OC1 493. The post-MS isochrones are from Barbaro et al. (1969) and the dashed lines represent the pre-MS isochrones taken from Iben (1965). The ages are indicated in years alongside the isochrones.

just to the right of the MS are in the process of reaching the main sequence and the faintest of these are close to the pre-MS isochrone of  $1.0 \times 10^6$  years. Thus, just as in the case of many other clusters, the total dispersion in the age of this cluster also seems to be from  $1.2 \times 10^7$  to  $5.0 \times 10^7$  years.

#### **4.3. OC 1 501 (NGC 2236)**

In 1899, Roberts identified this cluster on a photographic plate and it was later on observed by several authors, listed in Table 2.3. Shapley (1930) determined its distance to be 8320 parsecs and mentioned that it was one of the most remote open clusters. He estimated that it had an angular diameter of 5 arcmin and that it contained fifty stars. Trumpler (1930), on the other hand, gave a distance of 2290 parsecs, while Collinder (1931) and Barhatova (1950) gave 4750 parsecs and 1600 parsecs, respectively. Bok (1949) discussed the relationship of this cluster to the Milky Way. More recently, Rahim (1970) obtained a distance of 3430 parsecs through RGU photographic photometry. Its classification, given by Ruprecht (1966) is III 2 p, in the Trumpler system, while Trumpler (1930) himself had classified it as I 2 m. The finding chart is shown in Fig.4.16.

##### 4.3.1. Selection and Observations

This cluster also was selected through objective grating spectroscopy (cf. Section 2.2). The exposure time



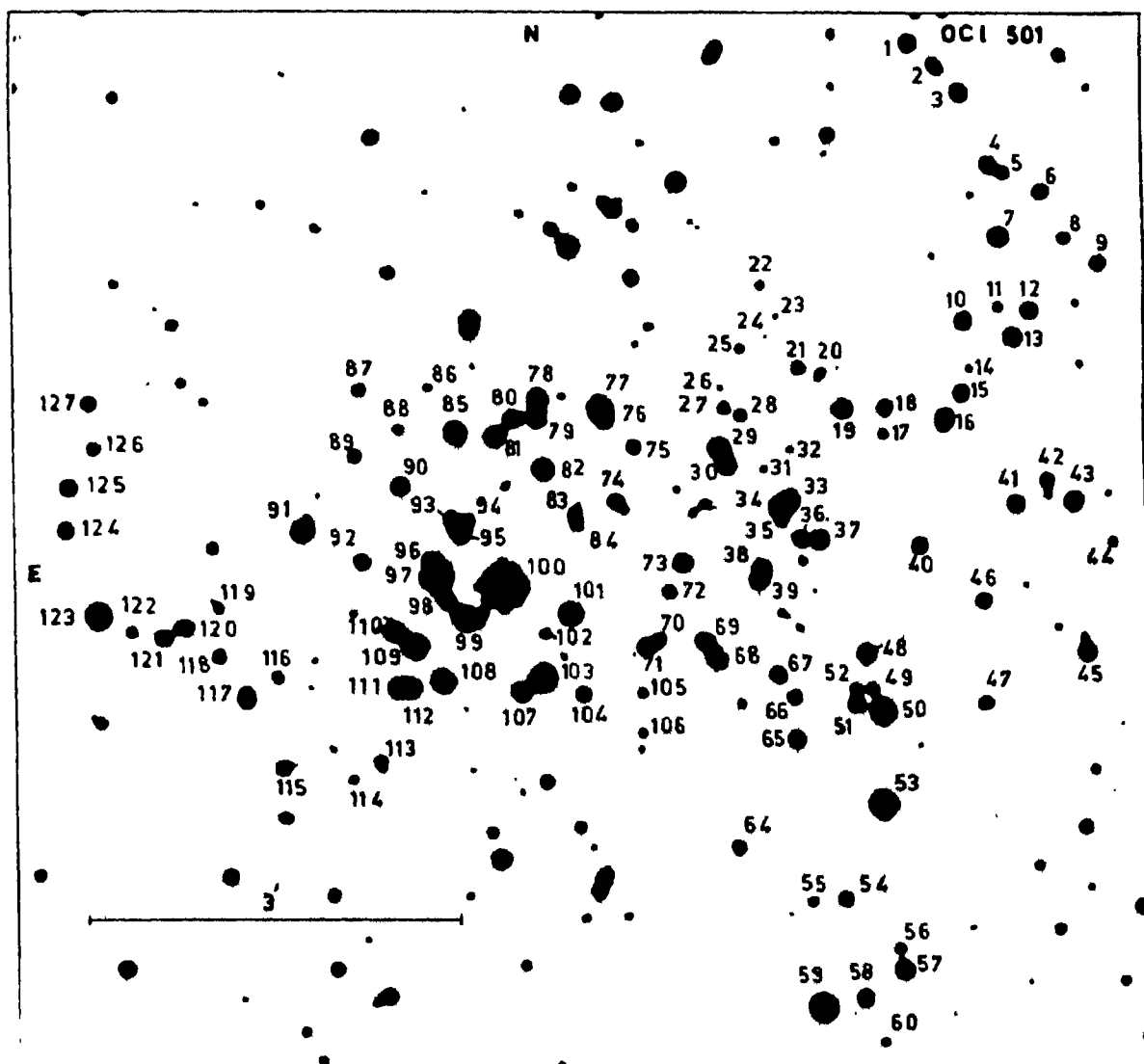


Fig. 4.16. Finding chart for the field of OC1 501.

was 120 minutes on the 103a-0 emulsion plate, on the basis of which spectral types could be estimated for a total of twentyfour stars. These spectral types and the corresponding V(POSS) magnitudes are listed in Table 4.3 and Fig. 4.17 shows a plot between them. In this diagram, stars 53 and 100, which are of spectral type B0, appear to be too bright and in spite of being located inside the field of the cluster, may not belong to the cluster. This preliminary inference is further strengthened by the location of the probable red giant members (star 19, 37, 58, 65, 81 and 99) in the diagram, which are much fainter than star 100. There are four stars 50, 59, 103 and 123 which are located to the right of the main sequence indicating a slightly evolved nature. The rest of the stars show some scatter which may be due to their faintness as well as the uncertainties involved in the estimation of the two parameters. They form the probable main sequence of the cluster. Finally, since star 101 is of the spectral type B3 with stars 57, 73 and 78 showing B5 type, this cluster is taken as belonging to the young category. However, Rahim (1970) estimated the earliest spectral type to be A0 and thereby pointed out that this cluster cannot be used as a spiral arm tracer.

The photoelectric photometry of the cluster was done using the 61-cm telescope of the Siding Spring Observatory (cf. Section 3.1). Following the procedures given in Sections 3.1.2 and 3.1.3, the standard magnitudes and colours for a total of twelve stars were obtained and the values are included

**Table 4.3.** The observational data for individual stars in the open cluster OC1 501.

| Star No.                 | Spectral Type | V (Sky survey) | V      | (B-V) | (U-B)  | $V_0$ | $(B-V)_0$ | $(U-B)_0$ | E(B-V) | Membership |
|--------------------------|---------------|----------------|--------|-------|--------|-------|-----------|-----------|--------|------------|
| 1                        | 2             | 3              | 4      | 5     | 6      | 7     | 8         | 9         | 10     | 11         |
| Photoelectric photometry |               |                |        |       |        |       |           |           |        |            |
| 1                        | B8            | 14.6           | 14.591 | 0.528 | 0.315  | 12.78 | -0.03     | -0.09     | 0.558  | m          |
| 3                        | B8            | 14.5           | 14.587 | 0.673 | 0.677  | -     | -         | -         | -      | -          |
| 6                        | -             | -              | 14.275 | 1.384 | 1.394  | 11.94 | 0.664     | 0.87      | 0.72   | m          |
| 7                        | B5            | 14.6           | 14.490 | 0.575 | 0.005  | 12.17 | -0.14     | -0.51     | 0.715  | m          |
| 13                       | -             | -              | 15.337 | 0.606 | 0.238  | 13.11 | -0.08     | -0.26     | 0.686  | m          |
| 48                       | B8            | 14.6           | 14.528 | 0.706 | 0.397  | 12.19 | -0.01     | -0.12     | 0.72   | m          |
| 53                       | B0            | 12.7           | 12.548 | 0.313 | -0.421 | -     | -         | -         | -      | -          |
| 59                       | B8            | 12.9           | 12.606 | 0.639 | -0.559 | -     | -         | -         | -      | m          |
| 73                       | B5            | 14.8           | 14.727 | 0.645 | -0.061 | 12.05 | -0.18     | -0.66     | 0.825  | m          |
| 100                      | B0            | 10.9           | 10.722 | 0.317 | -0.063 | -     | -         | -         | -      | -          |
| 101                      | B3            | 14.1           | 14.023 | 0.317 | -0.252 | -     | -         | -         | -      | -          |
| 123                      | B8            | 12.8           | 12.756 | 0.659 | -0.579 | -     | -         | -         | -      | -          |
| Photographic photometry  |               |                |        |       |        |       |           |           |        |            |
| 4                        | -             | -              | 15.37  | 0.59  | 0.26   | 13.27 | -0.06     | -0.20     | 0.65   | m          |
| 10                       | -             | -              | 15.27  | 0.46  | 0.07   | 13.48 | -0.09     | -0.34     | 0.55   | m          |
| 16                       | A0            | 15.0           | 14.96  | 0.47  | 0.27   | 13.32 | -0.04     | -0.10     | 0.51   | m          |
| 19                       | K5            | 13.5           | 13.28  | 1.53  | 0.94   | 10.94 | 0.81      | 0.41      | 0.72   | m          |
| 29                       | -             | -              | 14.25  | 0.42  | 0.17   | -     | -         | -         | -      | -          |
| 30                       | -             | -              | 14.46  | 0.63  | 0.57   | -     | -         | -         | -      | -          |
| 34                       | -             | -              | 13.28  | 1.45  | 0.96   | 10.94 | 0.73      | 0.44      | 0.72   | m          |
| 37                       | K0            | 14.0           | 13.93  | 1.37  | 1.13   | 11.59 | 0.64      | 0.61      | 0.72   | m          |
| 38                       | -             | -              | 14.45  | 0.56  | 0.60   | -     | -         | -         | -      | -          |
| 40                       | -             | -              | 15.07  | 0.48  | 0.05   | 13.15 | -0.11     | -0.38     | 0.59   | m          |
| 50                       | A0            | 13.1           | 12.92  | 0.71  | -0.47  | -     | -         | -         | -      | -          |
| 57                       | B5            | 14.7           | 14.55  | 0.79  | 0.30   | 11.66 | -0.10     | -0.34     | 0.89   | m          |

---

| 1   | 2  | 3    | 4     | 5    | 6     | 7     | 8     | 9     | 10   | 11 |
|-----|----|------|-------|------|-------|-------|-------|-------|------|----|
| 58  | K5 | 14.4 | 14.26 | 1.63 | 1.33  | 11.92 | 0.91  | 0.81  | 0.72 | m  |
| 65  | K5 | 13.9 | 13.70 | 1.68 | 1.38  | 11.36 | 0.96  | 0.86  | 0.72 | m  |
| 67  | -  | -    | 15.26 | 0.73 | 0.63  | -     | -     | -     | -    | -  |
| 68  | -  | -    | 14.01 | 0.87 | 0.56  | 11.67 | 0.15  | 0.04  | 0.72 | m  |
| 69  | -  | -    | 14.72 | 0.61 | 0.41  | 12.69 | -0.02 | -0.05 | 0.63 | m  |
| 70  | -  | -    | 14.64 | 0.65 | 0.62  | -     | -     | -     | -    | -  |
| 76  | -  | -    | 13.47 | 0.61 | 0.40  | -     | -     | -     | -    | -  |
| 78  | B5 | 14.5 | 14.28 | 0.83 | 0.24  | 11.20 | -0.12 | -0.45 | 0.95 | m  |
| 81  | K5 | 13.6 | 13.54 | 1.56 | 1.09  | 11.20 | 0.84  | 0.57  | 0.72 | m  |
| 85  | B8 | 13.9 | 13.78 | 0.74 | 0.40  | 11.44 | 0.02  | -0.12 | 0.72 | m  |
| 95  | -  | -    | 14.00 | 1.92 | 1.64  | 11.66 | 1.20  | 1.12  | 0.72 | m  |
| 97  | -  | -    | 13.57 | 0.63 | 0.31  | -     | -     | -     | -    | -  |
| 99  | K5 | 13.4 | 13.23 | 1.58 | 1.12  | 10.89 | 0.86  | 0.60  | 0.72 | m  |
| 103 | A0 | 12.8 | 12.65 | 0.79 | -0.57 | -     | -     | -     | -    | -  |
| 107 | -  | -    | 13.33 | 1.94 | 1.79  | 10.99 | 1.22  | 1.27  | 0.72 | m  |
| 108 | -  | -    | 13.05 | 1.50 | 0.96  | 10.71 | 0.78  | 0.44  | 0.72 | m  |
| 109 | -  | -    | 13.30 | 1.20 | 0.64  | -     | -     | -     | -    | -  |
| 110 | -  | -    | 14.38 | 0.95 | 0.41  | 12.04 | 0.23  | -0.11 | 0.72 | m  |
| 112 | -  | -    | 14.20 | 0.62 | 0.46  | -     | -     | -     | -    | -  |
| 120 | B8 | 15.0 | 14.79 | 0.73 | 0.30  | 12.11 | -0.09 | 0.30  | 0.82 | m  |
| 121 | B8 | 14.6 | 14.53 | 0.84 | 0.64  | 12.18 | 0.12  | 0.12  | 0.72 | m  |

---

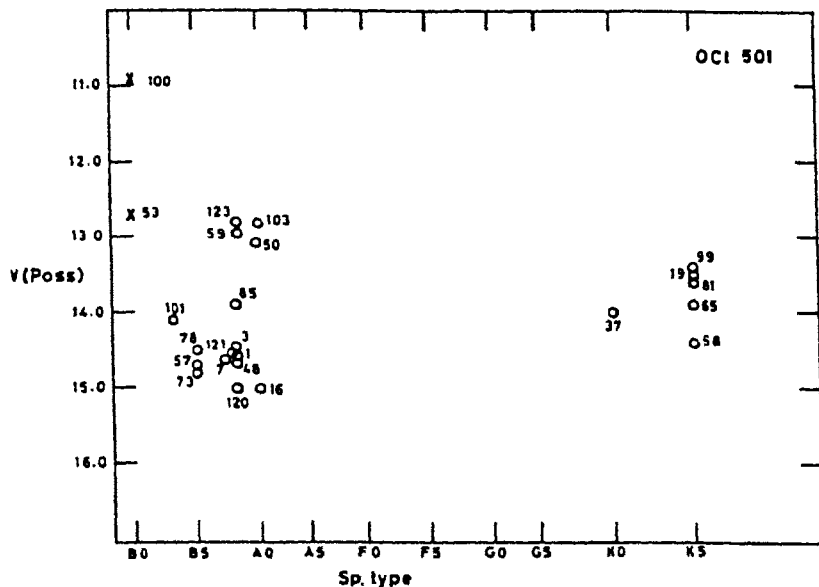


Fig. 4.17. Spectral type obtained from the modified objective-grating spectra plotted against the V magnitudes estimated from the POSS charts, for the stars in the field of OC1 501.

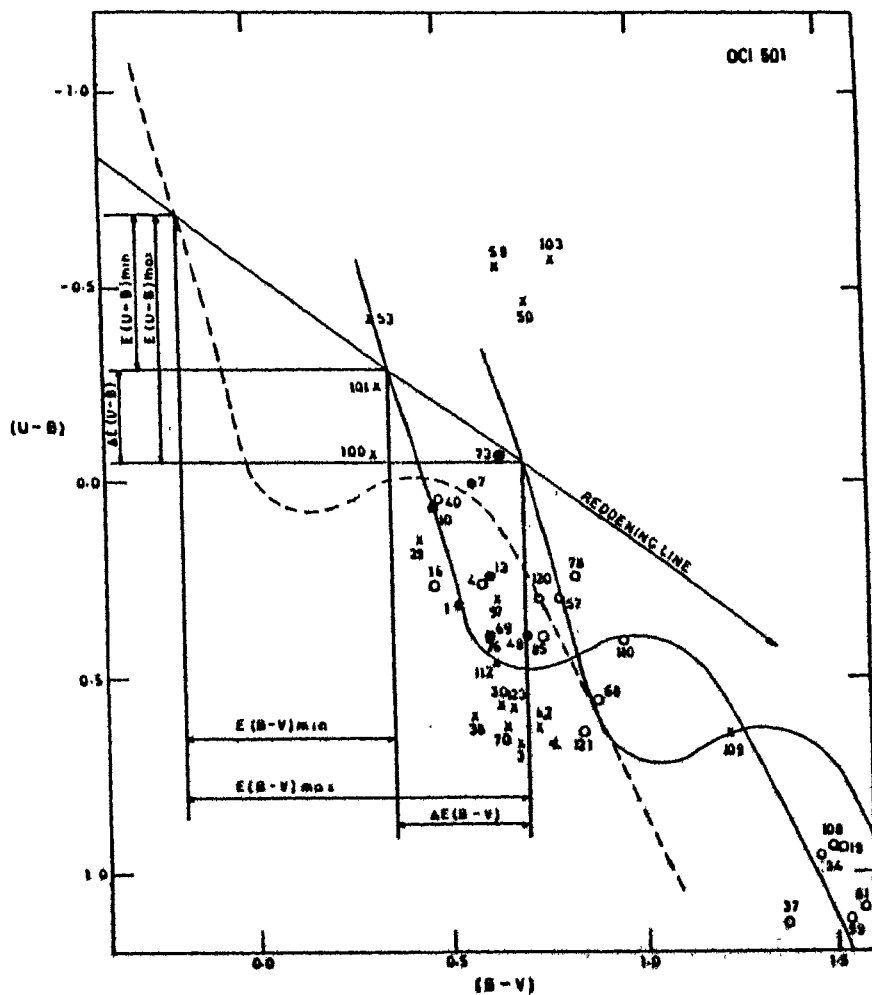


Fig. 4.18. The colour-colour diagram (CCD) of OC1 501. The dashed line is the unreddened main sequence (MS) taken from Schmidt-Kaler (1965).

in Table 4.3. The atmospheric extinction coefficients, the transformation coefficients and the zero-point constants (cf. Equations 3.6 to 3.11) are tabulated below.

$$\begin{aligned} K_v &= 0.160 & \epsilon &= 5.605 & \zeta_v &= 0.300 \\ K_{b-v} &= 0.155 & \mu &= 0.010 & \zeta_{bv} &= 0.865 \\ K_{u-b} &= 0.200 & \psi &= 2.400 & \zeta_{ub} &= -2.845 \end{aligned}$$

The direct photography of this cluster was carried out using both the 102-cm telescope of Kavalur Observatory (KO) and the 1-m telescope of Siding Spring Observatory (SSO) as described in Section 3.2.1. The following are the plate and filter combinations along with the exposure times.

| <u>Plate</u> | <u>Filter</u> | <u>Exposure time</u> |
|--------------|---------------|----------------------|
| IIa-0        | UG2           | 45 min for U(SSO)    |
| 103a-0       | GG13          | 30 min for B(SSO)    |
| IIa-D        | GG11          | 90 min for V(KO)     |

From these plates, the photographic magnitudes were obtained on an arbitrary scale, for a total of fortyfive stars, which included the ones observed photoelectrically. These were then standardized using the photoelectric observations following the procedure given in Section 3.2.2. All these magnitudes and colours are included in Table 4.3.

#### 4.3.2. Membership

Fig.4.18 shows the CCD of this cluster, where a considerable amount of scatter is seen. By shifting the unredd-

ened curve parallel to the reddening line and by marking the boundaries for the likely sequence, the probable candidates for the membership could be identified. Then, using the photometric criteria described in Section 3.3.1 on this CCD and on the two CMD's shown in Figs. 4.19 and 4.20, a total of twentyeight stars have been adopted as the most probable members of the cluster, out of the fortyfive stars observed. The brightest star (i.e star 100), which appears almost at the center of the cluster in the finding chart, is found to be a non-member on the basis of the photometric criteria. This conclusion matches with that found by Rahim (1970) through RGU study. Eleven of these members are located in the red giant region of the two CMD's with a few others showing evolved nature. All these stars are denoted by 'm' in Table 4.3.

#### 4.3.3. Reddening

The considerable scatter in the CCD (cf. Fig.4.18) indicates a variable reddening across the field of the cluster, which is supported by a similar scatter in the two CMD's (cf. Figs.4.19 and 4.20). The boundaries mentioned in section 4.3.3 show a difference  $\Delta$  between  $E(B-V)_{\max}$  and  $E(B-V)_{\min}$  as

$$\Delta E (B-V) = 0.34 \text{ mag}$$

and similarly

$$\Delta E (U-B) = 0.24 \text{ mag.}$$

These values are much larger than the natural dispersion values

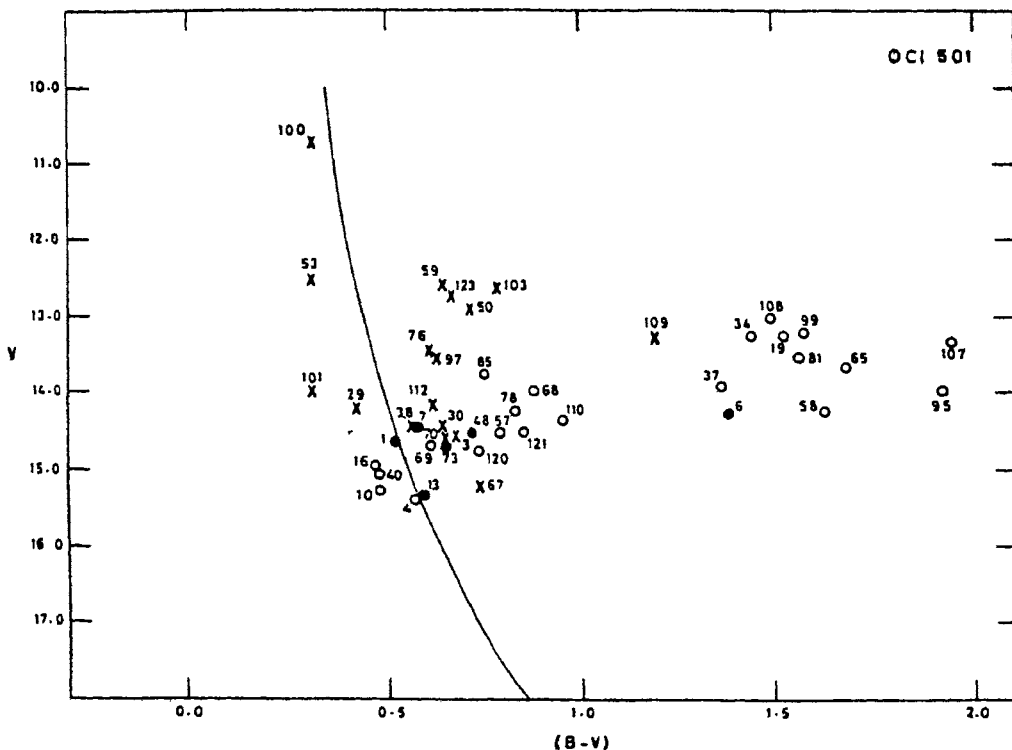


Fig. 4.19. The (B-V), V diagram (CMD) of OC1 501. The solid curve represents the zero age main sequence (ZAMS) fitted onto the cluster CMD.

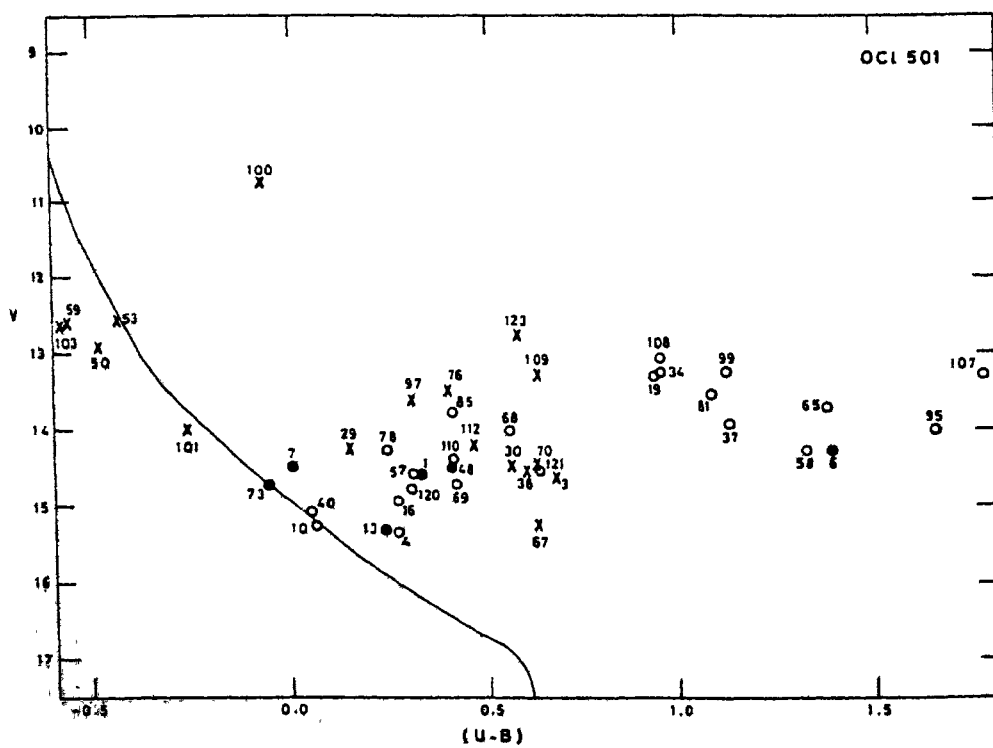


Fig. 4.20. The (U-B), V diagram (CMD) of OC1 501. The solid curve represents the ZAMS fitted onto the cluster CMD.



(cf. Section 3.4). Therefore, the concerned stars were individually corrected for the appropriate interstellar reddening. These corrections were found to be between  $E(B-V)_{\max} = 0.89$  mag and  $E(B-V)_{\min} = 0.55$  mag. Similarly,  $E(U-B)_{\max} = 0.64$  mag and  $E(U-B)_{\min} = 0.40$  mag. In this context, it may be noted that Rahim (1970) found a value for  $E(G-R)$  as 0.51 mag which is equivalent of  $E(B-V) = 0.37$  mag (cf. Steinlin, 1968 for the transformations) and did not mention anything about the variable reddening.

With the help of the individual  $E(B-V)$  values, which are included in Table 4.3, the corresponding values of  $A_V$  were obtained which were found to be between 2.89 mag and 1.79 mag as against the value of  $A_V = 1.19$  mag (or  $A_G = 1.37$  mag) given by Rahim (1970). The observed  $V$  values were then corrected by using the respective  $A_V$  values. All these corrected magnitudes and colours are also included in Table 4.3 as  $V_0$ ,  $(B-V)_0$  and  $(U-B)_0$ .

#### 4.3.4. Distance

The true distance modulus of this cluster has been determined by fitting ZAMS (Schmidt-Kaler, 1965) onto the cluster main sequence as shown in Fig.4.21. The long and short wavelength CMD's have been found to yield the distance moduli of 13.15 and 12.89 mag respectively giving an average value of 13.02 mag. Then the distance  $D$  to the cluster, based on the Equation 3.21 is

$$D = 4.02 \pm 0.23 \text{ kpc}$$

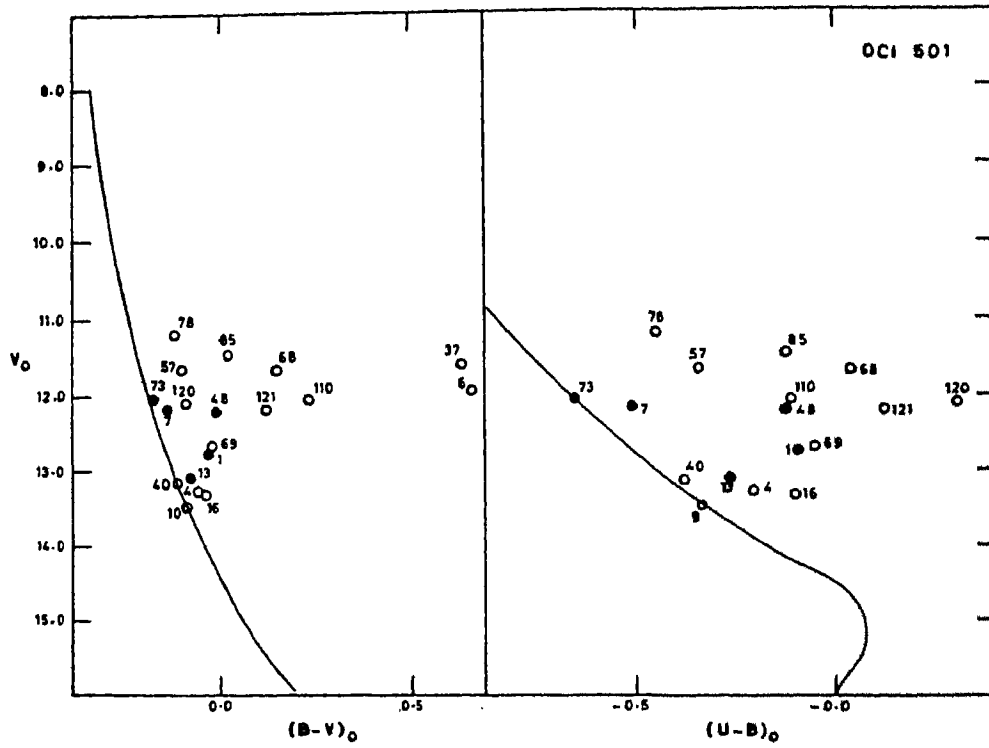


Fig. 4.21. The intrinsic  $(B-V)_0$ ,  $V_0$  and  $(U-B)_0$ ,  $V_0$  diagrams (CMDs) of OC1 501. The solid curves represent the ZAMS, taken from Schmidt-Kaler (1965), fitted onto the cluster CMDs.

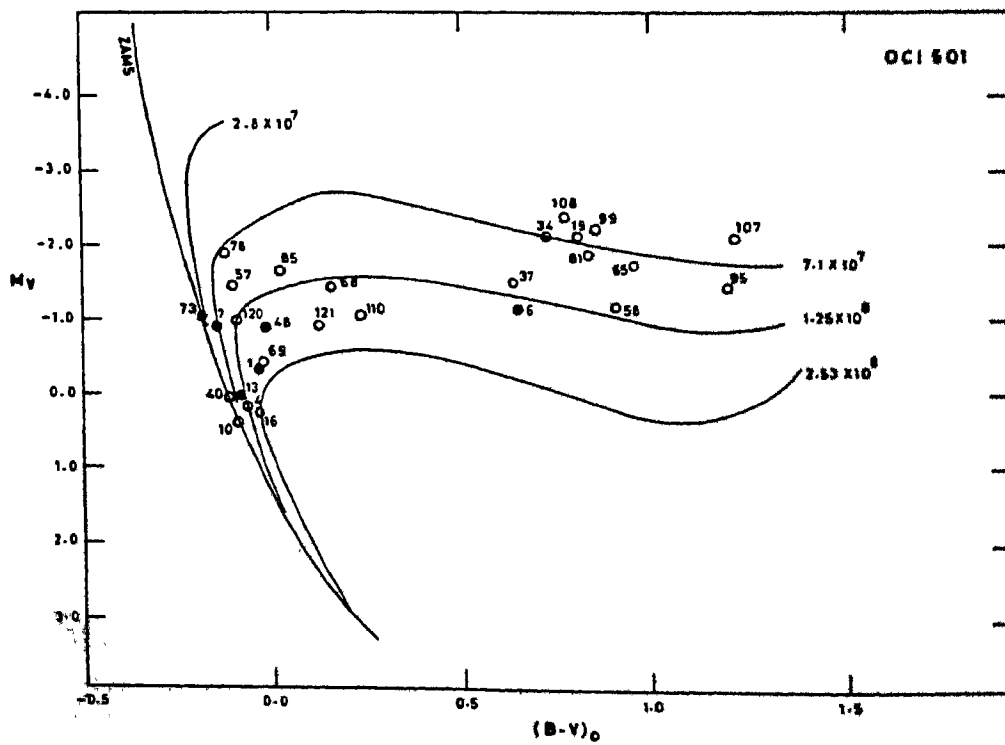


Fig. 4.22. HR-diagram of OC1 501. The post-MS isochrones are from Barbaro et al. (1969). The ages are indicated in years alongside the isochrones.

This value is at least 0.36 kpc greater than the one obtained by Rahim (1970).

#### 4.3.5. Age of the Cluster

The HR-diagram of the cluster is shown in Fig.4.22, which is plotted for the true distance modulus of 13.02 mag. The MS indicates an age of  $2.8 \times 10^7$  years, while the post-MS isochrones show a range of  $7.1 \times 10^7$  to  $12.5 \times 10^7$  years. Some of the stars appear to have evolved from the MS from which the red giants are clearly separated by the Hertzsprung gap as has also been noticed by Rahim (1970). Thus, the age spread in this cluster appears to be from  $2.8 \times 10^7$  to  $12.5 \times 10^7$  years.

#### **4.4. OC1 506 (Cr 97)**

This cluster of Trumpler class IV 3 p (Ruprecht 1966) was estimated to be at a distance of 610 parsecs by Collinder (1931). He also gave the angular diameter as 22.5 arcmin with only nine stars. He pointed out that this cluster has stars of spectral type B0 to A0 and that it is a bright cluster ( $m_{\text{total}} = 5.3$  mag). The finding chart is given in Fig.4.23. Even though, some of the stars in the field are bright enough to be included in SAO and BD charts, surprisingly no work has been done on them as members of this cluster.

##### 4.4.1. Selection and Observations

Spectral types could be obtained for a total of thirteen stars from the objective grating spectroscopy (cf.

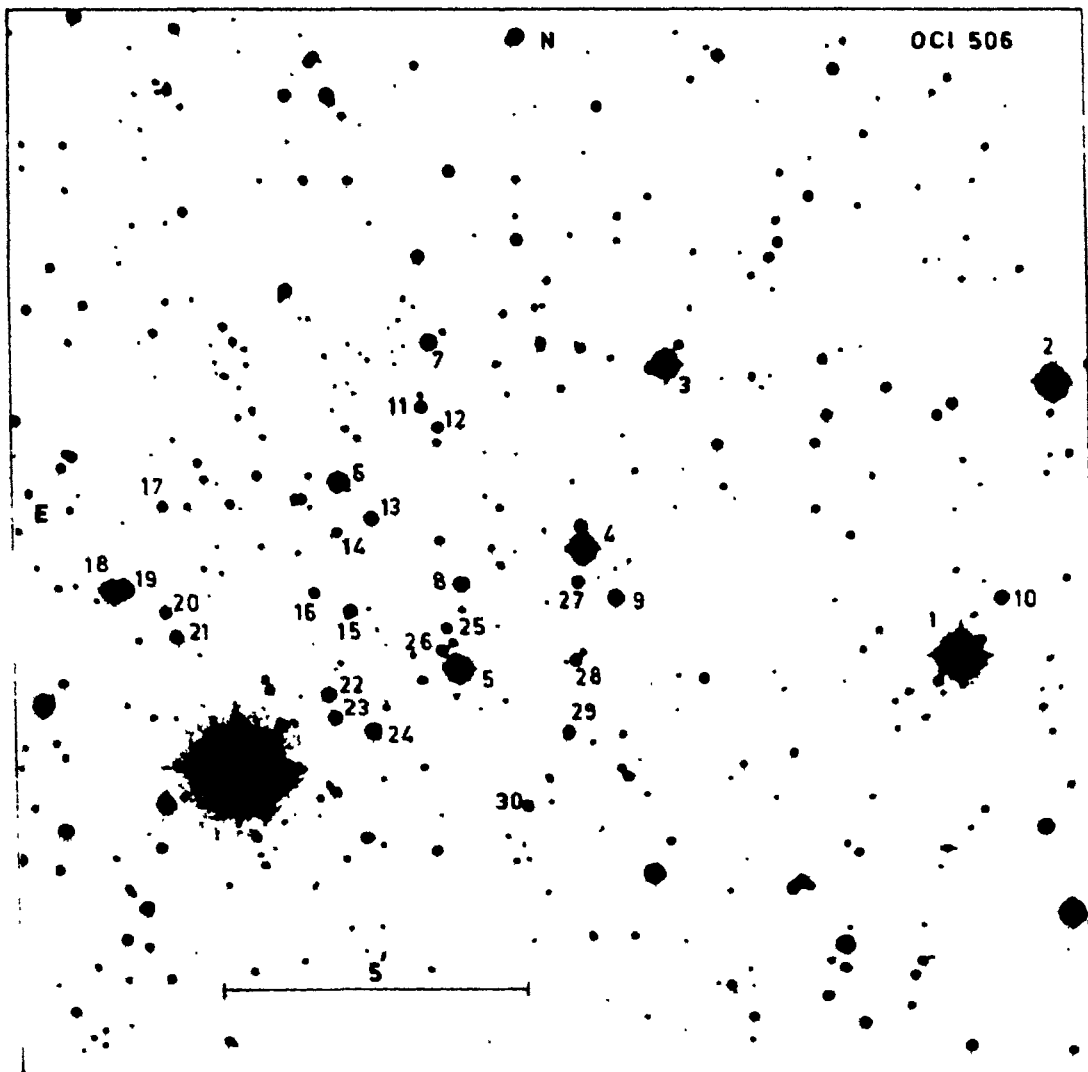


Fig. 4.23. Finding chart for the field of OC1 506.

Section 2.2), where the exposure time was 30 minutes on a 103 a-0 plate. A plot between these spectral types and the corresponding V(POSS) magnitudes is shown in Fig.4.24 which are tabulated in Table 4.4. In this figure, out of the five brightest stars, only star 4 is considered a member of the cluster. Stars 1 and 2 appear to be a little too bright to be members; yet they are given a doubtful membership because of the large angular diameter suggested by Collinder. Stars 3 and 5 have some chance of being members of the possible giant branch and thus they also get a doubtful membership. Star 10 is clearly a non-member. That makes a total of eight members and four doubtful members out of the thirteen observed stars. Since star 4 shows the spectral type of B5, it has been categorized as a marginally young cluster.

The photoelectric observations were obtained from Siding Spring Observatory, using the 61-cm telescope (cf. Section 3.1). Standardized magnitudes and colours for a total of seventeen stars were obtained and the values are included in Table 4.4. The atmospheric coefficients, the transformation coefficients and the zero-point constants (cf. Equations 3.6 to 3.11) are tabulated below:

$$\begin{aligned} K_V &= 0.165 & \epsilon &= 5.495 & \zeta_V &= 0.289 \quad ^1 \\ K_{b-v} &= 0.150 & \mu &= 0.005 & \zeta_{bV} &= 0.849 \quad ^1 \\ K_{u-b} &= 0.070 & \psi &= 2.385 & \zeta_{ub} &= -2.857 \end{aligned}$$

**Table 4.4.** The observational data for individual stars in the open cluster OC1 506.

| Star No.                        | Spectral Type | V (Sky survey) | V      | (B-V)  | (U-B)  | Membership |
|---------------------------------|---------------|----------------|--------|--------|--------|------------|
| 1                               | 2             | 3              | 4      | 5      | 6      | 7          |
| <b>Photoelectric photometry</b> |               |                |        |        |        |            |
| 1 (SAO 113979)                  | B8            | 7.6            | 8.398  | -0.021 | 0.054  | m          |
| 2 (SAO 113977)                  | A0            | 8.3            | 8.713  | 0.334  | 0.007  | m          |
| 3 (SAO 113987)                  | K0            | 8.3            | 8.686  | 0.992  | 0.655  | m          |
| 4 (BD+5°1274)                   | B5            | 9.3            | 9.757  | -0.054 | -0.231 | m          |
| 5 (BD+5°1276)                   | F5            | 9.3            | 9.566  | 0.641  | 0.273  | m          |
| 8 -                             | A0            | 12.0           | 12.716 | 0.379  | -0.031 | m          |
| 9 -                             | F0            | 11.8           | 12.255 | 0.390  | 0.044  | m          |
| 10 -                            | K5            | 12.5           | 12.866 | 0.851  | 0.347  | -          |
| 13 -                            | F0            | 12.4           | 12.729 | 0.486  | 0.049  | m          |
| 14 -                            | -             | -              | 15.044 | 0.804  | 0.877  | m          |
| 15 -                            | -             | -              | 13.996 | 0.674  | 0.285  | m          |
| 22 -                            | -             | -              | 13.798 | 0.607  | 0.227  | m          |
| 23 -                            | -             | -              | 12.673 | 1.622  | -      | -          |
| 24 -                            | -             | -              | 12.621 | 0.506  | 0.143  | m          |
| 25 -                            | -             | -              | 14.510 | 0.619  | 0.051  | m          |
| 27 -                            | -             | -              | 13.881 | 0.726  | 0.386  | m          |
| 30 -                            | -             | -              | 13.809 | 0.804  | 0.568  | -          |
| <b>Photographic photometry:</b> |               |                |        |        |        |            |
| 6 -                             | B8            | 10.3           | 10.81  | 0.15   | -      | m          |
| 7 -                             | A0            | 11.8           | 12.27  | 0.32   | -      | m          |
| 11 -                            | F5            | 13.2           | 13.34  | 0.64   | -      |            |
| 12 -                            | G0            | 13.3           | 13.63  | 0.60   | -      | m          |
| 16 -                            | -             | -              | 13.97  | 0.65   | -      | m          |
| 17 -                            | -             | -              | 14.24  | 1.17   | -      | -          |
| 18 -                            | -             | -              | 11.84  | 0.30   | -      | m          |

---

| 1  | 2 | 3 | 4      | 5     | 6 | 7 |
|----|---|---|--------|-------|---|---|
| 19 |   |   | 12.138 | 0.451 | - | m |
| 20 |   |   | 13.807 | 0.608 | - | m |
| 21 |   |   | 13.705 | 0.479 | - | m |
| 26 |   |   | 14.797 | 0.665 | - | m |
| 28 |   |   | 13.982 | 0.809 | - | m |

---

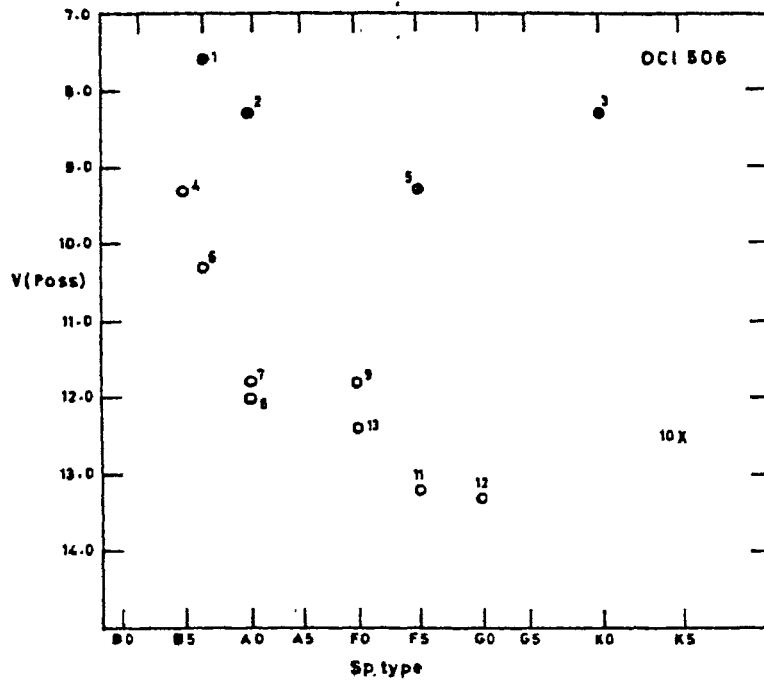


Fig. 4.24. Spectral types obtained from the modified objective-grating spectra plotted against the V magnitudes estimated from the POSS charts, for the stars in the field of OC1 506.

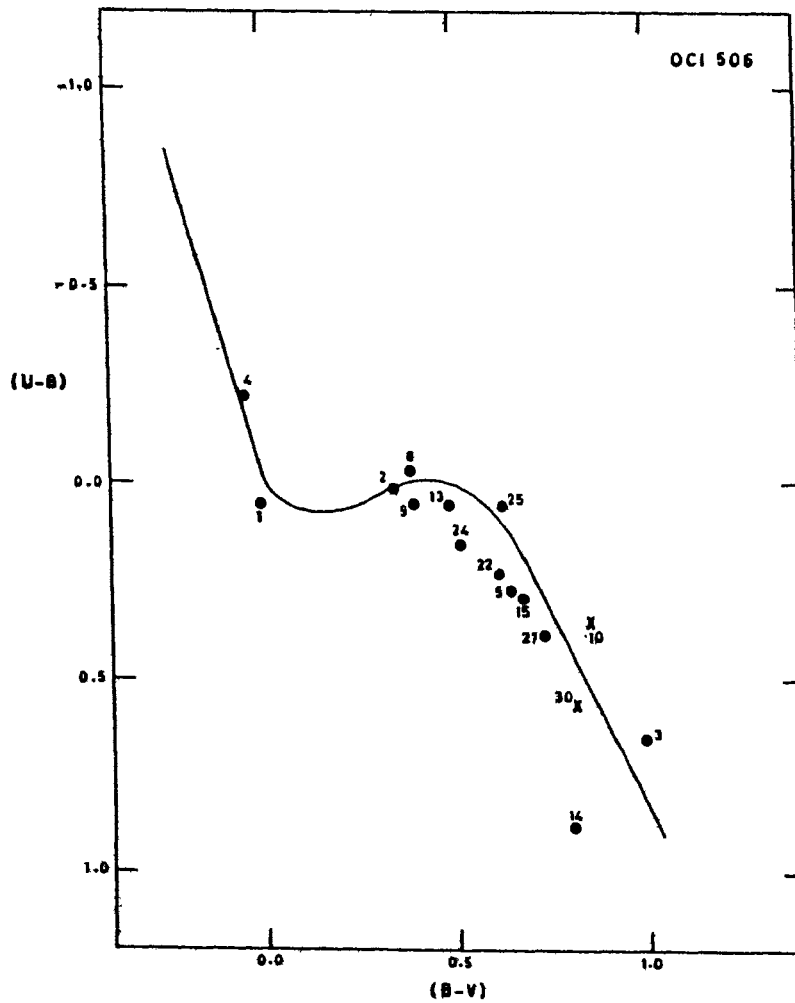


Fig. 4.25. The colour-colour diagram (CCD) of OC1 506. The solid line is the unreddened main sequence (MS) taken from Schmidt-Kaler (1965).



The direct U, B, V photography of this cluster was done using the 102-cm telescope at Kavalur Observatory (cf. Section 3.2.1). The plate and filter combination along with the exposure times are given below.

| <u>Plate</u> | <u>Filter</u> | <u>Exposure time</u> |
|--------------|---------------|----------------------|
| IIa-0        | UG2           | 35 min for U         |
| 103a-0       | GG13          | 20 min for B         |
| IIa-D        | GG11          | 40 min for V         |

From these plates, the photographic magnitudes in B and V were obtained for a total of twentynine stars, in which all the photoelectrically observed ones were included. The U photograph was affected by bad sky conditions on both occasions when it was attempted. However, since there were sufficient number of stars, observed photoelectrically in U to plot the CCD and the corresponding CMD, no further attempt was made to obtain the photographic U magnitudes. Thus, only B and V photographic magnitudes were standardized, which are listed in Table 4.4.

#### 4.4.2. Membership

The membership of the individual stars in the cluster has been determined with the help of the photometric criteria as described in Section 3.2.2. The CCD of this cluster, shown in Fig.4.25 indicates a clear sequence, which is also found in the two CMD's (cf. Figs. 4.26 and 4.27). Only stars 10, 17, 23, 28 and 30 have been considered as non-members, thus

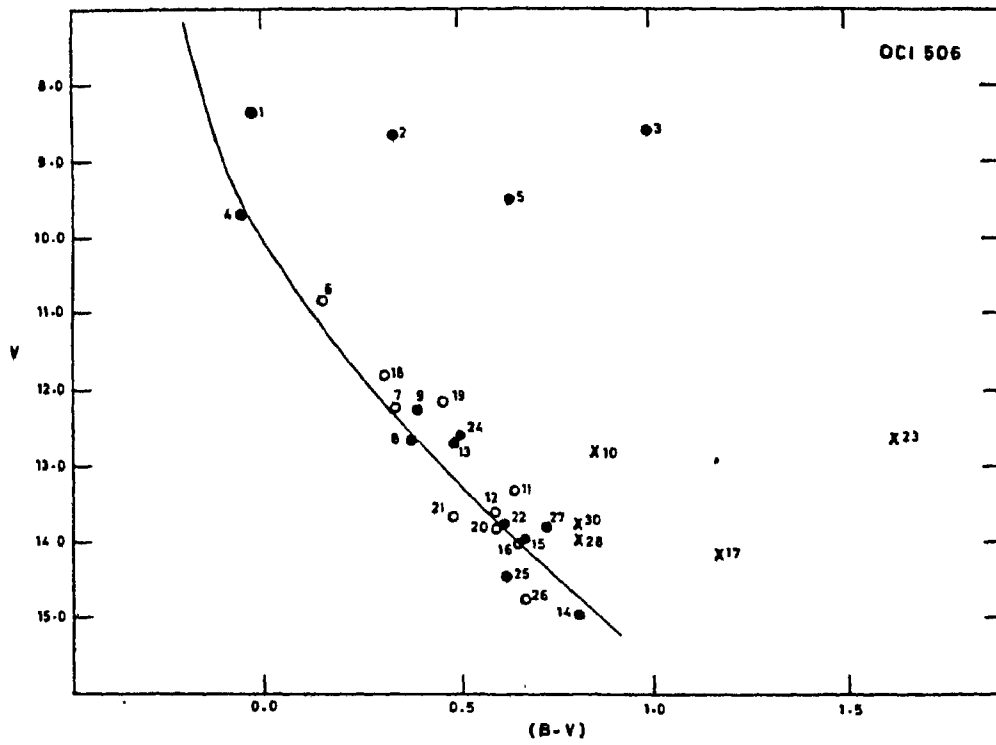


Fig. 4.26. The (B-V), V diagram (CMD) of OC1 506. The solid curve represents the zero age main sequence (ZAMS) fitted onto the cluster CMD.

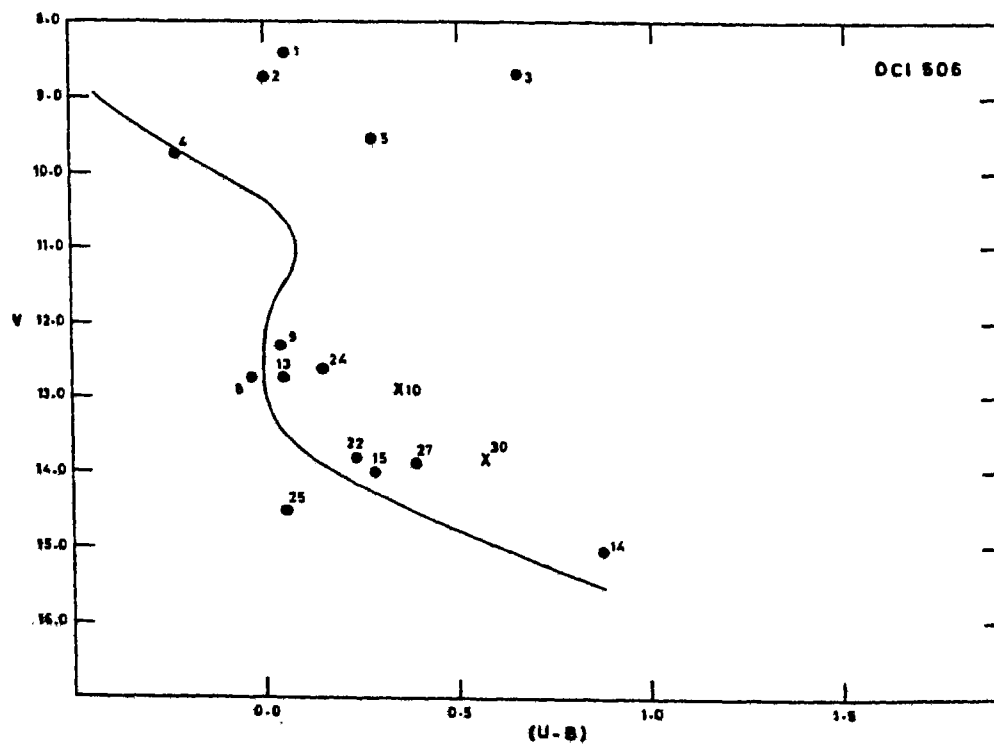


Fig. 4.27. The (U-B), V diagram (CMD) of OC1 506. The solid curve represents the ZAMS fitted onto the cluster CMD.

leaving a total of twentyfour stars as members. Out of these, stars 3 and 5 appear to be belonging to the red giant branch, while stars 1 and 2 show some evolved nature. All these members are denoted by 'm' in Table 4.41.

#### 4.4.3. Reddening

The CCD is given in Fig.4.25, where the sequence of all the member stars appear to be following the unreddened curve, indicating that there is no interstellar extinction between the cluster and the observer. Thus,

$$E (B-V) = 0.0 \text{ mag}$$

and  $E (U-B) = 0.0 \text{ mag} .$

That is, the observed magnitudes and colours need no further correction by way of interstellar reddening.

#### 4.4.4. Distance

The very fact that this cluster needs no corrections for the interstellar extinction, indicates that it is a nearby cluster. Its brightness and the large angular diameter (cf. Table 2.3) render support to this inference. Collinder (1931) also had estimated its distance to be only 610 parsecs. Thus, in order to determine its distance from the photometric data, the two CMD's shown in Figs.4.26 and 4.27 have been fitted with the ZAMS (Schmidt-Kaler, 1965) to match with the respective main sequences. They yielded the distance moduli of 8.7 mag and 8.8 mag respectively. Then, based on the Equation 3.21, the distance has been found to be

$$D = 0.56 \pm 0.01 \text{ kpc}$$

This, in fact, is the nearest of the clusters studied in the present programme.

#### 4.4.5. Age of the Cluster

The HR-diagram of this cluster is shown in Fig.4.28, which is plotted for the true distance modulus of 8.75 mag. The MS and the post-MS stars clearly indicate an age range of  $2.53 \times 10^8$  to  $5.90 \times 10^8$  years. Further, star 4, being the bluest on the MS with  $(B-V) = -0.05$ , gives the age as  $1 \times 10^8$  years. Thus, the total dispersion in the age of this cluster appears to be from  $1 \times 10^8$  to  $5.9 \times 10^8$  years. The average of this age range and the earliest spectral type B7, puts this cluster into an older age group, which is not specifically suitable as a spiral arm tracer.

#### **4.5 OC1 556 (Haffner 3)**

This group of stars was first listed as a cluster by Haffner (1957), who gave its angular diameter to be 2.7 arcmin with eleven stars in it. He also discussed its relationship with the spiral structure of our Galaxy. It has been classified as II 2 p in Trumpler system by Ruprecht (1966), though Haffner had earlier put it as IV 1 p. The finding chart is given in Fig.4.29. The interesting feature of the field of this cluster is that there are two distinct concentrations or physical groups separated by a small region of low star density.

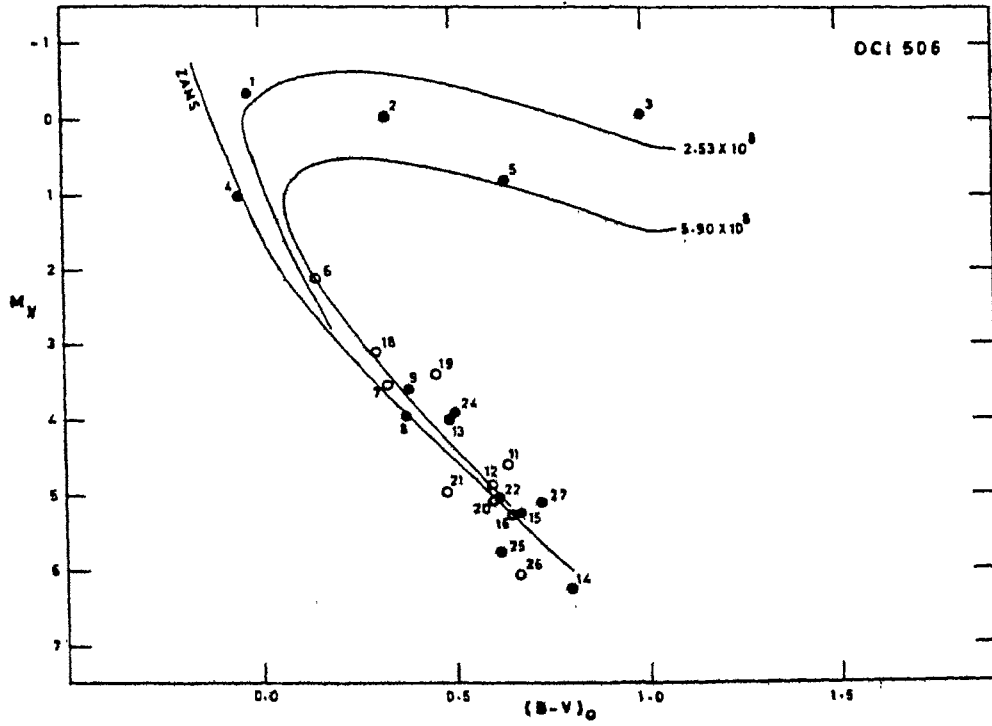


Fig. 4.28. HR-diagram of OC1 506. The post-MS isochrones are from Barbaro et al. (1969). The ages are indicated in years alongside the isochrones.

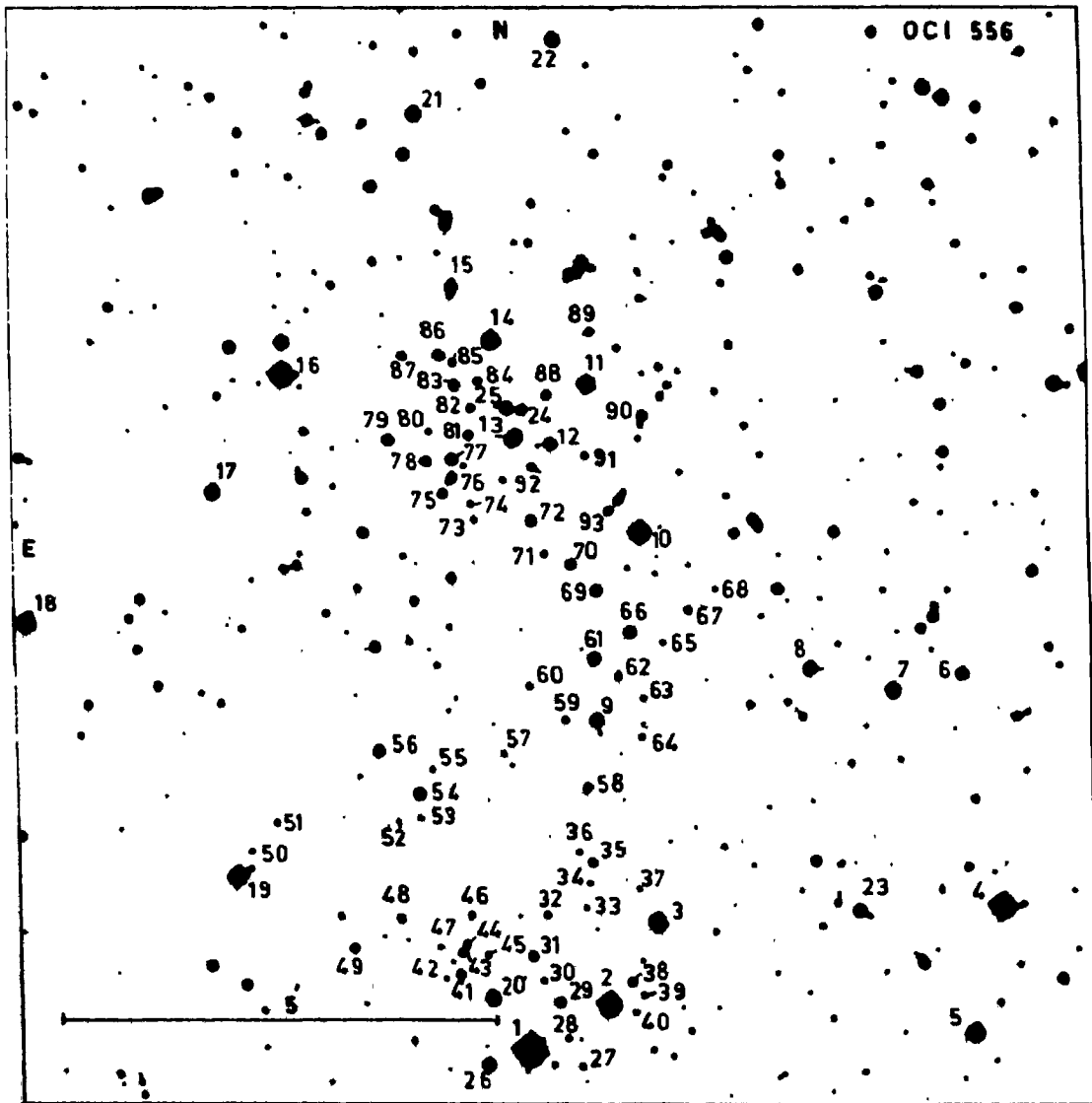


Fig. 4.29. Finding chart for the field of OC1 556.

#### 4.5.1. Selection and Observations

A photograph of this cluster, using the objective grating spectroscopic technique as described in Section 2.2, was taken with an exposure time of 45 minutes on a 103a-0 plate. From this plate, spectral types could be estimated for a total of twentyfour stars in the field of the cluster. From a plot between these spectral types and the V(POSS) magnitudes shown in Fig.4.30 (cf. Table 4.5), it may be seen that stars 5,7,9 and 17 are obvious non-members. Star 18 is discarded because of its location at the edge of the field. Since stars 1, 2, 3, 4, 19, 20 and 23 also are located as far from the core of physical group, they are not considered as members of this cluster. However, these stars appear to be members of a southern group and are denoted by triangles in Fig.4.30. On the same grounds, stars 10, 11, 12, 14, 15, 16, 21 and 25 are considered to be likely members of a northern group. Stars 6 and 8 have tentatively been included into the northern group, though they are situated at an intermediate position. The earliest spectral type in the southern group appears to be B0 and that in the northern group looks like A0.

The field configuration is quite similar to that around BD-16°1999 = Bo 4+5 (Moffat & Vogt, 1975). However, while Bo 4 and 5 appear to be at different distances, the main sequences of both the groups in the direction of OC1 556 are superimposed on each other as seen in Fig.4.30. Thus, OC1 556 could be

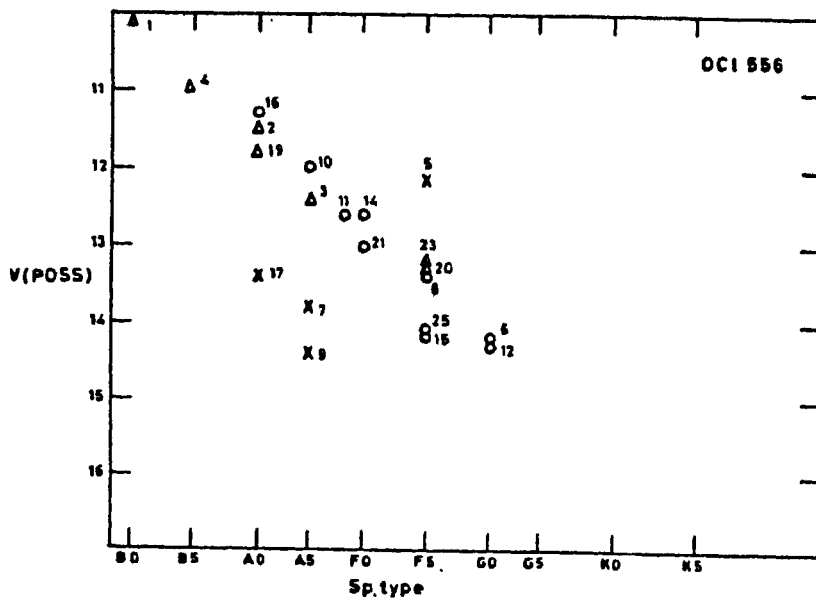


Fig. 4.30. Spectral type obtained from the modified objective-grating spectra plotted against the V magnitudes estimated from the POSS charts, for the stars in the field of OC1 556.

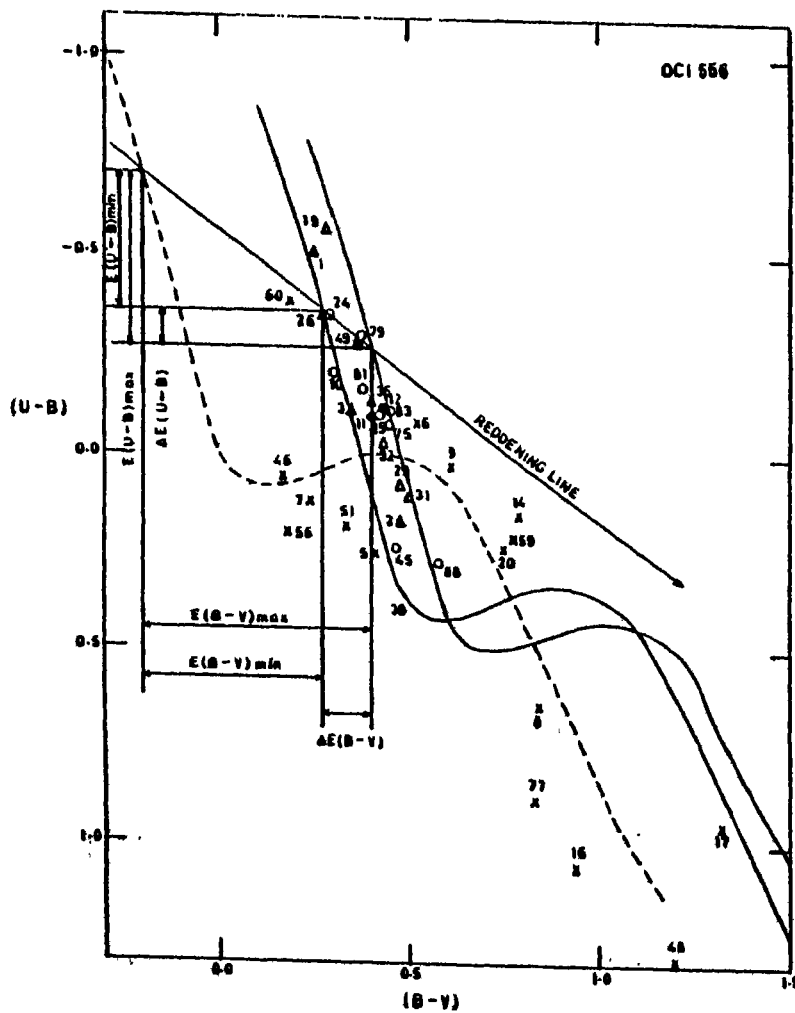


Fig. 4.31. The colour-colour diagram (CCD) of the stars in the region of OC1 556. The dashed line is the unreddened main sequence (MS) taken from Schmidt-Kaler (1965).



**Table 4.5.** The observational data for individual stars in the open cluster OC1 556

| Star No.                  | Spectral type | V (Sky survey) | V      | (B-V)  | (U-B)  | $V_0$  | $(B-V)_0$ | $(U-B)_0$ | Membership |
|---------------------------|---------------|----------------|--------|--------|--------|--------|-----------|-----------|------------|
| 1                         | 2             | 3              | 4      | 5      | 6      | 7      | 8         | 9         | 10         |
| Photoelectric photometry: |               |                |        |        |        |        |           |           |            |
| 1                         | B0            | 10.1           | 9.947  | 0.251  | -0.506 | 8.208  | -0.284    | -0.891    | mS         |
| 2                         | A0            | 11.5           | 11.041 | 0.481  | 0.172  | 9.302  | -0.054    | -0.213    | mS         |
| 3                         | A5            | 12.4           | 11.954 | 0.345  | -0.115 | 10.215 | -0.190    | -0.500    | mS         |
| 4                         | B5            | 11.0           |        |        |        |        |           |           |            |
| 9                         | A5            | 14.4           | 13.938 | 0.609  | 0.020  | -      | -         | -         | -          |
| 11                        | A8            | 12.6           | 12.250 | 0.397  | -0.100 | 10.511 | -0.138    | -0.485    | mN         |
| 12                        | G0            | 14.3           | 14.936 | 0.422  | -0.130 | 13.197 | -0.113    | -0.515    | mN         |
| 15                        | F5            | 14.1           | -      | -      | -      | -      | -         | -         | -          |
| 18                        | A0            | 12.1           | -      | -      | -      | -      | -         | -         | -          |
| 20                        | F5            | 13.3           | -      | -      | -      | -      | -         | -         | --         |
| 21                        | F0            | 13.0           | -      | -      | -      | -      | -         | -         | -          |
| 23                        | F5?           | 13.2           | -      | -      | -      | -      | -         | -         | -          |
| 26                        | -             | -              | 11.282 | 0.271  | 0.352  | 9.543  | -0.264    | -0.737    | mS         |
| 48                        | -             | -              | 14.159 | 1.183  | 1.290  | -      | -         | -         | -          |
| 49                        | -             | -              | 14.214 | 0.354  | -0.297 | 12.475 | -0.181    | -0.682    | mS         |
| Photographic photometry:  |               |                |        |        |        |        |           |           |            |
| 5                         | F5            | 12.2           | 12.629 | 0.415  | 0.250  | -      | -         | -         | -          |
| 6                         | G0            | 14.2           | 13.858 | 0.520  | -0.085 | -      | -         | -         | -          |
| 7                         | A5            | 13.8           | 13.419 | 0.234  | 0.113  | -      | -         | -         | --         |
| 8                         | F5            | 13.4           | 12.936 | 0.837  | 0.642  | -      | -         | -         | -          |
| 10                        | A5            | 12.0           | 12.508 | 0.297  | -0.210 | 10.769 | -0.238    | -0.595    | mN         |
| 14                        | F0            | 12.6           | 12.773 | 0.790  | 0.150  | -      | -         | -         | -          |
| 16                        | A0            | 11.3           | 12.054 | 0.932  | 1.057  | -      | -         | -         | -          |
| 17                        | A0            | 13.4           | 12.953 | 1.313  | 0.942  | -      | -         | -         | -          |
| 19                        | A0            | 11.8           | 12.204 | 0.277  | -0.561 | 10.465 | -0.258    | -0.946    | mS?        |
| 24                        | -             | -              | 14.527 | -0.281 | -0.360 | 12.788 | -0.254    | -0.745    | mN         |

---

| 1  | 2   | 3    | 4      | 5     | 6      | 7      | 8      | 9      | 10 |
|----|-----|------|--------|-------|--------|--------|--------|--------|----|
| 25 | F5? | 14.1 | 13.932 | 0.415 | -0.120 | 2.193  | -0.120 | -0.505 | mN |
| 29 | -   | -    | 15.246 | 0.476 | 0.072  | 13.507 | -0.059 | -0.313 | mS |
| 31 | -   | -    | 15.432 | 0.500 | 0.101  | 13.693 | -0.035 | -0.284 | mS |
| 32 | -   | -    | 16.014 | 0.436 | -0.036 | 14.275 | -0.099 | -0.421 | mS |
| 35 | -   | -    | 15.784 | 0.407 | -0.128 | 14.045 | -0.128 | -0.513 | mS |
| 38 | -   | -    | 15.682 | 0.458 | 0.027  | 13.943 | -0.077 | -0.358 | mS |
| 45 | -   | -    | 16.492 | 0.516 | 0.232  | 14.753 | -0.019 | -0.153 | mS |
| 46 | -   | -    | 16.671 | 0.164 | 0.053  | -      | -      | -      | -  |
| 51 | -   | -    | 16.541 | 0.337 | 0.185  | -      | -      | -      | -  |
| 54 | -   | -    | 13.311 | 1.536 | 1.728  | -      | -      | -      | -  |
| 56 | -   | -    | 13.836 | 0.174 | 0.199  | -      | -      | -      | -  |
| 58 | -   | -    | 14.662 | 1.676 | 1.129  | -      | -      | -      | -  |
| 59 | -   | -    | 15.625 | 0.774 | 0.206  | -      | -      | -      | -  |
| 60 | -   | -    | 15.776 | 0.186 | -0.382 | -      | -      | -      | -  |
| 61 | -   | -    | 13.086 | 1.955 | 1.595  | -      | -      | -      | -  |
| 69 | -   | -    | 14.202 | 1.777 | 1.376  | -      | -      | -      | -  |
| 72 | -   | -    | 14.227 | 1.999 | 1.293  | -      | -      | -      | -  |
| 75 | -   | -    | 14.589 | 0.448 | -0.082 | 12.850 | -0.087 | -0.467 | mN |
| 77 | -   | -    | 14.198 | 0.821 | 0.886  | -      | -      | -      | mN |
| 78 | -   | --   | 14.747 | 0.392 | 0.200  | 13.008 | -0.143 | -0.185 | mN |
| 79 | -   | --   | 14.145 | 0.374 | -0.305 | 12.406 | -0.161 | -0.690 | mN |
| 81 | -   | --   | 15.683 | 0.359 | -0.170 | 13.944 | -0.176 | -0.555 | mN |
| 83 | -   | -    | 14.324 | 0.448 | -0.119 | 12.585 | -0.087 | -0.504 | mN |
| 88 | -   | -    | 15.257 | 0.581 | 0.280  | 13.518 | 0.046  | -0.105 | mN |

---

either an extended cluster with a foreground strip of interstellar matter cutting across it or two different clusters located almost at the same distance. If the second case turns out to be true, this cluster may provide evidence for sequential star formation as proposed by Elmegreen and Lada (1977). With these points in view, the field of OC1 556 has been selected for further work in this programme.

The photoelectric observations of the stars in the field of this cluster were obtained using the 61-cm telescope at the Siding Spring Observatory (cf. Section 3.1). Standardized magnitudes and colours for a total of ten stars were obtained and the values are included in Table 4.5. The atmospheric coefficients, the transformation coefficients and the zero-point constants (cf. Equations 3.6 to 3.11) are tabulated below.

$$\begin{array}{lll} K_V = 0.165 & \epsilon = 5.495 & \zeta_V = 0.303 \quad ? \\ K_{b-v} = 0.155 & \mu = 0.034 & \zeta_{bv} = 0.785 \quad ? \\ K_{u-b} = 0.200 & \psi = 2.225 & \zeta_{ub} = -2.693 \end{array}$$

The direct photography of this field was carried out using both the 102-cm telescope of Kavalur Observatory (KO) and the 1-m telescope of Siding Spring Observatory (SSO) as described in Section 3.2.1. The following are the plate and filter combinations along with the exposure times.

| <u>Plate</u> | <u>Filter</u> | <u>Exposure time</u> |
|--------------|---------------|----------------------|
| IIa-0        | UG2           | 45 min for U(SSO)    |
| 103a-0       | GG13          | 30 min for B(SSO)    |
| 103a-D       | GG11          | 60 min for V(KO)     |

From these plates the photographic magnitudes were obtained on an arbitrary scale, for a total of fortyfour stars, in which the photoelectrically observed ones also were included. They were then standardized using the photoelectric observations (cf. Section 3.2.2). These magnitudes and colours are listed in Table 4.5.

#### 4.5.2. Membership

The membership of the individual stars in this cluster has been determined using the photometric criteria as described in Section 3.3.1. The CCD of this cluster shown in Fig.4.31 indicates a clear sequence of many stars. By marking the boundaries of the most likely sequence in this diagram and picking out the same stars on the two CMD's (cf. Figs. 4.32 and 4.33) a total of twentythree stars could be identified as members out of the observed fortyfour stars. Then a visual examination of the star field in Fig.4.29 reveals that twelve of the above mentioned twentythree belong to the southern group with one (star 19) being a doubtful case, due to its far off location from the main group of stars. The remaining eleven stars are members of the northern group.

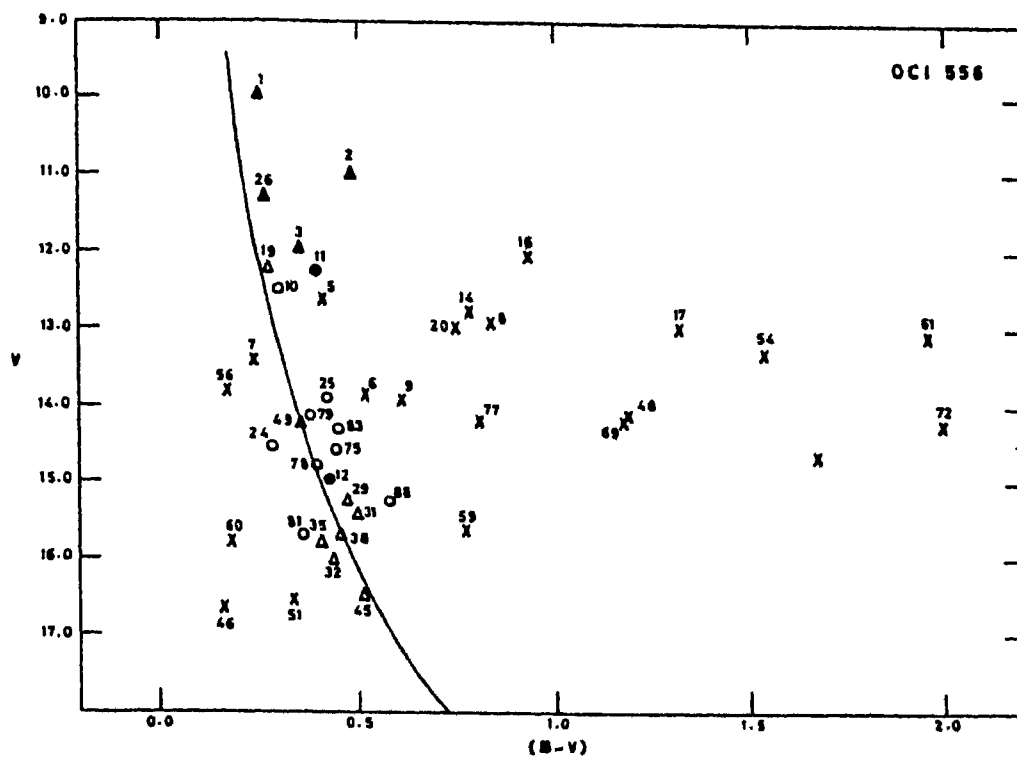


Fig. 4.32. The  $(B-V)$ ,  $V$  diagram (CMD) of OC1 556. The solid curve represents the zero age main sequence (ZAMS) fitted onto the cluster CMD.

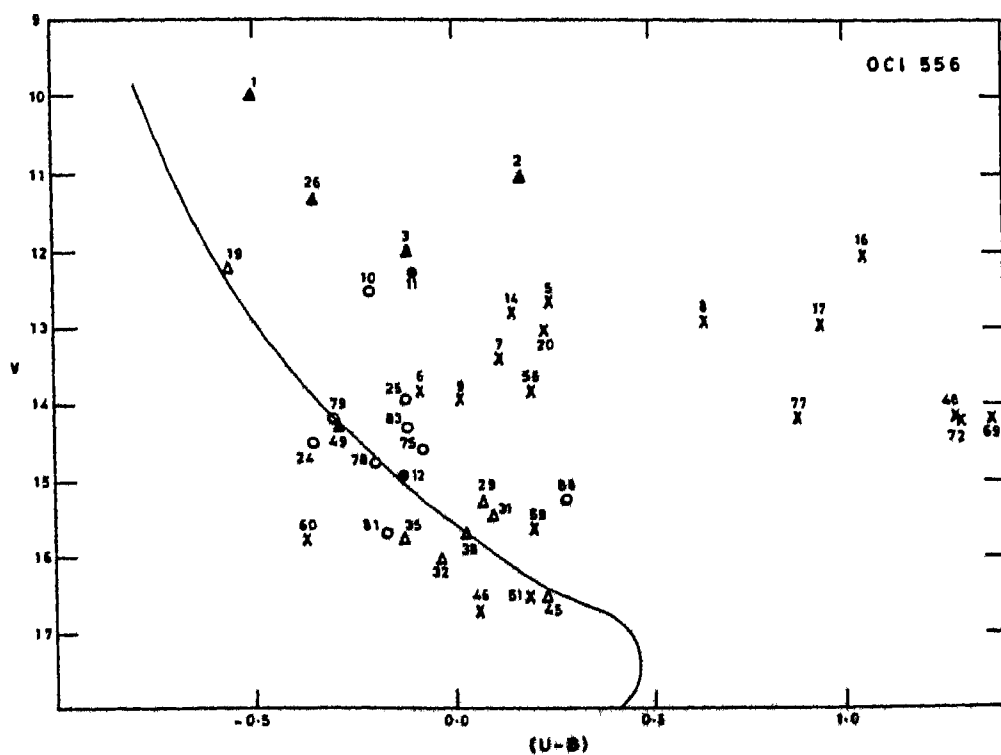


Fig. 4.33. The  $(U-B)$ ,  $V$  diagram (CMD) of OC1 556. The solid curve represents the ZAMS fitted onto the cluster CMD.

If there was any foreground interstellar matter cutting across the field, then the reddening should have been more for the stars which are behind the strip of this material as compared to the stars situated away from it. However such an excessive reddening is not noticed in the CCD of this region. Thus, there is no evidence for the existence of any 'extra' strip of interstellar matter between the star field and the observer. Further, most of the stars, which are located midway between the two groups in the chart (cf. Fig.4.29), appear to be more like foreground stars than being members of either group. They show much less reddening than the average reddening of the members. Thus, the possibility of the stars in the northern and the southern groups, together comprising an extended cluster, may be ruled out. Further, the stars of both groups are overlapping each other in all the above mentioned three diagrams indicating the likelihood that these two groups are two independent clusters located at the same distance with the same amount of interstellar matter in front of both of them. The members are denoted as 'mN' and 'mS' respectively for northern and southern groups, in Table 4.5. The southern group stars are indicated by triangles while those of the northern group are shown by circles in all the diagrams corresponding to these two groups of stars, which are now named as OC1 556S and OC1 556N respectively.

#### 4.5.3. Reddening

The CCD in Fig.4.31 shows a sequence formed by most of the stars and the boundaries of this sequence show that

$$\Delta E(B-V) = 0.13 \text{ mag}$$

$$\text{with } E(B-V)_{\text{max}} = 0.60 \text{ mag}$$

$$\text{and } E(B-V)_{\text{min}} = 0.47 \text{ mag.}$$

Similarly,

$$\Delta E(U-B) = 0.09 \text{ mag}$$

$$\text{with } E(U-B)_{\text{max}} = 0.43 \text{ mag}$$

$$\text{and } E(U-B)_{\text{min}} = 0.34 \text{ mag.}$$

These  $\Delta$  values are close to the ones arising from the natural dispersion (cf. Section 3.4) and therefore, an almost non-variable extinction across the field of both the groups is presumed. Hence, the following mean colour excesses have been adopted for the entire field.

$$\begin{aligned} E(B-V) &= 1/2 [ E(B-V)_{\text{max}} + E(B-V)_{\text{min}} ] \\ &= 0.535 \text{ mag.} \end{aligned}$$

and similarly

$$\begin{aligned} E(U-B) &= 1/2 [ E(U-B)_{\text{max}} + E(U-B)_{\text{min}} ] \\ &= 0.385 \text{ mag.} \end{aligned}$$

Then

$$A_V = 1.739 \pm 0.027 \text{ mag.}$$

Using these values in Equations 3.18 to 3.20, the intrinsic

magnitudes and colours were calculated, which are also included in Table 4.5 as  $V_0$ ,  $(B-V)_0$  and  $(U-B)_0$ .

#### 4.5.4. Distance

The main sequences of both the northern as well as the southern groups are plotted in Fig.4.34 using the above mentioned intrinsic magnitudes and colours. Both the main sequences are found to be overlapping each other. The ZAMS has been fitted onto the lower portions of these diagrams in order to determine the true distance modulus of the cluster. They are found to be 13.36 mag and 13.46 mag in the long and short wavelength CMD's, respectively. This gives an average value of 13.41 mag. Then the distance to the cluster based on Equation 3.21 is

$$D = 4.81 \pm 0.11 \text{ kpc.}$$

The overlapping of the main sequences of both the groups and the fitting of the ZAMS for a common distance modulus suggests that both the northern and southern groups of stars are situated at the same distance from the observer.

#### 4.5.5. Ages of the Two Clusters

Fig. 4.35 shows the HR diagrams of both the groups plotted for the true distance modulus of 13.41 mag. The stars of the southern group, denoted by triangles show a slightly evolved nature and indicate an age dispersion of  $1.0 \times 10^7$  to  $2.8 \times 10^7$  years, on the basis of the isochrones. On the other hand, the northern group seems to show a dispersion in the



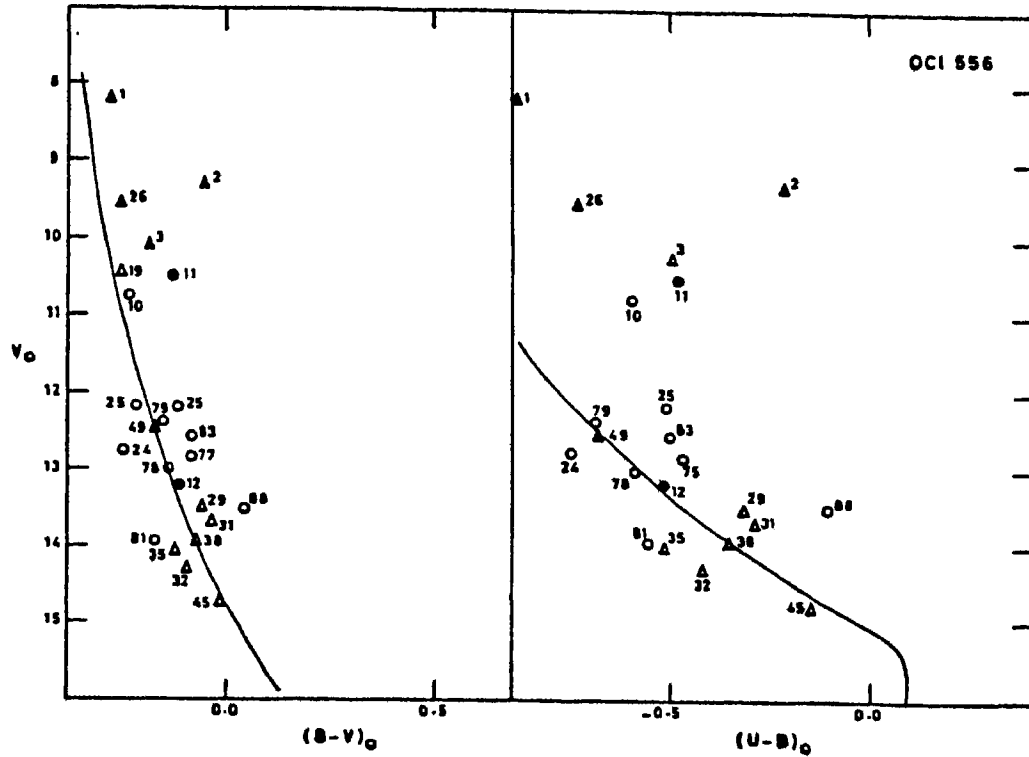


Fig. 4.34. The intrinsic  $(B-V)_0$ ,  $V_0$  and  $(U-B)_0$ ,  $V_0$  diagrams of both the clusters in the region of OC 1 556. The solid curves represent the ZAMS, taken from Schmidt-Kaler (1965), fitted onto the cluster CMDs.

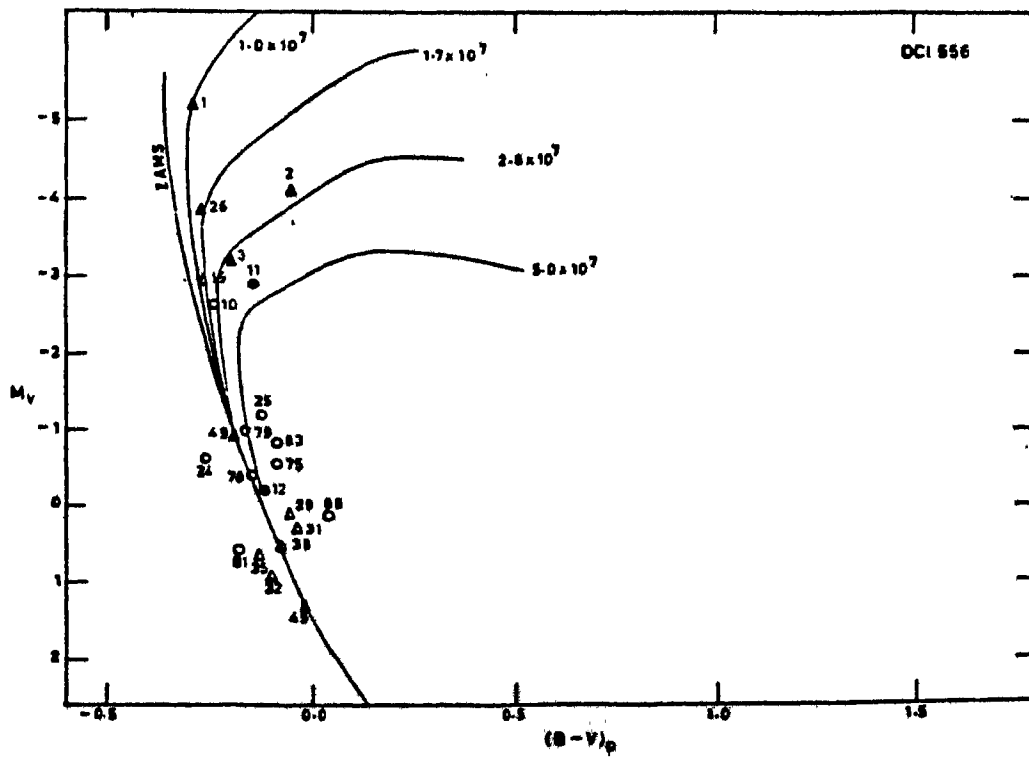


Fig. 4.35. HR-diagram of both the clusters in the region of OC 1 556. The post-MS isochrones are from Barbaro et al. (1969). The ages are indicated in years alongside the isochrones.

range of  $2.8 \times 10^7$  to  $5.0 \times 10^7$  years. Thus, it appears to have formed a little earlier than the southern cluster and hence both the clusters put together may provide an evidence for sequential star formation as theorized by Elmegreen and Lada (1977).

#### 4.6. OC 1 585 (NGC 2374)\*

The first systematic examination of this cluster was done by Trumpler (1930), who estimated an angular diameter of 4.5 arcmin and determined its distance to be 2600 parsecs. However, Collinder (1931) obtained a distance of 1240 parsecs and estimated the number of stars to be 100 and 40 respectively for two different angular diameters of 19.5 and 10 arcmin. Much later, Barhatova (1950) found its distance to be 930 parsec and gave an angular diameter of 15 arcmin. More recently, Fenkart et al. (1972) determined the distance of this cluster as 1260 parsec on the basis of photographic photometry. They found that the interstellar reddening was nil and gave twenty-nine stars as possible members. The age was estimated to be  $3.5 \times 10^8$  years by them. In the catalogue compiled by Lyngå (1980), a private communication by Buscombe mentions the distance as 1300 parsecs,  $E(B-V) = 0.0$  and the age as  $2 \times 10^9$  years. This entire information is reproduced in Table 2.3. Ruprecht (1966) has classified

The results included in this section have partially been published, vide: G.S.D.Babu, 1985 'A Study of the Open Cluster NGC 2374', *J. Astrophys. Astr.*, 6, 61.

this cluster as II 3p in the Trumpler classification system. The finding chart is given in Fig.4.36.

#### 4.6.1. Selection and Observations

Spectral types could be assigned to a total of twenty five stars in the field of the cluster from a modified objective grating plate of 2 hours exposure on 103a-0 emulsion (cf. Section 2.2). These estimates are plotted in Fig.4.37 against the V(POSS) magnitudes, both parameters being listed in Table 4.6. In this diagram, it may be seen that stars 1, 2, 3, 4, 5, 6 and 24 do not fit into the general sequence of the other stars. Among the rest of the stars, which are considered as possible members of the cluster, the earliest spectral type is found to be B5 for star 11. However, due to the uncertainty inherent in fixing the subclasses in the estimation of the spectral types, this has been selected as a marginally young cluster.

All the above mentioned stars were then observed photoelectrically using the 102-cm telescope of the Kavalur Observatory. Standardized magnitudes and colours for all these twentyfive stars were obtained and the values are included in Table 4.6. The atmospheric extinction coefficients, the transformation coefficients and the zero-point constants (cf. Equations 3.6 to 3.11) are tabulated below.

$$\begin{array}{lll} K_V = 0.686 & \epsilon = -0.137 & \zeta_V = 19.821 \\ K_{b-v} = 0.679 & \mu = 0.867 & \zeta_{bv} = 1.172 \\ K_{u-b} = 0.992 & \psi = 1.606 & \zeta_{ub} = -1.451 \end{array}$$

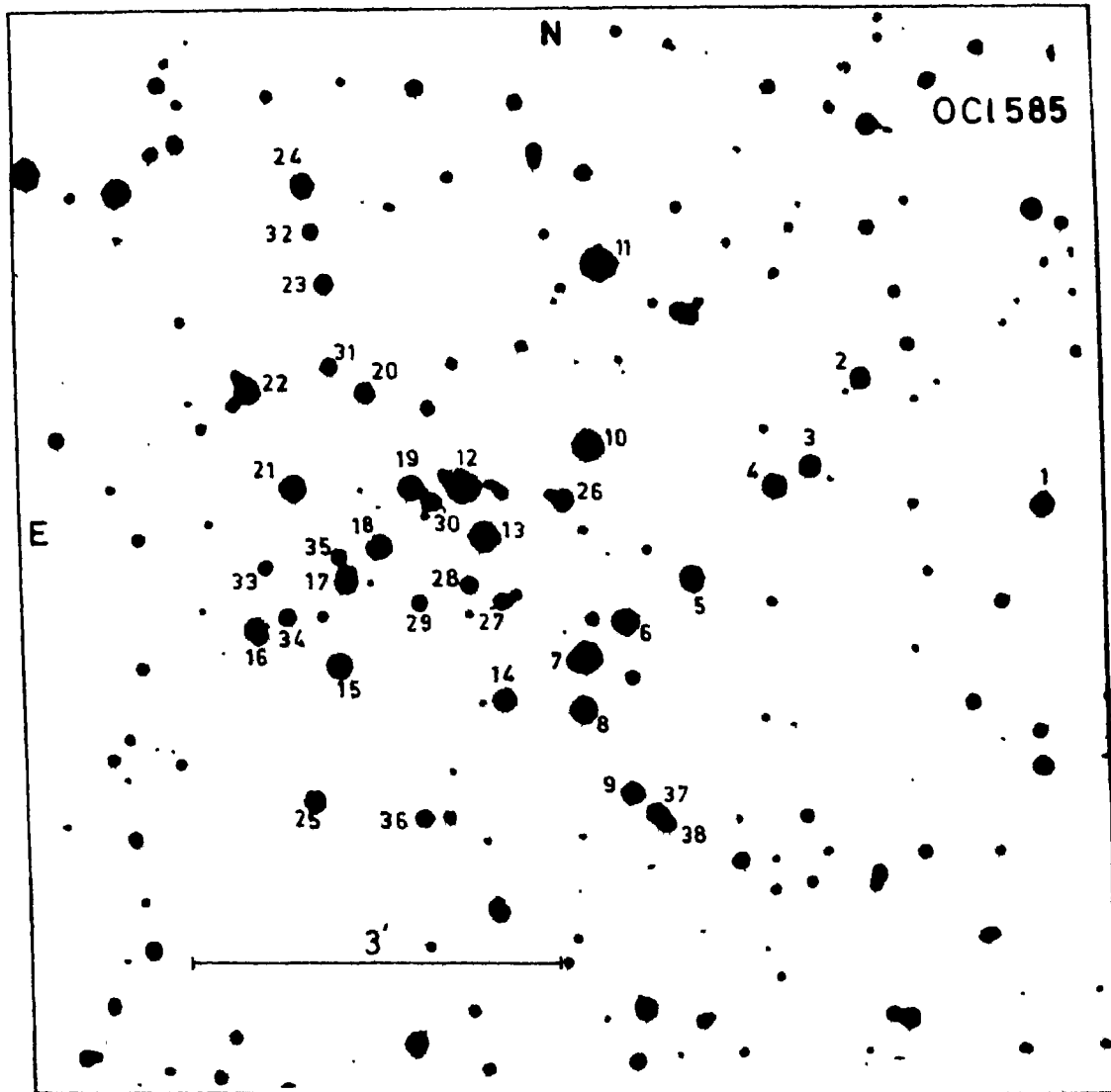


Fig. 4.36. Finding chart for the field of OC1585.

**Table 4.6.** The observational data for individual stars in the open cluster OC 1585.

| Star No.                 | Spectral type | V (POSS) | V      | (B-V) | (U-B)  | V <sub>0</sub> | (B-V) <sub>0</sub> | (U-B) <sub>0</sub> | Membership |
|--------------------------|---------------|----------|--------|-------|--------|----------------|--------------------|--------------------|------------|
| 1                        | 2             | 3        | 4      | 5     | 6      | 7              | 8                  | 9                  | 10         |
| Photoelectric photometry |               |          |        |       |        |                |                    |                    |            |
| 1                        | K5            | 12.25    | 11.750 | 1.340 | 0.910  | -              | -                  | -                  | -          |
| 2                        | A5            | 13.79    | 13.710 | 0.312 | 0.128  | 13.141         | 0.137              | -0.002             | m?         |
| 3                        | A5            | 13.58    | 13.721 | 0.255 | 0.021  | 13.152         | 0.080              | -0.109             | m?         |
| 4                        | K0            | 12.23    | 11.840 | 1.099 | 0.518  | 11.271         | 0.924              | 0.388              | m?         |
| 5                        | F0            | 12.45    | 12.334 | 0.469 | -0.155 | -              | -                  | -                  | -          |
| 6                        | F0            | 12.18    | 12.308 | 0.606 | -0.074 | -              | -                  | -                  | -          |
| 7                        | A0            | 11.67    | 11.866 | 0.179 | 0.040  | 11.297         | 0.004              | -0.090             | m          |
| 8                        | A0            | 12.44    | 12.637 | 0.292 | 0.109  | 12.068         | 0.117              | -0.021             | m          |
| 9                        | F5            | 13.23    | 13.380 | 0.444 | 0.104  | 12.811         | 0.269              | -0.026             | m          |
| 10                       | B7            | 11.43    | 11.664 | 0.128 | 0.069  | 11.095         | -0.047             | -0.199             | m          |
| 11                       | B5            | 10.59    | 10.653 | 0.449 | -0.125 | -              | -                  | -                  | -          |
| 12                       | B7            | 11.18    | 11.540 | 0.080 | -0.170 | 10.971         | -0.095             | -0.300             | m          |
| 13                       | A0            | 11.94    | 12.027 | 0.177 | -0.018 | 11.458         | 0.002              | -0.148             | m          |
| 14                       | A5            | 13.15    | 13.762 | 0.241 | 0.088  | 13.193         | 0.066              | -0.042             | m          |
| 15                       | A5            | 12.77    | 12.996 | 0.246 | 0.234  | 12.427         | 0.071              | 0.104              | m          |
| 16                       | A0            | 12.58    | 12.777 | 0.190 | 0.136  | 12.208         | 0.015              | 0.006              | m          |
| 17                       | A0            | 12.67    | 12.604 | 0.254 | 0.228  | 12.035         | 0.079              | 0.098              | m          |
| 18                       | A5            | 12.90    | 13.261 | 0.315 | 0.202  | 12.692         | 0.140              | 0.072              | m          |
| 19                       | F0            | 12.81    | 13.229 | 0.398 | 0.179  | 12.660         | 0.234              | 0.049              | m          |
| 20                       | F5            | 13.32    | 13.793 | 0.485 | 0.135  | 13.224         | 0.310              | 0.005              | m          |
| 21                       | A0            | 12.23    | 12.531 | 0.219 | 0.213  | 11.962         | 0.044              | 0.083              | m          |
| 22                       | A5            | 12.48    | 13.038 | 0.350 | 0.123  | 12.469         | 0.175              | -0.007             | m          |
| 23                       | F0            | 13.31    | 13.875 | 0.376 | 0.208  | 13.306         | 0.271              | 0.078              | m          |
| 24                       | K0            | 11.89    | 12.070 | 1.014 | 0.552  | 11.501         | 0.839              | 0.422              | m?         |
| 25                       | F0            | 13.01    | 13.133 | 0.399 | 0.173  | 12.564         | 0.224              | 0.043              | m          |

---

| 1                       | 2 | 3 | 4     | 5     | 6     | 7     | 8    | 9     | 10 |
|-------------------------|---|---|-------|-------|-------|-------|------|-------|----|
| Photographic photometry |   |   |       |       |       |       |      |       |    |
| 26                      | - | - | 13.80 | 0.35  | 0.20  | 13.23 | 0.18 | 0.07  | m  |
| 27                      | - | - | 15.12 | 0.21  | -0.46 | -     | -    | -     | -  |
| 28                      | - | - | 15.04 | 0.14  | 0.02  | -     | -    | -     | -  |
| 29                      | - | - | 14.95 | 0.63  | 0.07  | 14.38 | 0.46 | -0.06 | m  |
| 30                      | - | - | 14.79 | 0.15  | 0.07  | -     | -    | -     | -  |
| 31                      | - | - | 14.92 | 0.05  | -0.82 | -     | -    | -     | -  |
| 32                      | - | - | 15.14 | -0.12 | -0.12 | -     | -    | -     | -  |
| 33                      | - | - | 14.69 | 0.56  | 0.10  | 14.12 | 0.39 | -0.03 | m  |
| 34                      | - | - | 15.02 | 0.02  | -0.05 | -     | -    | -     | -  |
| 35                      | - | - | 15.49 | 0.00  | -0.36 | -     | -    | -     | -  |
| 37                      | - | - | 13.73 | 0.36  | 0.06  | 13.16 | 0.19 | -0.07 | m  |
| 38                      | - | - | 14.95 | 0.07  | -0.32 | -     | --   | -     | -  |

---

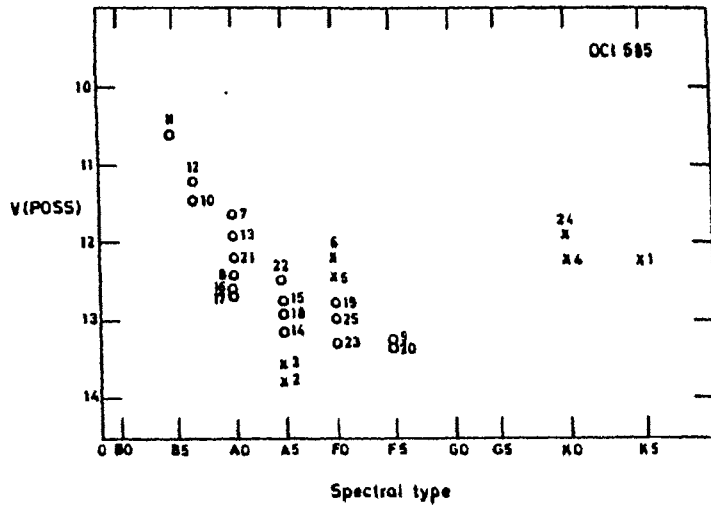


Fig. 4.37 Spectral type obtained from the modified objective grating spectra plotted against the V magnitudes estimated from the POSS charts, for the stars in the field of OC1 585.

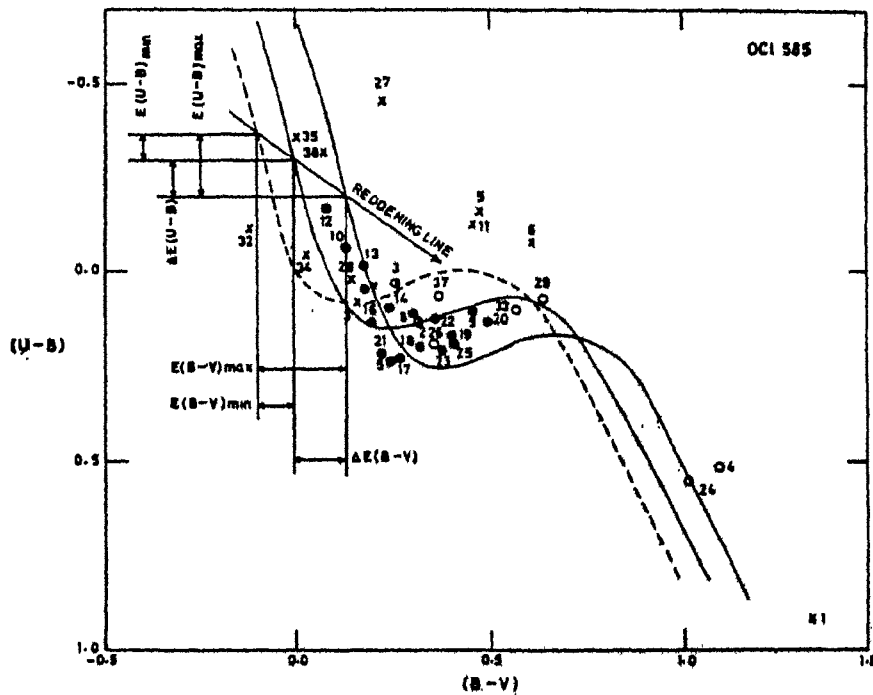


Fig. 4.38. The colour-colour diagram (CCD) of OC1 585. The dashed line is the unreddened main sequence (MS) taken from Schmidt-Kaler (1965).

The direct photography of this cluster was also done using the 102-cm telescope of the Kavalur Observatory, (cf. Section 3.2.1). The following are the plate and filter combinations along with the exposure times.

| <u>Plate</u> | <u>Filter</u> | <u>Exposure time</u> |
|--------------|---------------|----------------------|
| 103a-0       | UG2           | 50 min for U         |
| 103a-0       | GG13          | 30 min for B         |
| IIa-D        | GG11          | 30 min for V         |

The image diameters for a total of thirty eight individual stars were measured with the help of an X-Y coordinate measuring engine in the same manner as was done for the sky survey charts (cf. Section 2.3). These measurements also included all the photoelectrically observed stars in the field of this cluster on these plates. The diameters were then transformed to photographic magnitudes, using the photoelectrically observed stars for calibration. These magnitudes and colours are listed in Table 4.6.

#### 4.6.2. Membership

The photometric criteria (cf. Section 3.3.1) was used to determine the membership of the individual stars. The CCD of this cluster, shown in Fig.4.38, indicates a clear sequence for a majority of stars for which the boundaries are marked. Then by picking out these same stars on the two CMD's shown in Figs 4.39 and 4.40, a total of twenty stars have been adopted as the most probable members of the cluster out of the observed



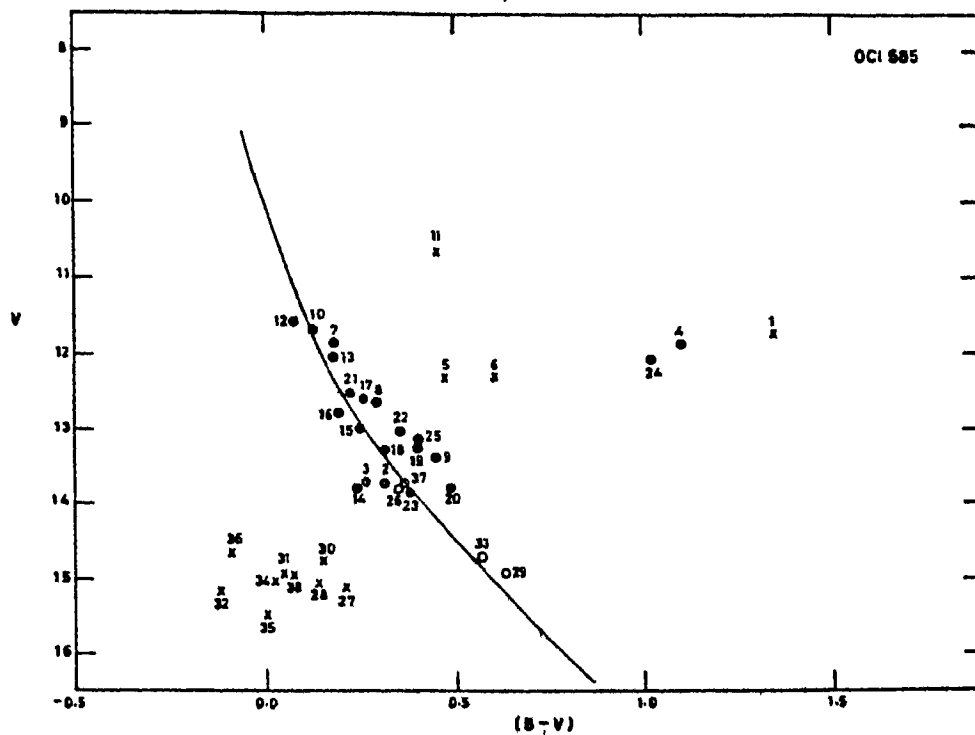


Fig. 4.39. The (B-V), V diagram (CMD) of OC1 585. The solid curve represents the zero age main sequence (ZAMS) fitted onto the cluster CMD.

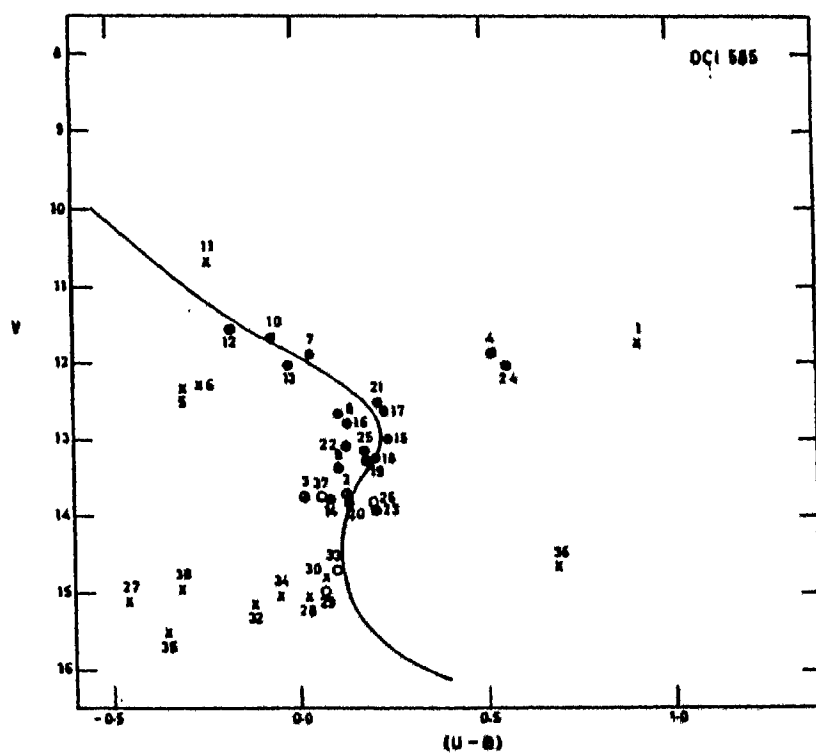


Fig. 4.40. The (U-B), V diagram (CMD) of OC1 585. The solid curve represents the ZAMS fitted onto the cluster CMD.

thirtyeight stars. There are two stars (4 and 24) which may belong to the giant branch of the cluster. But because of their slightly far off location from the main physical group, they have been marked as doubtful members. On similar grounds, stars 2 and 3 also are taken as doubtful members. Finally, star 11, being the brightest of the measured stars, (selection of the cluster depended on the spectral type of this star as mentioned in Section 4.6.1), is found to show much larger reddening which is not compatible with the cluster members. Thus, the star is considered as a non-member and thereby the cluster's earliest spectral type gets shifted to B7 (stars 10 and 12).

#### 4.6.3. Reddening

The CCD in Fig.4.38 shows a sequence formed by the member stars and the boundaries of this sequence show that

$$\begin{aligned} & \Delta E(B-V) = 0.13 \text{ mag} \\ \text{with} & \quad E(B-V)_{\text{max}} = 0.24 \text{ mag} \\ \text{and} & \quad E(B-V)_{\text{min}} = 0.11 \text{ mag.} \end{aligned}$$

Similarly,

$$\begin{aligned} & \Delta E(U-B) = 0.10 \text{ mag} \\ \text{with} & \quad E(U-B)_{\text{max}} = 0.18 \text{ mag} \\ \text{and} & \quad E(U-B)_{\text{min}} = 0.08 \text{ mag.} \end{aligned}$$

These  $\Delta$  values are close to the ones arising from the natural dispersion (cf. Section 3.4) and consequently an almost non-

variable extinction across the field of the cluster is presumed. Hence, the following mean colour excesses have been adopted.

$$\begin{aligned} E(B-V) &= 1/2 [E(B-V)_{\max} + E(B-V)_{\min}] \\ &= 0.175 \text{ mag} \end{aligned}$$

and similarly

$$\begin{aligned} E(U-B) &= 1/2 [E(U-B)_{\max} + E(U-B)_{\min}] \\ &= 0.13 \text{ mag.} \end{aligned}$$

Then

$$A_V = 0.569 \pm 0.009 \text{ mag}$$

Using these values in Equations 3.18 to 3.20, the intrinsic magnitudes and colours of the member stars were calculated, which have been included in Table 4.6 as  $V_0$ ,  $(B-V)_0$  and  $(U-B)_0$ .

#### 4.6.4. Distance

The cluster main sequences, composed of the probable members in both the CMD's are plotted in Fig.4.41, using the intrinsic magnitudes and colours mentioned above. The ZAMS has been shifted to match these main sequences in order to determine the true distance modulus of the cluster. This resulted in 10.33 mag and 10.13 mag respectively in the long and short wavelength CMD's, the average being 10.23 mag. Then the distance to the cluster based on Equation 3.21 is

$$D = 1.11 \pm 0.05.$$

This value is in a fair agreement with those obtained by Collinder (1931), Fenkart et al. (1972) and Buscombe (Lyngå, 1980), which are listed in Table 2.3.

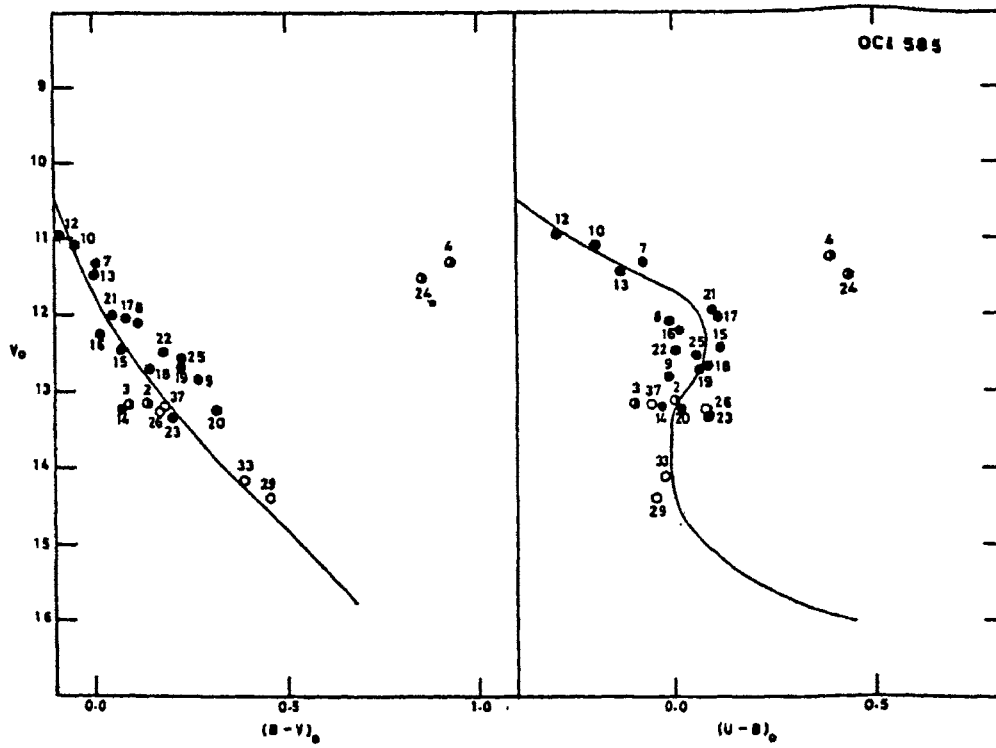


Fig. 4.41. The intrinsic  $(B-V)_0$ ,  $V_0$  and  $(U-B)_0$ ,  $V_0$  diagrams (CMDs) of OC1 585. The solid curves represent the ZAMS, taken from Schmidt-Kaler (1965), fitted onto the cluster CMDs.

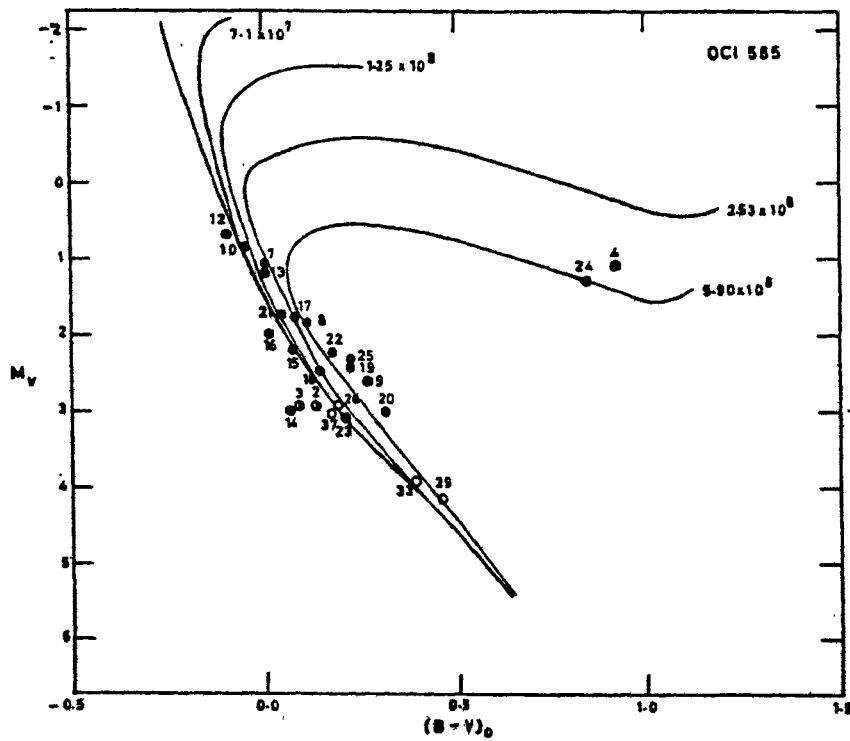


Fig. 4.42. HR-diagram of OC1 585. The post-MS isochrones are from Barbaro et al. (1969). The ages are indicated in years alongside the isochrones.

#### 4.6.5. Age of the Cluster

Fig.4.42 shows the HR-diagram of the cluster plotted for the true distance modulus of 10.23 mag. In this figure, it is found that the brighter MS stars extend upto the isochrone of  $7.1 \times 10^7$  years. It has also been estimated on the basis of the smallest  $(B-V)_0$  on the MS which gives  $6 \times 10^7$  years, agreeing fairly well with the isochrone age of the MS.

However, Fenkart et al. (1972) estimated the age of this cluster to be  $3.5 \times 10^8$  years based on the earliest spectral type using Hoerner's (1957) method. When the same method is applied to the earliest spectral type obtained in the present work (cf. Section 4.6.2) an age of  $1 \times 10^8$  years is obtained.

If the two doubtful members in the giant branch are considered as likely members of the cluster, then their apparent fitting close to the isochrone of  $5.9 \times 10^8$  years might indicate the non-coeval nature of this cluster. But the corresponding spread by the stars at the turn off area of the giant branch isochrone is not found in this diagram. Thus the membership of these two stars still remains doubtful. Therefore, considering only the main sequence, the age of the cluster is probably between 6 and  $7.1 \times 10^7$  years.

#### **4.7.OC1 674 (Haffner 14)**

Haffner (1957) identified this cluster and estimated its angular diameter to be 3.8 arcmin with fifty stars in it. He had also discussed its relationship with the spiral structure,

classifying it as III 3 m in the Trumpler system. However, Ruprecht (1966) reclassified it as III 2m. Fig.4.43 gives the finding chart for this cluster.

#### 4.7.1. Selection and Observations

This is the first cluster, for which the technique of visually inspecting the sky survey charts was applied (cf. Section 2.2). Stars 1, 2, 3, 13, 47, 58 and 59 appeared to be brighter on the blue than on the red print. Thus, considering these stars to be belonging to the B spectral type and assuming them to be cluster members, this cluster has been selected for the photometric investigations.

The photoelectric observations of this cluster were done using the 61-cm telescope of the Siding Spring Observatory (cf. Section 3.1). Standardized magnitudes and colours for total of ten stars were obtained and the values are included in Table 4.7. The atmospheric extinction co-efficients, the transformation coefficients and the zero-point constants (cf. Equations 3.6 to 3.11) are given below.

$$\begin{aligned} K_V &= 0.060 & \epsilon &= 0.337 & \zeta_V &= 5.148 \\ K_{b-v} &= 0.146 & \mu &= 0.762 & \zeta_{bv} &= 0.040 \\ K_{u-b} &= 0.080 & \psi &= -2.116 & \zeta_{ub} &= 1.765 \end{aligned}$$

The direct U,B,V photography of this cluster was done with the help of the 1-m telescope at Siding Spring Observatory (cf. Section 3.2.1). the plate and filter combinations along with the exposure times are as under.

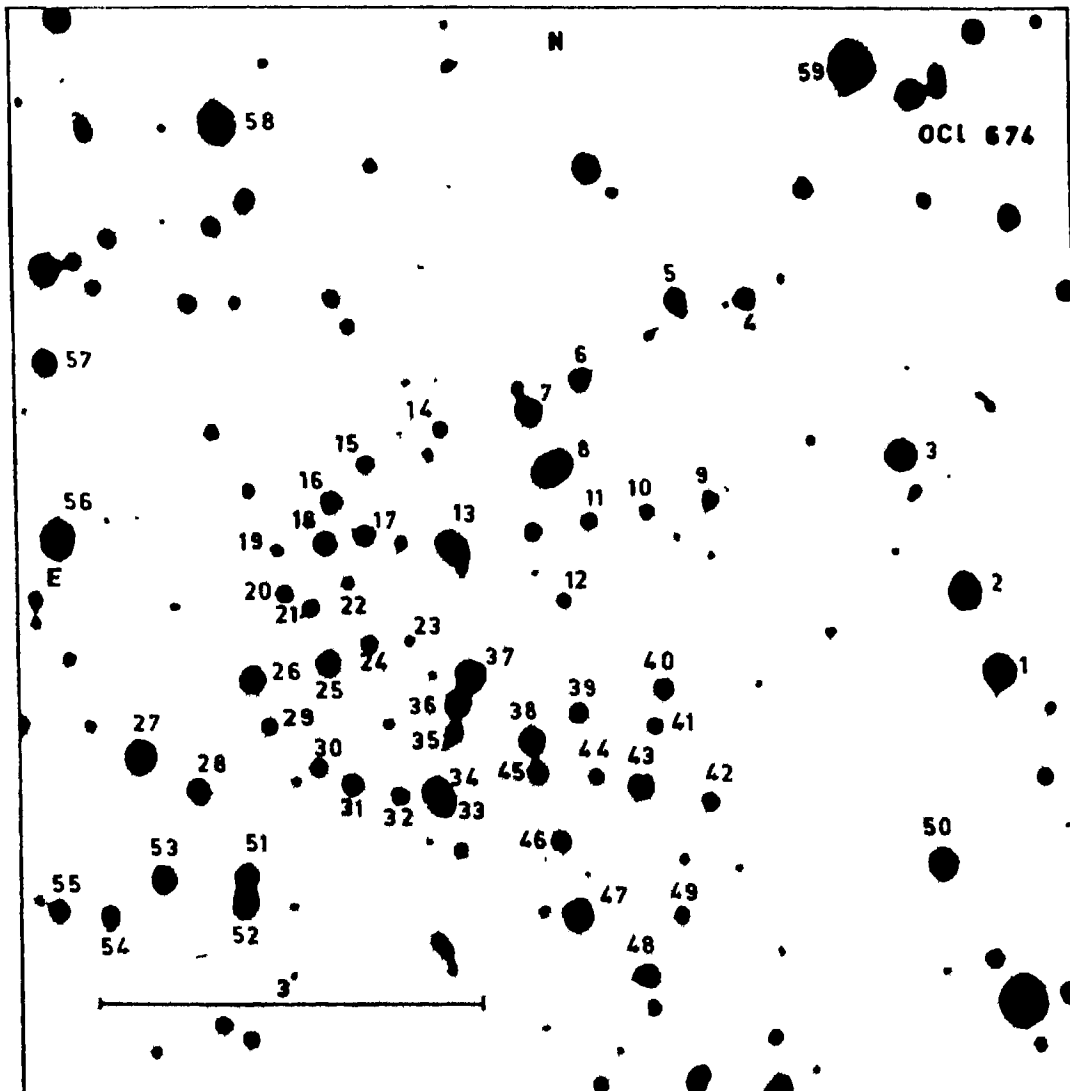


Fig. 4.43. Finding chart for the field of OC1 674.

**Table 4.7.** The observational data for individual stars in the open cluster OC1 674.

| Star No.                 | V      | (B-V) | (U-B)  | $V_0$  | $(B-V)_0$ | $(U-B)_0$ | E(B-V) | Membership |
|--------------------------|--------|-------|--------|--------|-----------|-----------|--------|------------|
| 1                        | 2      | 3     | 4      | 5      | 6         | 7         | 8      | 9          |
| Photoelectric photometry |        |       |        |        |           |           |        |            |
| 1                        | 12.863 | 0.406 | 0.049  | -      | -         | -         | -      | -          |
| 5                        | 14.338 | 0.645 | -0.144 | -      | -         | -         | -      | -          |
| 13                       | 13.727 | 0.428 | -0.240 | 11.719 | -0.190    | -0.685    | 0.618  | m          |
| 25                       | 14.368 | 0.652 | 0.214  | 11.940 | -0.095    | -0.325    | 0.747  | m          |
| 26                       | 14.084 | 0.515 | -0.095 | 11.890 | -0.160    | -0.580    | 0.675  | m          |
| 27                       | 12.470 | 0.480 | 0.186  | -      | -         | -         | -      | -          |
| 28                       | 13.778 | 0.533 | 0.343  | -      | -         | -         | -      | -          |
| 37                       | 13.173 | 0.589 | 0.332  | 11.129 | -0.040    | -0.130    | 0.629  | m          |
| 38                       | 14.033 | 0.527 | 0.070  | 11.963 | -0.110    | -0.385    | 0.637  | m          |
| 56                       | 12.086 | 0.573 | 0.275  | -      | -         | -         | -      | -          |
| Photographic photometry  |        |       |        |        |           |           |        |            |
| 2                        | 13.02  | 0.26  | -0.18  | -      | -         | -         | -      | -          |
| 3                        | 12.94  | 0.40  | 0.23   | -      | -         | -         | -      | -          |
| 6                        | 14.82  | 0.48  | 0.12   | 12.95  | -0.10     | -0.33     | 0.58   | m          |
| 7                        | 13.97  | 0.44  | -0.14  | 12.03  | -0.16     | -0.58     | 0.60   | m          |
| 8                        | 14.17  | 0.50  | 0.10   | 12.27  | -0.09     | -0.30     | 0.59   | m          |
| 11                       | 13.35  | 0.44  | -0.12  | 11.44  | -0.15     | -0.54     | 0.59   | m          |
| 14                       | 15.66  | 0.96  | 0.59   | 13.23  | +0.21     | 0.06      | 0.75   | m          |
| 15                       | 15.48  | 0.97  | 0.69   | 12.74  | +0.13     | 0.07      | 0.84   | m          |
| 16                       | 14.69  | 0.63  | 0.39   | 12.57  | -0.03     | -0.08     | 0.65   | m          |
| 17                       | 15.41  | 0.56  | 0.12   | 13.27  | -0.10     | -0.35     | 0.66   | m          |
| 18                       | 14.74  | 0.56  | 0.33   | 12.80  | -0.04     | -0.10     | 0.60   | m          |
| 21                       | 15.70  | 0.83  | 0.47   | 13.78  | +0.24     | 0.05      | 0.59   | m          |
| 31                       | 15.01  | 0.74  | 0.50   | 13.06  | +0.14     | 0.08      | 0.60   | m          |



---

| 1  | 2     | 3    | 4     | 5     | 6     | 7     | 8    | 9 |
|----|-------|------|-------|-------|-------|-------|------|---|
| 34 | 12.29 | 1.54 | 1.06  | 10.16 | 0.89  | 0.59  | 0.66 | m |
| 35 | 15.23 | 0.98 | 0.55  | 12.93 | 0.27  | 0.04  | 0.77 | m |
| 36 | 14.18 | 0.58 | 0.32  | 12.17 | -0.04 | -0.13 | 0.62 | m |
| 39 | 15.51 | 0.67 | 0.32  | 13.13 | -0.06 | -0.19 | 0.73 | m |
| 40 | 15.34 | 0.54 | 0.10  | 13.27 | -0.10 | -0.35 | 0.64 | m |
| 43 | 13.13 | 1.58 | 1.15  | 11.00 | -0.93 | 0.68  | 0.66 | m |
| 45 | 15.48 | 0.36 | 0.38  | -     | -     | -     | -    | - |
| 47 | 13.23 | 0.18 | 0.29  | -     | -     | -     | -    | - |
| 48 | 14.88 | 0.54 | 0.27  | -     | -     | -     | -    | - |
| 50 | 13.26 | 0.60 | 0.05  | -     | -     | -     | -    | - |
| 51 | 14.05 | 0.25 | -0.05 | -     | -     | -     | -    | - |
| 52 | 13.24 | 0.37 | 0.02  | -     | -     | -     | -    | - |
| 53 | 13.52 | 0.49 | 0.46  | -     | -     | -     | -    | - |
| 54 | 14.47 | 1.07 | 0.07  | -     | -     | -     | -    | - |
| 55 | 14.06 | 0.52 | 0.37  | -     | -     | -     | -    | - |
| 57 | 13.29 | 0.39 | 0.09  | -     | -     | -     | -    | - |
| 58 | 12.32 | 0.26 | -0.36 | -     | -     | -     | -    | - |
| 59 | 12.23 | 0.19 | -0.28 | -     | -     | -     | -    | - |

---

| <u>Plate</u> | <u>Filter</u> | <u>Exposure time</u> |
|--------------|---------------|----------------------|
| IIa-0        | UG2           | 60 min for U         |
| IIa-0        | GG13          | 30 min for B         |
| IIa-D        | GG14          | 30 min for V         |

From these plates, the photographic magnitudes were obtained for a total of fortyone stars, including the ten photoelectrically observed ones, on an arbitrary scale. These were then standardized using the above mentioned photoelectric observations as described in Section 3.2.2. These magnitudes and colours are also listed in Table 4.7.

#### 4.7.2. Membership

The CCD of this cluster, shown in Fig.4.44 indicated a clear sequence for some stars for which the boundaries are drawn in the diagram. By picking out the same stars in the two CMD's (cf. Figs. 4.45 and 4.46) and using the photometric criteria as described in Section 3.3.1 a total of twentytwo stars have been adopted as the most probable members of the cluster, out of the observed fortyone stars. Two of the members (stars 34 and 43) probably belong to the giant sequence. Among the adopted members, there are a few stars at the fainter end (stars 14, 15, 21, 31 and 35) which are located a little to the right of the MS. According to the photometric criteria for membership it is quite likely that these stars are pre-MS members. This last inference is based on the fairly young age of the cluster, which shall be discussed later on. All these members are denoted by 'm' in Table 4.7.

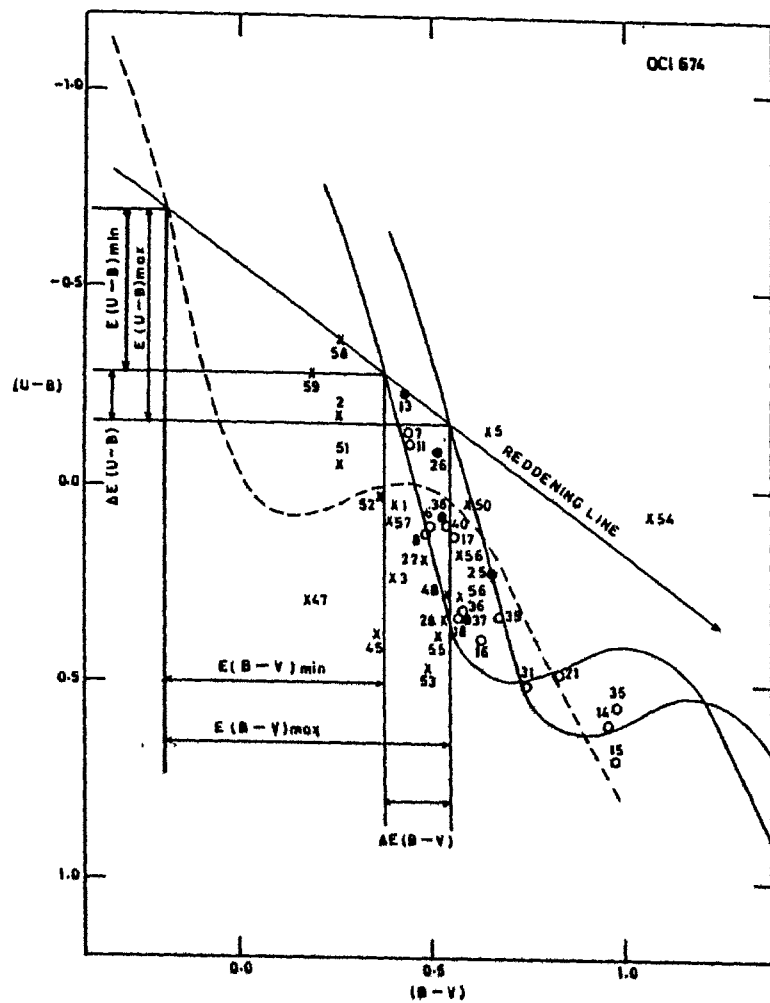


Fig. 4.44. The colour-colour diagram (CCD) of OC1 674. The dashed line is the unreddened main sequence (MS) taken from Schmidt-Kaler (1965).

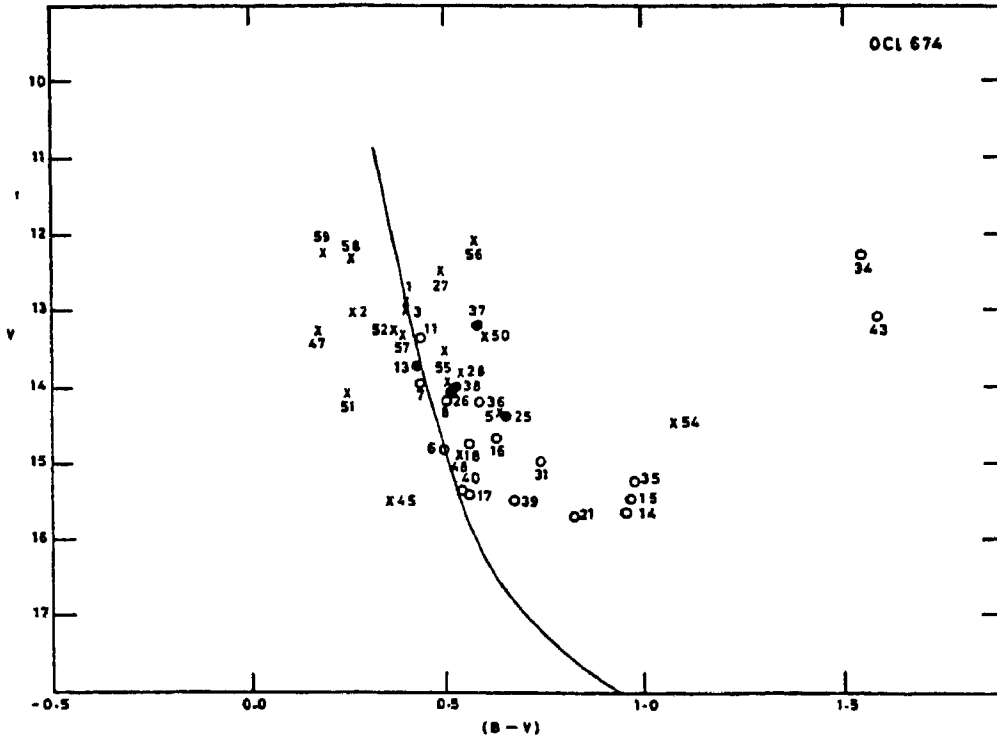


Fig. 4.45. The (B-V), V diagram (CMD) of OC1 674. The solid curve represents the zero age main sequence (ZAMS) fitted onto the cluster CMD.

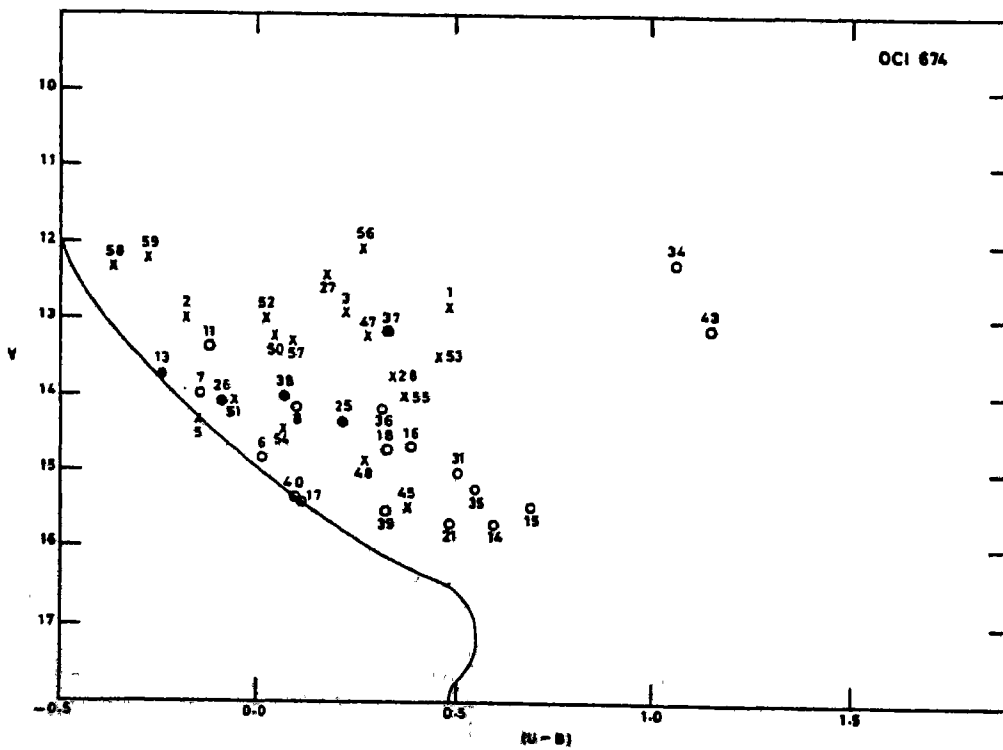


Fig. 4.46. The (U-B), V diagram (CMD) of OC1 674. The solid curve represents the ZAMS fitted onto the cluster CMD.

#### 4.7.3. Reddening

The CCD in Fig.4.44 shows a sequence formed by a majority of the stars and the boundaries of this sequence show that

$$\Delta E(B-V) = 0.17 \text{ mag}$$

and

$$\Delta E(U-B) = 0.12 \text{ mag.}$$

These values are much larger than the natural dispersion and therefore, the concerned stars were individually corrected for the appropriate interstellar reddening. These corrections were found to be between

$$E(B-V)_{\max} = 0.74 \text{ mag and } E(B-V)_{\min} = 0.57 \text{ mag}$$

and between

$$E(U-B)_{\max} = 0.53 \text{ mag and } E(U-B)_{\min} = 0.41 \text{ mag.}$$

With the help of the individual  $E(B-V)$  values, which are included in Table 4.7, the corresponding values of  $A_V$  were obtained, which were found to be between 2.41 mag and 1.85 mag. These, in turn, were used to correct the observed  $V$  values. All these corrected magnitudes and colours are also included in Table 4.7 as  $V_0$ ,  $(B-V)_0$  and  $(U-B)_0$ .

#### 4.7.4. Distance

The true distance modulus of this cluster has been determined by fitting ZAMS onto the cluster main sequences as shown in Fig.4.47. The long and short wavelength CMDs have been found to yield the distance moduli of 13.06 mag and 12.76 mag respectively, giving rise to an average value of 12.91 mag. Then the distance  $D$  to the cluster, based on Equation 3.21 is

$$D = 3.83 \pm 0.26 \text{ kpc.}$$

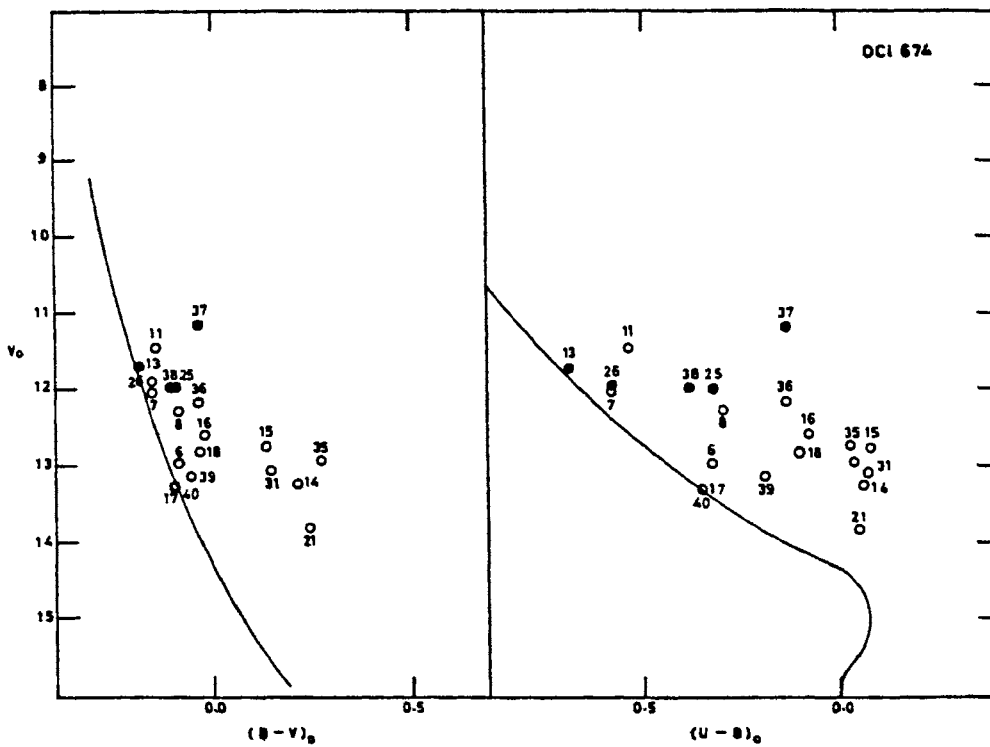


Fig. 4.47. The intrinsic  $(B-V)_0$ ,  $V_0$  and  $(U-B)_0$ ,  $V_0$  diagrams (CMDs) of OC1 674. The solid curves represent the ZAMS, taken from Schmidt-Kaler (1965), fitted onto the cluster CMDs.

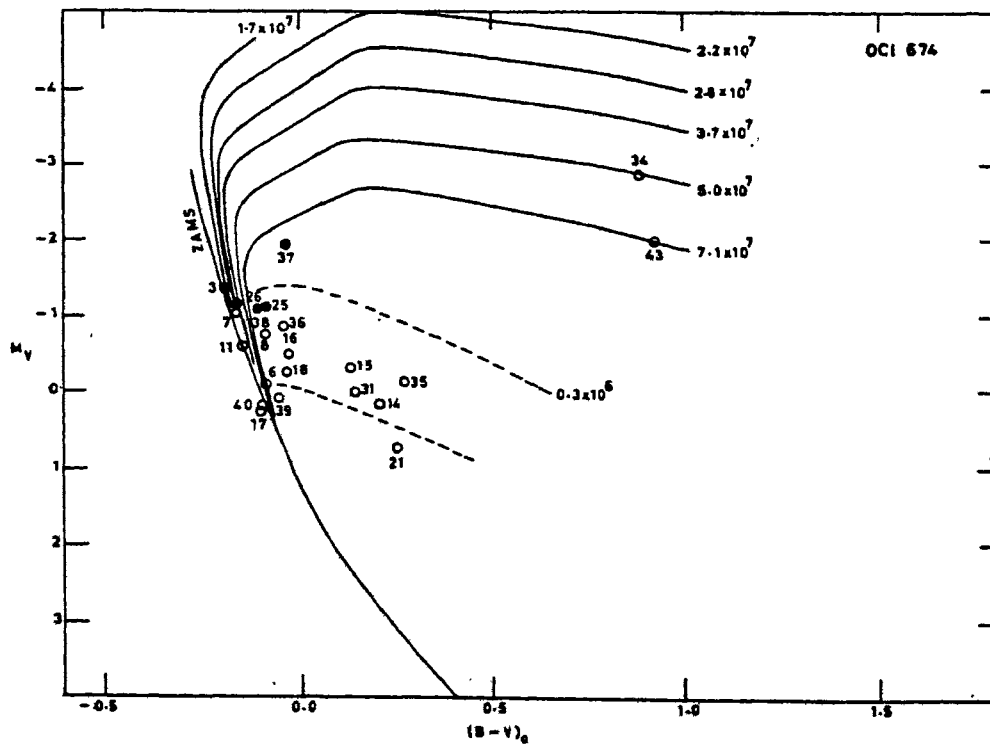


Fig. 4.48. HR-diagram of OC1 674. The post-MS isochrones are from Barbaro et al. (1969) and the dashed lines represent the pre-MS isochrones taken from Iben (1965). The ages are indicated in years alongside the isochrones.

#### 4.7.5. Age of the Cluster

Fig. 4.48 shows the HR-diagram of the cluster, plotted for the true distance modulus of 12.91 mag. The post-MS isochrones indicate an age range of  $5.0$  to  $7.1 \times 10^7$  years, while the MS itself appears to be following the curve of  $1.7 \times 10^7$  years. There are a few fainter stars, which are just to the right of the MS. It is quite likely that these stars are in the process of reaching the MS and they seem to be close to the pre-MS isochrone of  $1.0 \times 10^6$  years, thereby giving an additional support to the young age of the cluster. Further, the smallest  $(B-V)_0$  on the MS is 0.195 mag, which indicates an age of  $2 \times 10^7$  years. Thus, based on the MS and post-MS stars, the total dispersion in the age of this cluster appears to be from  $1.7$  to  $7.1 \times 10^7$  years.

#### **4.8. OC1 692 (Haffner 20)**

This cluster was also identified by Haffner (1957) who estimated its angular diameter to be 1.8 arcmin with twentyfive stars in it. He has also mentioned about its relationship with the spiral structure. It is classified as II 3 p by Ruprecht (1966) in the Trumpler system. Fig. 4.49 gives the finding chart for this cluster.

##### 4.8.1. Selection and observations

This cluster has been selected by visually inspecting the POSS charts (cf. Section 2.2), in which stars 2, 5, 10,

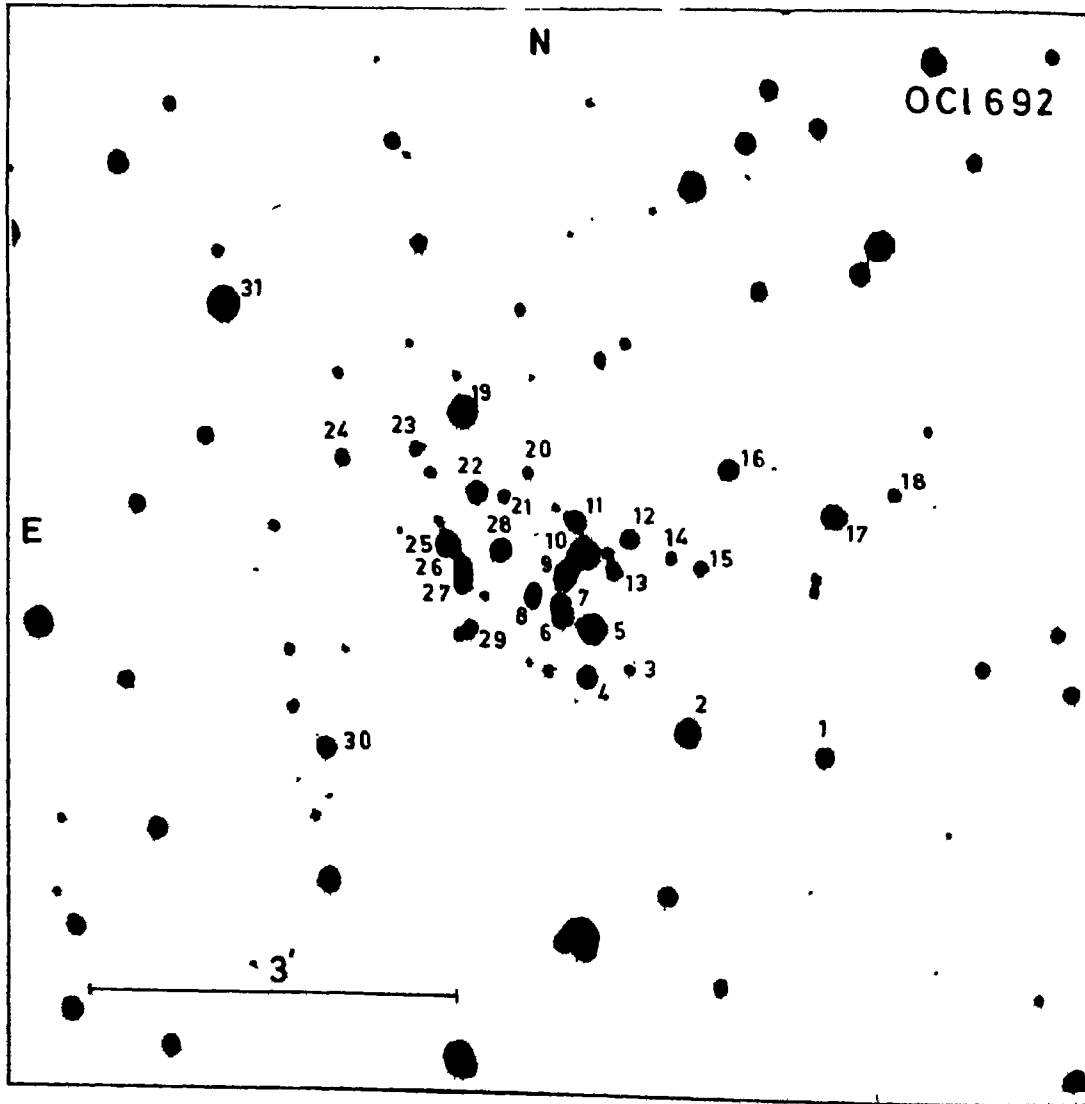


Fig. 4.49. Finding chart for the field of OC1 692.



19 and 31 appeared to be brighter on the blue print than on the red print. This indicated that their spectral types are close to B. Then, assuming these stars to be cluster members, this faint cluster was selected for the photoelectric investigations.

The photoelectric observations of this cluster were done using the 61-cm telescope of the Siding Spring Observatory (cf. Section 3.1). Standardized magnitudes and colours for a total of twelve stars were obtained and the values are included in Table 4.8. The atmospheric extinction coefficients, the transformation coefficients and the zero-point constants (cf. Equations 3.6 to 3.11) are given below.

$$\begin{array}{lll} K_V = 0.349 & \epsilon = 0.313 & \zeta_V = 5.797 \\ K_{b-v} = 0.153 & \mu = 0.808 & \zeta_{bv} = 0.024 \\ K_{u-b} = 0.161 & \psi = -2.467 & \zeta_{ub} = 1.828 \end{array}$$

The direct photography of this cluster for the purposes of U, B, V photometry was done with the help of the 1-m telescope at Siding Spring Observatory (cf. Section 3.2.1). The plate and filter combinations are given below along with the exposure times.

| <u>Plate</u> | <u>Filter</u> | <u>exposure time</u> |
|--------------|---------------|----------------------|
| 103a-0       | UG 2          | 55 min for U         |
| IIa-0        | GG 13         | 40 min for B         |
| 103a-D       | GG 14         | 35 min for V         |

From these plates, the photographic magnitudes were obtained on an arbitrary scale, for a total of twentyseven stars,

Table 4.8. The observational data for individual stars in the open cluster OC1 692.

| Star No                  | V      | (B-V)  | (U-B)  | $V_0$  | $(B-V)_0$ | $(U-B)_0$ | Membership |
|--------------------------|--------|--------|--------|--------|-----------|-----------|------------|
| Photoelectric photometry |        |        |        |        |           |           |            |
| 1                        | 14.812 | 0.867  | 0.531  | -      | -         | -         | -          |
| 2                        | 13.867 | 0.517  | 0.109  | -      | -         | -         | -          |
| 4                        | 15.136 | 0.627  | 0.164  | 12.617 | -0.148    | -0.396    | m          |
| 5                        | 13.944 | 0.626  | -0.038 | 11.425 | -0.149    | -0.598    | m          |
| 10                       | 13.900 | 0.609  | 0.054  | 11.381 | -0.166    | -0.506    | m          |
| 16                       | 12.837 | 1.494  | 1.373  | 10.318 | 0.719     | 0.813     | m          |
| 17                       | 14.072 | 0.466  | 0.196  | -      | -         | -         | -          |
| 19                       | 13.231 | 0.405  | -0.152 | -      | -         | -         | -          |
| 22                       | 15.151 | 0.570  | -0.077 | 12.632 | -0.205    | -0.637    | m          |
| 25                       | 14.331 | 0.599  | 0.036  | 11.812 | -0.176    | -0.524    | m          |
| 30                       | 14.881 | 0.600  | 0.500  | -      | -         | -         | m          |
| 31                       | 12.748 | 0.597  | 0.223  | -      | -         | -         | m          |
| Photographic photometry  |        |        |        |        |           |           |            |
| 6                        | 16.013 | 0.703  | 0.177  | 13.494 | -0.072    | -0.383    | m          |
| 7                        | 15.165 | 0.584  | 0.065  | 12.646 | -0.191    | -0.495    | m          |
| 8                        | 17.097 | 0.929  | 1.233  | -      | -         | -         | -          |
| 9                        | 14.855 | 0.557  | -0.104 | 12.336 | -0.218    | -0.664    | m          |
| 11                       | 15.519 | 0.583  | 0.016  | 13.000 | -0.192    | -0.544    | m          |
| 12                       | 15.861 | 0.629  | 0.148  | 13.342 | -0.146    | -0.412    | m          |
| 13                       | 17.099 | 0.871  | 0.755  | 14.580 | 0.096     | 0.195     | m          |
| 15                       | 16.779 | -0.013 | 0.191  | -      | -         | -         | -          |
| 20                       | 17.074 | 0.685  | 0.593  | 14.555 | -0.090    | 0.033     | m          |
| 23                       | 16.338 | 0.607  | 0.550  | 13.819 | -0.168    | -0.010    | m          |
| 24                       | 16.222 | 0.136  | 0.154  | -      | -         | -         | -          |
| 26                       | 16.959 | 0.746  | 0.673  | 14.440 | -0.029    | 0.113     | m          |
| 27                       | 15.397 | 0.587  | 0.038  | 12.878 | -0.188    | -0.522    | m          |
| 28                       | 15.390 | 0.655  | -0.047 | 12.871 | -0.120    | -0.607    | m          |
| 29                       | 16.030 | 0.851  | 1.076  | -      | -         | -         | -          |

including the twelve photoelectrically observed ones. These were then standardized using the above mentioned photoelectric observations (cf. Section 3.2.2). These magnitudes and colours are listed in Table 4.8.

#### 4.8.2. Membership

The CCD of this cluster, shown in Fig.4.50, indicates a clear sequence for most of the stars, for which the boundaries are drawn in the diagram. By picking out the same stars in the two CMD's given in Figs.4.51 and 4.52, and by using the photometric criteria as described in Section 3.3.1, a total of seventeen stars have been adopted as the most probable members of the cluster out of the observed twentyseven stars. One of the members, star 16, is a likely member of the red giant branch, while three other stars (5, 10 and 25) appear to have just evolved. All these members are denoted by 'm' in Table 4.8.

#### 4.8.3. Reddening

The CCD in Fig.4.50 shows a sequence formed by a majority of the stars and the boundaries of this sequence show that

$$\Delta E(B-V) = 0.11 \text{ mag}$$

and

$$\Delta E(U-B) = 0.08 \text{ mag.}$$

Since these values are same as the ones due to the natural dispersion (cf. Section 3.4), it is presumed that a non-variable interstellar extinction exists across the field of the cluster. Hence the following mean colour excesses have been adopted.

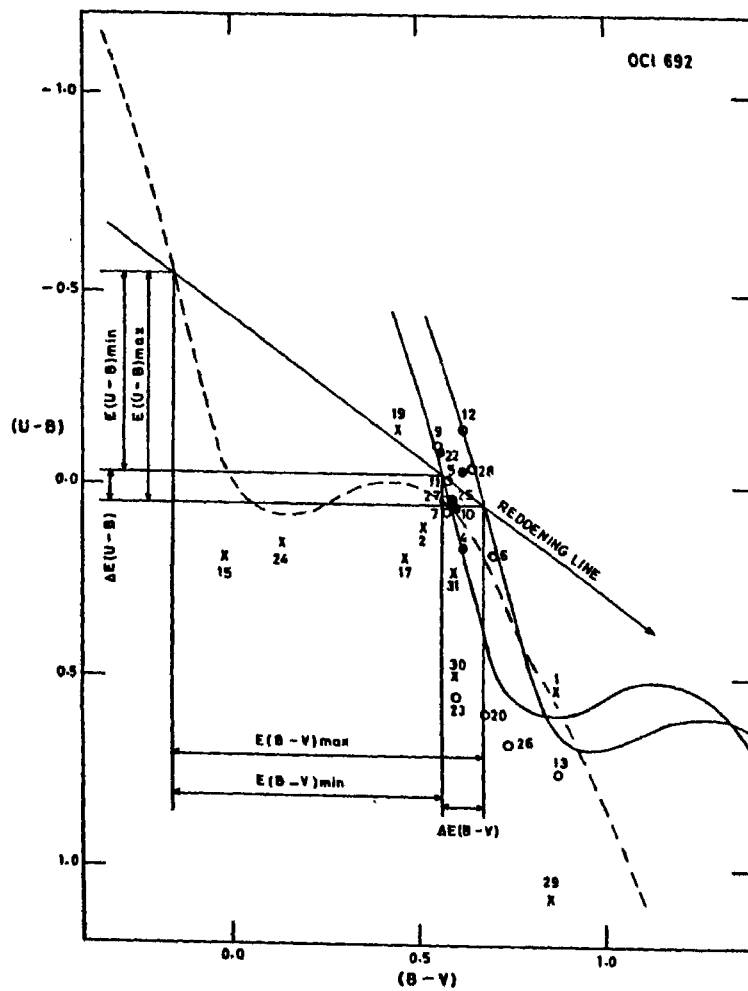


Fig. 4.50. The colour-colour diagram (CCD) of OC1 692. The dashed line is the unreddened main sequence (MS) taken from Schmidt-Kaler (1965).

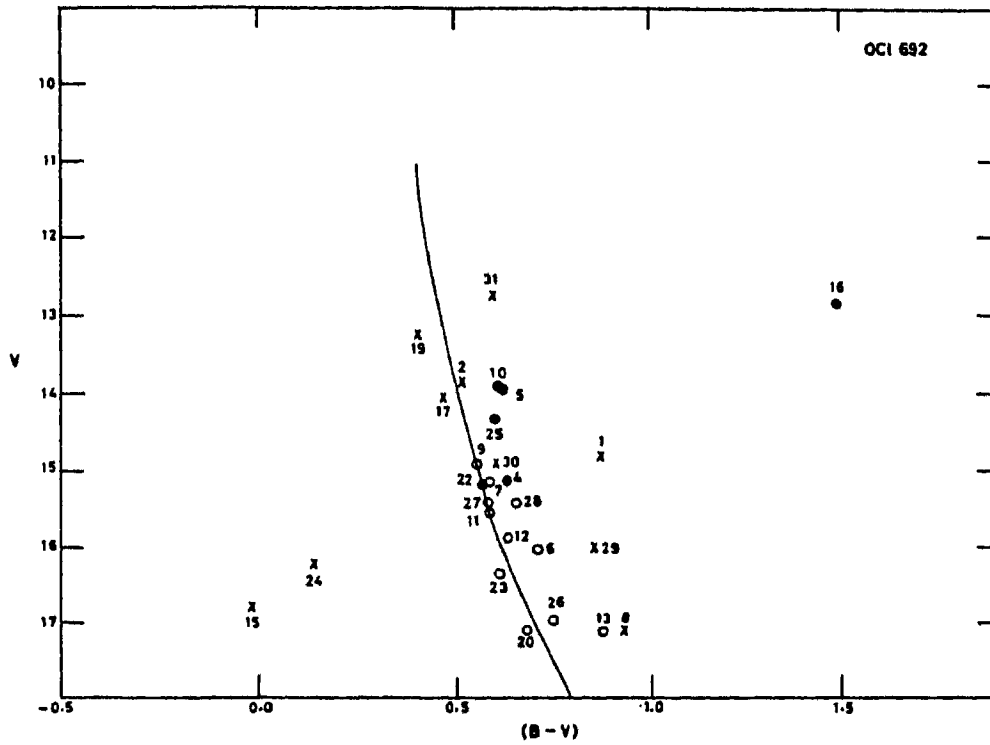


Fig. 4.51. The (B-V), V diagram (CMD) of OC1 692. The solid curve represents the zero age main sequence (ZAMS) fitted onto the cluster CMD.

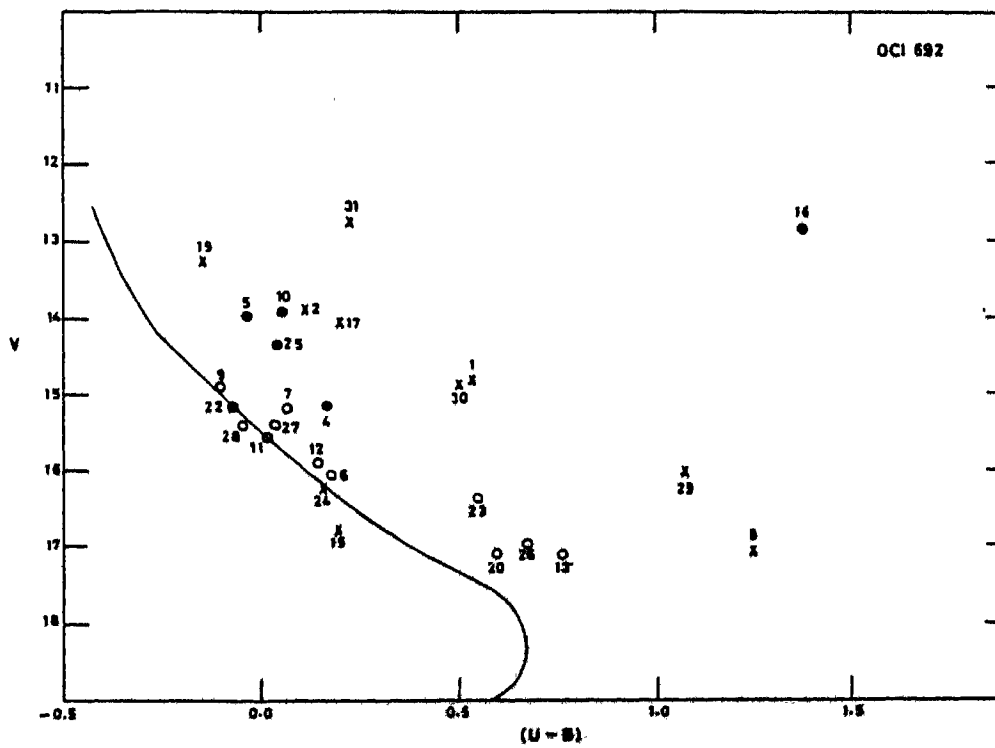


Fig. 4.52. The (U-B), V diagram (CMD) of OC1 692. The solid curve represents the ZAMS fitted onto the cluster CMD.

$$\begin{aligned} E(B-V) &= 1/2 [ E(B-V)_{\max} - E(B-V)_{\min} ] \\ &= 1/2 [ 0.83 + 0.72 ] = 0.775 \text{ mag} \end{aligned}$$

and similarly

$$\begin{aligned} E(U-B) &= 1/2 [ 0.60 + 0.52 ] \\ &= 0.56 \text{ mag.} \end{aligned}$$

Then  $A_V = 2.519 \pm 0.039$  mag.

Using these values in equation 3.18 to 3.20, the intrinsic magnitudes and colours were calculated, which are included in Table 4.8 as  $V_0$ ,  $(B-V)_0$  and  $(U-B)_0$ .

#### 4.8.4. Distance

The ZAMS has been fitted onto the cluster main sequences shown in Fig.4.53 in order to determine the true distance modulus of the cluster. They are found to be 13.73 mag and 13.48 mag in the long and short wavelength CMD's respectively, giving an average value of 13.61 mag. Then the distance to the cluster based on Equation 3.21 is

$$D = 5.27 \pm 0.30 \text{ kpc.}$$

#### 4.8.5. Age of the cluster

Fig.4.54 shows the HR-diagram of the cluster, plotted for the true distance modulus of 13.61 mag. The post-MS isochrones indicate an age range of  $5.0 \times 10^7$  to a little less than  $7.1 \times 10^7$  years, while the MS itself appears to be following the curve of  $1.7 \times 10^7$  years. Further, the smallest  $(B-V)_0$

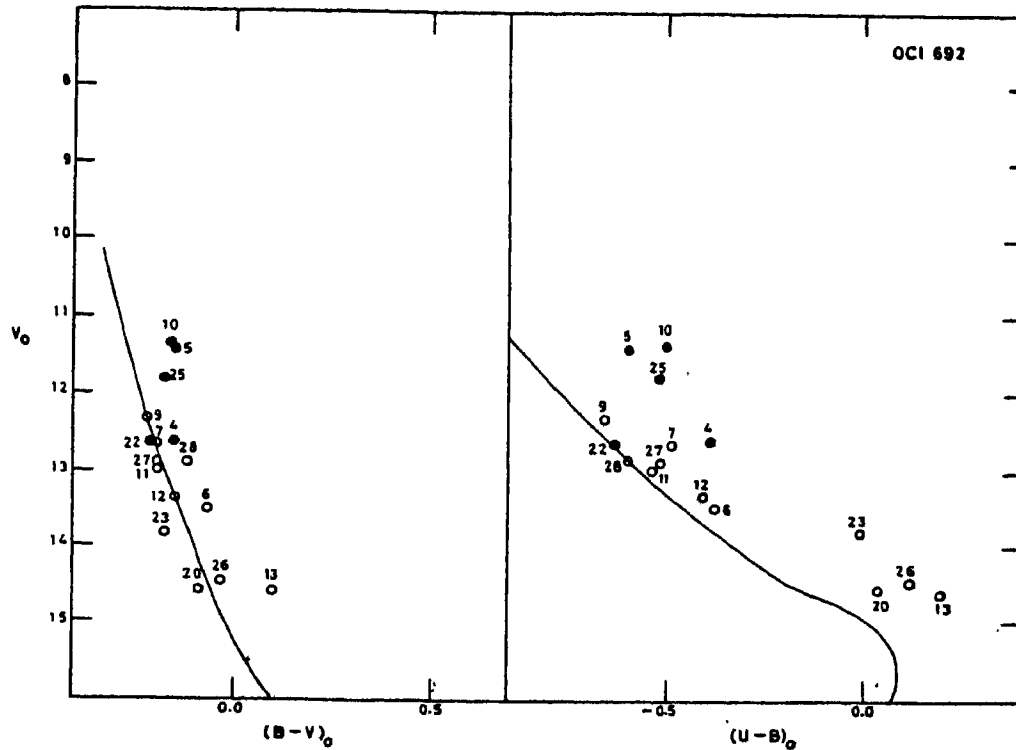


Fig. 4.53. The intrinsic  $(B-V)_0$ ,  $V_0$  and  $(U-B)_0$ ,  $V_0$  diagrams (CMDs) of OC1 692. The solid curves represent the ZAMS, taken from Schmidt-Kaler (1965), fitted onto the cluster CMDs.

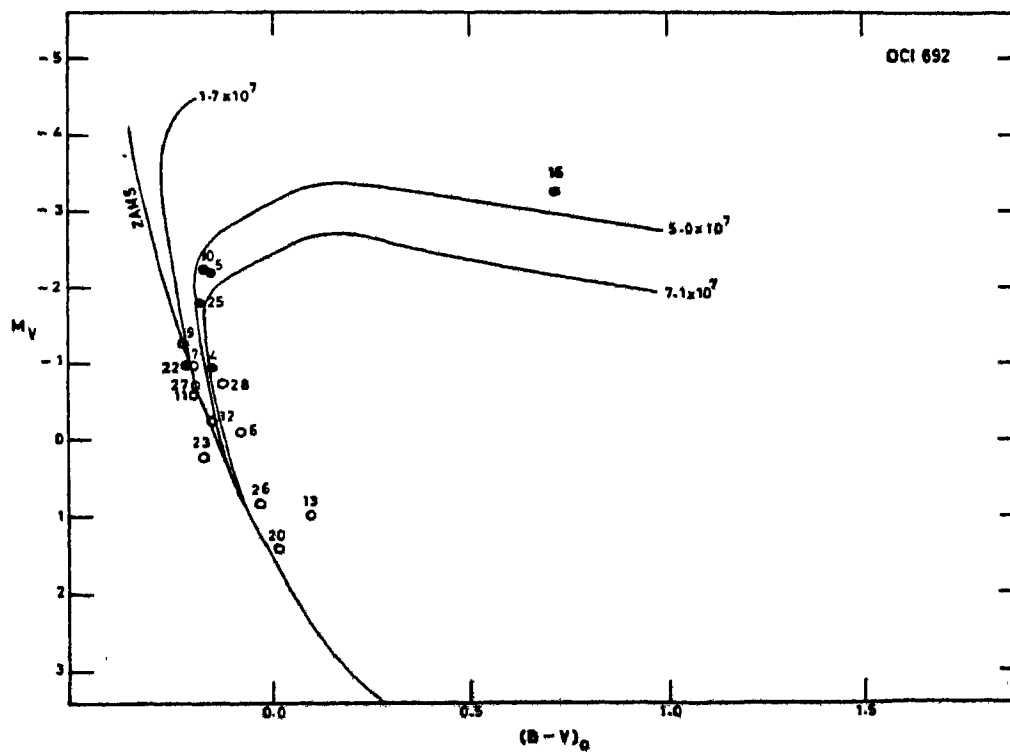


Fig. 4.54. HR-diagram of OC1 692. The post-MS isochrones are from Barbaro et al. (1969) and the dashed lines represent the pre-MS isochrones taken from Iben (1965). The ages are indicated in years alongside the isochrones.

on the MS is  $-0.218$  mag, which also indicates an age of  $1 \times 10^7$  years. It is quite likely that star 13, being at the fainter end as well as to the right of the MS, may be a pre-MS contracting star. Thus, the cluster is young with a dispersion of 1.0 to a little less than  $7.1 \times 10^7$  years in its age.

#### **4.9. OC1 694 (Haffner 17)**

This is the fourth cluster in the programme to be taken from the list given by Haffner (1957). He had estimated its angular diameter to be 1.6 arcmin with twentyfive stars in it. He had mentioned about its relationship with the spiral structure just as in the case of its neighbouring clusters, OC1 674 and OC1 692 (cf. Sections 4.7 and 4.8). This cluster had been classified as II 3p in the Trumpler system, which was slightly modified by Ruprecht (1966) to III 3p. Fig.4.55 gives the finding chart for this cluster.

##### 4.9.1. Selection and Observations

This cluster has been selected by visually inspecting the POSS charts (cf. Section 2.2), in which, star 38 appeared to be brighter on the blue print than on the red print. Assuming this star to be a member of the cluster and considering it to be of spectral type B, this cluster has been selected for the photometric investigations.

The photometric observations were done using the 61-cm telescope of the Siding Spring Observatory (cf. Section 3.1). Standardized magnitudes and colours for a total of ten stars



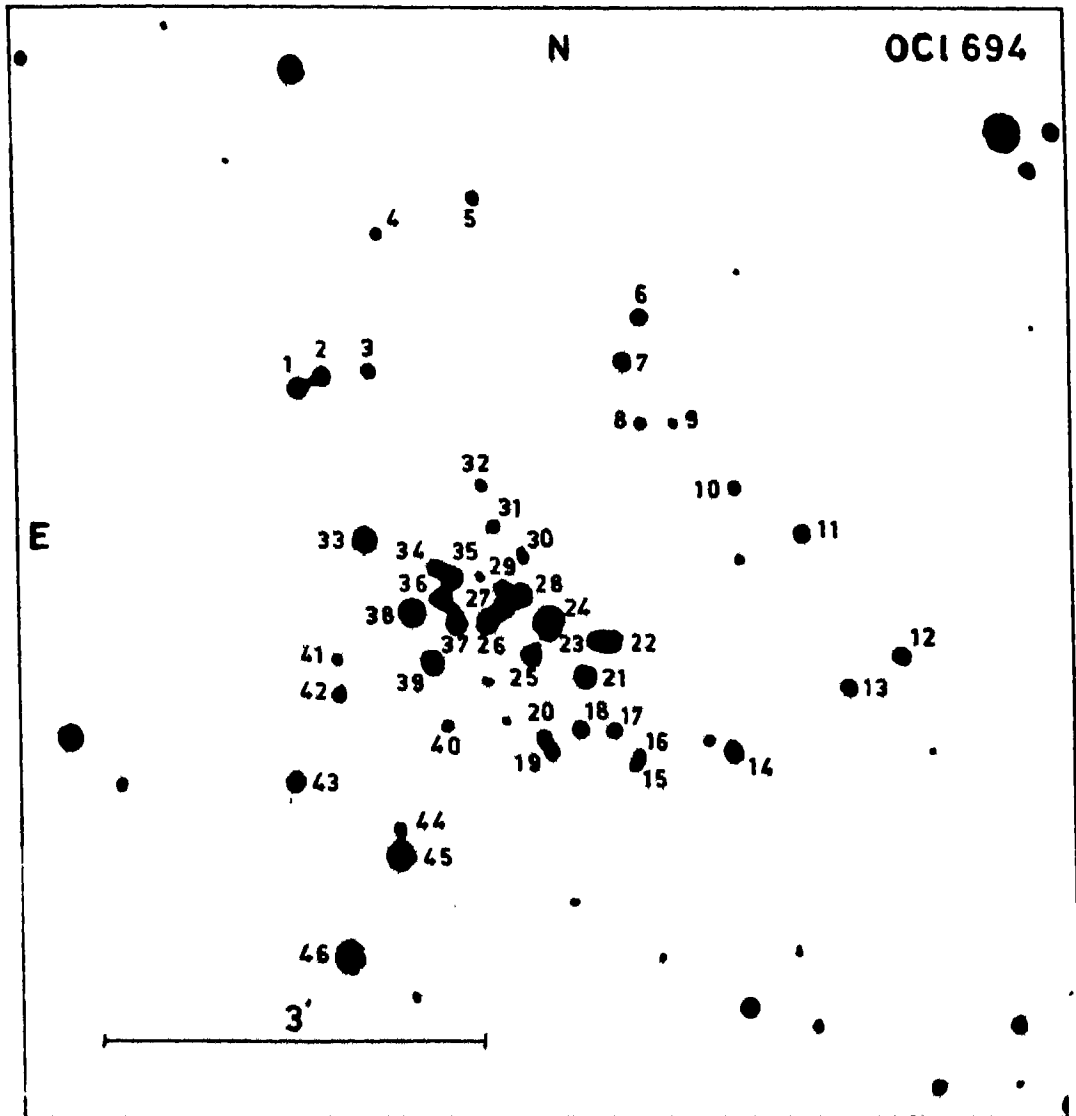


Fig. 4.55. Finding chart for the field of OC1 694.

were obtained and the values are included in Table 4.9. The atmospheric extinction coefficients, the transformation coefficients and the zero-point constants (cf. Equations 3.6 to 3.11) are given below.

$$\begin{aligned} K_V &= 0.377 & \epsilon &= 0.299 & \zeta_V &= 5.752 \\ K_{b-v} &= 0.194 & \mu &= 0.808 & \zeta_{bv} &= 0.081 \\ K_{u-b} &= 0.333 & \psi &= -3.008 & \zeta_{ub} &= 1.610 \end{aligned}$$

The direct U, B, V photography of this cluster was done with the help of the 1-m telescope at Siding Spring Observatory (cf. Section 3.2.1). The plate and filter combinations along with the exposure times are as under.

| <u>Plate</u> | <u>Filter</u> | <u>Exposure time</u> |
|--------------|---------------|----------------------|
| 103a-0       | UG 2          | 50 min for U         |
| IIa-0        | GG 13         | 40 min for B         |
| IIa-D        | GG 14         | 55 min for V         |

From these plates, the photographic magnitudes were obtained for a total of twenty-six stars, including the ten photoelectrically observed ones, on an arbitrary scale. These were then standardized using the above mentioned photoelectric observations as described in Section 3.2.2. These magnitudes and colours are listed in Table 4.9.

#### 4.9.2. Membership

The CCD of this cluster, shown in Fig.4.56, indicates a clear sequence for most of the stars, for which the boundaries

**Table 4.9.** The observational data for individual stars in the open cluster OC1 694.

| Star No.                 | V      | (B-V) | (U-B) | $V_0$ | $(B-V)_0$ | $(U-B)_0$ | E(B-V) | Membership |
|--------------------------|--------|-------|-------|-------|-----------|-----------|--------|------------|
| 1                        | 2      | 3     | 4     | 5     | 6         | 7         | 8      | 9          |
| Photoelectric photometry |        |       |       |       |           |           |        |            |
| 7                        | 13.497 | 1.914 | 2.611 | -     | -         | -         | -      | -          |
| 13                       | 13.428 | 2.095 | 2.444 | -     | -         | -         | -      | -          |
| 21                       | 14.40  | 1.45  | 0.77  | 10.92 | 0.38      | 0.00      | 1.07   | m          |
| 22                       | 15.37  | 0.94  | 0.35  | 11.96 | -0.11     | -0.41     | 1.05   | m          |
| 23                       | 15.24  | 0.98  | 0.53  | 11.83 | -0.07     | -0.22     | 1.05   | m          |
| 24                       | 13.701 | 1.071 | 0.992 | 10.24 | 0.006     | 0.222     | 1.065  | m          |
| 33                       | 14.387 | 0.782 | 0.527 | -     | -         | -         | -      | -          |
| 39                       | 14.43  | 1.19  | 0.72  | 11.38 | 0.25      | 0.04      | 0.94   | m          |
| 43                       | 14.855 | 1.163 | 2.121 | -     | -         | -         | -      | -          |
| 45                       | 13.389 | 1.297 | 2.224 | -     | -         | -         | -      | -          |
| Photographic photometry  |        |       |       |       |           |           |        |            |
| 14                       | 14.55  | 0.90  | 1.09  | -     | -         | -         | -      | -          |
| 17                       | 15.60  | 0.95  | 0.48  | 12.22 | -0.09     | -0.32     | 1.04   | m          |
| 25                       | 15.56  | 0.99  | 0.21  | 11.79 | -0.17     | -0.62     | 1.16   | m          |
| 26                       | 13.46  | 2.36  | 2.70  | -     | -         | -         | -      | -          |
| 27                       | 16.02  | 0.78  | -0.04 | 12.80 | -0.21     | -0.75     | 0.99   | m          |
| 28                       | 14.41  | 1.35  | 0.94  | 10.48 | 0.14      | 0.07      | 1.21   | m          |
| 29                       | 16.44  | 0.79  | 0.07  | 13.32 | -0.17     | -0.62     | 0.96   | m          |
| 30                       | 17.11  | 0.88  | 0.21  | 13.66 | -0.18     | -0.52     | 1.06   | m          |
| 31                       | 16.12  | 1.02  | 0.34  | 12.35 | -0.14     | -0.49     | 1.16   | m          |
| 32                       | 15.75  | 1.04  | 0.49  | 12.08 | -0.09     | -0.32     | 1.13   | m          |
| 34                       | 16.00  | 0.94  | 0.29  | 12.52 | -0.13     | -0.48     | 1.07   | m          |
| 35                       | 15.80  | 0.85  | 0.15  | 12.52 | -0.16     | -0.58     | 1.01   | m          |
| 36                       | 15.53  | 1.05  | 0.39  | 11.70 | -0.13     | -0.45     | 1.18   | m          |
| 37                       | 13.50  | 2.34  | 2.50  | -     | -         | -         | -      | -          |
| 38                       | 13.74  | 0.68  | 0.07  | -     | -         | -         | -      | -          |
| 40                       | 16.68  | 0.88  | 0.20  | 13.33 | 0.15      | -0.53     | 1.03   | m          |

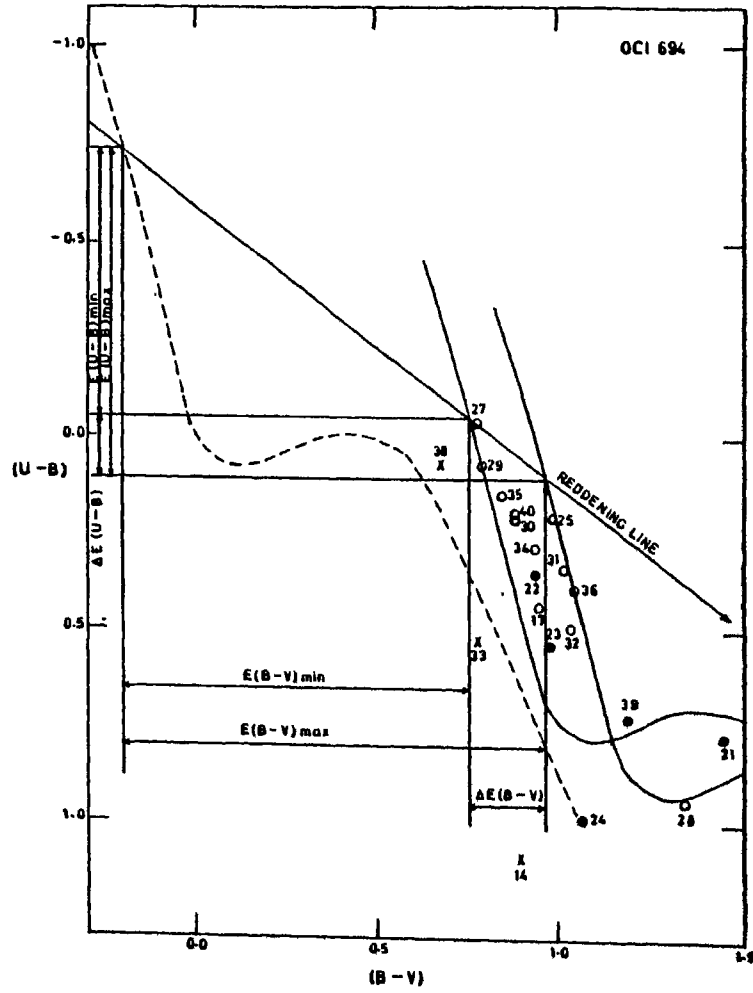


Fig. 4.56. The colour-colour diagram (CCD) of OC1 694. The dashed line is the unreddened main sequence (MS) taken from Schmidt-Kaler (1965).

are drawn in the diagram. By picking out the same stars in the two CMD's (cf. Figs. 4.57 and 4.58) and by using the photometric criteria as described in Section 3.3.1, a total of seventeen stars have been adopted as the most probable members of the cluster out of the observed twentysix stars. Star 38, on the basis of which the cluster has been selected, appears to be more like a foreground star and therefore considered as a non-member. Stars 21, 24, 28 and 39 are probably in the process of reaching the red giant region, while stars 17, 22, 23, 25, 31, 32, 34 and 36 appear to have just evolved. All these members are denoted by 'm' in Table 4.9.

#### 4.9.3. Reddening

The CCD in Fig. 4.56 shows a sequence formed by a majority of the stars and the boundaries of this sequence show that

$$\Delta E(B-V) = 0.21 \text{ mag}$$

and

$$\Delta E(U-B) = 0.16 \text{ mag.}$$

These values are much larger than the natural dispersion (cf. Section 3.4) and therefore, the concerned stars were individually corrected for the appropriate interstellar reddening. These corrections have been found to be between

$$E(B-V)_{\max} = 1.17 \text{ mag and } E(B-V)_{\min} = 0.96 \text{ mag}$$

and between

$$E(U-B)_{\max} = 0.85 \text{ mag and } E(U-B)_{\min} = 0.69 \text{ mag.}$$

With the help of the individual  $E(B-V)$  values, which are tabulated in Table 4.9, the corresponding values of  $A_V$  were

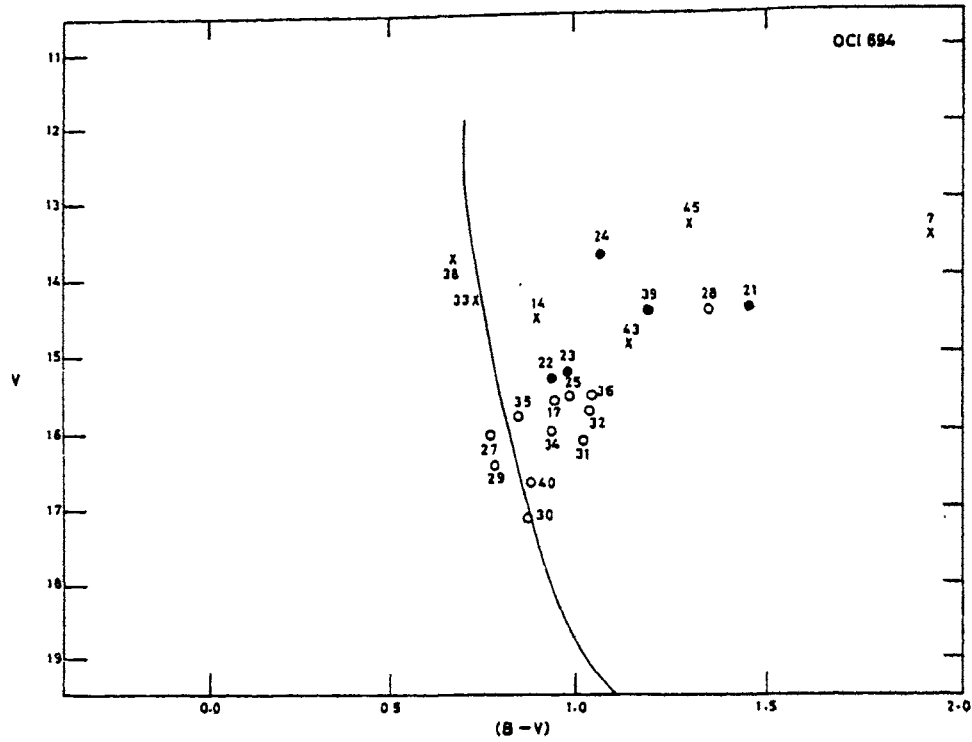


Fig. 4.57. The (B-V), V diagram (CMD) of OC1 694. The solid curve represents the zero age main sequence (ZAMS) fitted onto the cluster CMD.

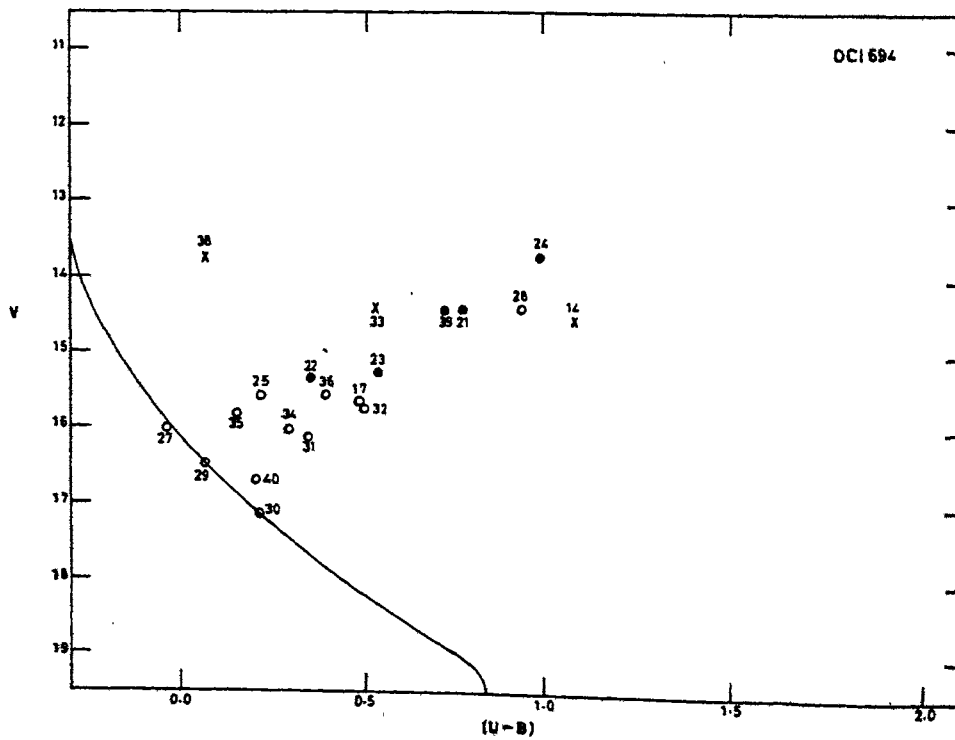


Fig. 4.58. The (U-B), V diagram (CMD) of OC1 694. The solid curve represents the ZAMS fitted onto the cluster CMD.

obtained, which were found to be between 3.80 mag and 3.12 mag. These, in turn, were used to correct the observed  $V$  values. All these corrected magnitudes and colours are also included in Table 4.9 as  $V_0$ ,  $(B-V)_0$  and  $(U-B)_0$ .

#### 4.9.4. Distance

The true distance modulus of this cluster has been determined by fitting ZAMS onto the cluster main sequences as shown in Fig.4.59. The long and short wavelength CMD's have been found to yield the distance modulus of 14.21 mag and 14.06 mag, respectively, giving rise to an average value of 14.14 mag. Then the distance  $D$  to the cluster, based on Equation 3.21 is

$$D = 6.73 \pm 0.23 \text{ kpc.}$$

#### 4.9.5. Age of the Cluster

Fig.4.60 shows the HR-diagram of the cluster, plotted for the true distance modulus of 14.14 mag. In this diagram, it appears that a majority of the stars are just evolving away from the MS. Out of the four stars (21, 24, 28 and 39), which look more evolved, the stars 21 and 39 are located well within the extension of the isochrones of the just evolved stars, while stars 24 and 28 are a little too bright. However, in view of the non-coeval nature of open clusters, all these four stars have been considered as belonging to the cluster. Thus, the post-MS isochrones indicate an age range of  $2.8$  to  $7.1 \times 10^7$  years. The smallest  $(B-V)_0$  on the MS is  $-0.21$  mag which indicates an age of about  $2 \times 10^7$  years. Thus, the dispersion in the age of this cluster appears to be from  $2$  to  $7.1 \times 10^7$  years.

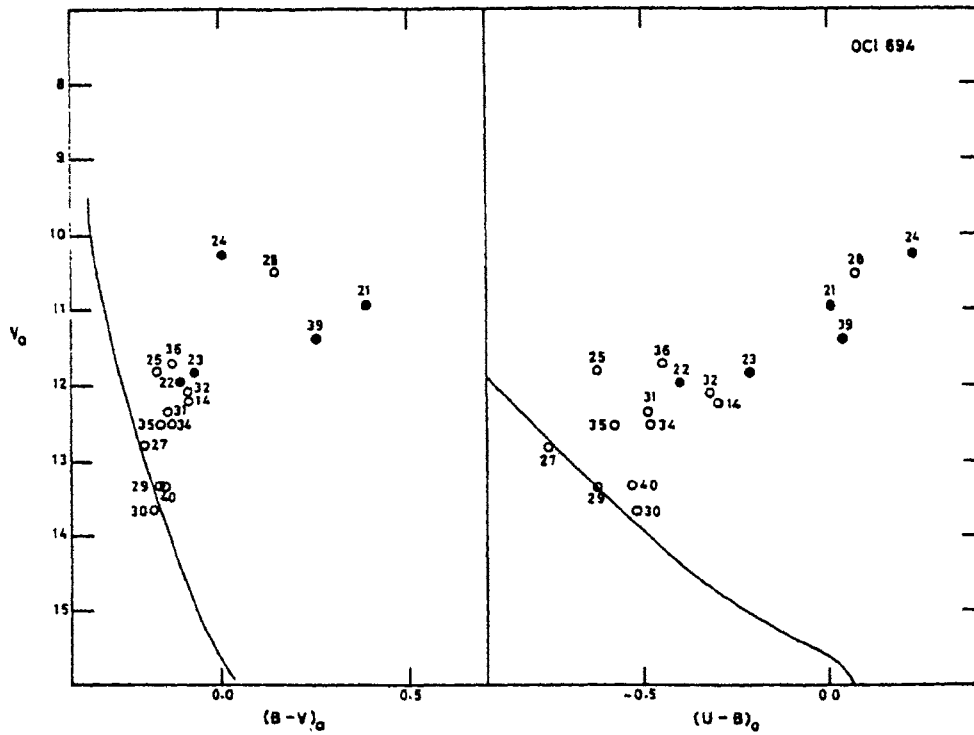


Fig. 4.59. The intrinsic  $(B-V)_0$ ,  $V_0$  and  $(U-B)_0$ ,  $V_0$  diagrams (CMDs) of OC1 694. The curves represent the ZAMS taken from Schmidt-Kaler (1965), fitted onto the cluster CMDs.

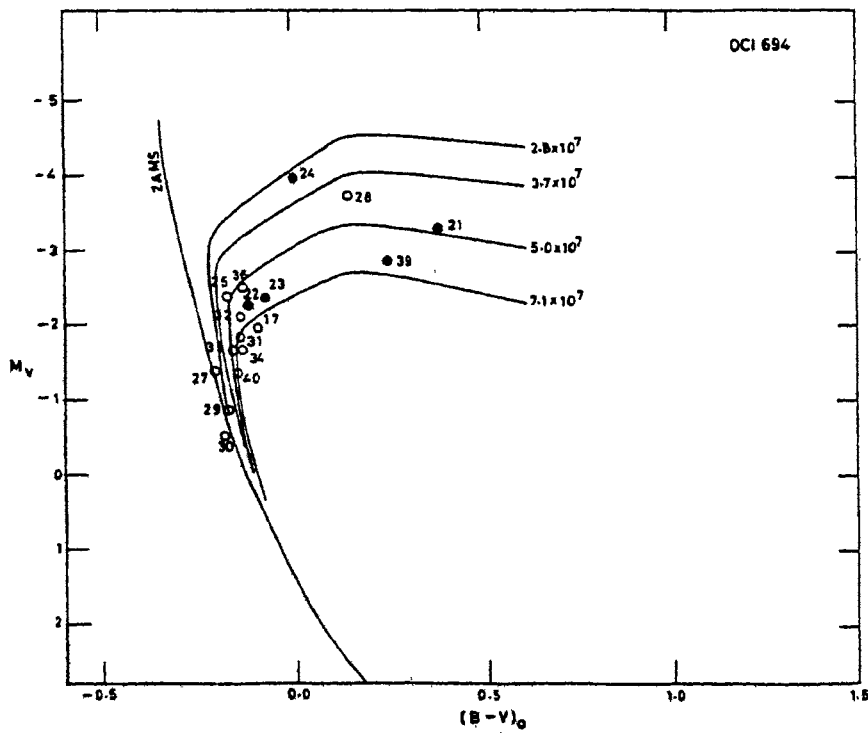


Fig. 4.60. HR-diagram of OC1 694. The post-MS isochrones are from Barbaro et al. (1969). The ages are indicated in years alongside the isochrones.



#### 4.10.0C1 715 (NGC 2588)

In 1930, Trumpler estimated its angular diameter to be 2.5 arcmin and adopted a distance of 4680 parsecs. But soon after, Collinder (1931) modified the angular diameter estimation to 2 arcmin and calculated its distance as 9100 parsec. Later on, Barhatova (1950) found its distance to be 2750 parsec with an angular diameter of 5 arcmin. This cluster is classified as II 1 p by Ruprecht (1966) in the Trumpler system. Fig.4.61 gives the finding chart for this cluster.

##### 4.10.1. Section and Observations

This cluster has been selected by visually inspecting the POSS charts (cf. Section 2.2) in which, stars 5, 12, 15 and 49 appeared brighter on the blue print as compared to the red print. This is an indication of their spectral type being B. Assuming these stars to be members, this faint cluster has been selected for the photometric investigations.

The photoelectric observations of this cluster were done using the 61-cm telescope of the Siding Spring Observatory (cf. Section 3.1). Standardized magnitudes and colours for a total of ten stars were obtained and the values are included in Table 4.10. The atmospheric extinction coefficients, the transformation coefficients and the zero-point constants (cf. Equations 3.6 to 3.11) are given below.

$$\begin{array}{lll} K_V & = & 0.155 \quad \epsilon = 0.303 \quad \zeta_V = 5.435 \\ K_{b-v} & = & 0.154 \quad \mu = 0.785 \quad \zeta_{bv} = 0.034 \\ K_{u-b} & = & 0.094 \quad \psi = -2.693 \quad \zeta_{ub} = 2.225. \end{array}$$

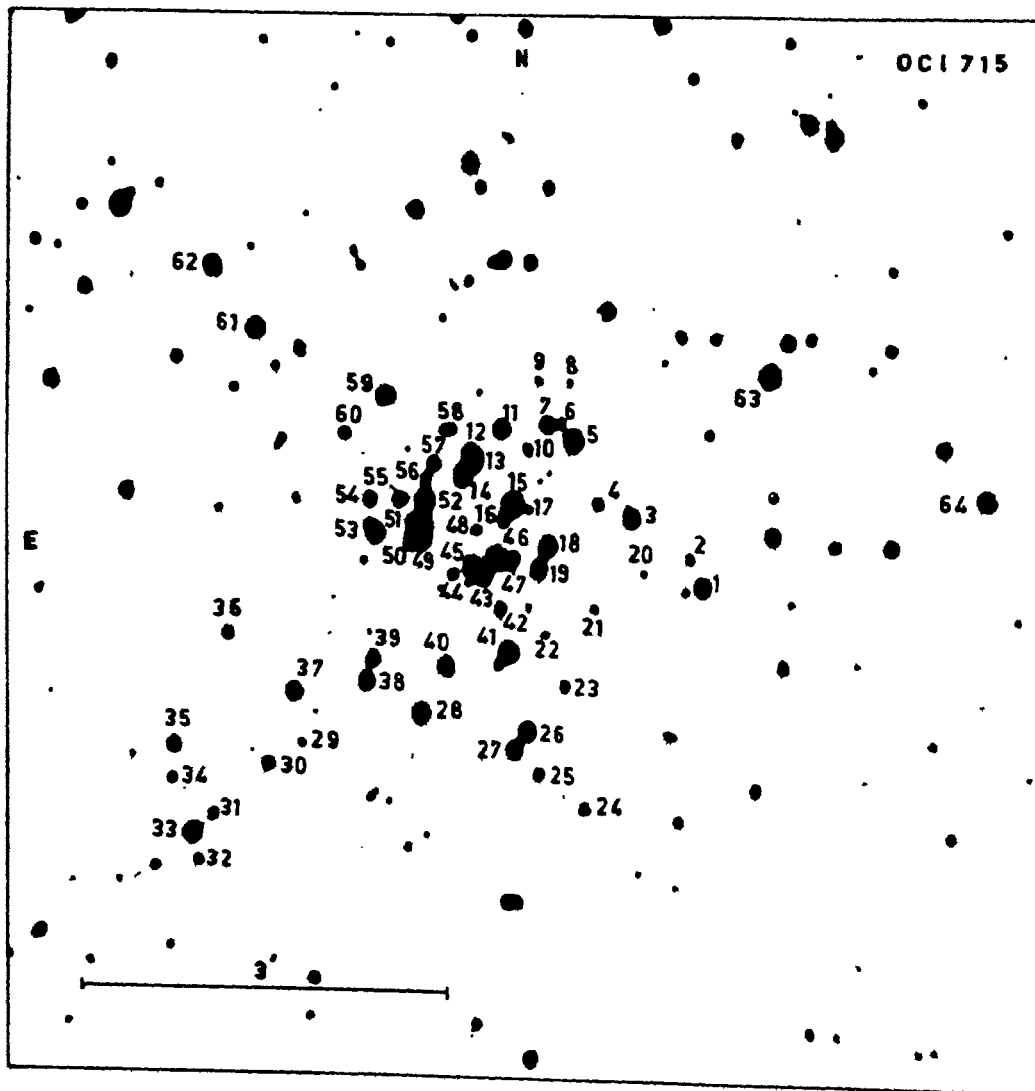


Fig. 4.61. Finding chart for the field of OC1 715.

**Table 4.10.** The observational data for individual stars in the open cluster OC1 715.

| Star No                  | V      | (B-V) | (U-B)  | $V_0$  | $(B-V)_0$ | $(U-B)_0$ | Membership |
|--------------------------|--------|-------|--------|--------|-----------|-----------|------------|
| Photoelectric photometry |        |       |        |        |           |           |            |
| 11                       | 13.867 | 1.354 | 0.861  | 12.096 | 0.809     | 0.471     | m          |
| 12                       | 14.243 | 0.318 | -0.226 | 12.472 | -0.227    | -0.616    | m          |
| 14                       | 14.983 | 0.521 | 0.124  | 13.212 | -0.024    | -0.266    | m          |
| 15                       | 14.103 | 0.343 | -0.349 | 12.332 | -0.202    | -0.739    | m          |
| 18                       | 14.840 | 0.384 | 0.006  | 13.069 | -0.161    | -0.384    | m          |
| 27                       | 14.765 | 0.346 | -0.323 | 12.994 | -0.199    | -0.713    | m          |
| 28                       | 13.385 | 1.231 | 0.674  | 11.614 | 0.686     | 0.284     | m          |
| 38                       | 15.046 | 0.496 | 0.041  | 13.275 | -0.049    | -0.349    | m          |
| 40                       | 14.696 | 0.399 | -0.122 | 12.925 | -0.146    | -0.512    | m          |
| 41                       | 13.178 | 1.146 | 0.552  | 11.407 | 0.601     | 0.162     | m          |
| Photographic photometry  |        |       |        |        |           |           |            |
| 1                        | 14.03  | 0.87  | 0.47   | -      | -         | -         | -          |
| 3                        | 13.76  | 1.19  | 0.64   | 11.99  | 0.65      | 0.25      | m          |
| 5                        | 13.97  | 0.34  | 0.12   | -      | -         | -         | -          |
| 7                        | 14.21  | 1.58  | 1.30   | 12.44  | 1.03      | 0.91      | m          |
| 19                       | 15.28  | 0.43  | -0.14  | 13.51  | -0.12     | -0.53     | m          |
| 25                       | 14.75  | 1.72  | 2.22   | -      | -         | -         | -          |
| 26                       | 14.69  | 0.24  | 0.32   | -      | -         | -         | -          |
| 33                       | 13.34  | 1.08  | 0.99   | -      | -         | -         | -          |
| 35                       | 15.28  | 0.52  | 0.53   | -      | -         | -         | -          |
| 46                       | 14.52  | 0.29  | -0.26  | 12.75  | -0.26     | -0.65     | m          |
| 49                       | 13.79  | 0.35  | -0.21  | 12.02  | -0.19     | -0.60     | m          |
| 50                       | 14.48  | 1.23  | 0.93   | 12.70  | 0.68      | 0.54      | m          |
| 52                       | 13.77  | 1.35  | 0.91   | 12.00  | 0.81      | 0.52      | m          |
| 53                       | 14.87  | 0.28  | 0.31   | -      | -         | -         | -          |
| 54                       | 15.88  | 0.87  | 0.48   | 14.11  | 0.32      | 0.09      | m          |
| 59                       | 15.22  | 0.26  | 0.36   | -      | -         | -         | -          |
| 61                       | 13.24  | 0.94  | 0.54   | -      | -         | -         | -          |
| 62                       | 13.99  | 0.42  | -0.31  | -      | -         | -         | -          |
| 63                       | 13.50  | 0.29  | -0.09  | -      | -         | -         | -          |
| 64                       | 14.09  | 0.41  | -0.03  | -      | -         | -         | -          |

The direct U, B, V photography of this cluster was done with the help of the 1-m telescope at Siding Spring Observatory (cf. Section 3.2.1). The plate and filter combinations are given below along with the exposure times.

| <u>Plate</u> | <u>Filter</u> | <u>Exposure time</u> |
|--------------|---------------|----------------------|
| IIa-0        | UG2           | 65 min for U         |
| IIa-0        | GG13          | 30 min for B         |
| IIa-D        | GG14          | 30 min for V         |

From these plates, the photographic magnitudes were obtained on an arbitrary scale, for a total of thirty stars, including the ten photoelectrically observed ones. These were then standardized using the above mentioned photoelectric observations (cf. Section 3.2.2). These magnitudes and colours are listed in Table 4.10.

#### 4.10.2. Membership

The CCD of this cluster, shown in Fig.4.62 indicates a clear sequence for most of the stars, for which the boundaries are drawn in the diagram. By picking out the same stars in the two CMD's given in Figs. 4.63 and 4.64 and by using the photometric criteria as described in Section 3.3.1, a total of eighteen stars have been adopted as the most probable members of the cluster out of the observed thirty stars. Seven stars of the members (stars 3, 7, 11, 28, 41, 50 and 52) appear to be forming the red giant branch, while one other (star 54) could be a pre-MS star, being at the faintest end and to the right of the MS. All these members are denoted by 'm' in Table 4.10.

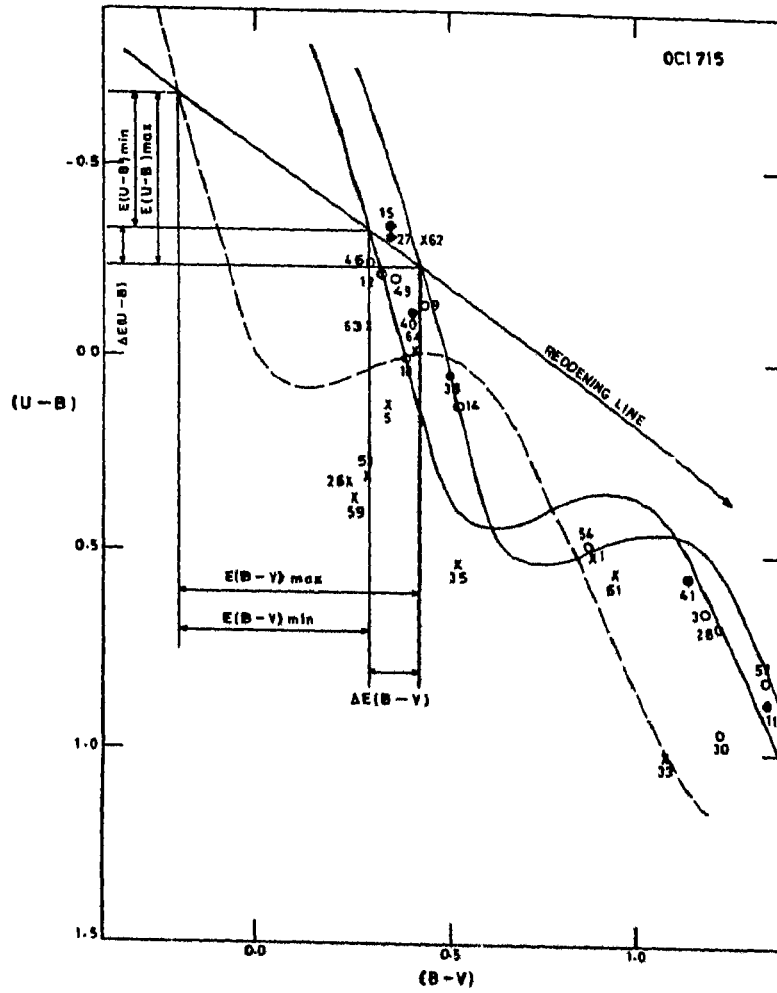


Fig. 4.62. The colour-colour diagram (CCD) of OC1 715. The dashed line is the unreddened main sequence (MS) taken from Schmidt-Kaler (1965).

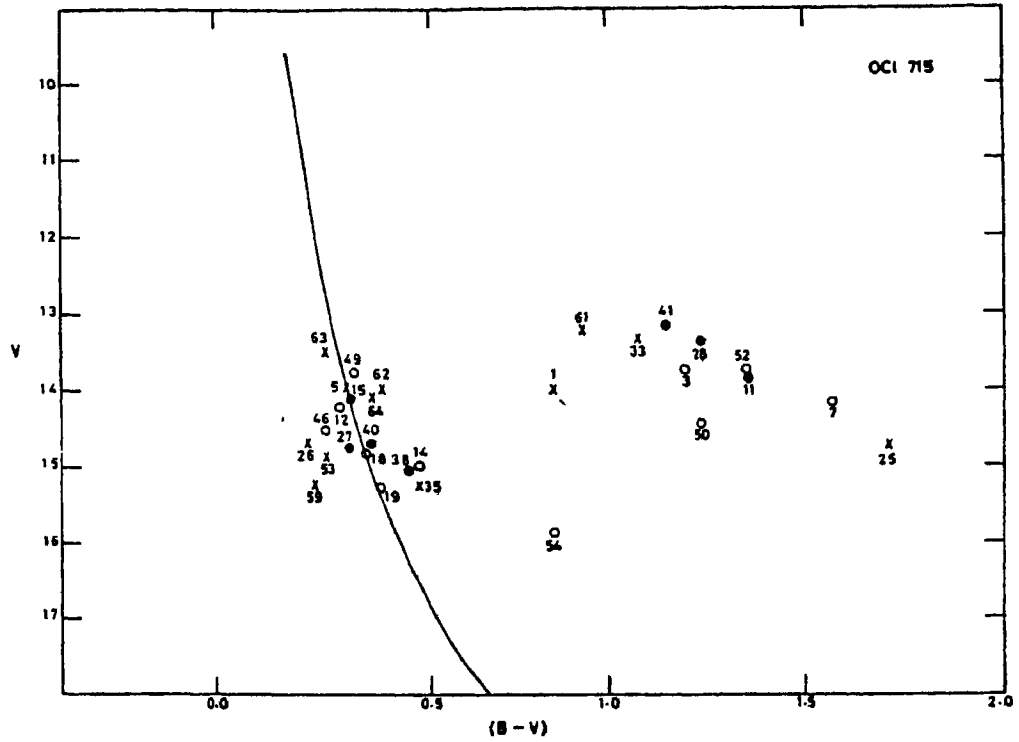


Fig. 4.63. The  $(B-V)$ ,  $V$  diagram (CMD) of OC1 715. The solid curve represents the zero age main sequence (ZAMS) fitted onto the cluster CMD.

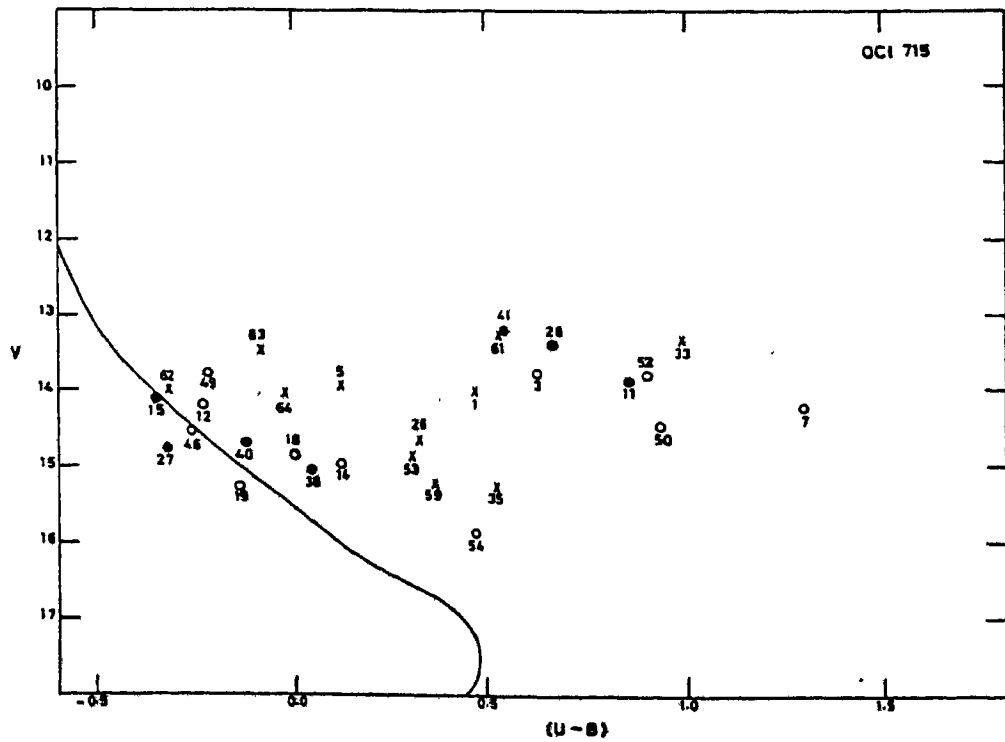


Fig. 4.64. The  $(U-B)$ ,  $V$  diagram (CMD) of OC1 715. The solid curve represents the ZAMS fitted onto the cluster CMD.

#### 4.10.3. Reddening

The CCD of this cluster in Fig.4.62 shows a sequence formed by a majority of the stars and the boundaries of this sequence show that

$$\Delta E(B-V) = 0.13 \text{ mag}$$

and

$$\Delta E(U-B) = 0.10 \text{ mag.}$$

Since these values are close to the ones arising from the natural dispersion (cf. Section 3.4), an almost non-variable extinction across the field of the cluster has been presumed. Hence, the following mean colour excesses have been adopted.

$$\begin{aligned} E(B-V) &= 1/2 [ E(B-V)_{\max} + E(B-V)_{\min} ] \\ &= 1/2 [ (0.61 + 0.48) ] = 0.545 \text{ mag} \end{aligned}$$

and similarly

$$\begin{aligned} E(U-B) &= 1/2 [ 0.44 + 0.34 ] \\ &= 0.39 \text{ mag.} \end{aligned}$$

Then

$$A_V = 1.771 \pm 0.027 \text{ mag.}$$

Using these values in Equations 3.18 to 3.20, the intrinsic magnitudes and colours were calculated, which are included in Table 4.10 as  $V_0$ ,  $(B-V)_0$  and  $(U-B)_0$ .

#### 4.10.4. Distance

The ZAMS has been fitted onto the cluster main sequences shown in Fig.4.65 in order to determine the true distance modulus

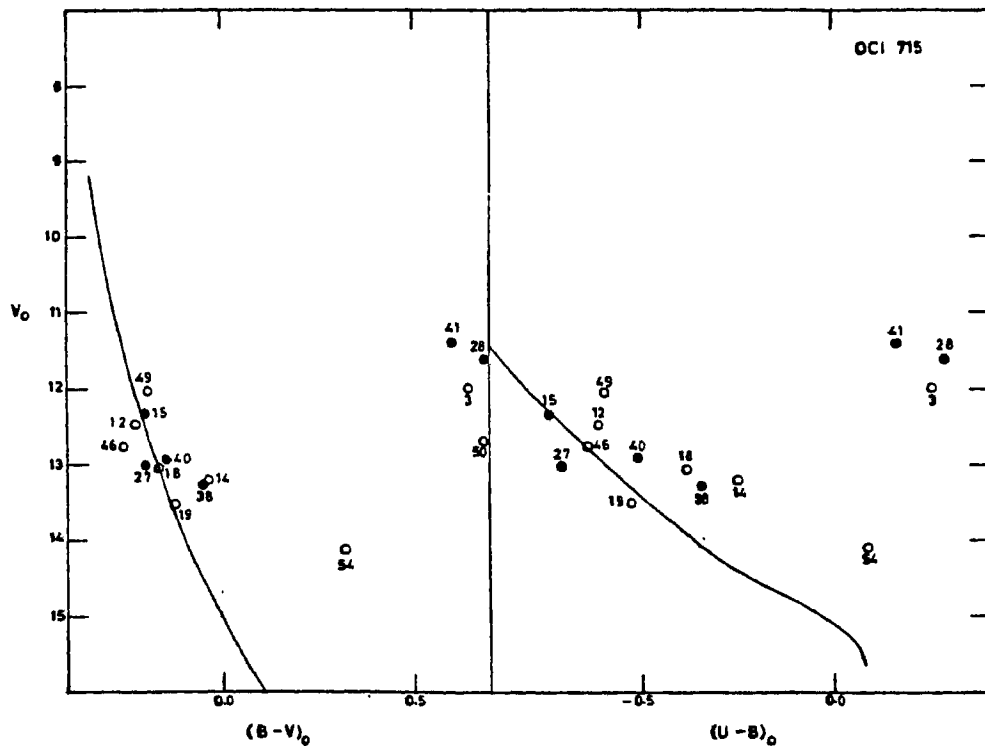


Fig. 4.65. The intrinsic  $(B-V)_0$ ,  $V_0$  and  $(U-B)_0$ ,  $V_0$  diagrams (CMDs) of OC1 715. The solid curves represent the ZAMS, taken from Schmidt-Kaler (1965), fitted onto the cluster CMDs.

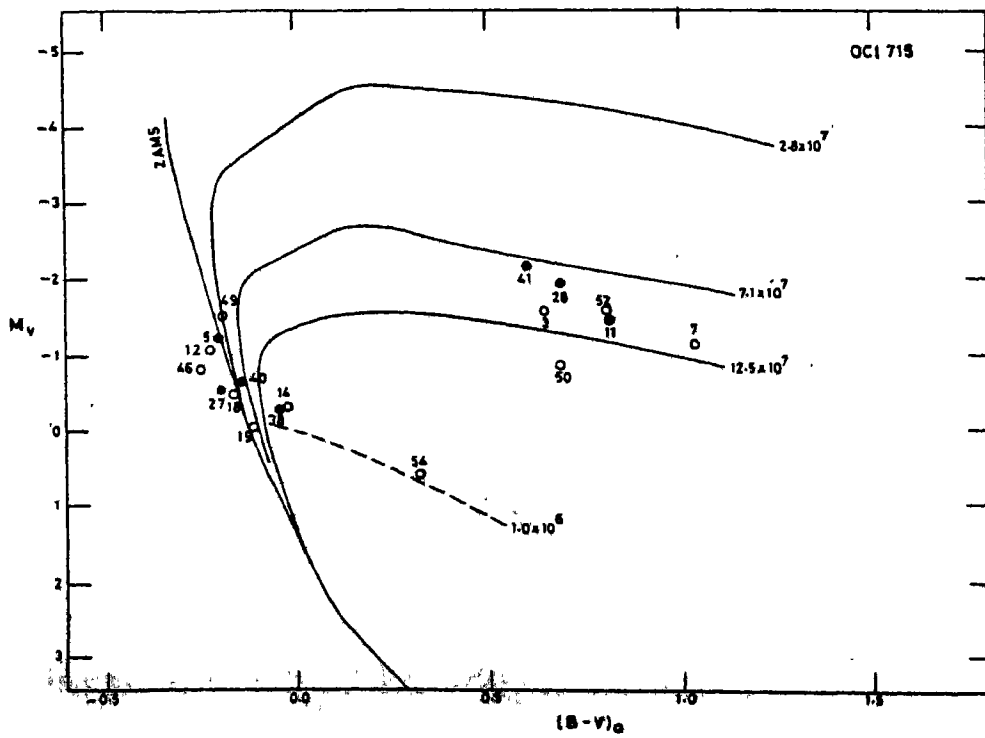


Fig. 4.66. The  $M_V$  vs  $(B-V)_0$  diagram for OC1 715. The post-MS isochrones are from Schaller et al. (1969) and the dashed line isochrone taken from Iben (1969). The ages indicated in years alongside the isochrones.



of the cluster. The distance moduli are found to be 13.63 mag and 13.48 mag in the long and short wavelength CMD's respectively, giving an average value of 13.56 mag. Then the distance to the cluster based on Equation 3.21 is

$$D = 5.14 \pm 0.18 \text{ kpc.}$$

#### 4.10.5. Age of the Cluster

Fig.4.66 shows the HR-diagram of the cluster, plotted for the true distance modulus of 13.56 mag. The post-MS isochrones indicate an age range of  $7.1 \times 10^7$  to  $12.5 \times 10^7$  years. However, the near MS stars seem to be following the isochrone of  $2.8 \times 10^7$  years. Further, the smallest  $(B-V)_0$  on the MS is -0.23 mag, which indicates an age of  $1 \times 10^7$  years. There is just one star (star 54) located to the right of the MS at its fainter end. This could be a pre-MS star, if it is a member of the cluster. Thus, the cluster is young, though with a dispersion of 1.0 to  $12.5 \times 10^7$  years, in its age.

#### **4.11.OC1 762 (Ruprecht 69)**

This faint cluster was identified by Ruprecht (1960), who gave its angular dimension as  $1.4 \times 2.2$  arcmin with twenty stars in it. He later on classified it as III 2 p in the Trumpler system (Ruprecht, 1966). Fig.4.67 gives the finding chart for this cluster.

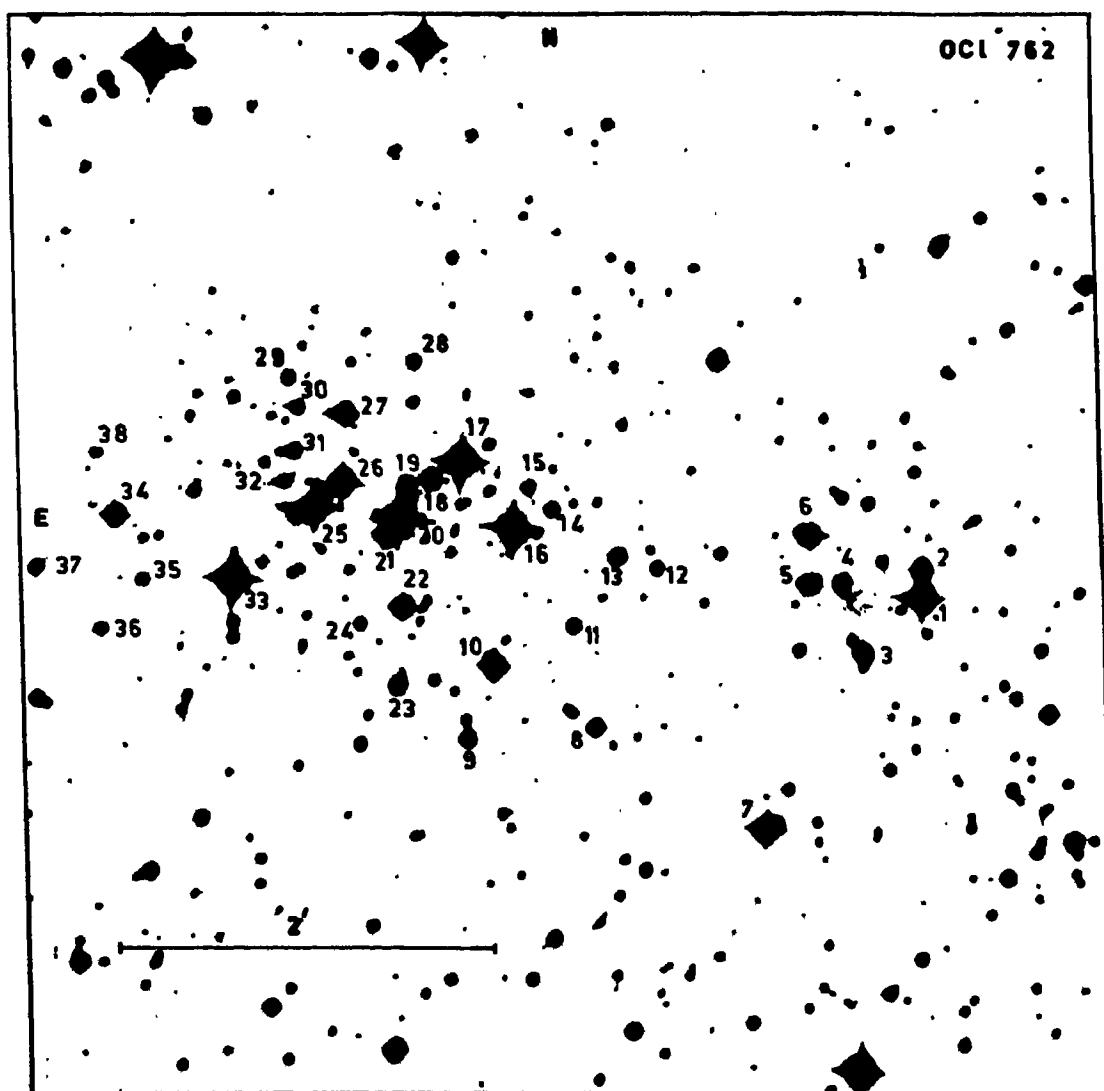


Fig. 4.67. Finding chart for the field of OC1 762.

#### 4.11.1. Selection and Observations

This cluster has been selected by visually inspecting the corresponding ESO/SERC (European Southern Observatory/Science and Engineering Research Council) Southern Sky Atlas Charts (cf. Section 2.2), in which stars 16, 25 and 33 appeared to be brighter on the blue print than on the red print. This is an indication of their B spectral types. On the basis of this finding and assuming these stars to be members, this faint cluster has been selected for the photometric investigations.

The photoelectric observations of this cluster were done using the 61-cm telescope of the Siding Spring Observatory (cf. Section 3.1). Standardized magnitudes and colours for a total of thirteen stars were obtained and the values are included in Table 4.11. The atmospheric extinction coefficients, the transformation coefficients and the zero-point constants (cf. Equations 3.6 to 3.11) are given below.

$$\begin{array}{lll} K_V & = & 0.155 \quad \epsilon = 0.303 \quad \zeta_V = 5.435 \\ K_{b-v} & = & 0.154 \quad \mu = 0.785 \quad \zeta_{bv} = 0.034 \\ K_{u-b} & = & 0.094 \quad \psi = -2.693 \quad \zeta_{ub} = 2.225 \end{array}$$

The direct U, B, V photography of this cluster was done with the help of the 1-m telescope at Siding Spring Observatory (cf. Section 3.2.1). The plate and filter combinations are given below along with the exposure times.

| <u>Plate</u> | <u>Filter</u> | <u>Exposure time</u> |
|--------------|---------------|----------------------|
| IIa-0        | UG2           | 55 min for U         |
| 103a-0       | GG13          | 35 min for B         |
| IIa-D        | GG14          | 20 min for V         |

**Table 4.11.** The observational data for individual stars  
in the open cluster OC1 762

| Star<br>No.              | V      | (B-V) | (U-B)  | V <sub>0</sub> | (B-V) <sub>0</sub> | (U-B) <sub>0</sub> | E(B-V) | Membership |
|--------------------------|--------|-------|--------|----------------|--------------------|--------------------|--------|------------|
| 1                        | 2      | 3     | 4      | 5              | 6                  | 7                  | 8      | 9          |
| Photoelectric photometry |        |       |        |                |                    |                    |        |            |
| 1                        | 12.184 | 1.377 | 1.323  |                |                    |                    |        |            |
| 5                        | 15.278 | 2.873 | 4.556  |                |                    |                    |        |            |
| 6                        | 14.246 | 0.749 | -1.041 |                |                    |                    |        |            |
| 8                        | 15.047 | 0.781 | 0.280  |                |                    |                    |        |            |
| 10                       | 13.447 | 0.584 | -0.166 | 10.802         | -0.23              | -0.74              | 0.814  | m          |
| 13                       | 14.909 | 4.685 | 2.162  | -              | -                  | -                  | -      | -          |
| 16                       | 12.465 | 0.596 | -0.482 | 9.488          | -0.32              | -1.05              | 0.916  | m          |
| 17                       | 11.861 | 1.387 | 0.884  | 8.708          | 0.417              | 0.174              | 0.97   | m          |
| 20                       | 11.974 | 1.773 | 1.498  | 8.822          | 0.803              | 0.788              | 0.97   | m          |
| 22                       | 14.255 | 0.875 | -0.052 | 10.631         | -0.24              | -0.86              | 1.115  | m          |
| 27                       | 14.803 | 0.846 | -0.108 | 11.209         | -0.26              | -0.90              | 1.106  | m          |
| 33                       | 11.947 | 0.669 | -0.467 | 8.700          | -0.33              | -1.08              | 0.999  | m          |
| 34                       | 13.729 | 0.671 | -0.416 | 10.508         | -0.32              | -1.05              | 0.991  | m          |
| Photographic photometry  |        |       |        |                |                    |                    |        |            |
| 2                        | 14.32  | 0.33  | -0.14  | -              | -                  | -                  | -      | -          |
| 3                        | 16.02  | 0.71  | -0.54  | -              | -                  | -                  | -      | -          |
| 4                        | 18.68  | 1.90  | -0.15  | -              | -                  | -                  | -      | -          |
| 7                        | 12.37  | 1.53  | 1.92   | -              | -                  | -                  | -      | -          |
| 9                        | 14.88  | 3.59  | 1.05   | -              | -                  | -                  | -      | -          |
| 11                       | 16.89  | 2.04  | -0.31  | -              | -                  | -                  | -      | -          |
| 12                       | 19.49  | 1.43  | -0.33  | -              | -                  | -                  | -      | -          |
| 14                       | 17.40  | 1.77  | -0.06  | -              | -                  | -                  | -      | -          |
| 15                       | 16.92  | 3.37  | 3.57   | -              | -                  | -                  | -      | -          |
| 18                       | 15.43  | 0.97  | 0.28   | 11.77          | -0.15              | -0.53              | 1.12   | m          |
| 19                       | 17.76  | 3.23  | 2.08   | -              | -                  | -                  | -      | -          |
| 21                       | 13.84  | 1.56  | -0.05  | -              | -                  | -                  | -      | -          |

---

| 1  | 2     | 3    | 4     | 5     | 6     | 7     | 8    | 9 |
|----|-------|------|-------|-------|-------|-------|------|---|
| 23 | 15.49 | 2.20 | 0.02  | -     | -     | -     | -    | - |
| 24 | 19.44 | 0.63 | -0.14 | -     | -     | -     | -    | - |
| 25 | 12.94 | 0.48 | -0.64 | 10.30 | -0.33 | -1.08 | 0.81 | m |
| 26 | 13.51 | 0.61 | -0.46 | 10.48 | -0.32 | -1.05 | 0.93 | m |
| 28 | 16.31 | 3.56 | 0.76  | -     | -     | -     | -    | - |
| 29 | 18.41 | 1.58 | -0.08 | -     | -     | -     | -    | - |
| 30 | 18.54 | 2.05 | -0.31 | -     | -     | -     | -    | - |
| 31 | 17.02 | 2.53 | -0.43 | -     | -     | -     | -    | - |
| 32 | 18.57 | 1.52 | 0.36  | -     | -     | -     | -    | - |
| 35 | 15.92 | 4.04 | 2.97  | -     | -     | -     | -    | - |
| 36 | 16.92 | 1.75 | -0.31 | -     | -     | -     | -    | - |
| 37 | 16.37 | 0.61 | -0.23 | 13.64 | -0.23 | -0.84 | 0.84 | m |

---

From these plates, the photographic magnitudes were obtained for a total of thirtyseven stars, including the thirteen photoelectrically observed ones. These values, which were on an arbitrary scale, were then standardized using the above mentioned photoelectric observations (cf. Section 3.2.2). These magnitudes and colours are listed in Table 4.11.

#### 4.11.2. Membership

The CCD of this cluster shown in Fig.4.68 indicates a clear sequence for some of the stars, for which the boundaries are drawn in the diagram. By picking out the same stars in the two CMD's given in Figs. 4.69 and 4.70 and by using the photometric criteria as described in Section 3.3.1, a total of twelve stars have been adopted as the most probable members of the cluster out of the observed thirtyseven stars. Two of the members (stars 17 and 20) appear to be located in the red giant branch of the cluster. All these members are denoted by 'm' in Table 4.11.

#### 4.11.3. Reddening

The sequence shown by the member stars in the CCD of this cluster (cf. Fig.4.68) appears to be much wider, which is also seen in the larger scatter of the members around the MS in the two CMD's (cf. Figs.4.69 and 4.70). Thus, non-uniform extinction across the field of the cluster is clearly indicated. Further, the boundaries of the sequence in the CCD show that



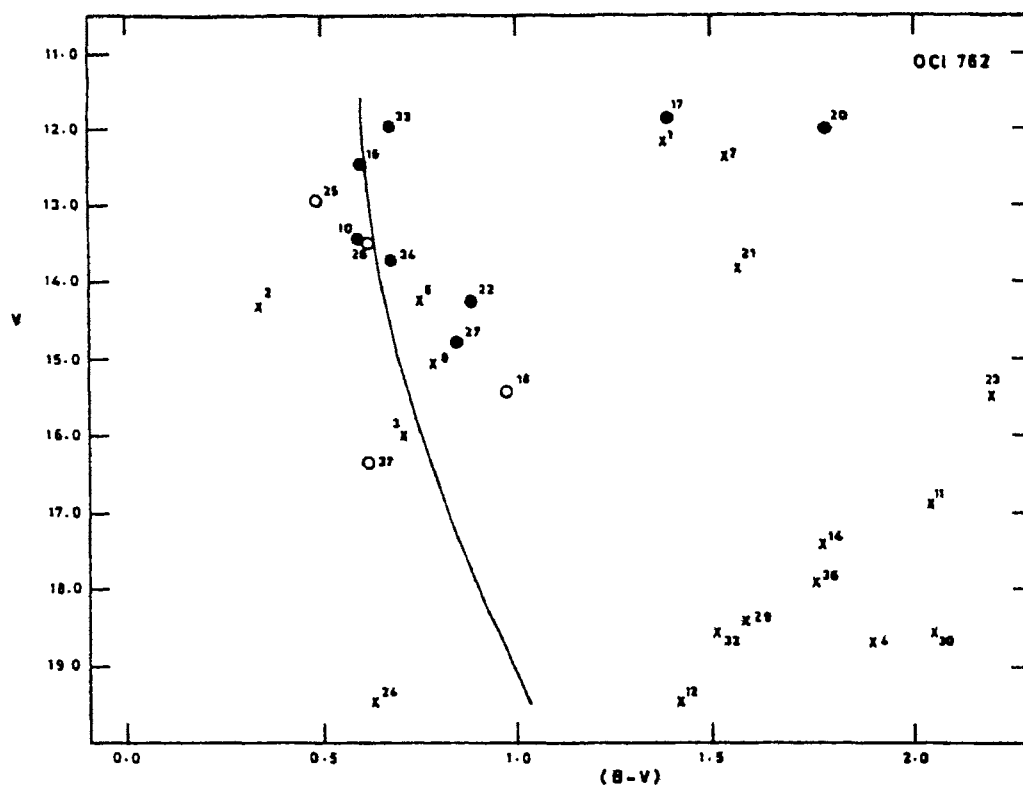


Fig. 4.69. The  $(B-V)$ ,  $V$  diagram (CMD) of OC1 762. The solid curve represents the zero age main sequence (ZAMS) fitted onto the cluster CMD.

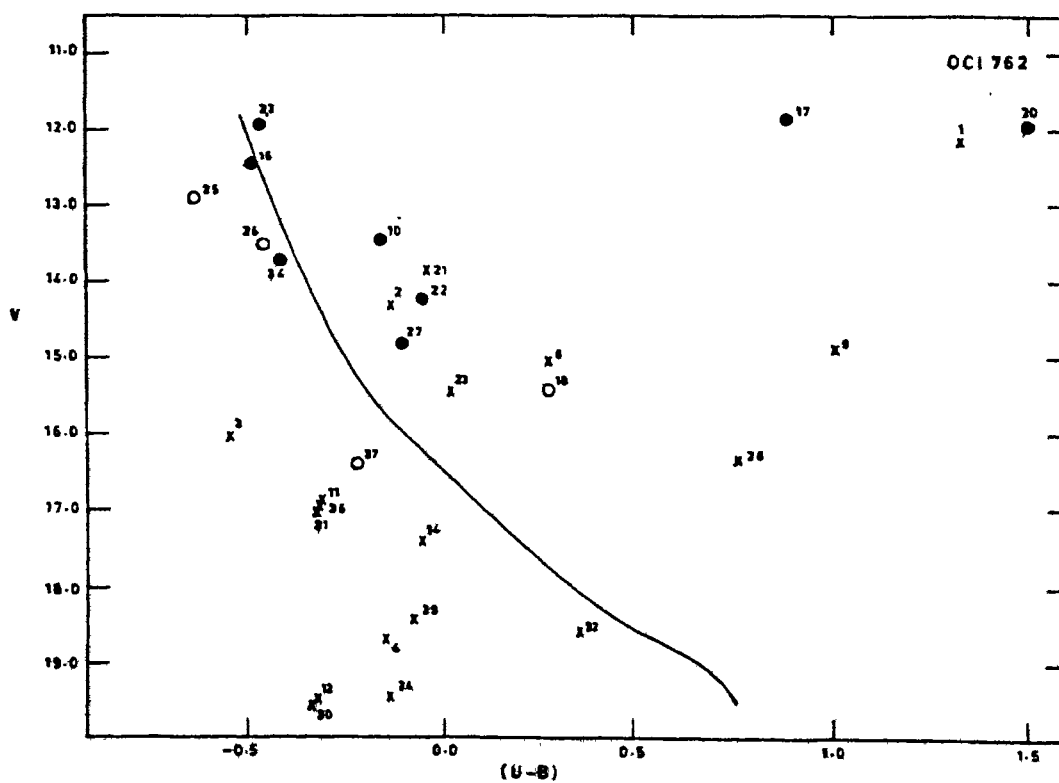


Fig. 4.70. The  $(U-B)$ ,  $V$  diagram (CMD) of OC1 762. The solid curve represents the ZAMS fitted onto the cluster CMD.



$$\Delta E(B-V) = 0.32 \text{ mag}$$

and

$$\Delta E(U-B) = 0.23 \text{ mag.}$$

These values are much larger than the natural dispersion (cf. Section 3.4) and therefore the concerned stars were individually corrected for the appropriate interstellar reddening. These corrections have been found to be between

$$E(B-V)_{\max} = 1.13 \text{ mag and } E(B-V)_{\min} = 0.81 \text{ mag}$$

and between

$$E(U-B)_{\max} = 0.82 \text{ mag and } E(U-B)_{\min} = 0.59 \text{ mag.}$$

With the help of the individual  $E(B-V)$  values, which are tabulated in Table 4.11, the corresponding values of  $A_V$  were obtained, which were found to be between 3.67 mag and 2.63 mag. These, in turn, were used to correct the observed  $V$  values. All these corrected magnitudes and colours are also included in Table 4.11 as  $V_0$ ,  $(B-V)_0$  and  $(U-B)_0$ .

#### 4.11.4. Distance

The true distance modulus of this cluster has been determined by fitting ZAMS onto the cluster main sequences as shown in Fig.4.71. The long and short wavelength CMD's have been found to yield the distance moduli of 14.21 mag and 14.31 mag, respectively, giving rise to an average value of 14.26 mag. Then the distance  $D$  to the cluster, based on Equation 3.21 is

$$D = 7.11 \pm 0.16 \text{ kpc.}$$

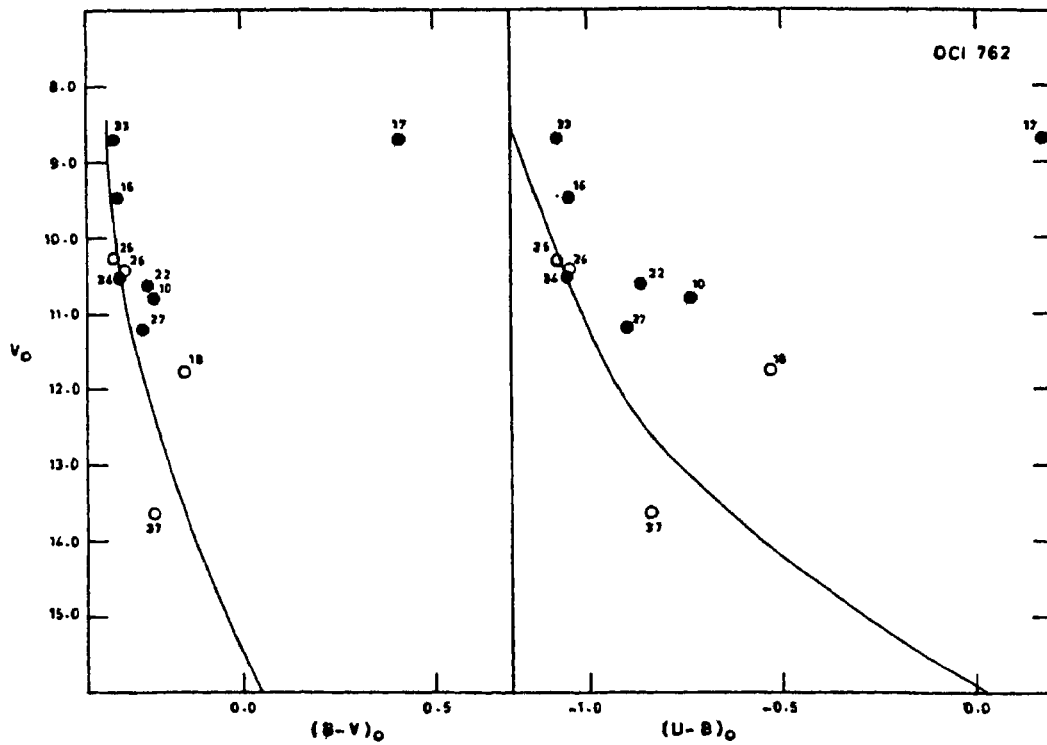


Fig. 4.71. The intrinsic  $(B-V)_0$ ,  $V_0$  and  $(U-B)_0$ ,  $V_0$  diagrams (CMDs) of OC1 762. The solid curves represent the ZAMS, taken from Schmidt-Kaler (1965), fitted onto the cluster CMDs.

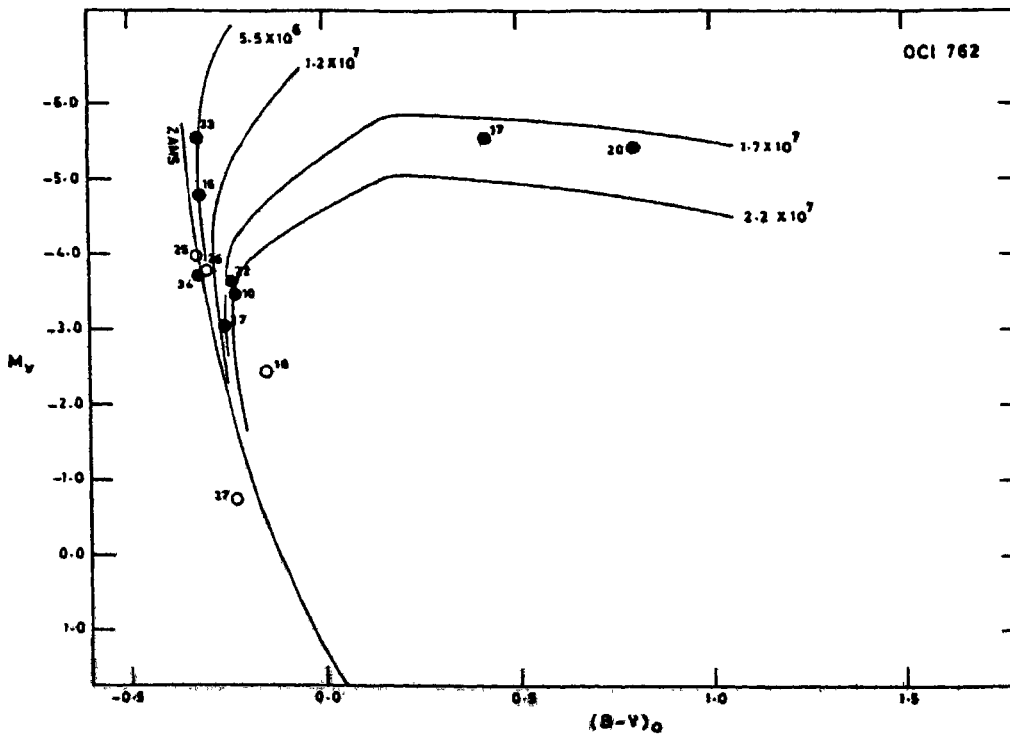


Fig. 4.72. HR-diagram of OC1 762. The post-MS isochrones are from Barbaro et al. (1969). The ages are indicated in years alongside the isochrones.

#### 4.11.5. Age of the Cluster

The HR-diagram of the cluster is shown in Fig.4.72, which is plotted for the true distance modulus of 14.26 mag. The post-MS isochrones indicate an age of  $1.8 \times 10^7$  years based on the location of the two probable red giant member stars. However, the near MS stars seem to indicate an age range of about  $5.5 \times 10^6$  years to  $2.2 \times 10^7$  years. The two brighter stars (16 and 33) near the upper end of the MS appear to be clearly following the isochrone of  $5.5 \times 10^6$  years, which is compatible with the age indicated by the smallest  $(B-V)_0$  on the MS. Under these circumstances, the two stars (17 and 20), which were presumed to be belonging to the red giant branch of the cluster, may turn out to be foreground stars rather than members of this cluster. However, in the absence of any other criteria, the membership of these two stars cannot be confirmed. Finally, it is quite clear that this is a very young cluster with a possible dispersion of  $5.5 \times 10^6$  to  $2.2 \times 10^7$  years, in its age.

#### **4.12. OC1 798 (NGC 3015)**

Trumpler (1930) estimated the distance of this cluster to be 4680 parsecs and gave an angular diameter of 2.5 arcmin. However, Shapley (1930) found its distance as 3980 parsecs and the angular diameter as 1.5 arcmin with fifteen stars in it. Soon after, Collinder (1931) determined the distance to be 7150 parsecs and gave an angular diameter of 2.5 arcmin with just ten stars in it. Much later, Barhatova (1950) estimated its angular diameter to be 8 arcmin and determined its distance as 2370 parsecs. Hogg (1965) gave an angular diameter of 2 arcmin and adopted seventeen stars as members.

Ruprecht (1966) classified it as I 3p in the Trumpler system. More recently Moffat & FitzGerald (1974) studied this cluster through UBV photometry, both photoelectric and photographic. They determined its distance as 8000 parsecs with  $E(B-V) = 1.09$  mag. But a little later, FitzGerald, Jackson & Moffat (1977) restudied this cluster exclusively through UBV photoelectric photometry and modified its distance to 5500 parsecs, the earliest spectral type being that of B2, the identification chart of this cluster, shown in Fig. 4.73, is printed from the direct photograph taken at the Cassegrain focus of the 1-m telescope at Siding Spring Observatory.

#### 4.12.1. Selection and Observations

This faint, young, remote and fairly well studied cluster was selected as a check for the results obtained in the present study. Eventhough, there seems to be some discrepancy in the estimation of the distance of the cluster by various earlier workers, the latest photoelectric study with the UBV filters done by FitzGerald, Jackson & Moffat (1977) has been adopted as a comparison for the present purposes.

The photoelectric observations of this cluster were done using the 61-cm telescope of the Siding Spring Observatory. (cf. Section 3.1). Standardized magnitudes and colours for a total of fourteen stars were obtained and the values are given in Table 4.12. The atmospheric extinction coefficients, the transformation coefficients and the zero-point constants (cf. Equations 3.6 to 3.11) are given below.

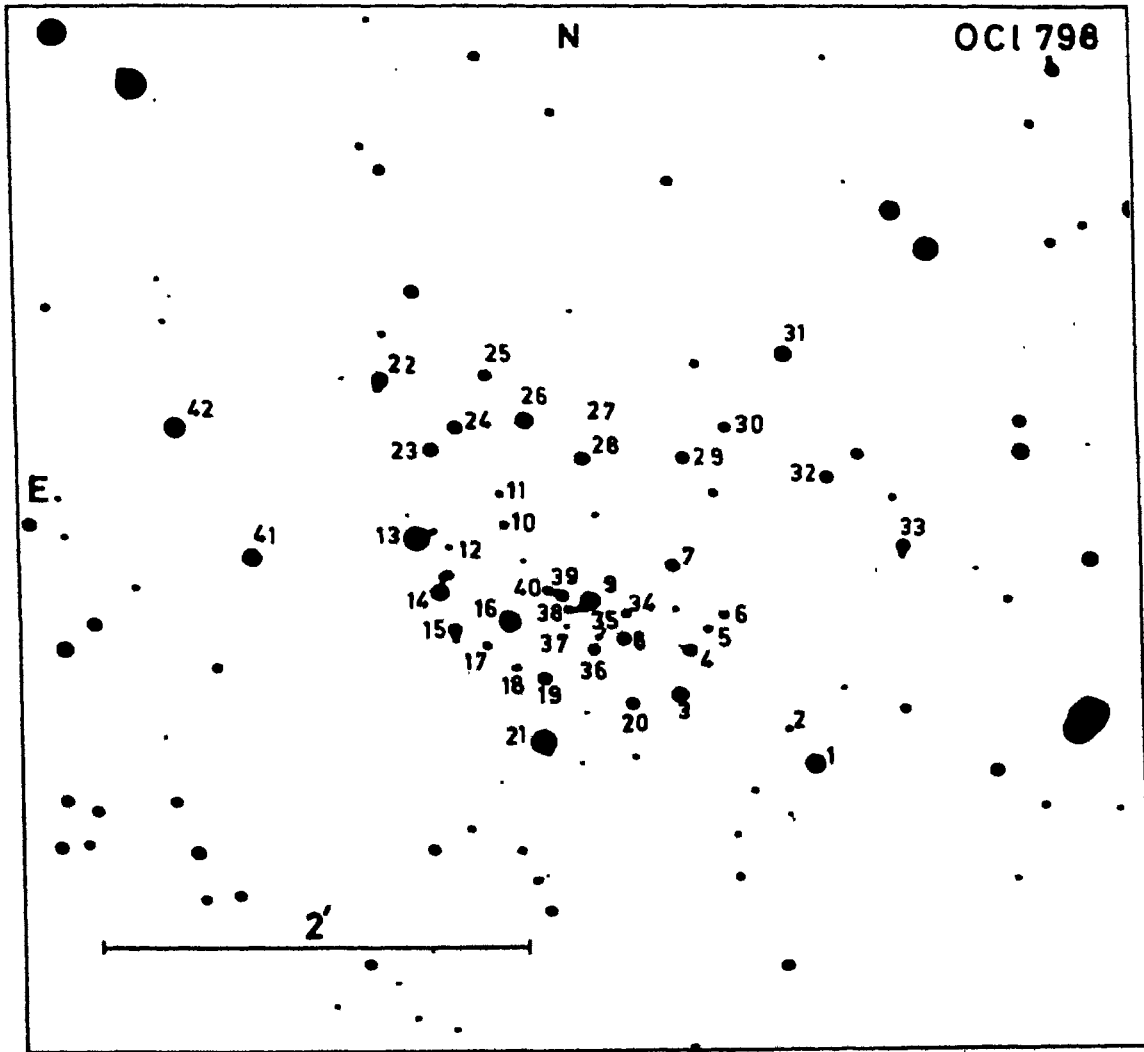


Fig. 4.73. Finding chart for the field of OC1 798.

**Table 4.12.** The observational data for individual stars in the open cluster OC1 798.

| Star No.                         | Star No.* | V      | (B-V) | (U-B)  | V*     | (B-V)* | (U-B)* | V <sub>o</sub> | (B-V) <sub>o</sub> | (U-B) <sub>o</sub> | E(B-V) | Membership |
|----------------------------------|-----------|--------|-------|--------|--------|--------|--------|----------------|--------------------|--------------------|--------|------------|
| 1                                | 2         | 3      | 4     | 5      | 6      | 7      | 8      | 9              | 10                 | 11                 | 12     | 13         |
| <b>Photoelectric photometry:</b> |           |        |       |        |        |        |        |                |                    |                    |        |            |
| 1                                | 88        | 13.892 | 0.478 | 0.233  | 13.93  | 0.38   | 0.24   | -              | -                  | -                  | -      | -          |
| 3                                | 33        | 12.690 | 2.627 | 2.572  | 12.56  | 2.56   | 2.50   | 9.164          | 1.542              | 1.787              | 1.085  | m          |
| 8                                | 12        | 14.850 | 0.880 | -0.150 | 14.99  | 0.81   | -0.04  | 11.110         | -0.270             | -0.940             | 1.150  | m          |
| 9                                | 14        | 13.734 | 0.865 | 0.047  | 13.64V | 0.86   | 0.09   | 10.273         | -0.200             | -0.720             | 1.065  | m          |
| 13                               | 1         | 12.288 | 0.989 | 0.435  | 12.36  | 0.92   | 0.47   | 8.911          | -0.050             | -0.350             | 1.039  | m          |
| 14                               | 4         | 13.767 | 0.930 | 0.253  | 14.07  | 0.85   | 0.20   | 10.257         | -0.15              | -0.520             | 1.080  | m          |
| 16                               | 7         | 13.177 | 0.973 | -0.224 | 13.25  | 0.99   | -0.42  | -              | -                  | -                  | -      | -          |
| 19                               | 9         | 13.509 | 2.060 | 2.108  | 13.31  | 2.33   | 2.50   | 9.983          | 0.975              | 1.233              | 1.085  | m          |
| 21                               | 37        | 13.321 | 0.229 | -0.258 | 13.44  | 0.26   | -0.03  | -              | -                  | -                  | -      | -          |
| 22                               | 59        | 14.619 | 0.617 | 0.302  | 14.61  | 0.56   | 0.27   | -              | -                  | -                  | -      | -          |
| 26                               | 24        | 12.948 | 1.757 | 0.152  | 13.03  | 1.77   | 0.51:  | -              | -                  | -                  | -      | -          |
| 31                               | 72        | 13.875 | 1.118 | -0.051 | 14.05  | 1.00   | -0.24  | -              | -                  | -                  | -      | -          |
| 41                               | 55        | 12.606 | 1.699 | 1.400  | 12.73  | 1.82   | 1.36   | 9.080          | 0.614              | 0.615              | 1.085  | m?         |
| 42                               | 56        | 12.855 | 1.104 | 0.509  | 13.04  | 1.07   | 0.52   | 9.072          | -0.060             | -0.370             | 1.160  | m?         |
| <b>Photographic photometry:</b>  |           |        |       |        |        |        |        |                |                    |                    |        |            |
| 2                                | 87        | 15.59  | 1.30  | 1.26   | 15.66  | 1.35   | 1.1:   | -              | -                  | -                  | -      | -          |
| 4                                | 32        | 15.17  | 0.82  | 0.13   | 15.18  | 0.86   | 0.14   | 11.99          | -0.16              | -0.58              | 0.98   | m          |
| 5                                | 31        | 16.11  | 1.00  | 0.32   | 15.92  | 0.9:   | 0.1:   | 12.40          | -0.14              | -0.50              | 1.14   | m          |
| 6                                | 30        | 15.77  | 0.99  | 0.29   | 15.66  | 1.10   | 0.35   | 12.07          | -0.15              | -0.53              | 1.14   | m          |
| 7                                | 28        | 15.10  | 0.63  | 0.37   | 15.23  | 0.63   | 0.22:  | -              | -                  | -                  | -      | -          |
| 10                               | 18        | 15.92  | 0.99  | 0.12   | 15.94  | 1.1:   | 1.0:   | 12.02          | -0.21              | -0.75              | 1.20   | m          |
| 11                               | 20        | 15.87  | 1.10  | 0.50   | 15.76  | 1.01   | 0.38:  | 11.94          | -0.11              | -0.37              | 1.21   | m?         |
| 12                               | 19        | 15.99  | 1.35  | 0.50   | 16.08  | 1.28   | 0.8:   | -              | -                  | -                  | -      | -          |
| 15                               | 5         | 14.99  | 0.84  | 0.14   | 15.20V | 0.81   | 0.02:  | 11.74          | -0.16              | -0.58              | 1.00   | m          |
| 17                               | 6         | 16.15  | 0.89  | 0.20   | 16.25  | 0.82   | 0.12   | 12.77          | -0.15              | -0.55              | 1.04   | m          |

| 1  | 2  | 3     | 4    | 5     | 6     | 7    | 8     | 9     | 10    | 11    | 12   | 13 |
|----|----|-------|------|-------|-------|------|-------|-------|-------|-------|------|----|
| 18 | 8  | 16.19 | 0.93 | 0.17  | 16.13 | 1.00 | 0.10  | 12.58 | -0.18 | -0.63 | 1.11 | m  |
| 20 | 34 | 15.43 | 0.85 | -0.11 | 15.41 | 0.85 | -0.06 | 11.82 | -0.26 | -0.91 | 1.11 | m  |
| 23 | 60 | 14.72 | 0.81 | 0.17  | 14.79 | 0.79 | 0.14  | -     | -     | -     | -    | -  |
| 24 | 61 | 14.94 | 0.71 | 0.43  | 14.93 | 0.76 | 0.40  | -     | -     | -     | -    | -  |
| 25 | 62 | 15.18 | 0.84 | 0.21  | 15.24 | 0.82 | 0.2:  | 12.00 | -0.14 | -0.5  | 0.98 | m  |
| 28 | 22 | 14.74 | 0.91 | 0.49  | 14.80 | 0.90 | 0.52  | -     | -     | -     | -    | -  |
| 29 | 25 | 15.15 | 0.83 | 0.08  | 15.19 | 0.85 | 0.01  | 11.87 | -0.18 | -0.65 | 1.01 | m  |
| 30 | 70 | 15.49 | 0.96 | 0.44  | 15.57 | 0.84 | 0.33  | -     | -     | -     | -    | -  |
| 32 | 77 | 14.69 | 0.97 | -0.01 | 14.78 | 0.95 | 0.06  | 10.69 | -0.26 | -0.90 | 1.23 | m  |
| 33 | 79 | 14.43 | 1.12 | 0.62  | 14.44 | 1.11 | 0.8:  | -     | -     | -     | -    | -  |
| 34 | 13 | 15.68 | 1.02 | 0.40  | 15.59 | 0.98 | 0.33  | 11.96 | -0.12 | -0.42 | 1.14 | m  |
| 35 | 11 | 15.73 | 1.04 | 0.29  | 15.79 | 1.1: | 0.1:  | 11.83 | -0.16 | -0.58 | 1.20 | m  |
| 36 | 10 | 15.36 | 0.99 | -0.33 | 15.26 | 1.10 | -0.2: | -     | -     | -     | -    | -  |
| 37 | 15 | 16.07 | 1.13 | 0.18  | 15.95 | 1.17 | -0.7: | -     | -     | -     | -    | -  |
| 38 | -  | 15.02 | 1.59 | 1.58  | -     | -    | -     | -     | -     | -     | -    | -  |
| 39 | 16 | 14.67 | 0.89 | -0.09 | 14.70 | 0.80 | -0.06 | 10.83 | -0.26 | -0.92 | 1.15 | m  |
| 40 | 17 | 15.50 | 0.92 | 0.04  | 15.5: | 1.1: | -0.03 | 11.80 | -0.22 | -0.79 | 1.14 | m  |

\* Moffat & FitzGerald (1974); or FitzGerald, Jackson & Moffat (1977).

$$\begin{aligned} K_V &= 0.155 & \epsilon &= 0.303 & \zeta_V &= 5.435 \\ K_{b-v} &= 0.154 & \mu &= 0.785 & \zeta_{bv} &= 0.034 \\ K_{u-b} &= 0.094 & \psi &= -2.693 & \zeta_{ub} &= 2.225 \end{aligned}$$

The direct UB<sub>V</sub> photography of this cluster was done with the help of the 1-m telescope at Siding Spring Observatory (cf. Section 3.2.1). The plate and filter combinations are given below along with the exposure times.

| <u>Plate</u> | <u>Filter</u> | <u>Exposure time</u> |
|--------------|---------------|----------------------|
| IIa-0        | UG2           | 65 min for U         |
| 103a-0       | GG13          | 40 min for B         |
| IIa-D        | GG14          | 30 min for V         |

From these plates, the photographic magnitudes were obtained for a total of fortyone stars, including the fourteen photoelectrically observed ones. These values, which were on an arbitrary scale, were then standardized using the above mentioned photoelectric observations (cf. Section 3.2.2). These magnitudes and colours are included in Table 4.12.

This Table also contains the star numbers given by Moffat & FitzGerald (1974) and by FitzGerald, Jackson & Moffat (1977) along with the numbers given in the present work. The magnitudes and colours in the form of V, (B-V) and (U-B) obtained by them are also included in the same Table. For an easy comparison of the observations, the values available in the literature (Moffat & FitzGerald, 1974; FitzGerald, Jackson & Moffat, 1977)



have been plotted against the present values in Figs. 4.74, 4.75 and 4.76. In the first figure (i.e. 4.74), the slope and the intercept obtained from the least squares solution of the linear relationship between the two quantities indicate an excellent match, which can be seen in the following equation.

$$V(\text{present}) = 1.019 V(\text{lit}) - 0.031.$$

The literature values of (B-V) for stars 5, 10 and 40 have been marked as uncertain and the same have been indicated in the next figure (i.e. 4.75) by their respective numbers. By neglecting these stars in the least squares solution, the two quantities of this figure also show an excellent match as seen below.

$$(B-V)_{\text{present}} = 0.972 (B-V)_{\text{lit}} + 0.035.$$

Similarly, after neglecting the uncertain (U-B) values as mentioned so in the literature (stars 2, 5, 7, 10, 11, 12, 15, 26, 33, 35, 36, 37 and 41), the two quantities of Fig.4.76 show a very good agreement. This is indicated by the following relationship.

$$(U-B)_{\text{present}} = 1.099 (U-B)_{\text{lit}} - 0.020.$$

In this last figure, there are two stars (16 and 31) at the upper end, which also seem to be deviating from the linear relationship. In fact, FitzGerald, Jackson & Moffat (1977) have found these two stars to be of Be spectral type.

#### 4.12.2. Membership

The CCD of this cluster, shown in Fig.4.77, indicates a clear sequence for a large number of the stars, for which

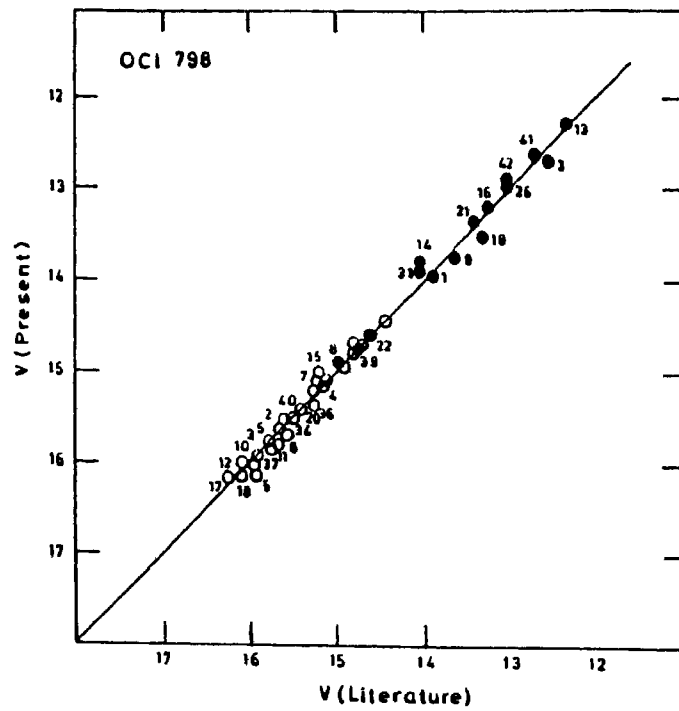


Fig. 4.74. The V magnitudes of the stars in the field of OC1 798, obtained in the present work, are plotted respectively against those available in the literature. V(literature) is taken from Moffat & FitzGerald (1974) and FitzGerald, Jackson & Moffat (1977).

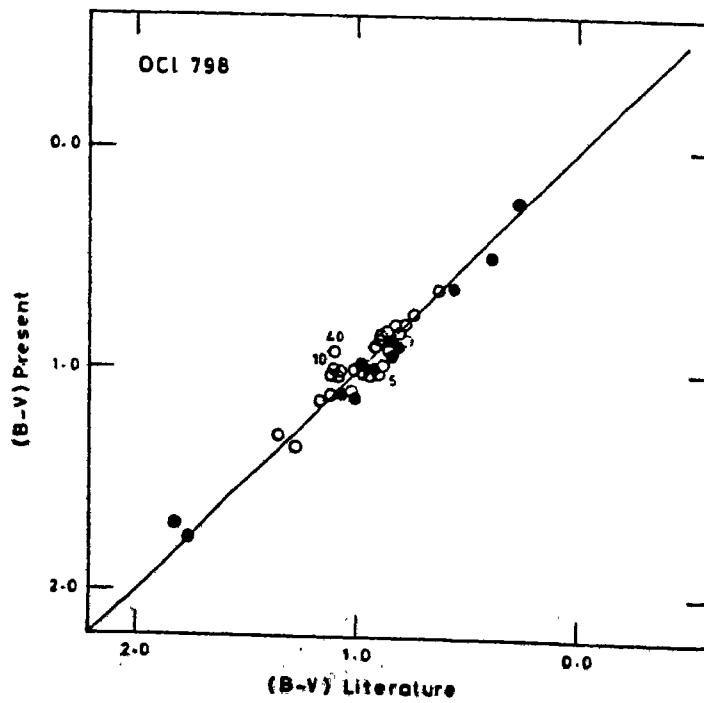
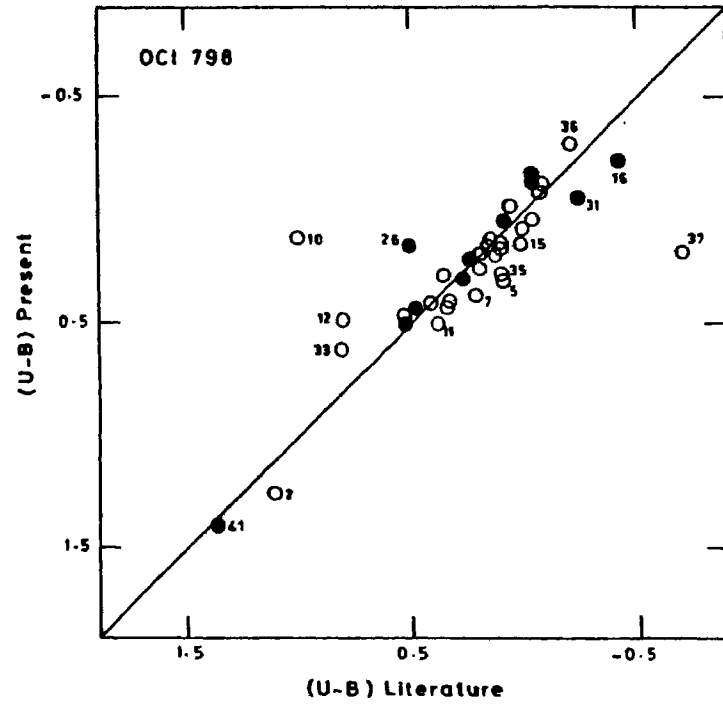


Fig. 4.75. The (B-V) values of the stars in the field of OC1 798, obtained in the present work, are plotted respectively against those available in the literature. (Literature as in Fig. 4.74).



**Fig. 4.76.** The (U-B) values of the stars in the field of OC1 798, obtained in the present work, are plotted respectively against those available in the literature. (Literature as in Fig. 4.74).

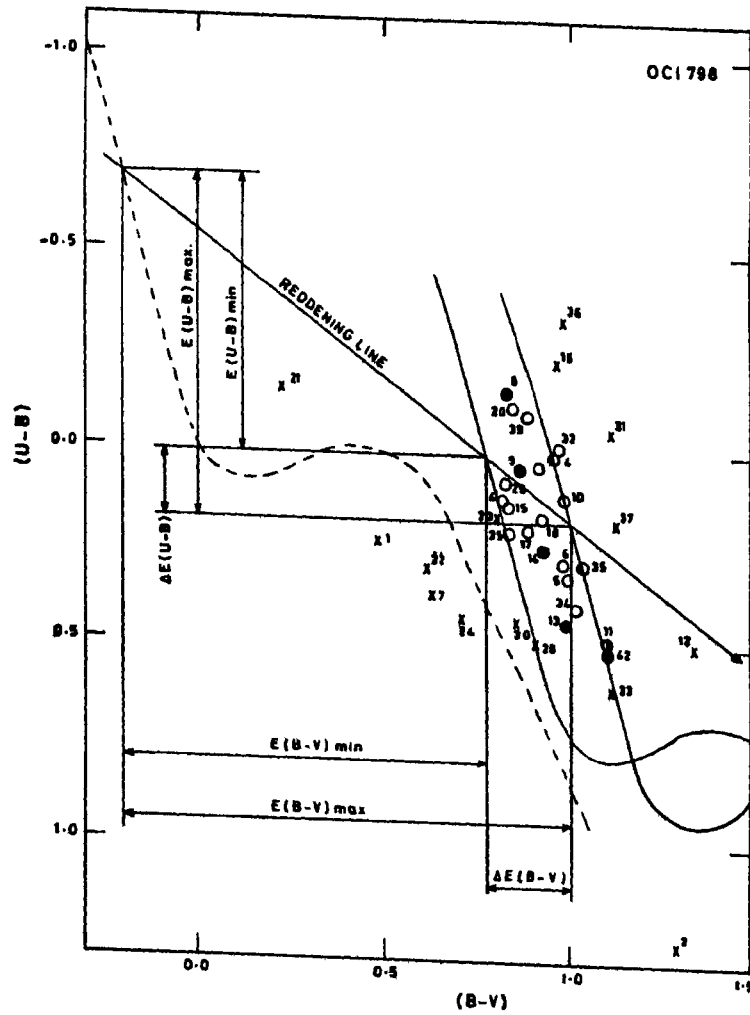


Fig. 4.77. The colour-colour diagram (CCD) of OC1 798. The dashed line is the unreddened main sequence (MS) taken from Schmidt-Kaler (1965).

the boundaries are drawn in the diagram. By picking out the same stars in the two CMD's given in Figs. 4.78 and 4.79 and by using the photometric criteria as described in Section 3.3.1, a total of twentyfour stars have been adopted as the most probable members of the cluster out of the observed fortyone stars. Three of the members (star 3, 19 and 41) appear to be belonging to the red giant branch of the cluster, while four others (stars 9, 13, 14 and 42) seem to have just evolved. Stars 41 and 42 are somewhat away from the actual physical group and yet they seem to be satisfying the rest of the photometric criteria. Therefore, these two stars have been given a doubtful membership. However, FitzGerald, Jackson & Moffat (1977) did not attribute any membership to star 42, while the other star was given a doubtful membership. Stars 13 and 25 have been adopted as members in this work, on the basis of photometric criteria only, even though Moffat & FitzGerald (1974) and FitzGerald, Jackson & Moffat (1977) considered them as non-members. Stars 16 and 31 have been found to be emission line stars by FitzGerald, Jackson & Moffat (1977), who adopted these two stars as a member and a doubtful member respectively. Therefore, it is obvious that the photometric criteria alone is not sufficient for fixing the membership of these two stars. Similarly, star 26 has been given as a double star with one blue and one red component by FitzGerald, Jackson & Moffat (1977) and therefore its membership could not be determined solely on the basis of the photometric criteria in the present work. Star 11 is one of the fainter

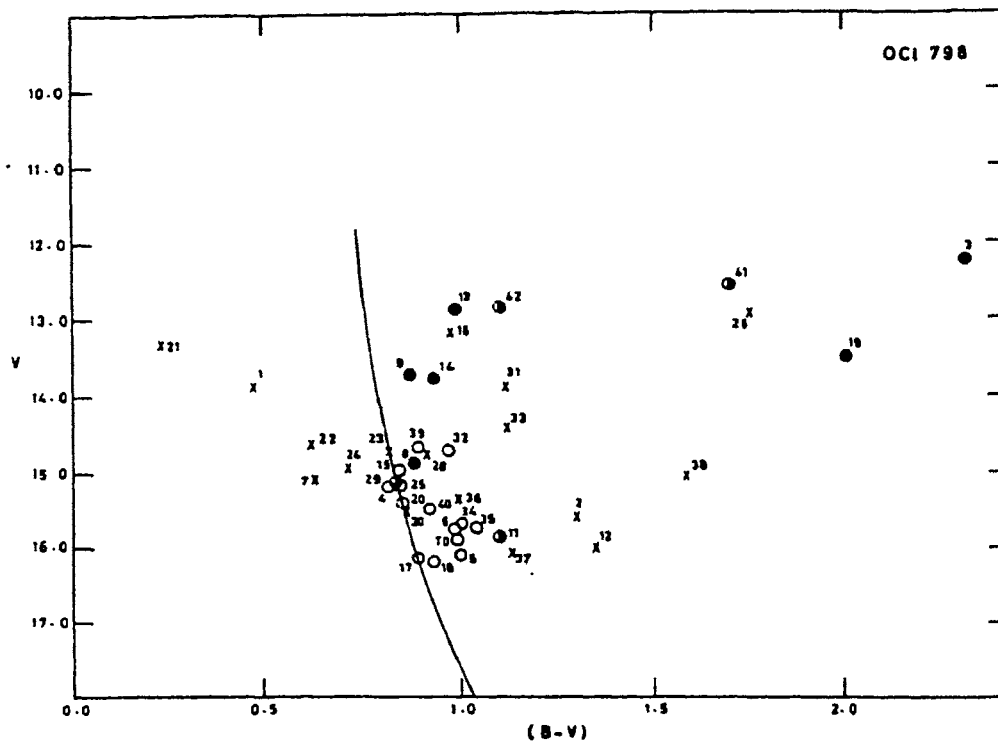


Fig. 4.78. The  $(B-V)$ ,  $V$  diagram (CMD) of OC1 798. The solid curve represents the zero age main sequence (ZAMS) fitted onto the cluster CMD.

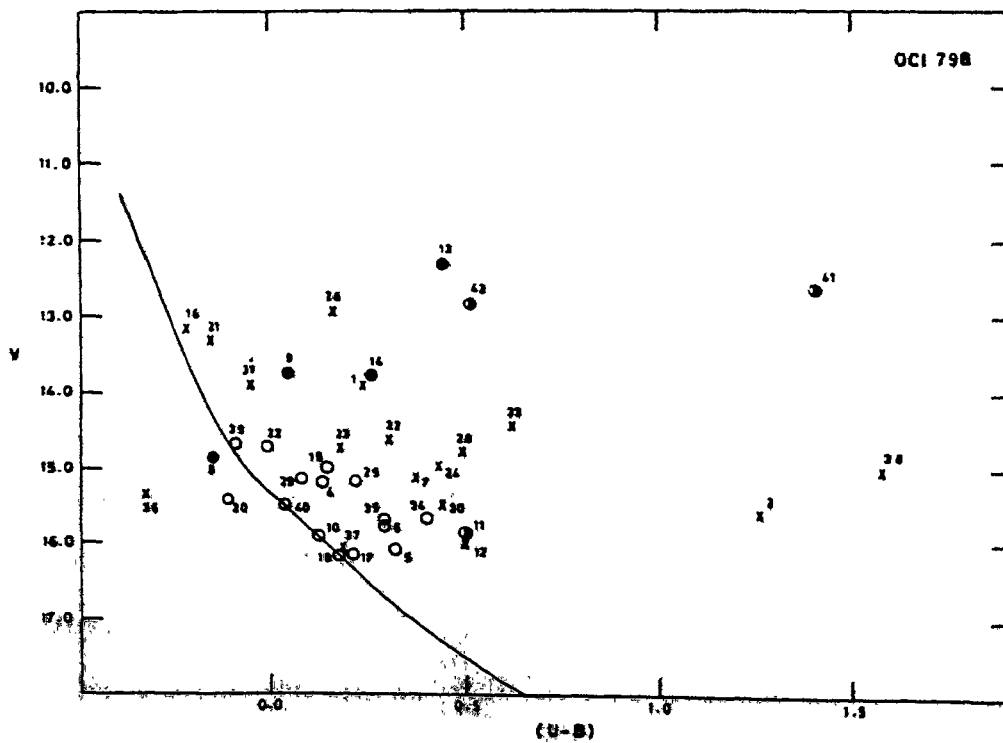


Fig. 4.79. The  $(U-B)$ ,  $V$  diagram (CMD) of OC1 798. The solid curve represents the ZAMS fitted onto the cluster CMD.

stars in the physical group and it seems to be marginally satisfying the photometric criteria in the present work. Therefore, it has been given a doubtful membership, while FitzGerald, Jackson & Moffat (1977) had considered it as a doubtful non-member. The photometric criteria of star 37 indicate it as a non-member in the present work, even though Moffat & FitzGerald (1974) had given a doubtful membership to it. There is just one star (no.38) which has been observed only in the present study and this turns out to be a non-member. All the other stars in this work agree very well with the membership or non-membership given to them by Moffat & FitzGerald (1974) and FitzGerald, Jackson & Moffat (1977). These are listed in Table 4.12 where the members and doubtful members are denoted by 'm' and 'm?' respectively.

#### 4.12.3. Reddening

FitzGerald, Jackson & Moffat (1977) pointed out a marginal evidence for a slight variable reddening across the field of the cluster and indicated that it might be due to photometric errors. However, the sequence shown by the member stars in the CCD of this cluster (cf. Fig. 4.77) appears to be wide enough to strongly indicate a non-uniform reddening. The boundaries of this sequence give rise to the following dispersions.

$$\Delta E(B-V) = 0.23 \text{ mag}$$

and

$$\Delta E(U-B) = 0.17 \text{ mag.}$$

These values are much larger than the natural dispersion (cf. Section 3.4) and therefore the concerned stars were individually

corrected for the appropriate interstellar reddening. These include all the stars for which the individual corrections have been applied by FitzGerald, Jackson & Moffat (1977). The corrections applied in the present work have been found to be between

$$E(B-V)_{\max} = 1.20 \text{ mag and } E(B-V)_{\min} = 0.97 \text{ mag}$$

and between

$$E(U-B)_{\max} = 0.87 \text{ mag and } E(U-B)_{\min} = 0.70 \text{ mag.}$$

However, the mean colour excess,  $E(B-V)_{\text{mean}} = 1.085 \text{ mag}$  is in excellent agreement with the value obtained by FitzGerald, Jackson & Moffat (1977).

With the help of the individual  $E(B-V)$  values, which are tabulated in Table 4.12, the corresponding values of  $A_V$  were obtained. These were found to be between 3.90 mag and 3.15 mag, which, in turn, were used to correct the observed  $V$  values. All these corrected magnitudes and colours are also included in Table 4.12 as  $V_0$ ,  $(B-V)_0$  and  $(U-B)_0$ .

#### 4.12.4. Distance

The true distance modulus of this cluster has been determined by fitting the ZAMS onto the cluster main sequences as shown in Fig.4.80. The long and short wavelength CMD's have been found to yield the distance moduli of 13.83 mag and 13.28 mag, respectively, giving rise to an average value of 13.56 mag. Then the distance  $D$  to the cluster, based on Equation 3.21 is

$$D = 5.16 \pm 0.65 \text{ kpc.}$$



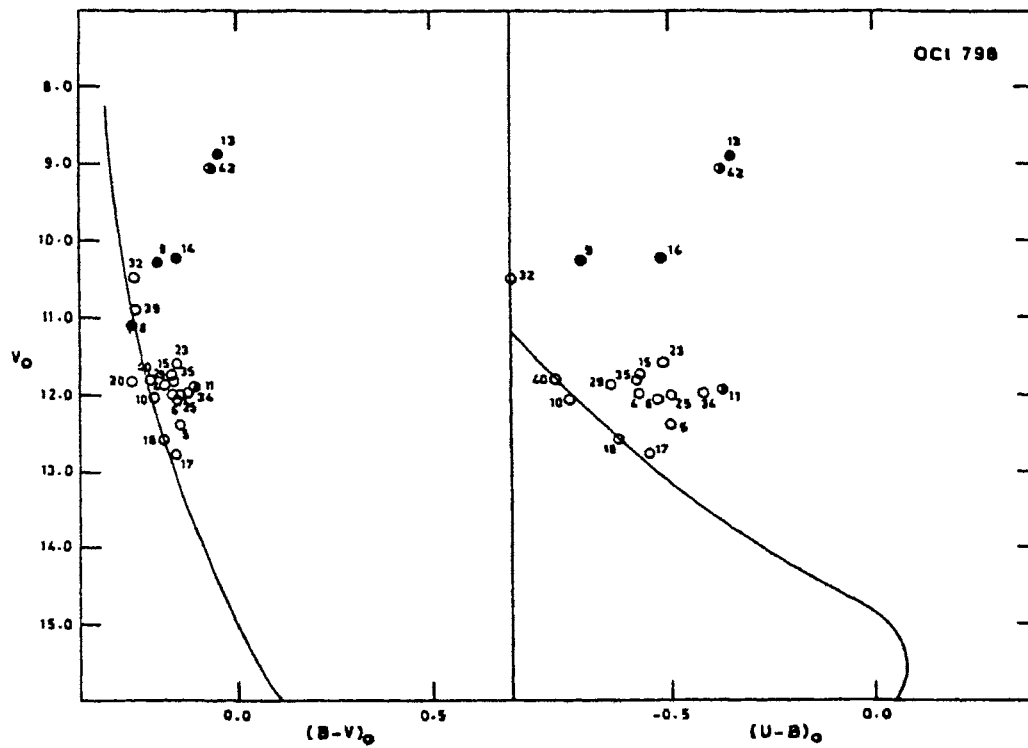


Fig. 4.80. The intrinsic  $(B-V)_0$ ,  $V_0$  and  $(U-B)_0$ ,  $V_0$  diagrams (CMDs) of OC1 798. The solid curves represent the ZAMS, taken from Schmidt-Kaler (1965), fitted onto the cluster CMDs.

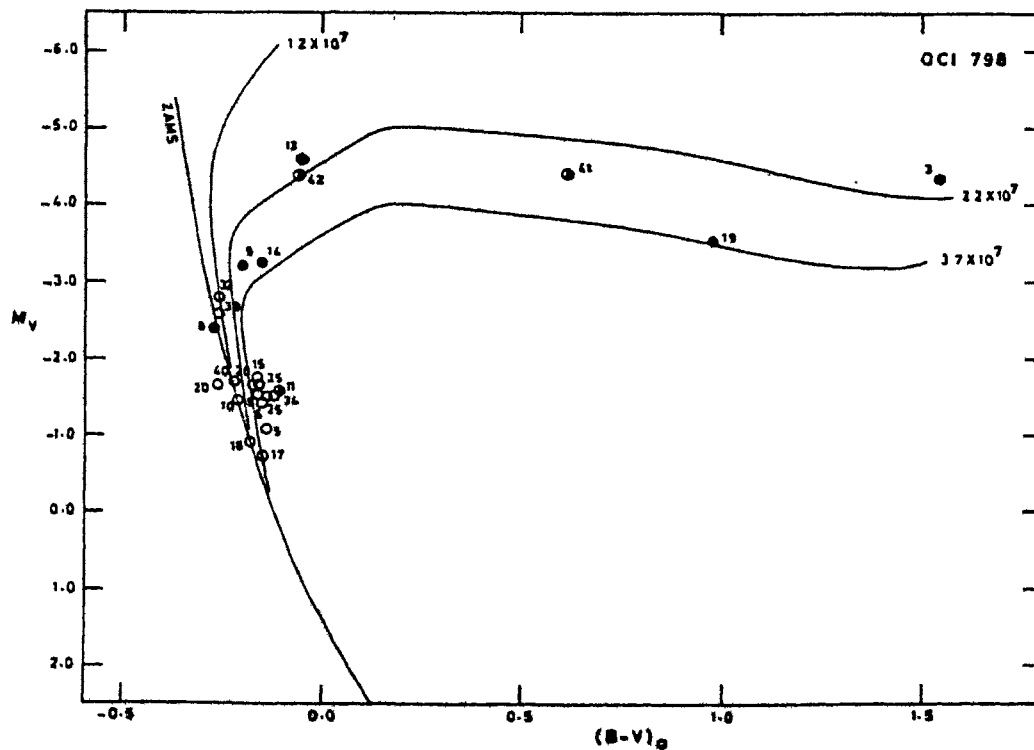


Fig. 4.81. HR-diagram of OC1 798. The post-MS isochrones are from Barbaro et al. (1969). The ages are indicated in years alongside the isochrones.

This value matches very well with the one ( $D = 5.5 \pm 0.8$  kpc) obtained by FitzGerald, Jackson & Moffat (1977).

#### 4.12.5. Age of the Cluster

The HR-diagram of the cluster is shown in Fig. 4.81, which is plotted for the true distance modulus of 13.56 mag. The post-MS isochrones indicate an age range of 2.2 to  $3.7 \times 10^7$  years, while the MS itself seems to be following the isochrone of  $1.2 \times 10^7$  years. Further, the smallest  $(B-V)_0$  on the MS, also indicates an age somewhat less than  $1 \times 10^7$ . In view of this young age, the slight scatter towards the right side of the MS by the fainter stars may include some pre-MS contracting stars also. Thus, this cluster is young enough to be a suitable tracer of spiral arms with a dispersion of 1.2 to  $3.7 \times 10^7$  years, in its age. The young age is in agreement with the finding of FitzGerald, Jackson & Moffat (1977), who have shown the earliest spectral type of this cluster to be around B2 type.

Thus, the observations and the results such as fixing the membership, finding the interstellar reddening, determining the distance and estimating the age of the cluster in this study are all showing excellent agreement with those obtained by the earlier authors (Moffat & FitzGerald, 1974; FitzGerald, Jackson & Moffat, 1977). On the basis of this matching found in this last mentioned cluster, the reliability of the observations and results obtained for the other eleven clusters may be inferred to be good.

\*\*\*\*\*

## CHAPTER 5

### EVOLUTIONARY ASPECTS OF THE SELECTED CLUSTERS AND THEIR RELATIONSHIP TO THE STRUCTURE OF THE GALAXY

The various parameters of the twelve selected clusters are discussed here in connection with their non-coeval nature, the presence of non-uniform reddening and their relationship to the structure of the Galaxy. All these clusters show a spread in their ages and most of them show variable extinction across their fields. The location of some of these young clusters in the anticentre direction of the Galaxy strongly supports the existence of an outer spiral feature at a distance of about 4 to 5 kpc. Also, a feature, which is branching off from the local arm and extending towards the Carina arm is indicated for the first time with the help of the present optical observations. A summary of the parameters obtained in this work is presented in Tables 5.1 and 5.2.

#### **5.1. Evolutionary Aspects**

It may be seen in Table 5.2 that an age dispersion of  $10^7$  to  $10^8$  years exists among cluster stars. The dispersion in age of the cluster stars has been discussed by various earlier authors (Strom et al., 1971, 1972a, 1972b; Bodenheimer, 1972; Breger, 1972; Jones, 1972; McNamara, 1976). According to Bodenheimer (1972), this dispersion can be due to

Table 5.1. Summary of cluster parameters - membership and reddening

| Open<br>Cluster<br>OC 1 | Name        | Galactic coordinates |        | No. of observed<br>Stars | Members | $E(B-V)_{\min}$<br>(mag) | $E(B-V)_{\max}$<br>(mag) | $E(B-V)$<br>(mag) | $E(B-V)_{\text{mean}}$<br>(mag) | Mean<br>$A_V$<br>(mag) |
|-------------------------|-------------|----------------------|--------|--------------------------|---------|--------------------------|--------------------------|-------------------|---------------------------------|------------------------|
|                         |             | l                    | b      |                          |         |                          |                          |                   |                                 |                        |
| 427                     | Czernik 20  | 168°.30              | 1°.32  | 77                       | 55      | 0.38                     | 0.53                     | 0.15              | 0.46                            | 1.48                   |
| 493                     | Czernik 25  | 202 .31              | -5 .26 | 31                       | 17      | 0.53                     | 0.64                     | 0.11              | 0.59                            | 1.90                   |
| 501                     | NGC 2236    | 204 .37              | -1.69  | 45                       | 28      | 0.55                     | 0.89                     | 0.34              | 0.72                            | 2.31                   |
| 506                     | Cr 97       | 205 .37              | -1.76  | 29                       | 24      | 0.00                     | 0.00                     | 0.00              | 0.00                            | 0.00                   |
| 556 S                   | Haffner 3   | 219.83               | 0.02   | 44                       | 12      | 0.47                     | 0.60                     | 0.13              | 0.54                            | 1.74                   |
| 556 N                   |             |                      |        |                          | 11      | 0.47                     | 0.60                     | 0.13              | 0.54                            | 1.74                   |
| 585                     | NGC 2374    | 228.43               | 1 .04  | 38                       | 20      | 0.11                     | 0.24                     | 0.13              | 0.18                            | 0.57                   |
| 674                     | Haffner 14  | 243 .99              | -2 .06 | 41                       | 22      | 0.57                     | 0.74                     | 0.17              | 0.66                            | 2.15                   |
| 692                     | Haffner 20  | 247 .01              | -0 .94 | 27                       | 17      | 0.72                     | 0.83                     | 0.11              | 0.78                            | 2.52                   |
| 694                     | Haffner 17  | 247 .72              | -2 .53 | 26                       | 17      | 0.96                     | 1.17                     | 0.21              | 1.07                            | 3.45                   |
| 715                     | NGC 2588    | 252 .28              | 2. 45  | 30                       | 18      | 0.48                     | 0.61                     | 0.13              | 0.55                            | 1.77                   |
| 762                     | Ruprecht 69 | 266 .45              | -2 .99 | 37                       | 12      | 0.81                     | 1.13                     | 0.32              | 0.97                            | 3.09                   |
| 798                     | NGC 3105    | 279 .92              | 0 .29  | 41                       | 24      | 0.97                     | 1.20                     | 0.23              | 1.09                            | 3.53                   |

Table 5.2. Summary of cluster parameters - distance and age

| Open Cluster | $(V_0 - M_V)$<br>(mag) | Distance<br>(kpc) | Earliest<br>(B-V) <sub>0</sub><br>(mag) | Age (in $10^7$ years)<br>based on<br>evolved stars<br>(going away from MS) | Pre-MS<br>stars | Median<br>age<br>in $10^7$ years |
|--------------|------------------------|-------------------|---|--|-----------------|----------------------------------|
| OC1          |                        |                   |   |  |                 |                                  |
| 427          | 13.15±0.10             | 4.16±0.14         | -0.26                                   | 2.2 to 7.1   | 0.1 to 0.2      | 4.1                              |
| 493          | 13.75±0.10             | 5.63±0.26         | -0.23                                   | 1.2 to 5.0   | 0.1             | 3.1                              |
| 501          | 13.02±0.13             | 4.02±0.23         | -0.18                                   | 2.8 to 12.5  | -               | 7.7                              |
| 506          | 8.75±0.05              | 0.56±0.01         | -0.05                                   | 10.0 to 59.0   | -               | 34.5                             |
| 556 S        | 13.41±0.05             | 4.81±0.11         | -0.18                                   | 1.0 to 2.8   | -               | 1.9                              |
| 556 N        | 13.41±0.05             | 4.81±0.11         | -0.14                                   | 2.8 to 5.0   | -               | 3.9                              |
| 585          | 10.23±0.10             | 1.11±0.05         | -0.10                                   | 6.0 to 7.1   | -               | 6.6                              |
| 674          | 12.91±0.15             | 3.83±0.26         | -0.20                                   | 1.7 to 7.1   | 0.03 to 0.1     | 4.4                              |
| 692          | 13.61±0.13             | 5.27±0.30         | -0.22                                   | 1.0 to 7.1   | -               | 4.1                              |
| 694          | 14.14±0.08             | 6.73±0.23         | -0.21                                   | 2.0 to 7.1   | -               | 4.6                              |
| 715          | 13.56±0.08             | 5.14±0.18         | -0.23                                   | 1.0 to 12.5  | ~0.1            | 6.8                              |
| 762          | 14.26±0.05             | 7.11±0.16         | -0.32                                   | 0.6 to 2.2   | -               | 1.4                              |
| 798          | 13.56±0.28             | 5.16±0.65         | -0.27                                   | 1.2 to 3.7   | -               | 2.5                              |

- mass loss at varying rates
- a contamination of the CMD's by field stars
- non-uniform reddening across the cluster
- stars in rapid rotation with different orientation of their rotational axes to the line of sight
- the presence of circumstellar shells
- the presence of spectroscopic binaries giving composite colours and magnitudes
- a real spread in the ages of the cluster stars.

Out of the above mentioned possibilities the effect of mass loss, according to Ezer & Cameron (1971), is to shift the evolutionary track and the time scale to that which is generally appropriate to a star of the resulting final mass. They, however, concluded that the spread of the stellar points on HR-diagrams of the young clusters cannot be explained as a result of variation in mass loss rate. Thus the observed position of stars which undergo mass loss should not be noticeably affected.

The chance of contamination of the CMD's by field star is small due to the fact that particular care has been taken to pick out the most probable members for each cluster.

To minimise the effect of non-uniform reddening, each individual star has been suitably dereddened.

A flattened fast rotating star viewed pole-on appears brighter than the same star viewed in the plane of its equator. Thus if this effect causes the luminosity spread, stars located

at the brightest apparent magnitude in CMD should have the smallest  $v \sin i$ . Contrary to this, McNamara (1976) has found that for some of the brightest stars in Orion cluster,  $v \sin i$  increases with luminosity, thus ruling out the effects of rapid rotation with different orientations on the luminosity spread.

Warner et al. (1977) have shown that a luminosity spread is clearly present in the cluster, even among such of the contracting stars which do not exhibit circumstellar shells.

McNamara (1976) measured the MK luminosity indicator  $\text{Sr II } (\lambda 4077)/\text{Fe I } (\lambda 4045)$  for some bright stars in Orion cluster and found that the spread in CMD is caused by an intrinsic difference in luminosities and not by spectroscopic binary nature of the stars. Further, the frequency of occurrence of binaries in clusters is noticeably small (Kopal, 1978).

Thus, it appears that the observed luminosity spread in the clusters is mainly caused by stars of differing ages. Therefore, it may be concluded that star formation in clusters is not coeval, and takes place in a time interval of approximately  $10^7 - 10^8$  years. This is in agreement with the earlier suggestions by various authors (Herbig, 1962; Iben & Talbot, 1966; Williams & Cremin, 1969; McNamara, 1976; Götz, 1977; Piskunov, 1977; Sagar & Joshi, 1978a, 1978b, 1979). Elmegreen & Lada (1977) have proposed that OB subgroups in a given association are formed in a step by step process and, therefore, are not coeval. This last aspect is quite likely to be seen in the field of OC1 556, (cf. Section 4.5) where two clusters of differ-

rent ages as well as of different age spreads are situated side by side, their distances being the same from the observer (Babu, 1983).

## 5.2. Presence of Gas-Dust in Cluster

From Table 5.1, it may be seen that the reddening of these young clusters is a function of the direction of the cluster and of its distance. Fig.5.1 clearly shows that as the cluster distance increases, the average value of the reddening,  $E(B-V)$ , increases, as is generally expected. That is, the amount of interstellar matter increases in the plane of the Galaxy with the increasing distance from Sun.

The remarkable feature, especially in the case of young clusters, is the relation of the variable reddening across the cluster with its age. As the age of the cluster increases the value of  $\Delta E(B-V)$  decreases which is clearly shown in Fig.5.2. One may expect this phenomenon because, at the beginning of star formation, only a part of the initial gas cloud is transformed into stars. With time, the remaining part of the gas is either swept away by radiation from the hot young stars or is used up in subsequent star formation (Tutukov, 1977, 1978). In earlier studies, stars belonging to several young stellar clusters or groups have been found to be embedded in gas (Mezger & Smith, 1977) such as the star cluster in the dark cloud in Ophiuchus (Grasdalen et al., 1973; Brown & Zuckerman, 1975; Encarnaz et al., 1975; Verba et al., 1975), the Trapezium



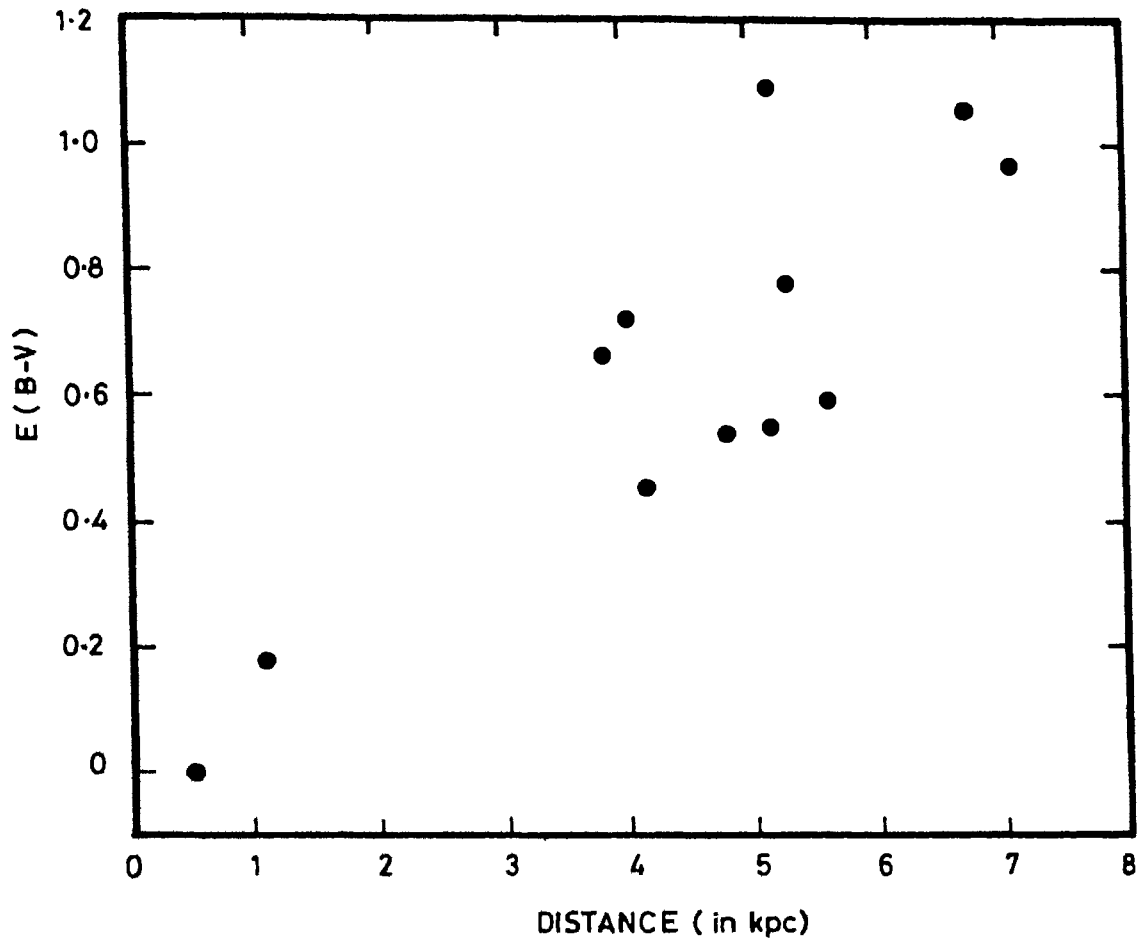


Fig. 5.1. The average values of  $E(B-V)$  of the individual clusters studied in this work are plotted against the respective distances.

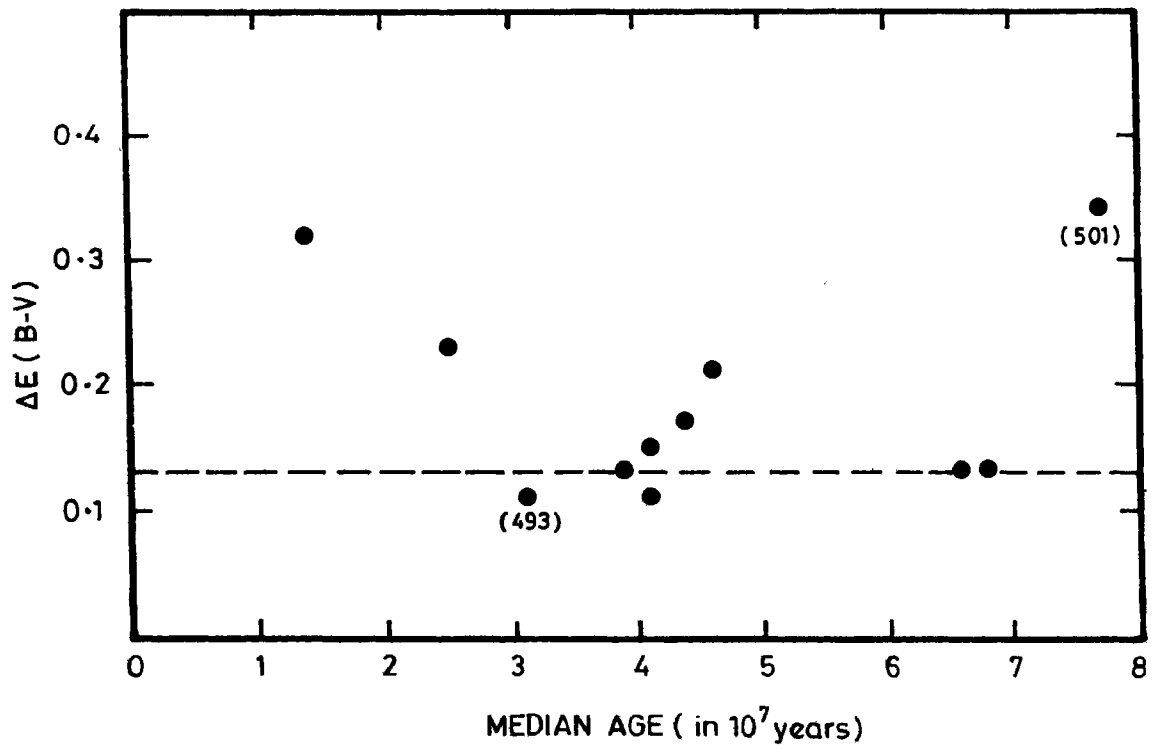


Fig. 5.2. The dispersions in the reddening,  $\Delta E(B-V)$ , of the individual clusters studied in this work are plotted against the respective median ages.

cluster and the IR star clusters in the Orion region (Sullivan & Downes, 1973; Harris & Wynn-Williams, 1976; Wynn-Williams & Becklin, 1974; Kutner et al., 1976; Mezger & Smith, 1977) and many others. The presence of gas and dust in all these clusters is a pointer to star forming activity in the cluster regions.

Thus, on the basis of the above discussions and according to the discussions in Section 3.4, a horizontal dashed line is drawn in Fig.5.2 at  $\Delta E(B-V) = 0.13$  mag, to indicate the border between the variable and non-variable reddening. In this work, the above mentioned value of 0.13 mag is adopted as the natural dispersion as against 0.11 mag which was discussed in Section 3.4, because three of the clusters studied here showed 0.13 mag and the same were considered as having a marginally non-variable reddening. Therefore it may now be concluded that gas is still present in the clusters OC1 427, OC1 674, OC1 694, OC1 762 and OC1 798 and that star formation may still be going on in these clusters. On the other hand, the star formation activity must have almost been completed or very close to completion in clusters OC1 506, OC1 556, OC1 585, OC1 692 and OC1 715. There is one cluster OC1 493, which contains the pre-MS contracting stars and yet is situated below the horizontal limiting line. Thus the border line shown in the diagram need not necessarily be considered as hard and fast. There is one other cluster OC1 501, which, in spite of being the second 'oldest' of the clusters studied here,

is showing the highest value for  $\Delta E(B-V)$ . One possibility could be that its median age is a little over-estimated. But Rahim (1970) had also suggested that this cluster was slightly old. Therefore, it may be more likely that some external effect is causing this. For example, the interstellar medium between the cluster and the observer could be non-uniformly distributed in a plane, perpendicular to the line of sight. However, this randomly distributed non-uniformity of the interstellar matter in the Galaxy could be a factor in all directions and it is only a matter of chance of where any cluster is physically located.

### **5.3. Relationship of the Open Cluster to the Structure of the Galaxy**

The location of the clusters studied in the present work are marked on the plane of the Galaxy in Fig.5.3, along with the already established features of the galactic structure. These are denoted by filled circles for which the error bars for the distances are indicated as seen from the Sun. Only one cluster namely OC1 506, has not been included in this figure because it is not considered as a spiral arm tracer due to its 'old' age.

In Fig.5.3, there are four clusters (OC1 585, 674, 692 and 715), which are clearly located along the local arm between  $1\sim 240^\circ$  to  $250^\circ$  with the distances ranging from about 1 kpc to 5 kpc. One cluster (OC1 798) is a definite member of the Sagitt-

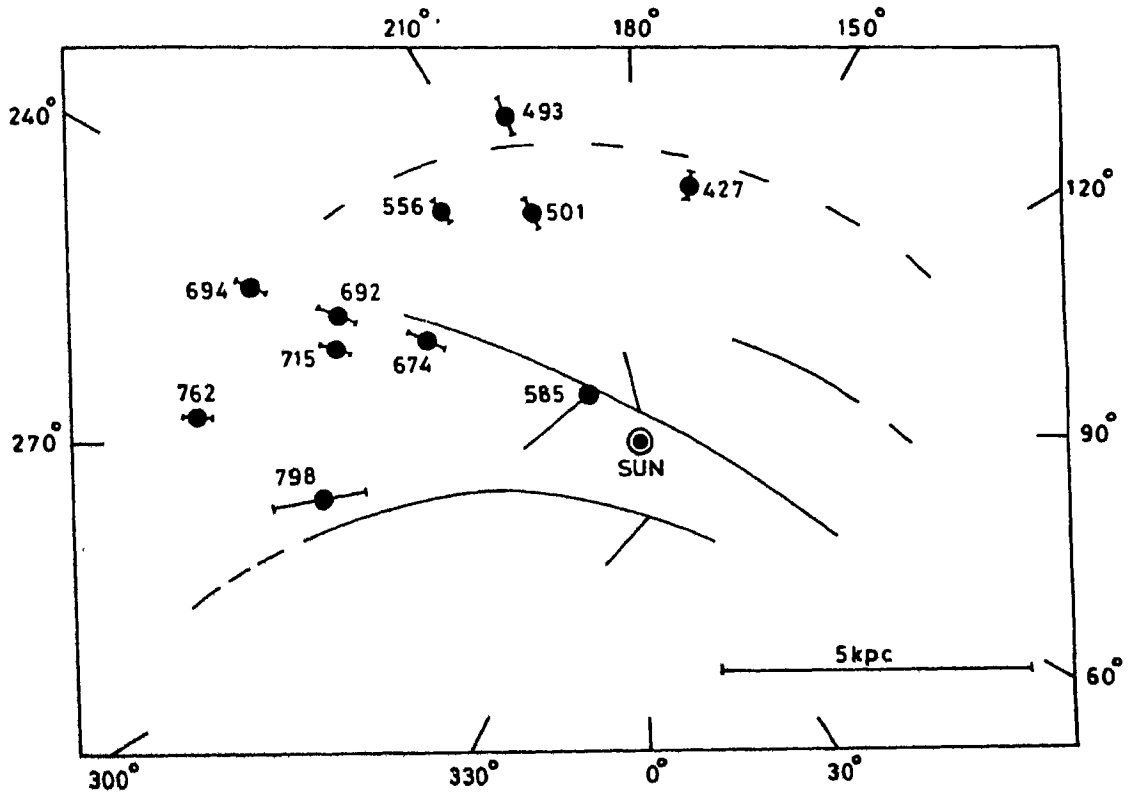


Fig. 5.3. The location of the clusters studied in the present work are marked on the plane of the Galaxy along with the already established optical features of the galactic structure. Error bars for the distances are indicated as seen from the Sun. Well determined spiral features are shown as solid lines while tentative features are shown as dashed lines.

arius-Carina arm in the direction  $l \sim 280^\circ$  at a distance of about 5 kpc.

Three of the remaining clusters (OC1 427, 493 and 556) studied in the present work are found in the outer Perseus region at distances of about 4 to 5.5 kpc in the direction  $l \sim 170^\circ$  to  $220^\circ$ . The slightly older cluster OC1 501 is also present in the same region at  $D \sim 4$  kpc and  $l \sim 200^\circ$ . The presence of even these few clusters indicate the existence of the outer Perseus spiral feature, some evidence for which was found earlier by Moffat & Vogt (1973) and Vogt & Moffat (1975).

Recently, Jackson, FitzGerald & Moffat (1979) studied the positions of H II regions along with the OB-star groups in the anticentre direction ( $l = 150^\circ$  to  $250^\circ$ ) and pointed out that the outer feature appears better defined than previous observations indicated, extending at least from  $l \sim 150^\circ, D \sim 5$  kpc to  $l \sim 245^\circ, D \sim 6.5$  kpc. When the diagram given by these authors is superimposed on Fig.5.3 of this work, along with the figure given by Vogt & Moffat (1975), the result is Fig.5.4. It can now be seen from this figure that the combined effort of the young open cluster studies (present and earlier works) as well as that of the H II region studies, puts the existence of the outer Perseus feature beyond doubts.

It can also be seen that in all likelihood, this outer feature is extending into the Puppis group of clusters in  $l \sim 240^\circ$  at  $D \sim 6$  to 7 kpc. This is also supported by the location of OC1 694, one of the presently studied clusters, at  $l \sim 245^\circ$  and  $D \sim 6.5$  kpc. Further, this Puppis cluster region seems

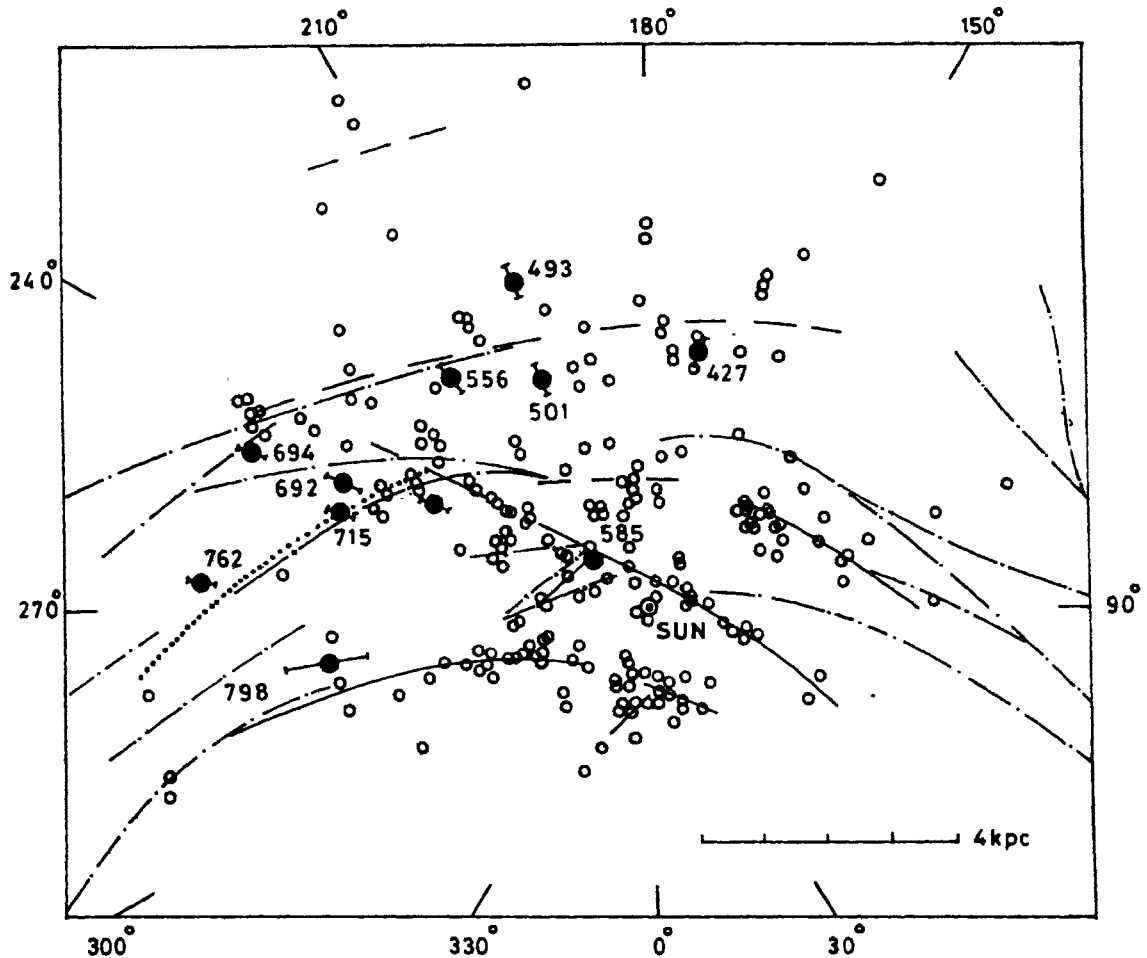


Fig. 5.4. The locations of the clusters studied in the present work (denoted by filled circles) are shown in the plane of the Galaxy along with the young clusters, associations and H II regions studied earlier (denoted by small unfilled circles). The solid lines and dashed lines show the well determined and tentative optical features respectively. The dot-dash lines indicate the features observed through radio wavelengths. The dotted line represents the branching off feature from the local arm for the first time from optical observations.

to be the junction for the merging of the local arm with the outer Perseus arm.

The location of OC1 762 at  $l \sim 270^\circ$  and  $D \sim 7$  kpc appears to be of particular importance, especially due to the presence of two already known clusters - one at  $l \sim 265^\circ$ ,  $D \sim 6$  kpc and the other at  $l \sim 280^\circ$ ,  $D \sim 8$  kpc. These positions along with those of OC1 692 and OC1 715 at  $l \sim 250^\circ$  and  $D \sim 5$  kpc give an indication of a feature which is originating from the local arm at  $D \sim 4.5$  kpc and extending towards  $l \sim 280^\circ$  and  $D \sim 8$  kpc. This branching off feature is clearly seen in the radio map of the Galaxy by Kerr (1970) and the same is marked by a dotted line in Fig.5.4. Thus, for the first time there seems to be an indication of this branching off feature from optical observations. However, it is essential to note the strong interstellar extinction found in this general direction, which indicates the presence of large quantities of interstellar matter (Garrison, 1985). Thus any further attempts to improve the evidence for this branching off feature must be made with extra care, especially while accounting for the interstellar reddening in the direction of  $l \sim 260^\circ$  to  $280^\circ$ .

\*\*\*\*\*



## CHAPTER 6

### **SUMMARY AND FUTURE PROSPECTS**

The study of faint young open clusters was undertaken on the suggestion of late Prof. M.K.V.Bappu in order to obtain the luminosities of stars contained in the very distant and hitherto not-well-studied clusters, with the hope of using these clusters as spiral arm tracers, if they were found sufficiently young.

A new technique was developed for the selection of the clusters where the spectral types of individual stars obtained by using modified objective-grating spectroscopy were combined with the V magnitudes which were estimated from the image diameters on the sky survey charts (for example, Palomar Observatory Sky Survey Charts). In this, the telescope time was needed only for obtaining the objective-grating spectra, while the other parameter was obtained from the already available survey charts. It was also possible to observe fainter stars upto  $V \sim 15$  mag with this method. This combination of spectral type (objective-grating) and V mag (sky survey chart) was found to work well in establishing the cluster reality by indicating the respective HR-diagram and consequently the possible members. A total of six young clusters were selected with this technique. Six more clusters were selected in the southern sky by visually picking up the bluer looking

clusters from the respective survey charts.

These twelve possibly young clusters extend in the galactic longitude  $l \sim 168^\circ$  to  $280^\circ$  with the galactic latitude  $b \sim +2.4$  to  $-5.2$ . All these clusters have been subjected to photoelectric and photographic photometry using the telescopes at the Kavalur Observatory as well as those at the Mount Stromlo and Siding Spring Observatories.

The members of each cluster have been carefully selected on the basis of the photometric criteria. OC1 762 contains twelve members out of the observed thirtyseven stars, while OC1 427 contains fiftyfive members out of the observed seventyseven stars. These two cases are about the minimum and maximum respectively showing the number of member stars. In almost all clusters, the observed faintest magnitude reached upto  $V \sim 15$  to  $16$  mag, sometimes going even upto  $17$  mag.

All the clusters studied in this program show various amounts of dispersions in their respective ages, supporting the earlier suggestions that star formation in clusters is not coeval, but is prolonged.

On the basis of the interstellar extinction found for the cluster, it may be seen that the average value of this extinction generally increases with the increasing distance from the Sun, as is normally expected. Further, as the age of the cluster increases, the differential reddening across the field of the respective cluster has been found to be

decreasing. This indicates that some amount of gas is still present in the younger clusters and it is a pointer to the star forming activity in the region of such clusters.

Four of the clusters studied in this program are located along the spiral arm in which the Sun also is located. Four others are situated in a more distant spiral feature, which is beyond the presently known Perseus arm. This distant feature, which is now called as the outer arm, is just about getting more clearly defined and the presence of four more clusters (from this study) in that region, renders a further support to the existence of this arm. It appears that this outer feature extends into Puppis group of clusters, where it probably merges with the local arm.

The presence of a few more clusters between the Puppis group of clusters and the Carina arm, including one from the present work, indicates a feature branching off from the local arm and extending towards the possible end of the Carina arm. These are perhaps the first optical observations of this feature which has been indicated earlier by radio studies.

#### **FUTURE PROSPECTS**

The present study was intended to apply a new observational technique of picking up and using the young clusters in tracing the large scale structure of the Milky Way Galaxy.

In the present work, this method could be used on thirty two out of about one hundred 'unknown' clusters in the galactic longitude  $l \sim 160^\circ$  to  $280^\circ$ , which appear to be likely physical groupings consisting of stars fainter than 12 mag. It may now be extended to the remaining ones which may reveal a few more faint clusters of young category. Photometric observations of these clusters would help us to further establish the distribution of interstellar extinction with distance. The ratio between the early type stars, and the late type stars in each cluster as related to its age and physical location would tell us about the nature of the star formation and eventually of the galactic disc. It would be interesting to see the effect of age on the linear diameter of the cluster at a given distance. This would again give us some information regarding the cluster formation.

The general luminosity function and the initial luminosity function of these young clusters would eventually lead to the initial physical conditions, such as, gas density, temperature, turbulent velocity, chemical composition and the magnetic field configuration prevailing in the protostellar clouds. This work needs the observations of almost all the stars in the field of any given cluster.

A search for the presence of Bok globules in the young clusters would throw more light on the star formation activity in these clusters, and consequently in the galactic disc.

Since interstellar extinction decreases as the wavelength of the observed radiation increases, studies in the infrared regions make it possible to observe the predominant radiation in the red giants and the pre-MS stars. Further, at longer wavelengths, thermal emission from dust becomes more important. From the IR studies, it is possible to obtain the line-of-sight column density of the interstellar dust, which is an important component in the structure of the Galaxy and the average temperature of the dust, which is a measure of the energy density of the stellar radiation heating it. Young clusters with interstellar matter in them are very good candidates for this work.

\*\*\*\*\*

## REFERENCES

- Alter, G. 1942, Mon. Not. R. astr. Soc., **102**, 205.
- Alter, G., Balazs, B., Ruprecht, J., 1970, **A Catalogue of Star Clusters and Associations**, 2nd Edn, Akademiai Kiado, Budapest.
- Ambartsumian, V.A. 1949, Astr. Zh., **26**, 3.
- Baade, W., Mayall, N.U., 1951, Symp. Motions of Gaseous Masses of Cosmical Dimensions, Paris, 1949, **Problems of Cosmical Aerodynamics**, Central Documents Office, Dayton, O.
- Babu, G.S.D. 1983, J. Astrophys. Astr. **4**, 235.
- Babu, G.S.D. 1985, J. Astrophys. Astr., **6**, 61.
- Bappu, M.K.V. 1978, in **Modern Techniques in Astronomical Photography**, Eds. R.M.West & J.L.Heudier, ESO, Munchen, p.263.
- Barbaro, G., Dallaporta, N., Fabris, G. 1969, Astrophys. Space Sci., **3**, 123.
- Barhatova, K.A. 1950, Astr. Zh., **27**, 183.
- Becker, W. 1963, Z. Astrophys., **57**, 117.
- Becker, W. 1972, Q.J.R. astr. Soc., **13**, 226.
- Becker, W., Fenkart, R. 1970, IAU Symp. **38**, "The Spiral Structure of our Galaxy", p.205.
- Becker, W., Fenkart, R. 1971, Astr. Astrophys. Suppl., **4**, 241.
- Becker, W., Stock, J. 1954, Z. Astrophys., **34**, 1.
- Bodenheimer, P. 1972, Rep. Prog. Phys. **35**, 1.
- Bok, B.J. 1949, Astrophys. J. **110**, 26.
- Bok, B.J. 1971, Highlights of Astronomy, **2**, 63.

- Bok, B.J. 1980, Personal Communication.
- Borgman, J., Koorneef, J. Slingerland, J., 1970, *Astr. Astrophys.* **4**, 248.
- Breger, M., 1972, *Astrophys. J.* **171**, 539.
- Brown, R.L., Zuckerman, B. 1975, *Astrophys. J. Letters.* **202**, L125.
- Burki, G. 1975, *Astr. Astrophys.* **43**, 37.
- Chromey, F.R. 1978, *Astrophys. J.* **83**, 162.
- Collinder, P. 1931a, *Lund Obs. Ann. No.2.*, Cr.
- Collinder, P. 1931b, *Lund Obs. Ann. No.2*, Lk.
- Czernik, M. 1966, *Acta Astr.*, **16**, 94.
- Dreyer, J. 1888, *Mem. R. astr. Soc.*, **49**, 1.
- Dreyer, J. 1895, *mem. R. astr. Soc.*, **51**, 185.
- Dreyer, J. 1908, *Mem. R. astr. Soc.*, **59**, 105.
- Elmergreen, B.G., Lada, C.J. 1977, *Astrophys. J.*, **214**, 725.
- Ezer, D., Cameron, A.G.W. 1971, *Astrophys. Sp. Sci.*, **10**, 52.
- Encrenaz, P.J., Falgarone, E., Lucas, R. 1975, *Astr. Astrophys.*, **44**, 73.
- Fenkart, R.P., Buser, R., Ritter, H., Schmitt, H., Steppe, H., Wagner, R., Weidemann, D. 1972, *Astr. Astrophys., Suppl. Ser.*, **7**, 487.
- FitzGerald, M.P., Moffat, A.F.J., 1976, *sky Telesc.*, **52**, 104.
- FitzGerald, M.P. Jackson, P.D., Moffat, A.F.J. 1977, *Astr. Astrophys.*, **59**, 141.
- Garrison, R.F., 1985, Personal Communication.
- Golay, M. 1974, **Introduction to Astronomical Photometry**, D.Reidel, Dordrecht, p.138.
- Gotz, W. 1977, in **The Role of Star Clusters in Cosmogony and in the Study of Galactic Structure**, Ed. B.A.Balazs, p.79.

- Grasdalen, G.L., Strom, K.M., Strom, S.E. 1973, *Astrophys. J. Letters*, **184**, L53.
- Gray, D.F. 1963, *Astr. J.*, **68**, 572.
- Haffner, H. 1957, *Z. Astrophys.*, **43**, 89.
- Hardie, R.H. 1962, in **Astronomical Techniques**, ed. W.A.Hiltner, p.178.
- Harris, G.L.H. 1976, *Astrophys. J. Suppl.*, **30**, 451.
- Harris, S., Wynn-Williams, C.G. 1976, *Mon. Not. R. astr. Soc.*, **174**, 649.
- Herbig, G.H. 1962, *Astrophys. J.*, **135**, 736.
- Hoag, A.A., Johnson, H.L., Iriarte, B., Mitchell, R.I., Hallam, K.L., Sharpless, S. 1961, *Publn. U.S. Naval Obs.*, **17**, 418.
- Hoag, A.A., Schroeder, D.J. 1970, *Publ. astr. Soc. Pacific*, **82**, 1141.
- Hoerner, V.S. 1957, *Z. Astrophys.* **42**, 273.
- Hogg, A.R. 1965, *Mem. Mt. Stromlo Obs.* **17**.
- Iben, I. Jr. 1965, *Astrophys. J.*, **141**, 993.
- Iben, I. Jr., Talbot, R.J. 1966, *Astrophys. J.*, **144**, 968.
- Jackson, P.D., FitzGerald, M.P., Moffat, A.F.J. 1979, *IAU Symp.84, The Large Scale Characteristics of the Galaxy*, p.221.
- Johnson, H.L., Morgan, W.W. 1953, *Astrophys. J.*, **117**, 313.
- Jones, B.F. 1972, *Astrophys. J. Letters* **171**, L57.
- Joshi, U.C. 1980, **Ph.D. Thesis**, Kumaon Univ., Nainital.
- Kamp, L.W., 1974, *Astr. Astrophys. Suppl.*, **16**, 1.
- Kerr, F.J. 1970, *IAU symp.38, The Spiral Structure of our Galaxy*, p.95.
- Koornneef, J. 1977, *Astr. Astrophys.* **55**, 469.
- Kopal, Z. 1978, in **Dynamics of Close Binary Systems**, D.Reidel, Dordrecht, p.15.



- Kutner, M.L., Evans II, N.J., Tucker, K.D. 1976, *Astrophys. J.*, **209**, 452.
- Landolt, A.U. 1973, *Astr. J.*, **78**, 959.
- Lindoff, U. 1968, *Arkiv Astr.* **5**, 1.
- Lockwood, G.W. 1974, *Astrophys. J.* **123**, 103.
- Lyngå, G. 1980, **A Computer Readable Catalogue of Open Cluster Data**, Stellar Data Centre, Observatoire de Strasbourg, France.
- Markarian, B.E. 1950, *Mitt. Obs. Bjurakan*, No.5.
- McCarthy, C.C., Miller, E.W. 1973, *Astr. J.*, **78**, 33.
- McNamara, B.J. 1976, *Astr. J.*, **81**, 845.
- Melotte, P.J. 1915, **A Catalogue of Star Clusters shown on Franklin-Adams Chart Plates**, *Mem. R. astr. Soc.*, **60**, Part V, 175.
- Mezger, P.G., Smith, L.F. 1977, *IAU Symp. 75, Star Formation*, p.133.
- Mezger, P.G., Wink, J. 1976, in *Proc. Infrared and Submillimeter Astronomy*, *Astrophys. Space Sci. Library*, D. Reidel, Dordrecht, **63**, p.55.
- Miller, E.W., Graham, J.A. 1974, *Publ. astr. Soc. Pacific*, **86**, 829.
- Moffat, A.F.J. 1972, *Astr. Astrophys. suppl.* **7**, 355.
- Moffat, A.F.J., FitzGerald, M.P. 1974, *Astr. Astrophys. Suppl.*, **16**, 25.
- Moffat, A.F.J., Schmidt-Kaler, Th. 1976, *Astr. Astrophys.* **48**, 115.
- Moffat, A.F.J., Vogt, N. 1973, *Astr. Astrophys.*, **23**, 317.
- Moffat, A.F.J., Vogt, N. 1975, *Astr. Astrophys. Suppl. Ser.*, **20**, 85.

- Morgan, W.W., Sharpless, S., Osterbrock, D. 1952, *Astr. J.*, **57**, 3.
- Muzzio, J.C., McCarthy, C.C. 1973, *Astr. J.*, **78**, 924.
- Ozsvath, I. 1960, *Astr. Abh. Hamburg Sternw., Bergedorf*, **5**, 129.
- Palous, J., Ruprecht, J., Dluhnevskaya, O.B., Piskunov, T. 1977, *Astr. Astrophys.* **61**, 27.
- Piskunov, A.E. 1977, *Nauch. Inform. astr. Council Acad. Sci., USSR*, **37**, 31.
- Rahim, M. 1970, *Astr. Astrophys.*, **9**, 221.
- Rufener, F. 1968, *Publ. Geneva Obs., Ser.A., No.74*.
- Ruprecht, J. 1960, *Bull. Astr. Inst. Czechoslovakia*, **12**, N1.
- Ruprecht, J. 1966, *Bull. Astr. Inst. Czechoslovakia*, **17**, 34.
- Sagar, R., Joshi, U.C. 1978a, *Bull. astr. Soc. India* **6**, 12.
- Sagar, R., Joshi, U.C. 1978b, *Mon. Not. R. astr. Soc.*, **184**, 467.
- Sagar, R., Joshi, U.C. 1979, *Astrophys. Sp. Sci.*, **66**, 3.
- Sandage, A. 1957a, *Astrophys. J.*, **127**, 422.
- Sandage, A. 1957b, *Astrophys. J.*, **125**, 435.
- Sandage, A. 1963, *Astrophys. J.*, **138**, 863.
- Sanders, W.L. 1971a, *Astr. Astrophys.*, **14**, 226.
- Sanders, W.L. 1971b, *Astr. Astrophys.*, **15**, 173.
- Schmidt-Kaler, Th. 1965, in Landolt-Bornstein, **Numerical Data and Functional Relationship in Science and Technology**, Ed. H.H.Voigt, Group VI, Vol.1, p.284.
- Shapley, H. 1930, **Star Clusters**, McGraw Hill, Cambridge, Mass.
- Slovak, M.H. 1977, *Astr. J.*, **82**, 818.
- Steinlin, U. 1968, *Z. Astrophys.*, **69**, 276.

- Stephenson, C.B., Sanduleak, N. 1971, Publ. Warner & Swassey Obs., 1, No.1.
- Strom, K.M., Strom, S.E. Yost, J. 1971, Astrophys. J., **165**, 479.
- Strom, S.E., Strom, K.M., Brooke, A.L., Bregman, J., Yost, J. 1972a, Astrophys. J. **171**, 267.
- Strom, S.E., Strom, K.M., Yost, J., Carrasco, L., Grasdalen, G. 1972b Astrophys. J., **173**, 353.
- Sullivan, III. W.T., Downes, D. 1973, Astr. Astrophys., **29**, 369.
- Taff, L.G., Littleton, J.E. 1973, Astrophys. Lett., **13**, 133.
- Trumpler, R.J. 1922, Allegheny Obs. Publ. **6**, 45.
- Trumpler, R.J. 1925, Publ. Astron. Soc. Pacific, **37**, 307.
- Trumpler, R.J. 1930, Lick Obs. Bull. **14**, 154.
- Trumpler, R.J., Weaver, H.F. 1953, **Statistical Astr.**, Univ. California Press, Berkeley, p.358.
- Tutukov, A.V. 1977, in Kiev (ed.) Early Stages of Stellar Evolution, "**Origin and Evolution of Open Clusters**", p.128 (in Russian).
- Tutukov, A.V. 1978, Astr. Astrophys., **70**, 57.
- van Altena, W.F. 1972, in IAU Coll.17: **Stellar Ages**, Eds. G.Cayrel de Strobel & A.M.De lplace, p.VIII-1.
- van den Bergh, S. 1957, Astr. J. **62**, 100.
- Vasilevskis, S., Klemola, A., Preston, G. 1958, Astr. J., **63**, 387.
- Verba, F.J., Strom, K.M., Strom, S.E, Grasdalen, G.L. 1975, Astrophys. J., **197**, 77.
- Vogt, N., 1971, Astr. Astrophys., **11**, 359.
- Vogt, N., Moffat, A.F.J. 1972, Astr. Astrophys. Suppl. Ser., **7**, 133.

- Vogt, N., Moffat, A.F.J. 1973, Astr. Astrophys. Suppl. Ser.,  
**9**, 97.
- Vogt, N., Moffat, A.F.J. 1975, Astr. Astrophys. **39**, 477.
- Wallenquist, A. 1975, Uppsala astr. Obs. Ann., **5**, No.8.
- Warner, J.W., Strom, S.E., Strom, K.M. 1977, Astrophys. J.  
**213**, 427.
- Watson, P.S. 1949, Popular Astr., **57**, 14.
- Westerlund, B.E. 1961, Publ. astr. Soc. Pacific, **73**, 51.
- Westerlund, B.E. 1968, Astrophys. J. Letters, **154**, L67.
- Wilde, K. 1968, Dissertation, Univ. Sternw., Gottingen.
- Williams, I.P., Cremin, A.W. 1969, Mon. Not. R. astr. Soc.,  
**144**, 359.
- Wynn-Williams, C.G., Becklin, E.E. 1974, Publ. astr. Soc.  
Pacific, **86**, 5.

\*\*\*\*\*